Synthesis of New Fullerides via the "Break-and-Seal" Approach and their Characterization

Von der Fakultät Chemie der Universität Stuttgart
zur Erlangung der Würde eines Doktors der
Naturwissenschaften (Dr. rer. nat.) genehmigte Abhandlung

Vorgelegt von

Nina V. Kozhemyakina

aus Moskau

Haupberichter:	Prof. Dr. M. Jansen
Mitberichter:	Prof. Dr. Th. Schleid
Prüfungsvorsitzender:	Prof. Dr. F. Gießelmann

Tag der Einreichung der Arbeit: 10.06.2009
Tag der Mündlichen Prüfung: 17.07.2009

Max Planck Institut für Festkörperforschung, Stuttgart

2009

Contents

Abbreviations

DB18C6	dibenzo-18-crown-6
DB24C8	dibenzo-24-crown-8
THF	tetrahydrofurane
DME	dimethoxyethane

Part I

Introduction

The chemistry of fullerenes offers a lot of fascinating potential that has still remained but partially exploited. Even isolation of individual fullerenes, including their respective isomers, and confirmation of their constitutions is far from being completed. Here, halogenation [1, 2, 3, 4] has proven to be a versatile and efficient tool for overcoming the notorious inclination of pristine fullerenes to form highly disordered crystalline solids. Particularly manifold are the options as offered by the fullerenes to organic chemistry [5, 6, 7, 8]. Basically behaving as a polyolefin, all reactivity schemes as commonly displayed by such a class of compounds have also been realized with fullerenes.

As another prominent feature, fullerenes have rather high electron affinities and are strong acceptors for electrons [9, 10]. By cyclovoltammetry it has been shown that C_{60} is able to take up as many as six electrons, and reacting C_{60} with elemental alkali metals is yielding the full range of alkali metal fullerenes from e.g. AC_{60} to A_6C_{60} [11, 10, 12]. These alkali metal fullerides offer rich solid state chemistry and physics, with the most spectacular finding of superconductivity for the A_3C_{60} family. However, the structures of the monomeric alkali fullerides are again heavily disordered, impairing a full microscopic understanding of the physical properties and the underlying electronic structures. Due to the high degeneracy of the frontier molecular orbitals of most of the fullerenes (for C_{60}, see Fig. 0.1), their reduction frequently leads to partial occupation of the LUMOs, thus originating an unstable electronic situation to which the system is expected to respond by a geometric distortion. However, such a kind of a Jahn-Teller distortion has not yet been observed for bulk fullerides experimentally. A crucial prerequisite to any attempts of understanding these phenomena, and the possibly related superconductivity of the A_3C_{60}, is to know the molecular structures of fullerides with high accuracy.

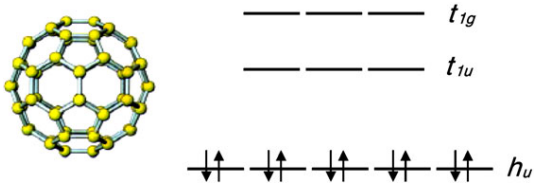

Figure 0.1: Fullerene C_{60} and its frontier molecular orbitals [13].

A series of $C_{60}{}^{2-}$ and based fullerides has been synthesized and crystallized from liquid ammonia by Jansen et al. [14, 15, 16, 17, 18, 19, 20]. Because of the low temperatures prevailing during crystal growth, all of them contained well ordered fulleride anions, and the accuracies achieved in the structure analyses were rather good. However, because of the high content of solvent molecules, all compounds degraded at ambient temperature, evolving ammonia. Thus, appropriate measurements characterizing the electronic struc-

tures, in particular for distinguishing between the two possible triplet or singlet ground states, have proven to be unmanageable.

In order to create a sound basis for in depth studies of the interesting physics and chemistry of fullerides, the present work has been started aiming at the synthesis and characterization of fullerides that are stable at room temperature and form structures containing ordered anions. The approach to achieving this goal has been to select cationic building blocs of sufficient sizes and having definite constituents that interact with the fulleride anion, i.e. to take measures that might fix the fulleride in a specific orientation. As a long term goal, the same factors of influence could be used to generate low dimensional partial structures that allow direct and collective fulleride-fulleride interactions.

For the cations, we have been focusing on complexed alkali ions, using crown-ethers as ligands that are available in a large choice with widely varying sizes and constituents. It has been proven beneficial to offer another degree of freedom to the system by adding further ether ligands of similar size.

Few examples of fullerides with crownether- or cryptand-coordinated alkali metals [21, 22, 23] have been reported, the fulleride molecules still being not fully ordered.

In the present work, a number of new alkali-metal intercalated fullerides have been synthesized in solution and characterized by single-crystal X-ray diffraction. In some of the structures, the fulleride anions are ordered due to additional interactions with the complexing agents of the metal. The dimerization of fullerene anion-ardicals takes place in some structures, observed previously by Jansen et al. [24, 25, 26] and by Konarev et al. [27, 28, 29].

The synthesis of fullerides was performed for the first time using the so-called "seal-and-break" technique (instead of the conventionally used "Schlenk-line"), employed formerly for electrides and alkalides synthesis by Dye [30, 31, 32, 33] and in "living anionic polymerization" [34, 35].

Part II

Literature overview

1 Fullerenes - general

1.1 Discovery

Fullerenes have been discovered in 1985 by Robert F. Kurl, Harold W. Kroto and Richard E. Smalley [36], but it was not till 1991 that studies of their properties have become possible when a method for production of macroscopic amounts has been developed by W. Krätschmer and D.R. Huffmann [37]. In 1996 R.F. Kurl, H.W. Kroto and R.E. Smalley shared the Nobel Prize in chemistry "for their discovery of fullerenes".

It is interesting to mention the prehistory of the discovery of fullerenes, an example when unknown species were first proven to exist, even several times and independently by different research groups, and only then discovered experimentally.

The story goes back to the 1960^s when a possibility of making large hollow carbon cages was considered [38]. At that time, no reaction from the scientific community followed. Four years later, in 1970, stimulated by the synthesis of the bowl-shaped corannulene [39] (Fig. 1.1), Osawa was the first to propose the spherical "football structure" for a C_{60} molecule [40]. During his efforts to find new three dimensional superaromatic π-systems, he recognized corannulene to be a part of the "football" framework. Subsequently, theoretical work has been done by Galpern and Bochvar in the USSR, in which, among others, Hückel calculations on C_{60} were performed [41, 42].

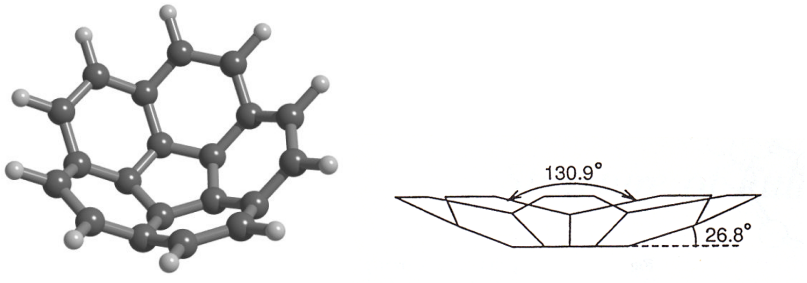

(a) (b)

Figure 1.1: Bowl-shaped corannulene.

In 1982 Huffmann came to the Max Planck Institute in Heidelberg for one year. In 1983, he and Krätschmer performed there a series of experiments [43] on graphite vaporization for simulating interstellar dust (presumably consisting of graphite particles) havig a diffuse UV absorption band at 215 nm for understanding its nature. The setup was not perfect, and the results of the experiments could have been ony published in "Communications on irreproducible results" [43]. Later, in 1987, Huffmann made some Raman spectra measurements at the Max Planck Institute for Solid State research in Stuttgart, proving the fact that the soot obtained at that time contained C_{60} fullerene already.

In 1984 it was observed that upon laser vaporization of graphite, large carbon clusters C_n with $n = 30 - 190$ can be produced [44]. By time-of-flight mass-spectroscopy it was determined that only ions with even numbers of carbon atoms were present with $n \geq 30$. Although C_{60} and C_{70} were among these clusters, their identity was not recognized at that time.

The breakthrough in the experimental discovery of fullerenes came in 1985 when J.W. Kroto from University of Sussex, United Kingdom, visited the Rice University in Houston.

In 1968, a veritable Pandora's box of molecules has been opened up by Townes and co-workers [45] who discovered ammonia in the Orion constellation (Fig. 1.2). After this discovery microwavers and radioastronomers joined forces and showed that the vast dark clouds (Orion and SgrB2 – richest known molecular clouds) harbor scores of molecules the galaxy could possibly need for a primordial pot of prebiotic soup (methanol, carbon monoxide, formaldehyde, ethanol, hydrogen cyanide, formic acid, formamide, etc.) [46].

Harold W. Kroto made his PhD on microwave spectroscopy. In 1972-1973, after the first molecule in space, HC_3N, cyanoacetylene, has been observed [47], Kroto, as well as rather many professionals in spectroscopy at that time, shifted into the field of radioastronomy and started working on polyynes – organic compounds with alternating single and triple bonds. Actually, he with co-workers was the first to discover the first polyyne – dicyanoacetylene, HC_5N, in space, which was detected in the giant molecular cloud SgrB2 [48]. The next synthesized and discovered in 1977 molecule was HC_7N [49]. This was the longest and the heaviest molecule among all observed by that time in interstellar matter, this fact bringing questions for scientists working on chemistry of interstellar space. Approximately at the same time when the chain with 7 carbon atoms was observed, a new star which became later famous under the name *IRC + 10216* was discovered – this was a red carbon giant. It is the closest to the Earth star, and can be visualized more in a detail. Besides, with time HC_7N, HC_9N and $HC_{11}N$ have been detected in this star, it was almost "evolving" carbon chains. Since this time Kroto had had

Figure 1.2: The Horsehead Nebula - dark nebula in the Orion constellation.

the idea that carbon molecules could be an important source for interstellar molecules.

In 1984 Robert F. Curl has invited H.W. Kroto to visit Rice University in Houston, where he met with Richard E. Smalley, who at that time wass working on silicon carbide SiC_2. This molecule turned out to be triangular unlike the analogous more or less linear C_3, and silicon, germanium and carbon arsenides [50]. Smalley had built an apparatus by which one could evaporate almost any material with a laser beam in order to obtain cluster bunches. It was then when Kroto had the idea to use carbon for obtaining a plasma similar to the plasma of the atmosphere of a carbon star, which should successively lead to formation of carbon chains. This experiment has been performed in September of 1985.

In the course of the experiment [36] carbon species have been vaporized from the surface of a solid disc of graphite into a high density helium flow, using a focused pulsed laser. The resulted carbon clusters were expanded in a supersonic molecular beam, photoionized using an excimer laser, and detected by time-of-flight mass spectrometry. The vaporization chamber is shown in Fig. 1.3. Carbon species were vaporized into the helium stream, cooled and transferred in the resulting molecular beam to the ionization region.

The vaporization of carbon has been studied previously in a very similar apparatus by another group [44]. In that work clusters of up to 190 carbon atoms have been observed

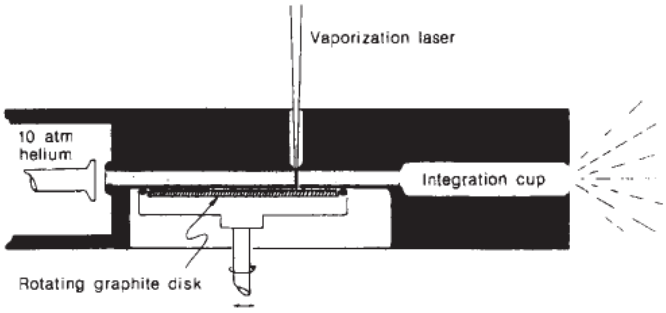

Figure 1.3: Schematic cross-section drawing of "AP2" – the supersonic laser vaporization nozzle source [36].

and it was noted that for clusters of more than 40 atoms only those containing an even number of atoms were observed. But the group in Rice re-examined this system and found that under certain clustering conditions the C_{60} peak can be made ca. 40 times larger than those of other clusters [36] (Fig. 1.4).

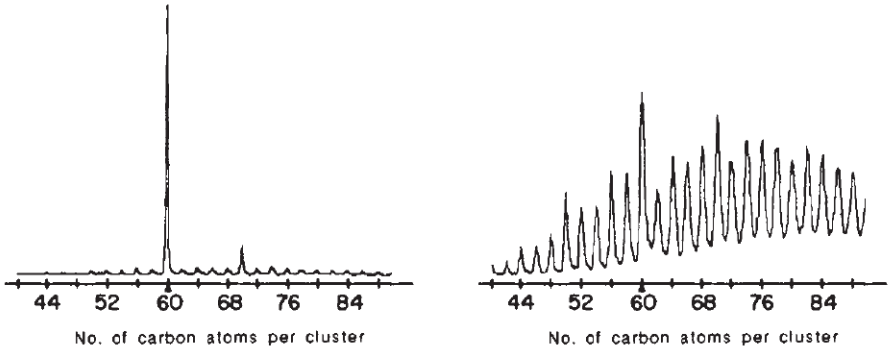

Figure 1.4: TOF-MS spectra of carbon clusters obtained from graphite laser vaporization at different conditions [36].

These clusters proved to be stable and more interesting than long-chained molecules of carbon. Two questions immediately arose. How are these clusters built? Does a new form of carbon exist besides the two well-known forms, graphite and diamond (Fig. 1.5)?

Not straightforwardly the structure of such big carbon clusters with even number of atoms, especially C_{60} and C_{70}, was proposed, first suggestions being based on linear chains, "four-stock sandwiches" hexagon/coronene/coronene/hexagon, "chicken coop", etc., neither of them appearing satisfactory and meaningful at a closer consideration [51, 52, 53]. The model of torn fragments of the planar graphite structure led to the problem of dangling valences at the edges. Same challenge as when the solution was

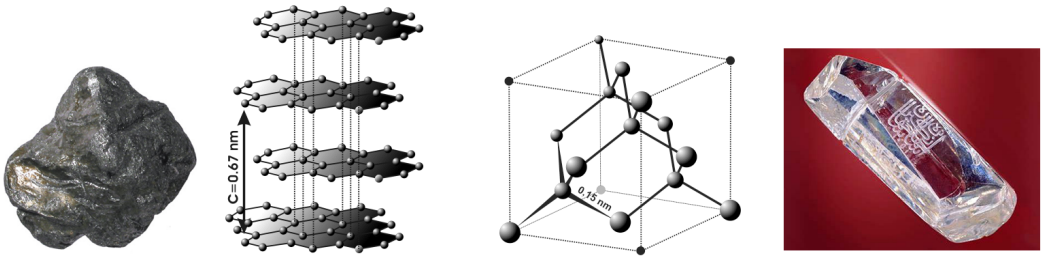

Figure 1.5: Graphite and diamond and their structures.

tried to be found suggesting microscopic particles of the tetrahedral diamond to be the stable clusters.

Only a *closed* spheroidal structure appeared likely to explain everything, all carbon atoms being sp^2-hybridized. Some pentagons, besides hexagons, should be present in the structure, what would give it the curvature. After all this considerations and multiple long discussions among Smalley, Kroto and Curl, within a few days when the experiment has been performed, Buckminster Fuller's work was consulted by Smalley, after him and Kroto having remembered to have seen the geodesic dome at the Expo-67 in Montreal (Fig. 1.6).

Figure 1.6: The geodesic dome designed by R. Buckminster Fuller for the USA exposition in Expo-67 in Montreal.

Richard Buckminster Fuller (1895-1983) was an American architect, designer, futurist and inventor. His ideas, among others, were related to the growth and development of cities, of how different infrastructures should be deliberately introduced during this growth, thus improving the macrostructure, as well. His *opus magnum* "Synergetics" [54] explains his views and concepts. One of them, i.e. "doing more with less", applies to the geodesic dome. A sphere has the largest internal volume with the smallest external

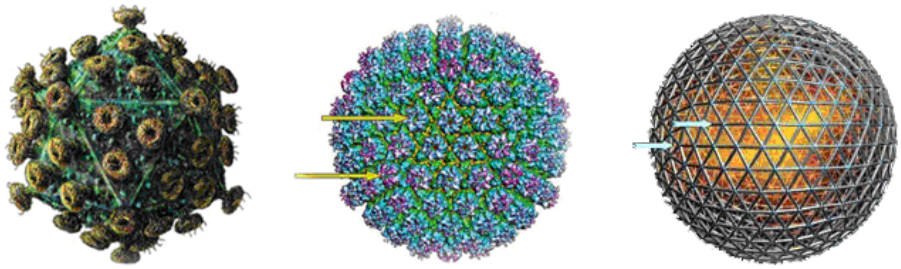

Figure 1.7: Icosahedral symmetry in viruses: HIV (human immunodeficiency virus) and HPV (human papilloma virus) and the similarity of the latter with the dome structure showing hexagons and pentagons.

surface area which means there are less materials required to build a dome than are needed for a conventional shelter. The stability of triangles combined with the stability of arches forms a self supporting super structure that is synergistic in nature (Fig. 1.7). It's worth mentioning that the physical geometry of Buckminsterfuller has influenced significantly other scientists, too, e.g. Klug and Caspar in their pioneering research on icosahedral viral structures [55].

The new discovered species, C_{60}, got a "rather fanciful but highly appropriate name" [36] after him: "buckminsterfullerene".

The structure was proposed to be a truncated icosahedron – a polygon with 60 vertices and 32 faces, 12 of which are pentagonal and 20 hexagonal.

1.2 Methods of production

In 1990, the synthesis of fullerenes in macroscopic amounts [37] has been performed for the first time, what made possible to prove experimentally the calculated properties and suggested applications of fullerenes by that time.

Krätschmer and Huffman [37], by producing laboratory analogues of interstellar dust by vaporizing graphite rods in helium atmosphere, got a material which revealed some features (bands in IR spectrum, Fig. 1.8) close to those predicted by theory for Buckminsterfullerene [56]. The fullerenes were isolated from the soot by sublimation or extraction with benzene. This allowed their verification [57] by spectroscopic and crystallographic methods as well as by controlled experiments with ^{13}C-enriched material. Along with C_{60}, higher homologues are also obtained by this technique, which subsequently should

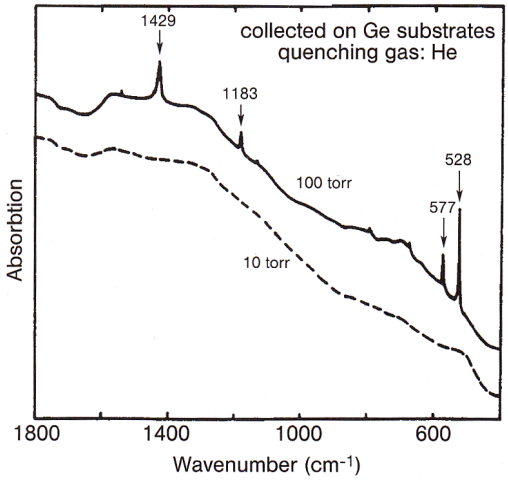

Figure 1.8: IR spectra of soot particles produced by evaporation of graphite under different helium pressure [57].

be separated by chromatographic methods.

Several methods can be used for obtaining fullerenes, i.e. vaporization of graphite, combustion in sooting flames, pyrolysis of hydrocarbons, and direct synthesis. When compared, yield of fullerenes, temperatures of fullerene generation and the C_{60} : C_{70} ratios of these processes are being considered. Not all of them are suitable for production of big amounts of fullerenes; nevertheless, the fundamentals of all approaches are very important and remain prospective.

1.2.1 Generation by vaporization of graphite

Nowadays, the so-called "Krätschmer-Huffman method" is being used for fullerene synthesis for scientific purposes, and synthesis in combustion on industrial scale.

1.2.1.1 Resistive heating of graphite

The apparatus (Fig. 1.9) that Krätschmer et al. used for the first production of fullerenes consisted of a bell jar as a recipient [58], connected to a pump system and a gas inlet. In the interior of the recipient two graphite rods are kept in contact by a soft spring. One graphite rod is sharpened to a conical point, the end of the other is flat. The graphite rods are connected to copper electrodes.

For producing the soot, the apparatus is repeatedly evacuated and purged with helium and finally filled with ca. 140 mbar of helium. After applying a voltage, the electric current passing through the rods dissipates most of its Ohmic power heating at the

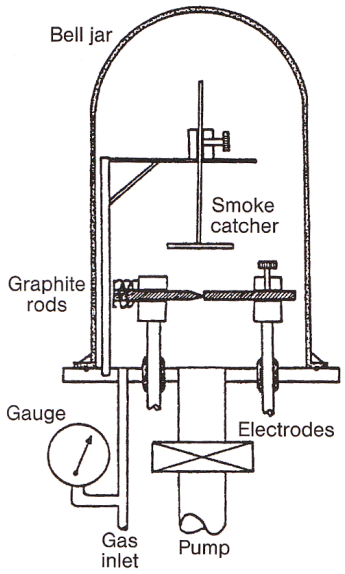

Figure 1.9: Fullerene generator originally used by Krätschmer et al. [58].

narrow point of the contact. This leads to a bright glowing in this area at 2500-3000 °C (the final temperature reaching up to 6000 °C). Simultaneously, smoke develops at the contact zone, being transported away by convection and collected on the cooler areas (smoke catcher) of the apparatus.

The buffer gas cools the plasma by collisions with the carbon vapor. The gas has to be inert to prevent reactions with smaller carbon clusters or atoms. The highest yields of fullerenes are obtained if helium is used as a buffer gas. Also, the concentration of the buffer gas is important (Fig. 1.10), with maximum yields obtained between 140 and 160 mbar [59]. With a very low buffer gas pressure the carbon radicals diffuse far from the hot zone and the clusters continue to grow in an area that is too cool for allowing an annealing to spherical carbon molecules. Conversely, if the pressure of the buffer gas is too high, a very high concentration of carbon radicals results in the hot reaction zone. This leads to a fast growth of clusters far beyond 60 atoms and the annealing process to fullerenes can not complete.

After the reaction is over, fullerenes are extracted from the soot e.g. with benzene or toluene in about 10-15 % yield. It must be noted that although yields are always being reported, these numbers are often not exact and often higher than they really are.

Only thin graphite rods can be used for efficient fullerene production by this method. For graphite rods with diameters of 6 mm or greater the resistive layer doesn't remain

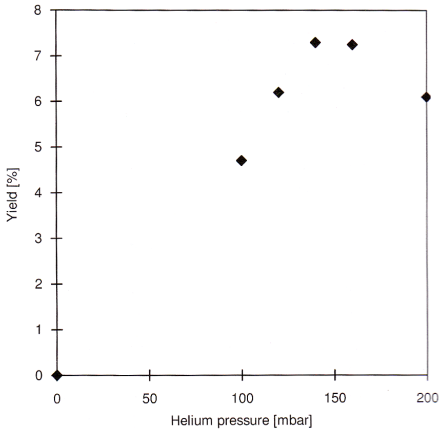

Figure 1.10: Dependence of the fullerene yield on the helium gas pressure in the fullerene generator [59].

sufficiently resistive and the entire length of the graphite rod begins to glow. This causes inefficient evaporation of carbon from the center of the rod.

1.2.1.2 Arc heating of graphite

An alternative to resistive heating is arc vaporization of graphite, first developed by Smalley [60]. If the tips of two sharpened graphite rods are kept in close proximity, but not in a direct contact, the bulk of the electrical power is dissipated in an arc and not in Ohmic heating. The most efficient operation occurs when the electrodes are barely touching. The yield of fullerenes was found to be ca. 15%. However, the yield decreases almost linearly by increasing the rod diameter [60], which also prevents an upscaling to very large rod sizes.

The reason for the low yields observed by using larger rod-sizes is the fullerene sensitivity towards UV-radiation. Very intense UV-radiation originates from the central part of the arc plasma. Newly formed fullerenes moving from the region around the arc are exposed to this intense light flux. The absorption of UV-light produces a triplet state (T_1) with a very short half-life time (few microseconds):

$$C_{60}(S_0) + h\nu \rightarrow C^*_{60}(T_1).$$

In the T_1 state the fullerene is an open shell system and very susceptible to other carbon species C_n. As a result of such a reaction a non-vaporizable insoluble product may be formed [61]:

$$C_{60}^{*}(T_1) + C_n \rightarrow insoluble\ carbon.$$

The ratio of C_{60} to higher fullerenes is typically about 8:2. Fullerenes have also been synthesized by a pulse arc discharge with graphite electrodes and ambient helium. Instead of graphite, coal was also used as carbon source [62].

1.2.1.3 Solar generators

The problem of intense UV-radiation as in the case of arc heating is avoided by the use of solar furnaces as fullerene generators [61]. As an example solar generator, "Solar 1" developed by Smalley [61] can be considered (Fig. 1.11).

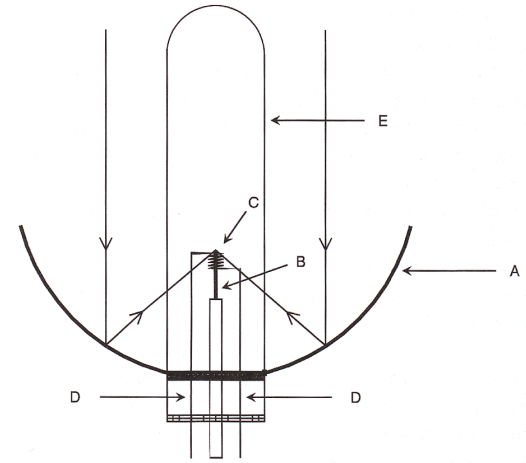

Figure 1.11: "Solar 1" fullerene generator. A – parabolic mirror, B – graphite target, C – preheater, D – insulated preheater connectors, E – glass tube [61].

Sunlight is collected by parabolic mirrors and focused onto a tip of a graphite rod. This rod, enclosed by helical tungsten preheater, is mounted inside a Pyrex tube. After degassing the system, it is filled with ca. 50 Torr of argon and sealed off. To run the reaction the apparatus is adjusted so that the sunlight is focused directly onto the tip of the graphite target. The argon gas heated by the tungsten preheater is carried up over the solar-irradiated carbon tip by convection. The condensing carbon vapor deposits on the upper walls. Although fullerenes can be obtained by this way, the efficiency is not very high.

1.2.1.4 Inductive heating of graphite and other carbon sources

Fullerenes can also be produced by direct inductive heating of a carbon sample held in a boron nitride support (Fig. 1.12) [63, 64], at much lower temperatures than with the method developed by Krätschmer and Huffman. Evaporation at 2700 °C in helium atmosphere affords fullerene-containing soot that is collected on the cold Pyrex glass of the reaction tube. This method allows a continuous operation by keeping the graphite sample in the heating zone. Upon evaporating 1 g of graphite, 80 to 120 mg of fullerene extract can be obtained in 10 min.

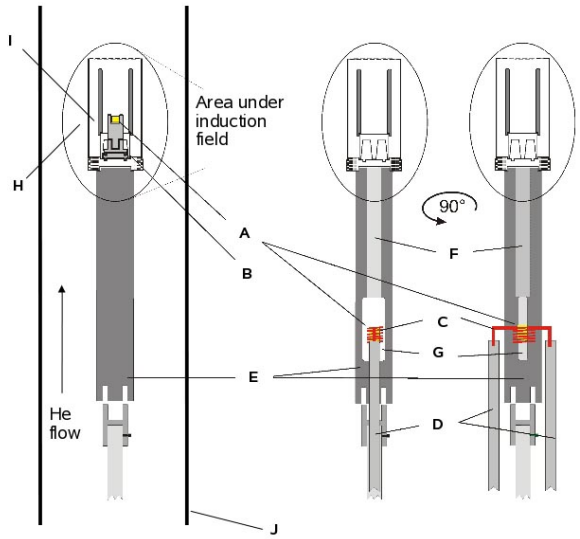

Figure 1.12: Cross-section of the high-frequency apparatus for the preparation of fullerenes. A – foreign element, B – graphite cone, C – heating resistance, D – power supply for the resistance, E – PBN support column, F – tunnel, G – cavity for the resistance, H – PBN shield, I – carbon body, J – quartz glass.

1.2.2 Fullerene synthesis in combustion

The existence of fullerenes in sooting flames has been proven by mass spectroscopy [65, 66]. The production of fullerenes is possible in optimized sooting flames. For this purpose premixed laminar benzene-oxygen-argon flames have been operated under a range of conditions. Along with fullerene soot, polyaromatic hydrocarbons (PAHs) are formed simultaneously. The amount of C_{60} and C_{70} produced is in the range of 0.003 - 9 % of the soot mass at temperatures ca. 1800 K, the C_{70}:C_{60} ratio varies from 0.26 to 5.7, which is much larger than that observed for graphite vaporization methods (0.02 - 0.18) [67].

Further optimization of the process led to the development of pilot plants [68]. Currently, a combustion system that can produce fullerenes at the tons per year scale has been developed [69].

However, fullerene production in combustion plants remains not very essential because nowadays the demand for fullerenes is not so big, and the most widely used method remains the Krätschmer-Huffman method.

1.2.3 Pyrolysis of hydrocarbons

Fullerenes can also be obtained by pyrolysis of hydrocarbons, preferably aromatics, e.g. naphthalene or perchlorofulvalene [70, 71]. Naphthalene skeleton is a monomer of the C_{60} structure. Fullerenes are formed by dehydrogenative coupling reactions. The yields of C_{60} and C_{70} are less than 0.5 %.

1.2.4 Total synthesis approaches

Total synthesis approaches are attractive because specific fullerenes could be made selectively and exclusively, as well as heterofullerenes and other cluster modified fullerenes.

One of the approaches is the zipping up of fullerene precursors (Fig. 1.13).

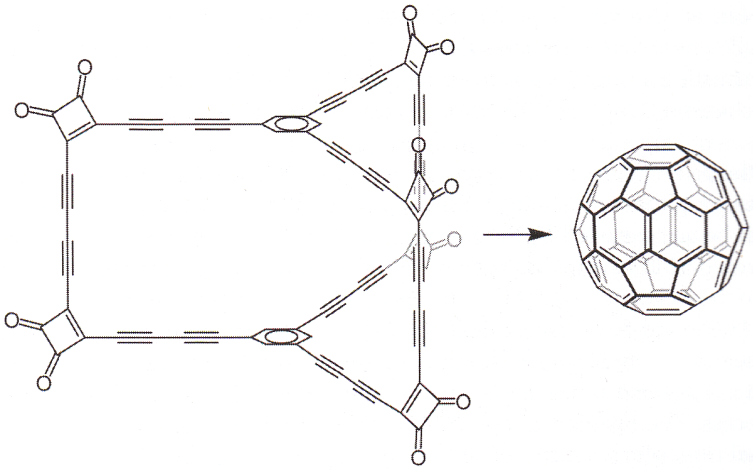

Figure 1.13: Conversion of cyclophane into C_{60} in the gas phase in laser desorption spectrometry.

The second approach is based on the idea of synthesizing bowl-shaped hydrocarbons in which curved networks of trigonal C-atoms map out the same patterns of five- and six-membered rings as those found on the surface of fullerenes (Fig. 1.14) [72, 73, 74, 75, 76, 77].

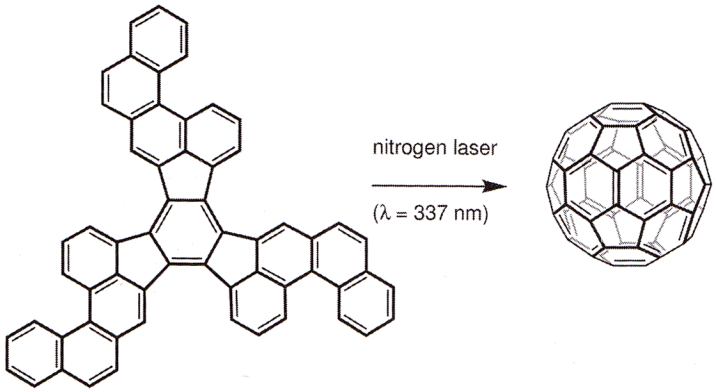

Figure 1.14: Generation of C_{60} by cyclodehydrogenation of polyarene.

1.3 Separation and purification

The raw product obtained by the evaporation of graphite is soot and slag. Next to soluble fullerenes the soot and slag contain other kinds of closed carbon structures, e.g. higher fullerenes [78] and nanotubes [79, 80], the rest is amorphous carbon. Fullerenes must be efficiently dissolved in order to extract them from soot and functionalize them by organic reactions.

The most common method for isolating the fullerenes form soot is extraction with organic solvents [37, 78, 81]. In general, toluene is used since it provides a sufficient solubility and is less toxic than benzene or carbon disulfide. Either a hot extraction of the soot followed by a filtration or a Soxhlet extraction is possible. Longer extraction times lead to higher yields of fullerenes [78].

To separate fullerenes predominantly chromatographic methods are used.

1.4 Structure of fullerenes

1.4.1 Platonic bodies

There are 5 regular convex polyhedra known since ancient times – polyhedra containing regular polygons as faces, all faces being the same. They are called "platonic solids" after Plato (427-348 BC) having written about them in his work "Timaeus" (ca. 340 BC) to identify five principles upon which everything is modelled: he identified these principles as fire, earth, air, water, and cosmos (or divine force), even though Pythagoras used them 150 years earlier; he called them the "perfect solids" (Fig. 1.15).

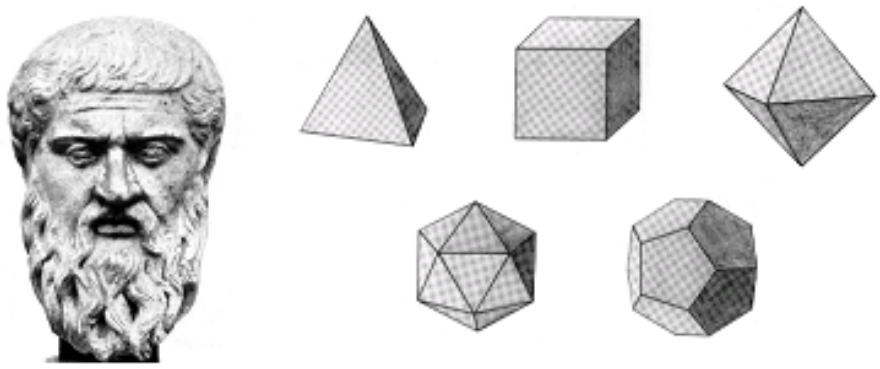

Figure 1.15: Plato and the five Platonic bodies: tetrahedron, cube, octahedron, icosahedron and dodecahedron.

The fullerene C_{60} has a shape of a truncated icosahedron (Fig. 1.16a), which in its turn belongs to the Archimedean bodies - regular polyhedra containing two or more different types of faces which are regular polygons, as well.

One more example showing that such shapes of bodies were predicted to exist long ago befor being really discovered is the truncated icosahedron from the Italian translation of the libellus published in 1509 by the mathematician Luca Pacioli in his book "De divina proportione" (Fig. 1.16b). The design is supposed to be by Leonardo da Vinci [82, 83].

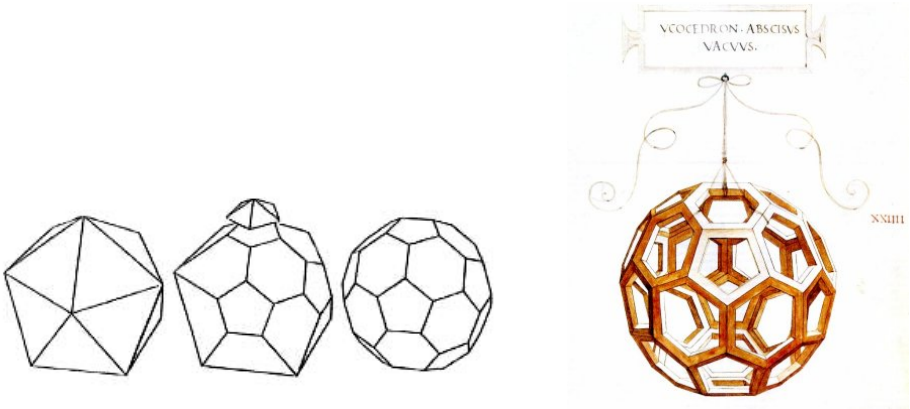

(a) (b)

Figure 1.16: a) Truncating an icosahedron. b) A regular truncated icosahedron from the book by Luca Pacioli "De divina proportione", 1509. In the C_{60} molecule each carbon atom is at an equivalent position on the corners of a regular truncated icosahedron.

1.4.2 Euler's theorem

For fullerenes the Euler characteristic applies [84, 85].

It is a topological invariant, a number that describes shape or structure regardless of the way it is bent. The Euler characteristic χ was originally defined for polyhedra, according to the formula:

$$\chi = V - E + F, \tag{1.1}$$

where V is the number of vertices, E - edges, and F - faces.

For convex polyhedra

$$\chi = V - E + F = 2. \tag{1.2}$$

Expression (1.2) is known as Euler's formula or Euler's theorem[1] [87].

Thus, for a tetrahedron holds $4 - 6 + 4 = 2$, $8 - 12 + 6 = 2$ for a cube, $6 - 12 + 8 = 2$ for an octahedron, etc.

If we consider a fullerene with the general formula C_n, then the number of its vertices

$$V = n. \tag{1.3}$$

Each atom in a fullerene is bonded to three other atoms, and every atom ("edge") joins 2 vertices. Thus,

$$E = \frac{3V}{2}. \tag{1.4}$$

On the other hand, E may be expressed form (1.2):

$$E = V + F - 2. \tag{1.5}$$

By equating (1.4) and (1.5) and substituting V for n (1.3), we obtain:

$$F = \frac{n}{2} + 2. \tag{1.6}$$

The faces of a fullerene are hexagons and pentagons (a structure complied of hexagons

[1] Actually, the original problem was the classification of polyhedra: "While in plane geometry polygons (*figurae rectilinae*) could be satisfied very easily according to the number of their sides, which of course is always equal to the number of their angles, in stereometry the classification of polyhedra (*corpora hedris planis inclusa*) represents a much more difficult problem, since the number of faces alone is insufficient for this purpose" [86]. The key to Euler's result was the invention of the concepts of *vertex* and *edge*.

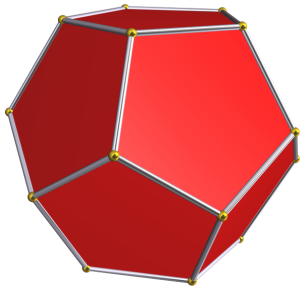

Figure 1.17: The smallest fullerene: C_{20}, a dodecahedron.

exclusively is planar, and the pentagons give it the curvature). Thus,

$$F = p + h, \tag{1.7}$$

where p is the number of pentagons, and h - hexagons. One can rerwrite (1.6) taking (1.7) into account:

$$p + h = \frac{n}{2} + 2. \tag{1.8}$$

On the other hand, the number of vertices is:

$$V = n = \frac{5p + 6H}{3}. \tag{1.9}$$

By solving the system of two equations, (1.8) and (1.9), one obtains the solution

$$\begin{cases} p = 12 \\ h = \frac{n}{2} - 10. \end{cases} \tag{1.10}$$

Hence, all fullerenes contain twelve five-membered rings, whereas the number of six-membered rings can vary.

As a consequence of Euler's theorem, one can see that a fullerene C_n contains $(20+2h)$ carbon atoms. Therefore, the smallest fullerene one can think of is C_{20}, consisting of pentagons exclusively - a dodecahedron (Fig. 1.17).

Starting with C_{20}, any even-numbered carbon cluster, except C_{22}[2] [87, 88], can form at least one fullerene structure.

[2]Fullerene C_{22} does not admit a fullerene isomer. It is impossible to construct a trivalent planar graph with a single hexagon at the centre and every other face a pentagon. The construction fails because the final face of the graph has to be another hexagon, giving a total of two hexagons and 24 vertices - i.e., the unique structure of C_{24} [87].

1.4.3 The isolated pentagon rule (IPR)

The pentagons and hexagons can be arranged in a diferent way in such structures, what gives rise to fullerene isomerism. With increasing n, the number of possible fullerene isomers rises dramatically [87] (Tab. 1.1).

Table 1.1: Enumeration of C_n fullerene isomers found by the spiral algorithm in the range $n = 20$ to 100. The left entry for each value of n is the isomer count obtained when enantiomers are regarded as equivalent, and the right (bracketed) entry is for the isomer count obtained when they are regarded as distinct [87].

n	Isomers		n	Isomers	
20	1	(1)	62	2385	(4670)
24	1	(1)	64	3465	(6769)
26	1	(1)	66	4478	(8825)
28	2	(3)	68	6332	(12501)
30	3	(3)	70	8149	(16091)
32	6	(10)	72	11190	(22142)
34	6	(9)	74	14246	(28232)
36	15	(23)	76	19151	(38016)
38	17	(30)	78	24109	(47868)
40	40	(66)	80	31924	(63416)
42	45	(80)	82	39718	(79023)
44	89	(162)	84	51592	(102684)
46	116	(209)	86	63761	(126973)
48	199	(374)	88	81738	(162793)
50	271	(507)	90	99918	(199128)
52	437	(835)	92	126409	(252082)
54	580	(1113)	94	153493	(306061)
56	924	(1778)	96	191839	(382627)
58	1205	(2344)	98	231017	(461020)
60	1812	(3532)	100	285913	(570602)

For instance, the most abundant fullerene, C_{60}, has 1812 isomers. The soccer-ball shaped icosahedral isomer [60-I_h]fullerene is the smallest stable fullerene. In this structure, all twelve pentagons are isolated by hexagons, and it is the only C_{60} isomer to obey the "isolated pentagon rule" (IPR) [89, 90], and is the smallest possible fullerene which can obey this rule. Adjacent pentagons lead to destabilization of the structure [88]. The number of fullerene structures obeying the IPR is a small share of all possible isomers (e.g. compare C_{70}-C_{100} from Tab. 1.1 and Tab. 1.2).

Even though fullerenes are significantly destabilized with respect to graphite [91], they readily form out of a chaotic plasma at about 3000 K. The ratio C_{60}:C_{70} in the toluene

Table 1.2: Enumeration of isolated-pentagon C_n fullerene isomers found by the spiral algorithm in the range $n = 70$ to 140. Left and right (bracketed) entries for each n have same meaning as in Tab. 1.1 [87].

n	Isomers		n	Isomers	
70	1	(1)	106	1233	(2401)
72	1	(1)	108	1799	(3502)
74	1	(1)	110	1355	(4645)
76	2	(3)	112	3342	(6658)
78	5	(6)	114	4468	(8820)
80	7	(9)	116	6063	(11997)
82	9	(12)	118	8148	(16132)
84	24	(34)	120	10774	(21326)
86	19	(33)	122	13977	(27763)
88	35	(56)	124	18769	(37313)
90	46	(78)	126	23589	(46907)
92	86	(161)	128	30683	(61069)
94	134	(252)	130	39393	(78476)
96	187	(349)	132	49878	(99343)
98	259	(483)	134	62372	(124282)
100	450	(862)	136	79362	(158258)
102	616	(1179)	138	98541	(196532)
104	823	(1606)	140	121354	(242126)

extract of the soot obtained by vaporization is about 85:15 [92], the latter suggesting kinetic control for the fullerene generation, since C_{70} is more stable than C_{60} [93, 94]. Locally, [60-I_h]Fullerene is in a deep potential well and, if once formed from clustering carbon, it is chemically inert. This explains the much lower abundance of higher fullerenes.

With these constraints, "magic numbers" n for stable fullerenes C_n can be predicted, where $n = 60$, 72, 76, 78, 84, etc.

2 Fullerene C_{60}

2.1 Crystalline structure of C_{60}

The diameter of [60-I_h]fullerene has been determined to be 7.10±0.07 Å [95, 96]. When taking into account the size of the π-electron cloud, the outer diameter of C_{60} can be estimated as 10.34 Å [96]. The volume per C_{60} molecule is estimated to be 1.87×10^{-22} cm^3.

A spherical shape distributes the strain as evenly as possible [89]. The bond length alternation in C_{60} fullerene shows that the double bonds are located at the junctions of the hexagons ("short" [6,6]-bonds, 1.38 Å), the bonds at the junctions of a hexagon and a pentagon are "single" ("long" [5,6]-bonds, 1.45 Å) (Fig. 2.1).

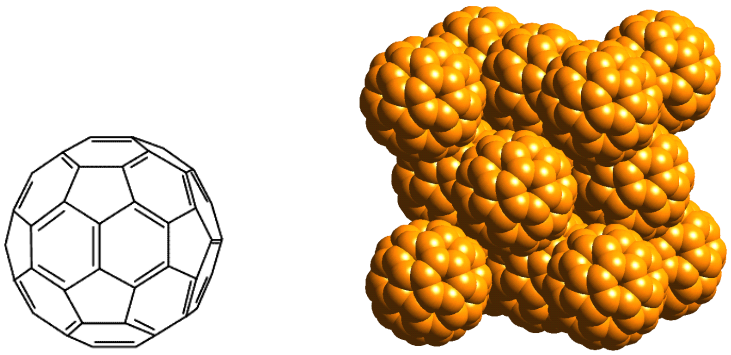

(a) (b)

Figure 2.1: Double and single bonds in C_{60} (a) and *fcc* packing of the molecules in the solid (b).

At room temperature C_{60} has an *fcc* crystal structure (Fig. 2.1), the fullerene molecules being orientationally disordered and cubic lattice constant being 14.1569(5) Å (crystal symmetry $Fm\bar{3}m$). In this phase the C_{60} molecules rotate almost freely. Rotational correlation times τ_{rot} of 9-12 ps are faster than in any other known solid state rotor [97, 98].

At 250 K [99] C_{60} fullerene undergoes an orientational ordering phase transition to *bcc*

structure, the space group becoming $Pa\bar{3}$ and lattice constant 10.0408(1) Å [100].

At 90 K a freezing transition [101] takes place: a finite amount of orientational disorder is frozen in, as the thermal energies become much smaller than the rotational barriers.

2.2 Physical properties of C_{60}

Solid C_{60} is a black crystalline powder as produced (Fig. 2.2) with density 1.72 g/cm^3, melting point 1180 °C, sublimation temperature 434 °C [96]. C_{60} is a hydrophobic molecule with high refraction index (n_D =1.96) and nonpolar (dielectric constant ε = 3.61), molar volume V = 429 cm^3/mol [102].

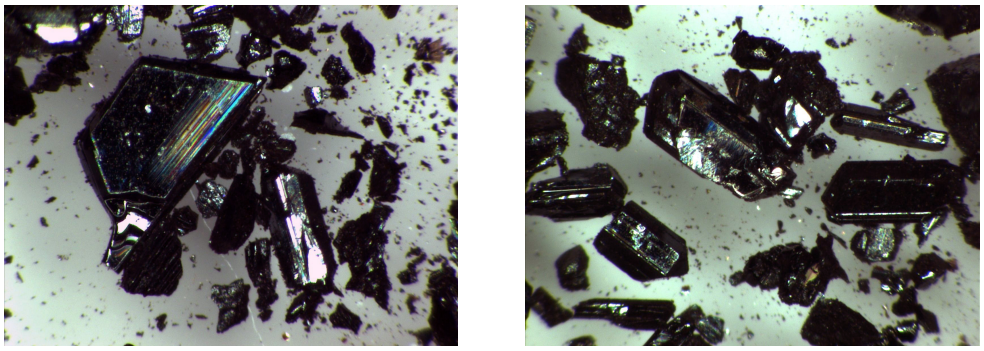

(a) (b)

Figure 2.2: Crystalline C_{60}.

Solubility of C_{60} is crucial for its extraction and separation from other fullerenes, the solvent is influencing much some of the properties of C_{60} in solution.

The practical problem of fullerene solubility has partially been solved just by collecting experimental data. The solubility of C_{60} in almost 150 solvents is known - probably, the highest number among all chemical substances [103]. Effective, relatively inexpensive, and readily available solvents were soon found: aromatic solvents (toluene, 1,2-dimethylbenzene and 1,2-dichlorobenzene) and carbon disulfide CS_2. However, there is still no good theory to explain or to predict absolute values of fullerene solubility and changes in solubility when changing the solvent or the fullerene itself.

In early 1990s an examination of the solubilities of C_{60} as a function of solvent characteristics has been carried out [102]. Solvent properties that might be expected to influence the solubility of C_{60} were chosen: polarizability, polarity, cohesive energy density, molecular size and H-bonding strength. To investigate the influence of these properties, following solvent parameters were selected:

polarizability parameter - measure of *polarizability*:

$$\frac{n^2-1}{n^2+2},$$

where n is index of refraction;

polarity parameter - measure of *polarity*:

$$\frac{\varepsilon-1}{\varepsilon+2},$$

where ε is dielectric constant;

Hildebrand solubility parameter - measure of *cohesive energy density*:

$$\delta = \left(\frac{\triangle E}{V}\right)^{\frac{1}{2}} = \left[\frac{\rho(\triangle_{vap}H - RT)}{M}\right]^{\frac{1}{2}},$$

where $\triangle E$ is the cohesive energy, $\triangle_{vap}H$[1] - enthalpy of vaporization, ρ - density, M - molar mass. The cohesive energy is the energy required to convert a mole of liquid at 298 K to a mole of noninteracting gas;

molar volume - measure of *molecular size*:

$$V = \frac{M}{\rho},$$

where M is the molar mass, ρ - density.

No single solvent parameter could uniformly predict the solubility of C_{60}, but a composite picture of solvents with high solubility for C_{60} emerged, having large refraction indices, dielectric constants around 4, large molecular volumes, Hildebrand solubiblty parameters ca. 10 $cal^{1/2}/cm^{-3/2}$, etc. [102]. That is, the old principle *similia similibus solvuntur* holds [103].

In Table 2.1 solubilities of C_{60} in some solvents are presented. Last column of the table shows the solid phase in equilibrium with the saturated liquid solution at 298 K. As is shown later, for many fullerene-solvent systems, the phase is a solid solvate rather than pristine C_{60}. For other cases, the equilibrium solid phase has not been identified. C_{60} is essentially insoluble in polar H-bonding solvents like tetrahydrofurane, acetonitrile, ethanol, etc. It is spairingly soluble in alkalnes, with the solubility increasing with the number of carbons. And is best of all soluble in aromatic solvents. Increasing the size

[1]For use in solubility theory, the parameter δ is defined for a liquid solute. If the solute is a solid, a hypothetical supercooled liquid should be used as reference liquid, and $\triangle_{vap}H$ for this liquid should be used. C_{60} has not yet been induced to melt, therefore no experimental information exists. However, if $\triangle_{vap}H$ is replaced with $\triangle_{subl}H$, a value of $\delta = 9.8$ $cal^{1/2}/cm^{-3/2}$ is obtained for C_{60}.

of the aromatic system (benzene to naphtalene) increases the solubility. Thus, all other things being equal, a solvent with a solvent parameter whose value is close to that of C_{60} will win over a solvent whose parameter differs significantly [102].

Because C_{60} is good electron pair acceptor (Lewis acid), it can form charge-transfer complexes with electron pair donors (Lewis bases) [104, 105]. Dissolution of fullerenes in tertiary amines and substituted anilines is accompained by the formation of such donor-acceptor complexes in the liquid state as evidenced by the appearence of new visible and near-infrared absorption bands. The room temperature solubilities of C_{60} in aniline, N-methylaniline and N,N'-dimethylaniline were found to be 1.05, 1.16 and 3.89 mg/mL, respectively. These solubilities definitely correspond to the saturation relative to the donor-acceptor complexes rather than the pure fullerene. Complexation with aniline was applied to separate C_{60} from different endohedral complexes [106].

Solubilities of solids in liquids exhibit a temperature dependence that is correlated with the energetics of dissolution [102]. For organic solutes in organic solvents the common experience is that solubility increases on warming (i.e., dissolution is endothermic), what forms a basis for purification by crystallization [108]. Interactions of inorganic compounds with water are often more energetic, and may lead to complicated temperature-dependent solubilities, often associated with the formation of hydrated solid phases [109]. A solubility extremum for organic compounds in non-electrolytes is highly unusual.

The solubility of C_{60} in various solvents has been investigated by Ruoff et al. [102], and a solubility maximum was observed near room temperature for some solvents. Although the absolute solubilities differed by some orders of magnitude, the temperature dependence of the relative solubilities was much the same in all cases (Fig. 2.3).

It was concluded that the dissolution is endothermic below room temperature and exothermic above. It was also clear that the unusual temperature dependence is likely to be caused by the changes in the solid phase and that the first-order phase transition of pure C_{60} at ca. 250 K could not explain it [110].

This phenomenon could have been explained after careful calorimetric measurements combined with single-crystal X-ray diffraction were carried out, and a thermodynamic theory of the temperature dependence of fullerene solubility was presented [111, 112]. The reason for the temperature of maximum solubility (TMS) of fullerenes in a number of solvents turned out to be the formation of ctystallosolvates and their incongruent melting, the temperature of incongruent melting being the TMS.

As an example the system C_{60}-bromobenzene can be considered in which the crystallosolvate with the composition $C_{60} \cdot nB$ (where B is bromobenzene, $n = 2$) is formed (Fig. 2.4) [111]. At 350 K - the incongruent melting temperature,- the following reaction

Table 2.1: Solubility of C_{60} in some organic solvents at T = 298 K (combined data from [103, 107] and [102]). V [cm^3/mol], δ [$cal^{1/2}/cm^{-3/2}$].

Solvent	Solubility of C_{60}		n	ε	V	δ	Equilibrium solid phase
	Mole fraction$\times 10^4$	[C_{60}], mg/ml					mol C_{60}:mol solvent
Aromatic hydrocarbons							
Benzene	1.09-2.30	1.7	1.5	2.28	89	9.2	1:4
Toluene	3.18-4.71	2.8	1.5	2.44	106	8.9	C_{60}
Benzonitrile	0.58	0.41	1.53	25.6	97	8.4	—
Bromobenzene	4.8	3.3	1.56	5.40	105	9.5	1:2
Nitrobenzene	1.14	0.80	1.56	35.74	103	10.0	—
Alkanes							
n-Pentane	0.008	0.005	1.36	1.84	115	7.0	1:1
n-Hexane	0.066-0.095	0.043	1.38	1.89	131	7.3	1:1
n-Decane	0.19	0.071	1.41	1.99	195	8.0	—
Cyclohexane	0.053-0.081	0.036	1.43	2.02	108	8.2	1:13
Miscellaneous							
Ethanol	0.00082-0.001	0.001	1.36	24.30	59	12.7	—
Acetonitrile	0.000	0.000	1.34	37.50	52	11.8	—
Carbon disulfide	4.31-9.87	7.9	1.63	2.64	54	10.0	—
Tetrahydrofurane	0.000	0.000	1.41	7.60	81	9.1	—
Pyridine	0.33-1.00	0.89	1.51	12.30	80	10.7	—
N-Methyl-2-pyrrolidone	1.24	0.89	1.47	—	96	11.3	—

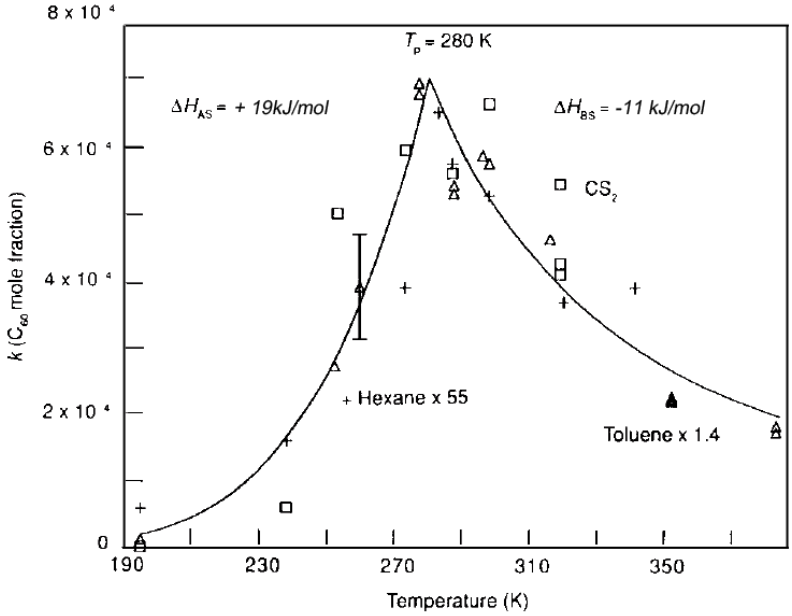

Figure 2.3: Temperature dependent solubility of C_{60} in hexane (+, $\times 55$), toluene ($\triangle$, $\times 1.4$) and CS_2 ($\boxdot$) [110].

takes place:

$$C_{60} \cdot nB_{(s)} = C_{60(s)} + nB_{(liq).} \tag{2.1}$$

Solid C_{60} is being formed, and a saturated solution of C_{60} in B.

Below the incongruent melting point, the saturated solution of C_{60} in B is in equilibrium with solid $C_{60} \cdot nB$. The equilibrium condition is

$$\mu_{C_{60} \cdot nB_{(s)}} = \mu_{c_{60\,(sat)}} + n\mu_{B_{(sat)}}, \tag{2.2}$$

where $\mu_{C_{60} \cdot nB_{(s)}}$ is the chemical potential of $C_{60} \cdot nB$ in the solid phase, $\mu_{C_{60}(sat)}$ - the chemical potential of C_{60} in the saturated solution, $\mu_{B_{(sat)}}$ - chemical potential of the solvent B in the saturated solution of C_{60}. Since the "saturated" solution is still rather diluted in a common sence, it is possible to replace the chemical potential $\mu_{B_{(sat)}}$ for that one of the pure solvent:

$$\mu_{C_{60} \cdot nB_{(s)}} = \mu_{c_{60\,(sat)}} + n\mu_{B_{(liq)}}. \tag{2.3}$$

The temperature dependence of solubility is given by

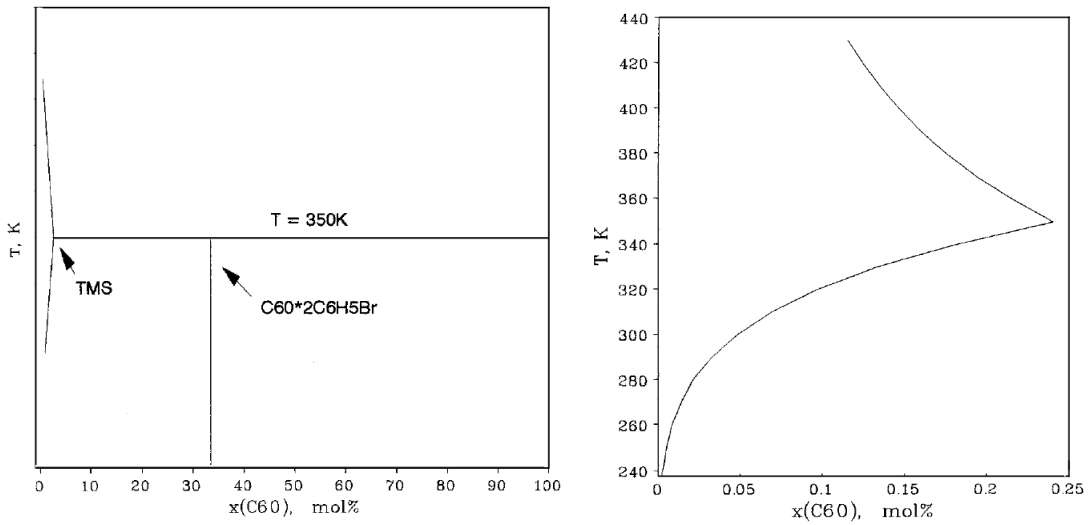

Figure 2.4: Phase diagram of the system C_{60}-bromobenzene. a) General view; b) part of the diagram close to pure bromobenzene showing the temperature vs solubility curve. [111].

$$\frac{d\,lnx_{C_{60}}}{dT} = \frac{\triangle_{sol}H_{C_{60(s)}} - \triangle_f H_{C_{60}\cdot nB_{(s)}}}{RT^2}. \tag{2.4}$$

Mole fractions are used instead of activities, and solubilization enthalpies are assumed to equal the partial molar enthalpies. $\triangle_{sol}H_{C_{60(s)}}$ is the enthalpy of dissolution of solid C_{60}, $\triangle_f H_{C_{60}\cdot nB_{(s)}}$ - enthalpy of formation of the crystallosolvate.

Above the temperature of incongruenting melting, the equilibrium is between the saturated solution and solid C_{60}:

$$\mu_{C_{60\,(s)}} = \mu_{C_{60\,(sat)}} \tag{2.5}$$

and the temperature dependence of solubility is

$$\frac{d\,lnx_{C_{60}}}{dT} = \frac{\triangle_{sol}H_{C_{60(s)}}}{RT^2}. \tag{2.6}$$

The maximum of solubility is caused by the unusual relation between the enthalpies in equations (2.4) and (2.6).

In Fig. 2.4 the phase diagram of C_{60}-bromobenzene is shown. The predicted solubility curve is adjusted to the experimental solubility of 3.3. mg/mL at 298 K [102], which

represents the solubility of $C_{60}{\cdot}2B$, not C_{60}. The part of the solubility curve above 350 K represents the solubility of pure C_{60}. If extrapolated to 298 K, it represents the hypothetical solubility of pure C_{60}, an unachievable state.

As shown by calorimetric measurements, the enthalpies of fullerene dissolution are negative, at least in aromatic solvents. Hence, at high temperatures where C_{60} is the equilibrium phase, Eq. 2.6 predicts a decrease of solubility when increasing temperature. In contrast, for lower temperatures, when the solid phase is solvated C_{60}, the sign of the numerator in Eq. 2.4 determines the temperature dependence of the solubility.

It is the unusual thermodynamic properties of fullerenes - namely, their negative enthalpies of dissolution - and the stability of their solvated crystals which causes their abnormal solubility behavior [103].

It should be clear that interpretations of measurements of the solubility of fullerenes are subject to large uncertainties as long as the composition of the solid phase in equilibrium with the saturated solution is unknown [112].

May be worth mentioning, that the first published picture of "solid C_{60}" on the cover of 1990 issue in Nature in which the article by Krätschmer et al. appeared, is not really of pure C_{60} crystals, but of a benzene crystallosolvate of composition $C_{60}{\cdot}4C_6H_6$ [103].

2.3 Chemical properties of C_{60}

2.3.1 Reduction

The high electron affinity of fullerenes was theoretically predicted before their solution electrochemistry was actually recorded [113]. The estimated electron affinity and ionization potential for C_{60} are 2.7 eV and 7.8 eV, respectively. Most easily C_{60} is reduced to oxidation states ranging from -1 to -6. It was not until 1992 (Fig. 2.5) that all six one-electron reductions were electrochemically detected by three independent groups [114, 115, 116].

The fullerenes undergo reduction to form a family of fulleride anions. For C_{60} the lowest unoccupied molecular orbitals (LUMOs, the triply degenerate t_{1u} orbital) are relatively low in energy, and C_{60} is readily reduced. As predicted by the nature of the LUMO, six reversible one-electron reductions can be observed for C_{60} [117, 9]. The reduction potentials are uniformly spaced with approximately a 0.5 V difference between successive reduction waves as observed by cyclic voltammetry. The reduction potentials show only modest variations when the solvent and/or supporting electrolyte are changed. In toluene/acetonitrile (4:1, v/v) with tetra(n-butyl)ammonium hexafluorophosphate as

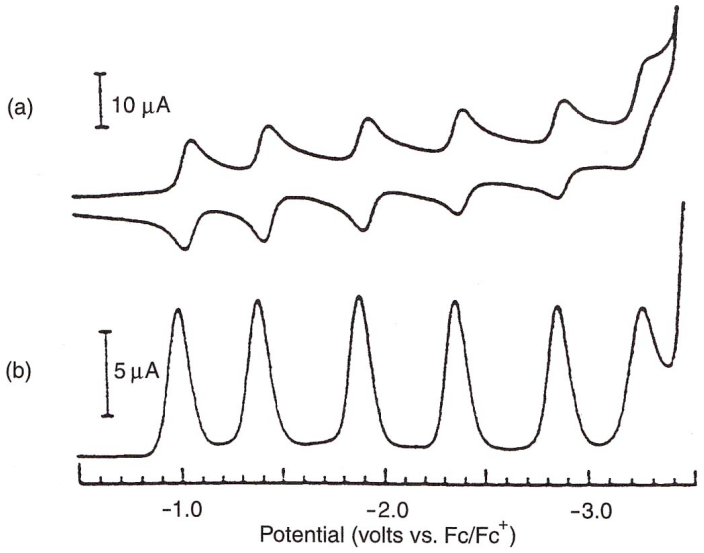

Figure 2.5: Reduction of C_{60} in acetonitrile/toluene using (a) cyclic voltammetry at a 100 mV/s scan rate and (b) differential pulse voltammetry (50 mV pulse, 50 ms pulse width, 300 ms period, 25 mV/s scan rate) [114].

supporting electrolyte, the reduction potentials for C_{60} are -0.98, -1.37, -1.87, -2.35, -2.85 and -3.26 V versus a ferrocene/ferrocinium electrode.

The solubility of the generated anionic species is highly dependent on the choice of the solvent. Thus, C_{60} is insoluble in dimethylformamide (DMF) and tetrahydrofurane (THF), but all of its anions readily dissolve in these solvents.

Most prominent are the salts A_3C_{60} which are metallic and become superconducting at T_c as high as 33 K (ambient pressure), for $RbCsC_{60}$ [118].

2.4 Applications in medicine

Medical applications of fullerenes are a good example of direct properties-application relation of the material.

It was already 1993 when first work concerning possible applications of C_{60} derivatives in drug industry has been reported [119]. Great attention to fullerenes was explained not only by almost perfectly spherical shape, but also by the compactness of the molecule. If one considers the molecular weight of C_{60} as a measure of size (MW = 720), it is "big". But based on the calculations of the molecular surface area, C_{60} has the effective size of a $C_{16}H_{34}$ hydrocarbon (MW = 226) [120]. The size of a potential drug is an important

factor in assessing oral bioavailability. Compounds of lower molecular weight (less than 700) have higher prospects. For such a purpose, the effective MW of C_{60} fits very well.

Already in the article on fullerene discovery it was speculated to make use of the inner volume of the cage in future by including some atoms, while a remarkable shift in the NMR of the central atom has been expected because of the ring currents [36]. Nowadays one of the bioapplications of fullerenes involves placing radioactive metal atoms inside the fullerene cage, leading to products with the potential for radiotherapy or magnetic resonance imaging as e.g. Gd@C_n [121].

Many applications find chemically modified fullerenes. Thus, water soluble fullerols $C_{60}(OH)_n$ can be used as anticancer drugs [122]. Fullerols were shown to decrease the free radical content by up to 86 % in human blood samples from patients with pancreatitis or gastritic cancer [123].

C_{60} accepts readily up to 6 electrons. The electron affinity of C_{60} can be explained by considering its numerous pyracylene units, which upon receiving two electrons go from an unstable $4n$ π-system to a stable aromatic $(4n+2)$ π-system [124]. This leads to applications in quenching of oxygen radicals and as antioxodant [125].

It can be also used as neuroprotective antioxidant [126] for treating Alzheimer and Parkinson diseases.

Fullerene C_{60} has been called a "free radical sponge" [127]. It rapidly reacts with all sorts of reactive free radicals and a number of biomedical applications take advantage of this. Besides, it exhibits antiviral [128] and anti-HIV [119] activity.

C_{60} is efficiently converted to the triplet excited state on UV radiation, and the triplet state efficiently sensitizes the formation of singlet molecular oxygen $^1O_2$. For this reason, one of the earliest suggestions for possible biological activity was the potential application in photodynamic therapy [129]. In 1995, the first photodynamic therapy drug "Photofrin" was approved [130]. Its action is based on the localization of the hydrophobic drug in tumor cells and sensitization of singlet oxygen.

Taking advantage of the UV absorbing ability of C_{60}, sunscreen cosmetics with UV-protection effects have been prepared [131].

Although rather many prospective biomedical properties of fullerenes have been reported up to now, the question of biotoxicity of fullerenes remains open [132]. However, there are already fullerene containing products on the market, i.e. anti-aging skin cremes. Among these are three products that contain engineered C_{60} nanoparticles: "Radical Sponge", made by Tokyo-based "Vitamin C60 Bioresearch Corporation", "Dr. Brandt Lineless Cream" from the New York-based "Dr. Brandt", and "Zelens Fullerene C-60 Day Cream" made by "Zelens" in London [133]. Such cosmetics being rather expensive ($

200-300 for 100-200 mL), it is marketed touting the antioxidant and radical scavenging proprerties of fullerenes, as well as their occurence in nature. Its "Nobel Prize winning" origin is also being stressed as a proof for cutting-edge science, but the opinion of the Nobel Prize winners, e.g. R. Curl, is not widely spread: "I would take the conservative path of avoiding using such cosmetics while withholding judgement on the actual merits or demerits of their use" [133].

3 Intercalation of fullerenes with metals

The structure of pristine *fcc* C_{60} is characterized by the presence of two types of unoccupied interstitial holes: the smaller tetrahedral (2 per C_{60} unit, r = 1.12 Å), and the larger octahedral (1 per C_{60} unit, r = 2.06 Å). Fig. 3.1 shows the *fcc* structure for C_{60} and the interstitial sites where metal ions can intercalate.

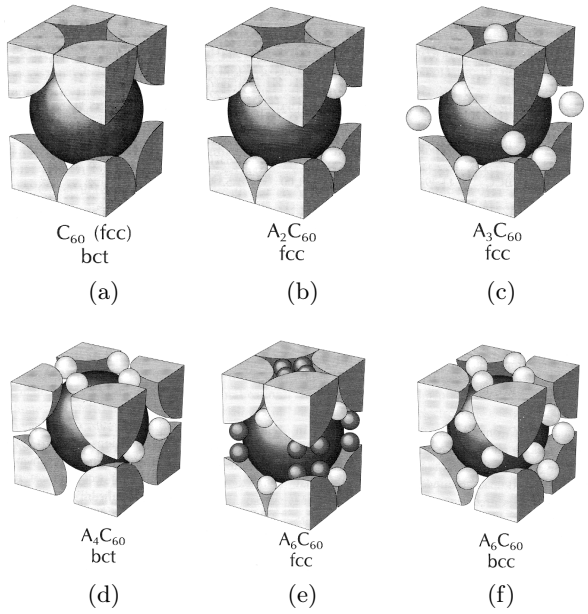

Figure 3.1: Schematic representation of A_xC_{60} structures [134].

Intercalation of C_{60} with electron donors, like the alkali metals, results in a variety of fulleride salts with stoichiometries A_xC_{60}, where x can be as low as 1 (CsC_{60}) or as high as 15 ($Li_{15}C_{60}$) [135].

Solids containing fulleride ions have been obtained principally through two different routes: intercalation of metal atoms into the solid fullerene via vapor transport or by solution techniques. The intercalation route has been heavily investigated as a route to salts of the type A_3C_{60}, which exhibit superconductivity at temperatures up to ca. 40 K. A number of reviews covers the physics and chemistry of this type of products as well

as the nonsuperconducting phases A_4C_{60} and A_6C_{60} [136, 137, 138, 139, 140].

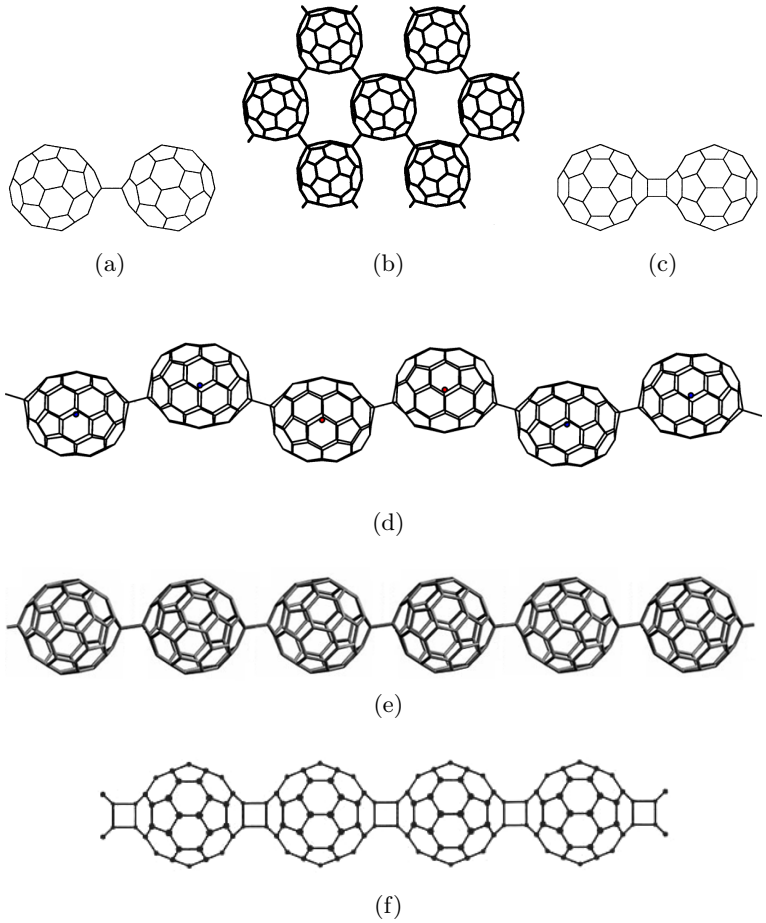

Figure 3.2: Different type of bonding occuring in metal intercalated fullerides. a) σ-dimer $(C_{60}{}^{-})_2$ with a single covalent interfullerene C-C bond observed in some fullerides [24, 25, 26]; b) two-dimensional polymer in Na_4C_{60} [141]; c) π-dimer of $(C_{60}{}^{-})_2$ formed via a [2+2] cycloaddition [142, 143]; d) linear anionic polymeric chain in C_{70} fullerides [20, 144, 19]; e) single-bonded polymer observed in Li_3CsC_{60} ([145]) and Na_2RbC_{60} ([146]); f) linear polymeric chain in C_{60} fullerides [147].

The fullerene cages can undergo transformations when being intercalated with metals and form a variety of newly bonded structures, which under certain conditions can even transform from one into another, e.g. dimers, polymeric chains or two-dimensional dimers (Fig. 3.2). The latter depends on the metal (or different metals) being intercalated, the metal-to-fullerene ratio, the sample preparation and its thermal history, among others.

3.1 Methods of intercalation with metals

3.1.1 High temperature synthesis

3.1.1.1 Vapor phase intercalation

The first method used for the preparation of fullerides was the direct reaction of stoichiometric amounts of alkali metal with C_{60} powder, followed by an appropriate annealing - the "vapor phase intercalation" [148]. The C_{60} powder and the metal are placed in a quartz or Pyrex tube which is equipped with a vacuum valve and removed from the glove-box. The inert atmosphere is evacuated, and the ampoule is sealed under vacuum. The reaction tube is placed in an oven and annealed at 200-400 °C (depends on the vapor pressure of the metal) for the diffusion of the alkali metal in the C_{60} lattice. The annealing time depends on the size of the C_{60} particles and is between several hours (for powder) and weeks (for crystals).

However, this method presents some experimental difficulties regarding the weighing of the alkali metals. If the alkali metal is loaded into a capillary with known diameter, the amount of the metal can be measured from the length of the capillary, besides, the "open" surface of the alkali metal exposed to the glove box atmosphere is very small.

Another procedure adopted for avoiding the difficulty of measuring the precise amount of the alkaline metal A is overdoping C_{60} with an excess of alkali metal in order to obtain a compound with stoichiometry A_6C_{60}. Because no more than six alkali ions (K, Rb and Cs, but not Li and Na) can be intercalated into the C_{60} lattice, it is possible to synthesize A_6C_{60} as a well-defined homogeneous compound and then to anneal a proper mixture of A_6C_{60} and C_{60} to produce the desired final stoichiometry.

3.1.1.2 Decomposition of metal azides

An alternative doping procedure doesn't require a glove-box while weighing and is based on the thermal decomposition of alkali metal azides [149]. Azides are not air sensitive and, when heated above their decomposition temperature, produce pure alkali metals and nitrogen:

$$2AN_3 \rightarrow 2A + 3N_2 \uparrow .$$

The decomposition temperature ranges from 360 °C to 520 °C (depending on A). A further annealing is sometimes required.

3.1.2 Synthesis in solution

3.1.2.1 Synthesis in ammonia

The next method is doping of C_{60} in a solution of liquid ammonia. It gives homogeneously doped samples and doesn't require the use of high temperature treatment [150]. This method takes advantage of the good solubility of alkali metals and C_{60}-anion in liquid ammonia, which can be evaporated slowly after the reaction took place. A possible disadvantage of this method is that ammonia may be incorporated as an impurity in the fullerides lattice.

3.1.2.2 Synthesis in organic solvents

Alkali-doped C_{60} can be prepared in organic solvents, as well [151]. The first procedure reported was the following. A toluene solution containing pure C_{60} was freeze-thaw-degassed 3 times. Small potassium chips were then added while the C_{60}-toluene solution was kept frozen. The reaction flask was immediately evacuated and back-filled with Ar three times. The mixture was warmed to room temperature and then refluxed. The color of the solution turned from purple (pure C_{60}) to burgundy and finally to black with a large amount of black precipitate (the fulleride) being formed.

3.1.3 Intercalation with metal alloys

One more approach to doping is to use metal alloys [152, 153]. The procedure is similar to described earlier, only instead of azides or ammonia, metal alloys such as AHg are used. The molar mass of AHg is more than that of pure A. This allows the preparations of a more precise stoichiometric mixture. Besides, these alloys are solid and can be ground and mixed directly with C_{60} powder and are less sensitive to oxygen and moisture.

3.2 A_xC_{60} fullerides

3.2.1 Monoanions

Intercalation of alkali metal atoms into C_{60} leads to an array of different phases with the composition AC_{60} [154]. For A = K, Rb and Cs above 400 °C, the high-temperature rocksalt-type structure with freely rotating fulleride ions is stable [155].

On slow cooling below 400 °C, an orthorhombic conducting phase, $\{A[C_{60}]\}_n$, forms which is a linear polymer of fulleride anoins connected by the [2+2] cycloaddition reaction between double bonds of the adjacent fullerenes, shrinking the interfullerene distance

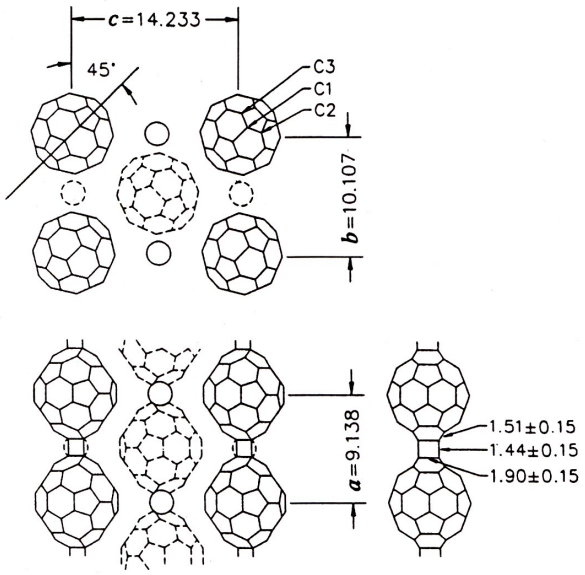

Figure 3.3: Structure of $\{Rb[C_{60}]\}_n$, showing covalently bonded chains along the a direction. Solid (broken) lines show species centered at $x = 0$ ($x = \frac{1}{2}$) in the bc plane at the top, and $y = 0$ ($y = \frac{1}{2}$) in the ac plane in the middle. Solid line through the upper-left fullerene denotes the molecular mirror plane, and the fragment to the right is a projection of one chain perpendicular to that plane (distances given in Å) [147].

from the usual van der Waals value [147, 156, 157, 158, 159]. Such type of bonding also occurs in pressure polymerized C_{60} [160, 161, 162].

When the high-temperature rocksalt phase is quenched below 273 K, a monoclinic insulating phase is being formed, preventing polymerization. In this case discrete dimers are being formed [163, 164]. Such a single covalent interfullerene bond has been already found in solution for dimerized C_{60} radicals [165] and for $(C_{59}N)_2$ [166], which is isoelectronic to ${(C_{60})_2}^{2-}$.

Fig. 3.3 shows a drawing of the structure of the air stable polymeric phase $\{Rb[C_{60}]\}_n$ [147]. In this solid a [2+2] cycloaddition between adjacent fullerides forms the four-membered rings that covalently link the fulleride ions. Metallic conductivity has been observed for $\{A[C_{60}]\}_n$ (A = K, Rb and Cs) [167].

Solution phase methods have been used to prepare the solid salts $[(\eta^2\text{-}C_5H_5)_2Co^+][C_{60}^-]$, $[Na(\text{dibenzo-18-crown-6})^+][C_{60}^-]$ and $[\text{bis(N-methyl-imidazole)-(tetraphenylporphyrinato)-tin(IV)}^{+2}][C_{60}^-]_2$ which are believed to contain isolated $[C_{60}]^-$ units [168]. These have been characterized extensively by electron paramagnetic resonance (EPR) and ultraviolet/visible (UV/Vis) spectroscopy, and $[(\eta^2\text{-}C_5H_5)_2Co^+][C_{60}^-]$ has been examined by single-crystal X-ray diffraction. Electrocrystallization techniques have been effective in

producing crystalline forms of $[C_{60}^{-}]$ [169, 170, 171, 172]. The air stable salt $[Ph_4P]_2[C_{60}][I]_n$, with n in the range 0.15-0.35, has been characterized by single-crystal X-ray diffraction [169]. Despite the non-stoichiometric formulation, the spectroscopic data are consistent with the presence of $[C_{60}^{-}]$ only (no C_{60} or C_{60}^{2-}) in the solid. The stoichiometric compound $[Ph_4P^{+}]_2[C_{60}{}^{-}][Cl^{-}]$ has also been formed by electrocrystallization and has been characterized by single-crystal X-ray diffraction [170]. Other salts related, $[Ph_4P^{+}]_2[C_{60}^{-}][X^{-}]$, with X = Br or I, and $[Ph_4As^{+}]_2[C_{60}^{-}][Cl^{-}]$, have similarly been characterized [172]. Due to issues of disorder and crystal quality, these structure determinations have not allowed to examine the fullerene geometry in sufficient precision to detect any possible distortion that results from addition of an electron to C_{60}.

Dark red crystals of $[(\eta^5\text{-}C_5H_5)_2Ni^{+}][C_{60}^{-}]\cdot CS_2$ form from carbon disulfide solutions of $(\eta^5\text{-}C_5H_5)_2Ni$ and C_{60} [173]. An X-ray crystallographic study shows that the fulleride undergoes axial compression so that there is a short axis dimension, 6.878(6) Å (from the midpoint of a C-C bond at a 6:6 ring junction to the opposite midpoint), and two corresponding longer orthogonal distances, 6.965(5) and 6.976(5) Å. This structural change may result from a Jahn-Teller distortion, but the framework of $[(\eta^5\text{-}C_5H_5)_2Ni]^{+}$ cations may also reshape the fulleride ion.

3.2.1.1 Similarity with azafullerene $C_{59}N$

The first bulk synthesis of the azafullerene with stoichiometry $C_{59}N$ was achieved in 1995 [166, 174]. As a result of the trivalency of nitrogen, compared to the tetravalency of carbon, nitrogen substitution of a single carbon atom on the C_{60} skeleton leads to the azafullerene radical $C_{59}N$, isoelectronic with the $C_{60}{}^{\cdot -}$ radical anion. $C_{59}N$ is found to rapidly dimerize and form a dimer $(C_{59}N)_2$. If the synthetic procedure is somewhat modified, dimerization is prevented, and the monomeric hydroazafullerene $C_{59}HN$ can be isolated [175].

The introduction of the nitrogen atom in the fullerene cluster strongly perturbs the electronic and geometric character of the parent C_{60}, resulting in a very reactive $C_{59}N$ radical. Theoretical calculations [176] find that the $C_{59}N$ molecule is particularly stable (binding energy $\approx$ 72 kcal/mol), while the $(C_{59}N)_2$ dimer adopts a closed shell structure (binding energy $\approx$ 18 kcal/mol) in which the nitrogen atoms are *trans* to each other with an intermolecular C-C bond, formed by C atoms neighboring the N atoms on each monomer, of length 1.61 Å. Experimentally $(C_{59}N)_2$ is found to be a diamagnetic, insulating solid. The g-value of the $C_{59}N$ radical is 2.0013(2), higher than that reported for the Jahn-Teller distorted C_{60} radical anion, 1.9991.

Solid $(C_{59}N)_2$ adopts a monoclinic cell (space group $P2_1/a$) with lattice dimensions a

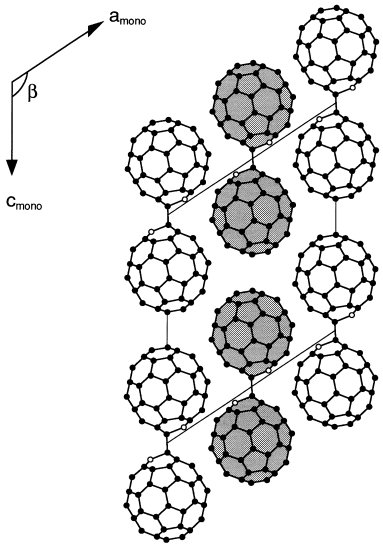

Figure 3.4: Unit cell basal plane projection of the structure of $(C_{59}N)_2$ down the b-axis. Only one of the two merohedral images is shown. The open circles label the nitrogen atoms. Shaded molecules lie at b = $\frac{1}{2}$ [177].

= 17.25 Å, b = 9.96 Å, c = 19.44 Å, and β = 124.3° (Fig. 3.4) [177]. This resembles the situation encountered for the metastable phase of RbC_{60} in which $C_{60}^{\cdot -}$ form dimeric units.

It is instructive to compare the properties of this salt with those of its C_{60} analog, K_6C_{60}. C_{60} has a triply degenerate t_{1u} lowest unoccupied molecular orbital (LUMO), which, when half-filled with electrons stemming from alkali metal atoms, gives rise to the metallic A_3C_{60} salts with half-filled electronic bands. When the t_{1u} level is completely filled, the stoichiometry requires six alkali metal ions, the resistivity reaches a maximum, and the resulting insulating A_6C_{60} salts adopt a body-centered cubic (*bcc*) structure. In the case of the $C_{59}N$ molecule, as a result of the symmetry lowering, the t_{1u} triplet LUMO is no longer degenerate:

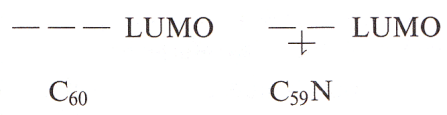

Complete filling of the levels should require, in principle, only five alkali metal atoms. Thus, reduction of $C_{59}N$ with six electrons necessitates population of the LUMO+1 state:

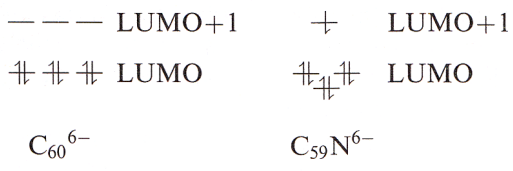

The resulting $A_6C_{59}N$ salts adopt *bcc* structures (space group $Im\bar{3}$), essentially isostructural with A_6C_{60}, with somewhat smaller lattice constants.

3.2.2 Dianions

Na_2C_{60}, not superconducting, is formed via intercalation and possesses a fluorite structure with all tetrahedral voids occupied in the *fcc* closed-packed structure [178]. Treatment of Na_2C_{60} with ammonia at room temperature produces $[Na(NH_3)^{4+}]_2[C_{60}^{2-}]$ in which the close-packed structure is expanded so that the intralayer $[C_{60}^{2-}] \cdots [C_{60}^{2-}]$ separation is 12.22 Å while the corresponding interlayer separation is 10.24 Å [179].

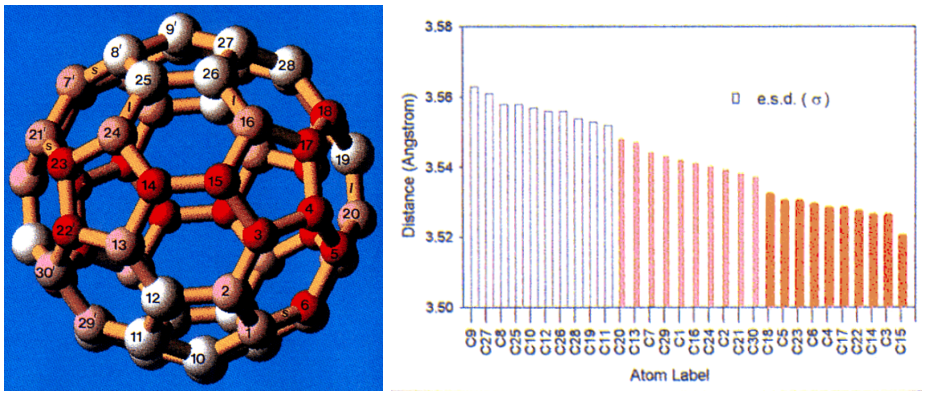

(a) Color visualization of the distortions in C_{60}^{2-}.

(b) Center-to-C-atom-distances.

Figure 3.5: Distortion of the fullerene in $[PPN^+]_2[C_{60}^{2-}]$ [180].

Crystals of $[(Ph_3P)_2N^+]_2[C_{60}^{2-}]$ have been obtained by mixing $[(Ph_3P)_2N]Cl$ with $[Na(crown)^+]_2[C_{60}^{2-}]$ in acetonitrile [180, 181]. Within the solid, the fulleride ions are ordered and the data are of sufficient precision to reveal a significant distortion in the fulleride (Fig. 3.5), which has been described as an "axial elongation with an apparent rhombic squash" with a long diameter of 7.126(5) Å and a short diameter of 7.040(5) Å [180, 181]. A bar graph that shows the distribution of distances within the fulleride is contained in Fig. 3.6.

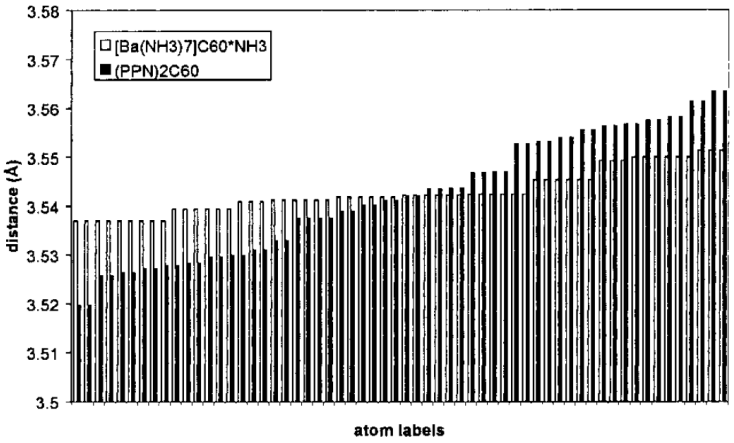

Figure 3.6: A comparison of the distances from the center of the fulleride ion to the carbon atoms in $[Ba(NH_3)_7{}^{2+}][C_{60}{}^{2-}] \cdot NH_3$ and $[(Ph_3P)_2N^+]_2[C_{60}{}^{2-}]$ [14].

The salt $[Ba(NH_3)_7{}^{2+}][C_{60}{}^{2-}]\cdot NH_3$ has been prepared by the reaction of C_{60} and barium metal in liquid ammonia and has also been characterized by X-ray crystallography [14]. In this salt the fulleride anion is also ordered, but the structural analysis shows a much less pronounced distortion than that seen in $[(Ph_3P)_2N^+]_2[C_{60}{}^{2-}]$. Relevant data for comparison are shown in Fig. 3.6. The structure of the related salt, $[Ni(NH_3)_6]C_{60}\cdot 6NH_3$ is shown in Fig. 3.7.

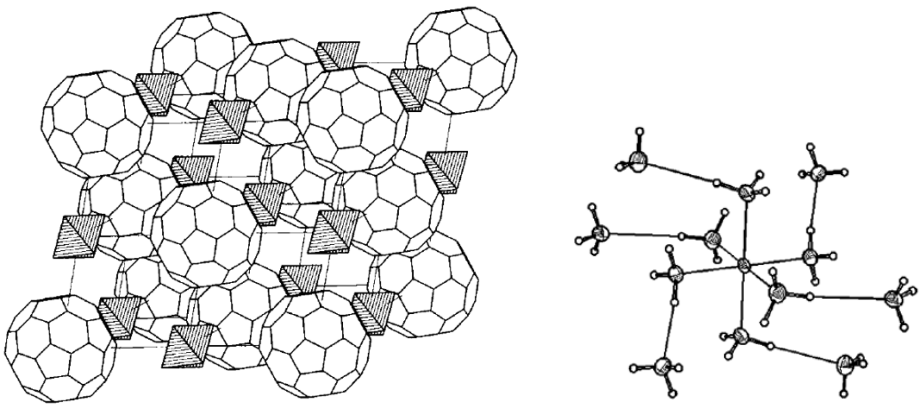

(a) The packing within the solid.

(b) The hydrogen bonding that occurs between the cation and the adjacent ammonia molecules.

Figure 3.7: A view of the structure $[Ni(NH_3)_6{}^{2+}][C_{60}{}^{2-}] \cdot 6NH_3$ as determined by X-ray crystallography [15].

Another $[C_{60}{}^{2-}]$ containing salt, $[K([2.2.2.]crypt)^{+}]_2[C_{60}{}^{2-}] \cdot 4(C_6H_5CH_3)$, has been formed by reaction of C_{60} with potassium metal in the presence of [2.2.2.]crypt in dimethylformamide [21]. It crystallizes in a layered structure that consists of fulleride layers with distorted hexagonal close packing separated by layers of the cationic complexes.

3.2.3 Trianions. Superconductivity

The electronic structure of the molecule is important in determining the properties of the intercalates. The lowest unoccupied molecular orbital (LUMO) of C_{60} is almost nonbonding in nature and is triply degenerate with t_{1u} symmetry (Fig. 3.8, Fig. 3.9). The t_{1g} (LUMO + 1) level is also chemically accessible, with possible anion charges rising up to -12 (Fig. 3.8) [182].

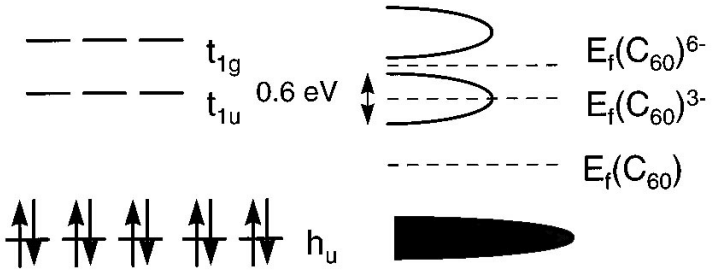

Figure 3.8: The HOMO, LUMO and (LUMO + 1) levels of the C_{60} molecule, and their evolution into narrow bands on the formation of the *fcc* solid. Dashed lines show the Fermi levels for neutral C_{60}, metallic K_3C_{60} and insulating K_6C_{60} [182].

After many years of attempt to increase the superconducting transition temperature, T_c, in the conventional superconductors, the highest T_c obtained was 23.2 K in Nb_3Ge in 1973, and it was widely believed that this transition temperature could be hardly improved significantly. The new era in superconductivity started in 1986, after Bendorz and Müller [183] discovered superconductivity in cuprates (La_2CuO_4) with T_c of 30 K. They were awarded the 1987 Nobel Prize in physics. Soon after, it was followed by discoveries of a large number of cuprate superconductors with T_c up to 150 K, which is above the boiling point of liquid nitrogen (77 K) and promising commercial applications. Five years later, superconductivity in alkali-doped fullerenes was discovered [184] with T_c as high as 33 K in $RbCs_2C_{60}$ [185, 186]. The highest T_c in fullerides so far was observed in $Cs_xRb_{3-x}C_{60}$ at ambient pressure (T_c = 33 K) [118] and in Cs_3C_{60} at 12 kbar (T_c = 40 K) [187] under pressure (Tab. 3.1).

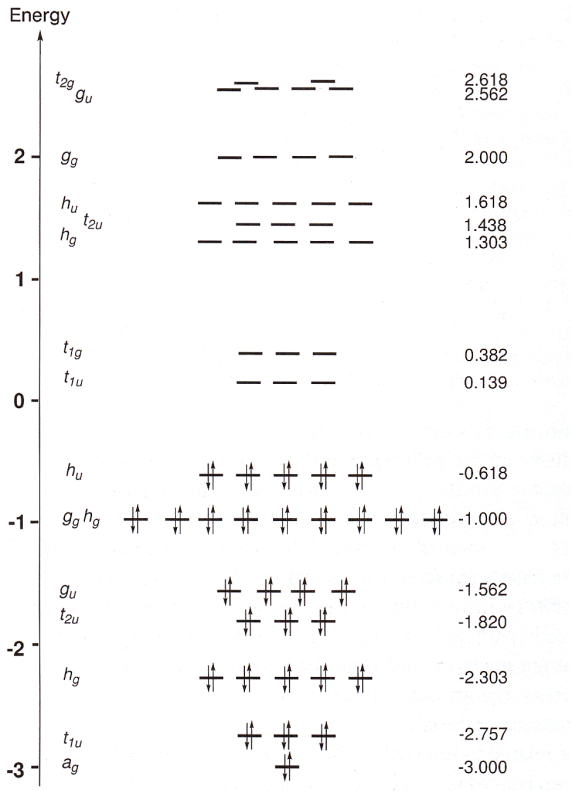

Figure 3.9: Hückel molecular orbital diagram for C_{60}.

The superconducting phases adopt, in general, either face-centered cubic (*fcc*) or primitive cubic structures, in which the three cations occupy the available tetrahedral and octahedral interstitial sites. The conduction band of C_{60}, which arises from its lowest unoccupied molecular orbital (LUMO) of t_{1u} symmetry is half filled (Fig. 3.9).

Experimental evidence derived from the relationship between lattice parameters (i.e. interfullerene spacing) and superconducting transition temperatures in A_3C_{60} (Fig. 3.10) is consistent with T_c being modulated by the density-of-states at the Fermi level, $N(\varepsilon_F)$ [185].

The superconducting T_c is a sharply peaked function of the anion charge (Fig. 3.11), maximized at 3-, and with a narrow superconducting composition range before nonsuperconducting behavior occurs at the integral anion 4- and 5- charges [188].

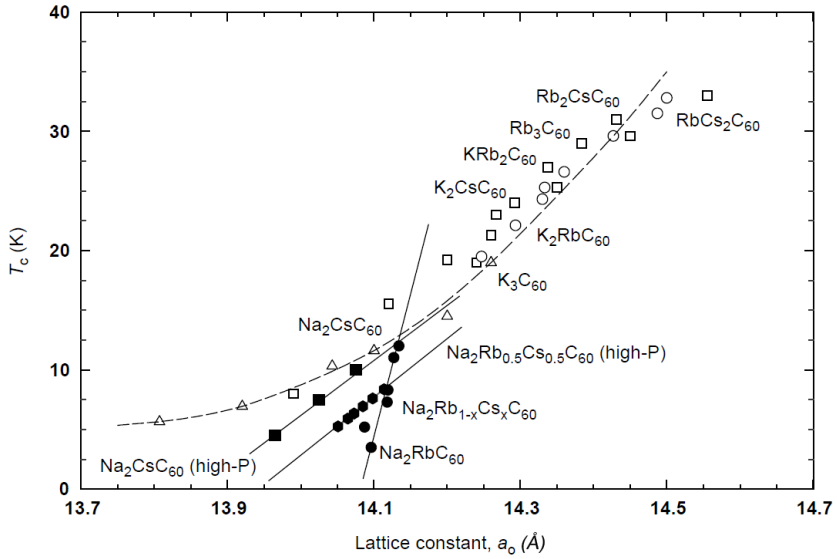

Figure 3.10: Variation of T_c with lattice parameter for various compositions of A_3C_{60} and $Na_2A'C_{60}$ (A' = Rb, Cs). The dotted line is the T_c-a relationship expected from BCS theory using $N(\varepsilon_F)$ values obtained by LDA calculations, the straight lines are guide to the eye [185, 189].

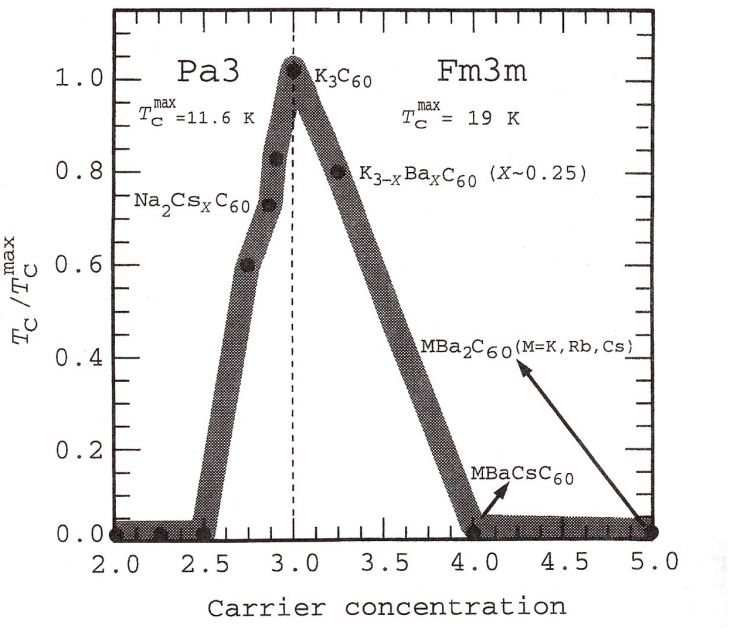

Figure 3.11: $T_c/T_{c_{max}}$ versus conducting electron concentration n in fulleride superconductors. Here T_c is scaled by the values of the end members Na_2CsC_{60} and K_3C_{60}. The heavy line is a guide for the eye [188].

Table 3.1: Solid state structures and superconducting transition temperatures for fullerene-based superconductors [190].

Compound	Structure	T_c, K
	Alkali	
Li_2CsC_{60}	$fcc(Fm\bar{3}m)$	12
K_3C_{60}	$fcc(Fm\bar{3}m)$	19.5
K_2RbC_{60}	$fcc(Fm\bar{3}m)$	23 , 21.8
K_2CsC_{60}	$fcc(Fm\bar{3}m)$	24
KRb_2C_{60}	$fcc(Fm\bar{3}m)$	27 , 24
Rb_3C_{60}	$fcc(Fm\bar{3}m)$	29.5
Rb_2CsC_{60}	$fcc(Fm\bar{3}m)$	31.3 , 31
$RbCs_2C_{60}$	$fcc(Fm\bar{3}m)$	33
Cs_3C_{60}	—	40 (at 12 kbar)
Sodium-containing		
$NaKC_{60}$	sc $(Pa\bar{3})$	2.5
$NaRbC_{60}$	$sc(Pa\bar{3})$	2.5 , 3.5
$NaCsC_{60}$	$sc(Pa\bar{3})$	12 , 10.5
$Na_2Rb_xCs_{1-x}C_{60}$	$sc(Pa\bar{3})$	3-12
Alkali/alkaline-earth		
$K_{3-x}Ba_xC_{60}$	$fcc(Fm\bar{3}m)$	15 ($x = 0.25$)
Rb3-xBaxC$_{60}$	$fcc(Fm\bar{3}m)$	24 ($x = 0.5$)
$K_3Ba_3C_{60}$	$bcc(Im\bar{3})$	5.6
$Rb_3Ba_3C_{60}$	$bcc(Im\bar{3})$	2
Alkaline-earth		
Ba_4C_{60}	$bcc(Immm)$	7
Sr_6C_{60}	$bcc(Im\bar{3})$	4
Ca_5C_{60}	$sc(Pa\bar{3})$	8.4
Rare-earth		
$Yb_{2.75}C_{60}$	Orthorhombic	6
Sm_3C_{60}	Orthorhombic	8
Ammonia-containing		
$Na_2Cs(NH_3)_4C_{60}$	$fcc(Fm\bar{3}m)$	29.6

3.3 Ferromagnetism

A compound which is worth mentioning in the section of metal intercalated fullerenes, is a "charge transfer" complex $[TDAE^+]C_{60}^-$ (TDAE – tetrakis(dimethylamino)ethylene), synthesized by Wudl et al. [191] and exhibiting unique solid-state properties. It undergoes a transition to ferromagnetic state at $T_c = 16.1$ K. $[TDAE^+]C_{60}^-$ has a C-centered monoclinic unit cell [192] with dimensions $a = 15.85$ Å, $b = 12.99$ Å, $c = 9.97$ Å and $\beta =$

93.3°. The intermolecular contacts along c are less than, or comparable, to those of alkali metal doped superconductors A_3C_{60}. This short separation suggests the formation of a conduction band which is partially filled [193]. The pronounced structural anisotropy implies a fairly low-dimensional band structure.

Part III

General methods

4 Measurements

4.1 Single-crystal X-ray diffraction

The experimental intensity data of the single crystals were collected with a Smart APEX I diffractometer (Bruker AXS, Karlsruhe, Germany, Mo-K_α radiation, λ = 0.71073 Å) and a dual wavelength three circle single crystal diffractometer - Smart APEX II (Bruker AXS, Karlsruhe, Germany) equipped with a CCD-detector, a Siemens X-ray sealed tube (Mo-K_α radiation, λ = 0.71073 Å), an Incoatec (Geesthacht, Germany) microfocus X-ray source IμS (Cu-K_α radiation, λ= 1.54178 Å). The cooling was provided either by Cryostream 700 plus system (Oxford Cryosystems, Oxford, United Kingdom, (80-500 K)) or by the N-Helix low temperature device (Oxford Cryosystems, Oxford, United Kingdom (28-300 K)). Because of the light elements contained in all the structures, almost all crystals were measured with both radiation sources, molibdenum and copper. The X-ray beam of the copper-source was generated with Incoatec IG150 and monochromatized by using a Montel optic monochromator (Incoatec, Geesthacht, Germany). The collection and reduction of data were carried out with the Bruker Suite software package [194]. Intensities were corrected for absorption effects applying a semi-empirical method [195]. The structures were solved by direct methods and refined by full-matrix least-squares fitting with the SHELXTL software package [196]. Hydrogen atoms were inserted as "riding atoms" geometrically and refined together with the "heavy" corresponding atoms.

Refinement was performed till converging the residual factors, on basis of which the quality of the model can be judged, or "R-factors". The unweighted R-factor was calculated as:

$$R_1 = \frac{\Sigma \mid\mid F_0 \mid - \mid F_c \mid\mid}{\Sigma \mid F_0 \mid}.$$

The weighted R-factor as:

$$wR_2 = \sqrt{\left[\frac{\Sigma w(F_0^2 - F_c^2)^2}{\Sigma w F_0^2}\right]^{1/2}}.$$

The weighing factor w is individually derived from the standard uncertainties of the

measured reflections and expresses the confidence in every single reflection.

4.2 Powder X-ray diffraction

Powder X-ray diffarction was performed for samples sealed in capillaries under argon on a "STOE" Cu-PSD1 diffractometer (Position Sensitive Detector, $\lambda = 1.54178$ Å, angle range 35°, resolution $\triangle 2\theta = 0.15°$) for fast routine measurements and a "Bruker" "AXS D8 Advance" diffractometer for high resolution powder diffractograms (Cu-Kα_1, Ge(111)-Johanson monochromator, Debye-Scherrer geometry).

4.3 UV/Vis/NIR spectroscopy

UV/Vis/NIR spectra were recorded on a "Lambda 19" "Perkin-Elmer" spectrophotometer.

4.4 EDX analysis

Elemental composition of the samples was determined on an EDX-system ("EDAX", Traunstein-Neuhof) with a S-UTW-Si(Li) detector and an integrated electron microscope. The samples were prepared in the glove-box and transferred in a special sluice into the electron microscope.

4.5 Digital microscope

Single crystals were examined and their photographs were made on a "VHX" "Keyence" digital microscope.

4.6 Magnetic measurements

Magnetic measurements of powder samples were performed on a "Quantum Design" "MPMS XL" magnetometer (sample holder - suprasil ampoule; magnetic field - 0.1 T, 1 T and 7 T) and on a "Quantum Design" "MPMS SQUID VSM" magnetometer - for single crystalline samples (sample holder - quartz ampoule in brass sample holder).

4.7 Quantum chemical calculations

Quantum chemical calculations were performed using the DFT method of B3LYP/6-31G with Gaussian 03 [197].

Part IV

Special part

5 Choice of method of synthesis

Several methods of synthesis were checked before a suitable one was found.

At first, the solid state synthesis was considered, using alkali metal azides as source of metal (as described elsewhere for the synthesis of alkalioxometallates along the azide-nitrate route [198]). Pellets of ground C_{60} fullerene and potassium azide, taken in respective amounts for stoichiometry desired, were prepared on air, enclosed into a special silver container allowing the nitrogen evolved during decomposition to escape, and annealed at a special temperature program in a furnace, the furnace being under argon flow. The temperature and time of annealing was chosen in a way for allowing decomposing the metal azide, and reacting the *in situ* formed metal with fullerene. Afterwards, the solid was removed under argon flow from the container after cooling, ground and sealed into capillaries under argon for powder X-ray diffraction measurements. It was possible to determine the composition for some samples (Appendix A, Fig. 8.1), but no reproducible results could be obtained at all.

Next, a synthesis of $C_{60}^{\cdot -}$ species in solution was reproduced [199]. The experiment consisted in mixing C_{60} powder with excess of Zn powder and KOH pellets (NaOH in [199]) in a flask under argon in a Schlenk line and adding THF. Neither of starting materials did dissolve in THF. Afterwards, water was added. NaOH pellets dissolved in water, but C_{60} and Zn pellets were suspended and aggregated at the interface of aqueous and organic layers. The reduction took place rapidly, and the red reaction product diffused into the THF layer, where it turned to dark red-purple. Subsequently, the red THF layer was separated from the colorless aqueous layer.

UV/Vis/NIR spectra of the solution were recorded, confirming the formation of $C_{60}^{\cdot -}$ (Appendix A, Fig. 8.2). Single crystals were grown. Admixtures of Zn were found on performing the REM/EDX analysis. Besides, time storing of the solution was limited by 3-4 weeks, the connections with grease being not hermetic enough for preventing from oxidation. The solution was contaminated, as well, by grease residues being dissolved at the connections by the solvent vapor (Appendix A, Fig. 8.3).

Therefore, "cleaner" conditions were necessary for performing the experiment and storing the products for a longer time. The "break-and-seal" technique was considered. The

two-phase system was changed only for one organic solvent, for avoiding using Zn and contamination of the product. For providing introducing the alkaline component, the approach used by Fässler was employed, based on complexing alkali metals with crown-ethers or cryptands [21, 22, 23].

6 Experimental: the "break-and-seal" technique

All experiments were conducted in all-glass apparatus sealed under vacuum equipped with breakseals and seal-offs (constrictions) in order to fulfill the high purity conditions required – the so-called "break-and-seal" technique [34, 35]. All starting compounds were purified as follows in the corresponding paragraphs prior to use.

The solvents – tetrahydrofurane ("Carl Roth", $\geq$ 99.9 %, $H_2O \leq 50$ ppm), *n*-octane ("Alfa Aesar", 98+ %), dimethoxyethane ("Reagentplus", $\geq$ 90%), in future "THF", "octane" and "DME", respectively, were distilled and refluxed over sodium under argon for 3 h, THF being additionally refluxed at first over potassium hydroxide for 3 h. The purified solvents were degassed by the "freeze-thaw-pumping" technique, never exposed to air, distilled under vacuum and sealed into ampoules over Na/K alloy. Crown-ethers (dibenzo-18-crown-6, "Acros Organics", $\geqslant$98 %; dibenzo-24-crown-8, "Fluka", $\geqslant$98 %) were recrystallized from octane.

Picking of single crystals was performed on air under oil or in the glove-box. Crystals were stable on both conditions.

Subsequent manipulations (filling capillaries for powder X-ray diffraction or sample preparation for SQUID measurements) was carried out in the glove-box.

6.1 Preparation of solvents

The sealing of the solvents into ampoules is schematically shown in Fig. 6.1. A 500 ml flask *A*, with dried and distilled THF (250 ml), was connected through a stopcock to the vacuum line and an empty ampoule *B* equipped with a breakseal and a constriction. The solvents were degassed using the freeze-thaw-purging technique.

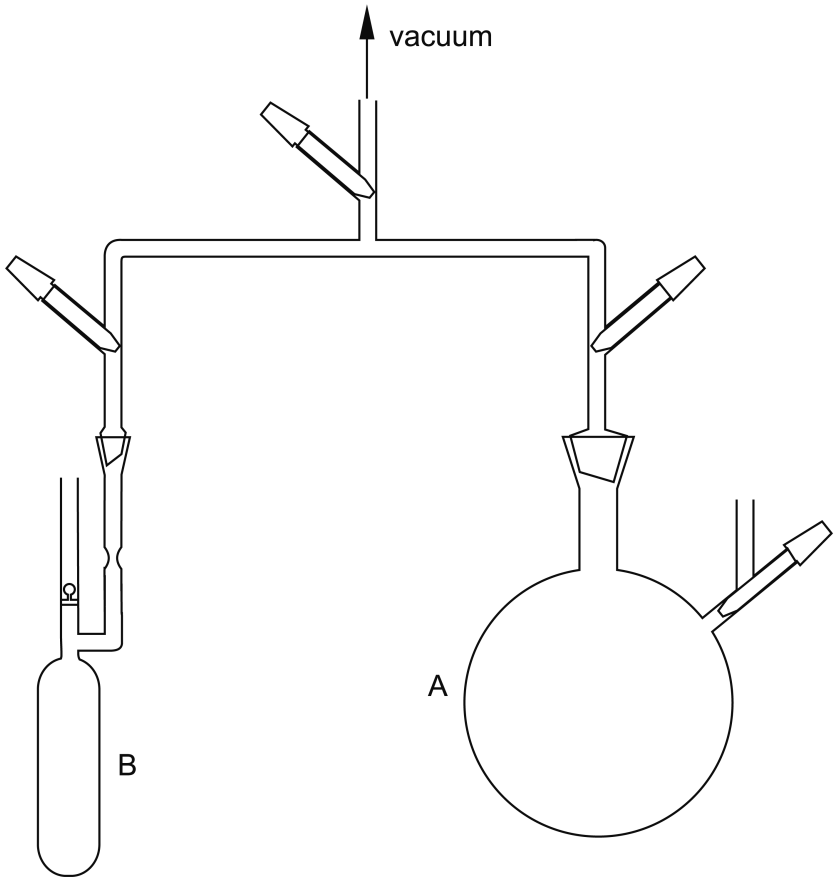

Figure 6.1: Apparatus for sealing solvents into ampoules over Na/K alloy.

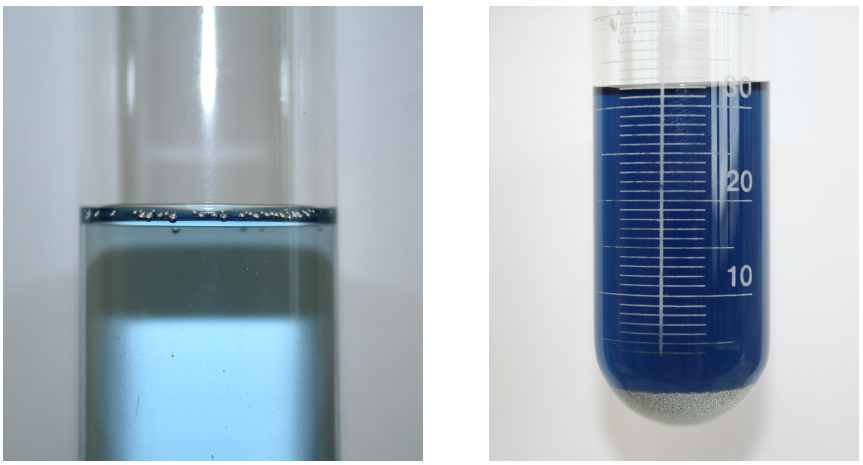

(a) Tetrahydrofurane (b) Dimethoxyethane

Figure 6.2: Characteristic blue color of THF and DME sealed into ampoules under vacuum over Na/K alloy induced by the formation of solvated electrons.

The Na/K alloy was prepared. For this purpose, pieces of metallic Na ("Merck", cubes under protective liquid for synthesis) and K ("Merck", cubes under protective liquid for synthesis) with 1:3 mass ratio were placed in a 50 ml round bottom flask under argon flow. They were molten by gentle heating (60-70 °C). After the alloy has been formed, it was let cooling to room temperature under argon flow.

After this, the alloy was rapidly transferred into the ampoule *B* through the connection with a pipette, purged several times before this with argon. The solvent was condensed from *A* by cooling *B* in liquid nitrogen. The ampoule *B* was sealed off at the constriction. THF got blue with time with the alloy because of the generation of solvated electrons (Fig. 6.2).

6.2 The glassware for fullerides synthesis in solution

The glassware for fullerides synthesis in solution is shown on Fig. 6.3. Connected to the vacuum line and prior to use, it was thoroughly checked for possible leakages with the high frequency spark vacuum-tester (Fig. 6.4) and heated under dynamic vacuum.

Below a typical synthesis in THF is described.

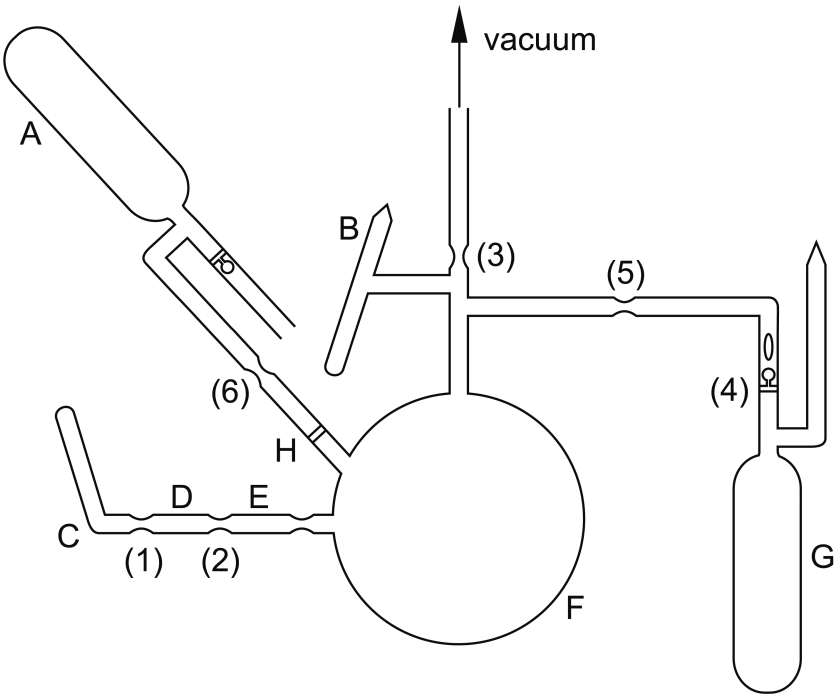

Figure 6.3: Scheme of the glassware for synthesis in solution.

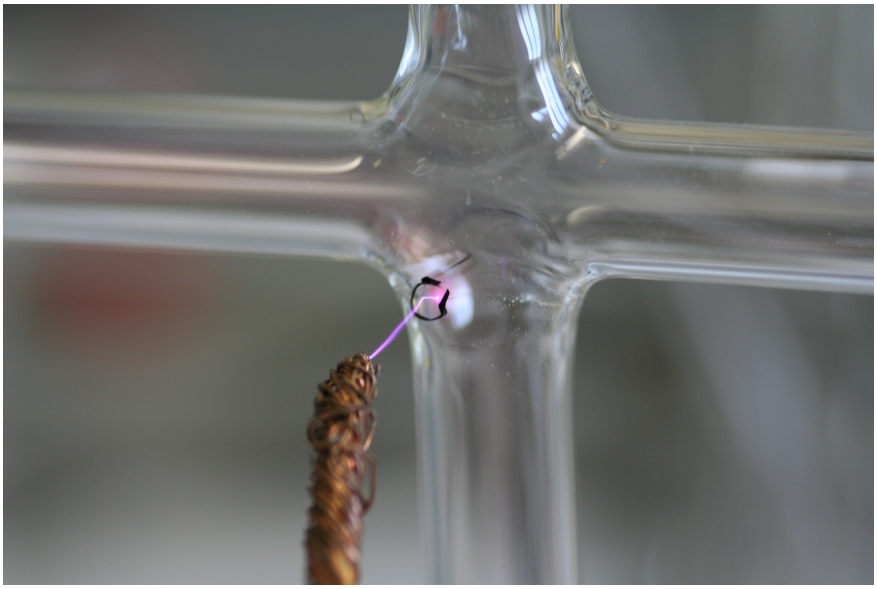

Figure 6.4: Microleakage in glass easily visible with the spark-vacuum tester under dynamic vacuum.

Commercially available C_{60} was ground and placed in the ampoule *A*. Equimolar amount of recrystallized crown-ether was placed into *B*. The open tubes through which the compounds have been introduced were sealed, the glassware evacuated and heated carefully with "cold" flame under dynamic vacuum. The glassware was checked for leakages again. The system was flown with argon, and a piece of metallic potassium (excess) was placed into *C* under argon flow. All open parts of the system were sealed and the glassware was evacuated (1×10^{-3} mbar).

Potassium was distilled three times by gentle heating of the glass from *C* to *D*, from *D* to *E*, and, finally, from *E* to *F*, the first two steps followed by subsequent sealing off at the constrictions *(1)* and *(2)*. A silver-violet potassium "mirror" was formed on the internal surface of *F* (Fig. 6.5). The system was sealed off from the vacuum at the constriction *(3)*. The ampoule with THF (30 ml) over Na/K alloy was cooled in liquid nitrogen for decreasing the vapor pressure inside (general procedure for the future before breaking a breakseal on the way to an ampoule containing a solvent or a solution), and the breakseal *(4)* was broken. THF was distilled into *F* by gentle chilling with liquid nitrogen. The constriction *(5)* was sealed off.

Some THF was condensed in *B* by cooling it with liquid nitrogen, and the crown-ether in *B* was dissolved. The solution of the crown-ether in THF was poured from *B* to *F* by inclining the system and shaked gently for 1-2 min. During this time the colour of THF

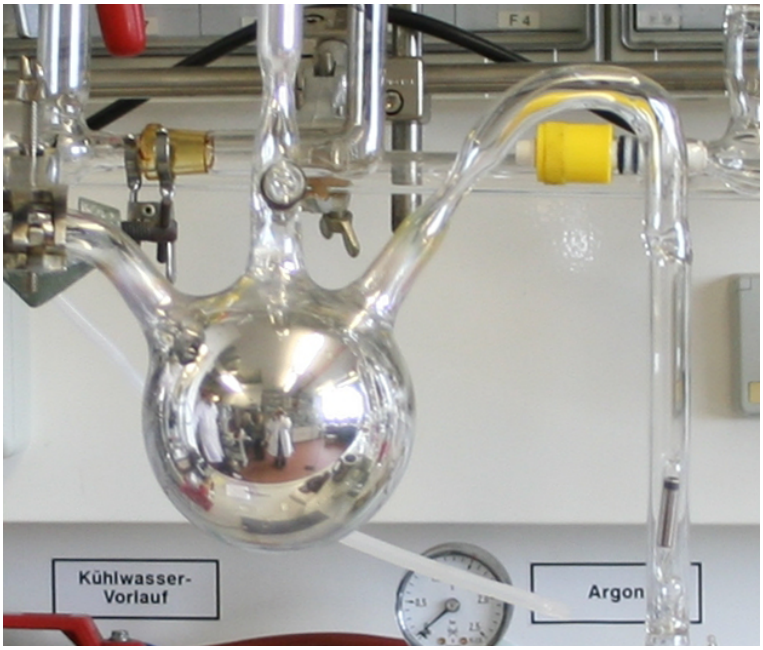

Figure 6.5: Potassium “mirror”.

changed from blue to yellowish. (Note that the solvent must be cold while it is known that crown-ethers are being slowly decomposed by potassium [200]).

The glassware was inclined, and the resulting solution mixture was filtered from the possible potassium residues in the solution through a glass filter № 3 H into the ampoule A by chilling it with liquid nitrogen. The constriction *(6)* was “washed” with solvent by chilling the constriction with liquid nitrogen (general procedure before sealing off a constriction through which a solution was overflown) and sealed off. On warming to room temperature and shaking the solution in A got reddish-black.

The scheme of the glassware for filtering the solution and its separation into small individual ampoules is presented in Fig. 6.6.

It consists of the ampoule with the solution, A, equipped with a breakseal and a magnet inside, a glass filter, an ampoule with a breakseal into which the solution should be filtered and small ampoules C_n. The system was checked for leakages, heated under vacuum and sealed off from the vacuum line at the constriction *(1)*. The ampoule A was cooled in liquid nitrogen, the breakseal *(2)* was broken, and the solution was filtered from A to B by cooling B with liquid nitrogen and gently warming up A, if necessary. The small ampoules C_n were filled with solution one after another; the constrictions were washed by condensing the solvent on chilling, and sealed off.

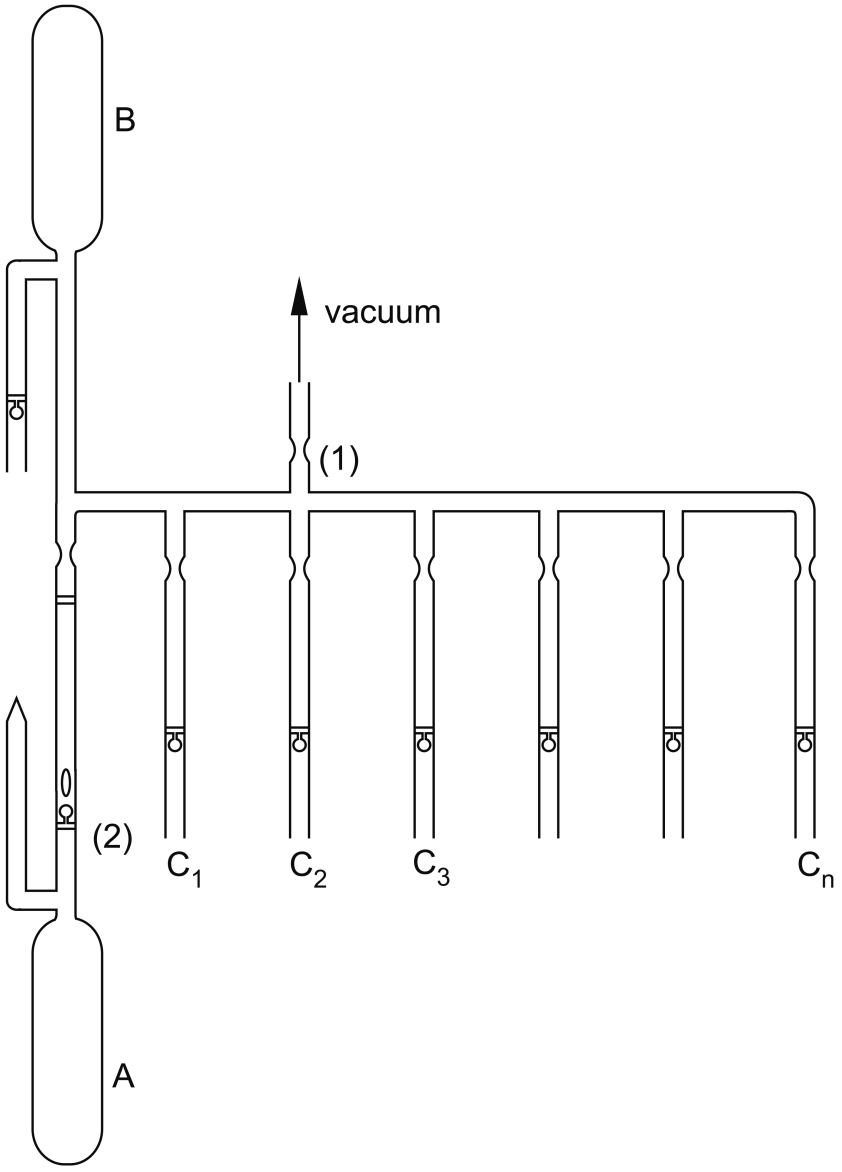

Figure 6.6: Scheme of the glassware for filtering the solution and its separation into small individual ampoules.

6.3 Crystallization

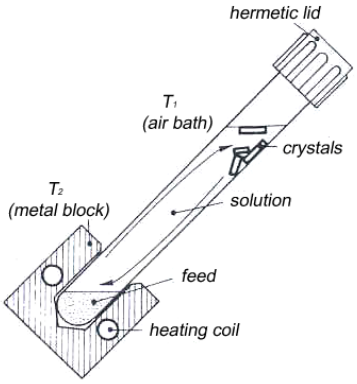

Figure 6.7: Crystallization by the "temperature difference method" [201].

The "temperature difference method" [201, 202, 203, 204] was used for crystallization.

This method consists in growing single crystals in a glass vessel having small temperature gradient ($\triangle T = 1 - 5$ K) between the bottom of the vessel which is heated and its upper part exposed to air. A saturated solution is placed into it with a small excess of solid at the bottom (Fig. 6.7). The solution, rising by natural convection, becomes supersaturated, and begins to form nuclei spontaneously.

The method is most suitable for solvents yielding a moderate solubility (in the range of 5 to 30 wt. %) [204]. The tube diameter and the angle of inclination influence the convection rate, too, as well as the shape of the glass (e.g. round or rectangular).

Fullerides have very good solubilities in THF or DME, one drop is mostly enough to dissolve completely single crystals. The solutions obtained in THF or DME during the experiment described previously are far below from their saturation limit, which is restricted by the experiment performance. These reasons taken into account, some modifications were made for crystallization by the temperature difference method. Besides, no solid "feed" could have been present prior to crystallization in the solution. The problem of good solubility of fullerides, preventing crystallization, was solved by adding a second, "poor" (nonpolar) solvent for the fullerides, to the solution. After considering the miscibility of the two solvents (good and poor), changes in solubility and, very important, means of purification and highest possibly purity achievable, and after test experiments, n-octane was chosen as the second, poor, solvent. One of the advantages, as it turned later, was that it would not include into the crystal structure of the crystals formed at all, unlike THF or DME.

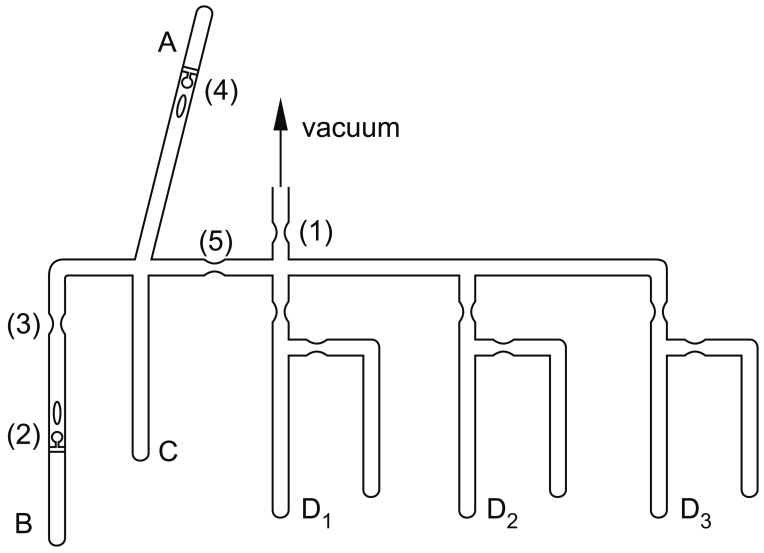

Figure 6.8: Scheme of the glassware for the preparation of the solution for crystallization.

As the solution would still be much diluted for giving crystals, and much of the solvent needed to be just "evaporated", and not "convected", the vessel for crystallization has been modified: a two-thigh ampoules where used instead, one thigh being inserted into a moderately heating furnace, and the other being exposed to air. In such a way, the "convected" solvent was gradually removed from the solution and condensed in the second, colder thigh. During crystallization, the good solvent, which was always the solvent with lower boiling point in comparence with octane, would evaporate, thus leading to very slow gradual change of the volume ratios of the good and poor solvents for fullerides, at some point leading to spontaneous crystallization.

The glassware for crystallization (Fig. 6.8) consists of an ampoule with fulleride solution, A, an ampoule with octane, B, both equipped with breakseals, a vessel for mixing the solution and the solvent, C, as well as ampoules for crystallization, D_n. After all the glassware has been checked for leakages and heated under vacuum, it was sealed off from the vacuum line at the constriction *(1)*. B was carefully cooled with liquid nitrogen, the breakseal *(2)* was broken, and octane was condensed into C by chilling it with liquid nitrogen. (Typically, the amount of condensed octane equaled to $\frac{1}{4}$ or less of the volume of the fulleride solution, otherwise a precipitate was formed after mixing THF solution and octane). B was then sealed off at *(3)*. A was carefully chilled with liquid nitrogen, the breakseal *(4)* was broken, and the solution was poured into C[1]. The mixture in C

[1]The reverse sequence would also work: first break the breakseal *(4)*, pour the solution from A into C, and then condense octane on it.

was shortly mixed and transferred to the right-hand part of the glassware. The constriction *(5)* was washed with solvent by chilling and sealed off. The mixture was divided into ampoules D_n, each of them was subsequently sealed off after the constrictions being washed with solvent.

The ampoules prepared as described above were placed (Fig. 6.9) with one thigh A into a programmable furnace (angle of inclination ca. 30 degrees), the other, B, being left at room temperature, the temperature difference between the two edges being 2-3 degrees. Within 2-3 days dark violet-reddish crystals were formed on the walls of the ampoules in the remaining solvent mixture in A. A was sealed off at the constriction *(1)*.

Time of crystallization could take from some days to weeks, depending on the volume of the solution. The temperature difference in most cases was kept 2 - 4 degrees, inclination of the ampoule - 30° - 40°.

After 2 or 3 days in furnace, the ampoules were regularily checked for crystal formation. Must be noted that even during this short time of checking, 1-2 min, if done under the microscope, part of the solvent from B could evaporate back to A because of the equal temperature on both thighs, A and B, what could lead to partial damage or complete dissolution of the crystals. The check must be performed as fast as possible. For avoiding solvent condensation in A during this procedure, B can be cooled slightly in liquid nitrogen (only for few seconds, while "long" cooling can damage the crystals formed, as well).

The constriction *(1)* was sealed after fine crystals (at least optically) having formed. By this point, the solvent from A could have evaporated completely or still remained, as a colored solution or colorless solvent. It was noticed that crystals picked from a "dry" ampoule were more fragile than the ones picked from solution, but it didn't lead to differences in the crystal structures for different crystallizations performed with the same solution.

It is important not to exceed the volume of condensed octane (in a typical experiment, 1-2 mL of octane were added to 6 mL fulleride solution) and keep in mind that the solvents used here shrink on cooling. If too much octane is added (what can be unfortunately seen only after melting of the cooled mixture), a precipitate is being formed, and there is no way of redissolving it again or recovering something. If crystals of poor quality are formed, when checked under the microscope directly in the sealed ampoule, they can be redissolved with pure solvent by pouring it from B to A and putting the ampoule into the furnace with the thigh A again. Such a repetition of crystallization very often would lead to crystal formation, again.

Sometimes a precipitate is being gradually formed during crystallization instead of

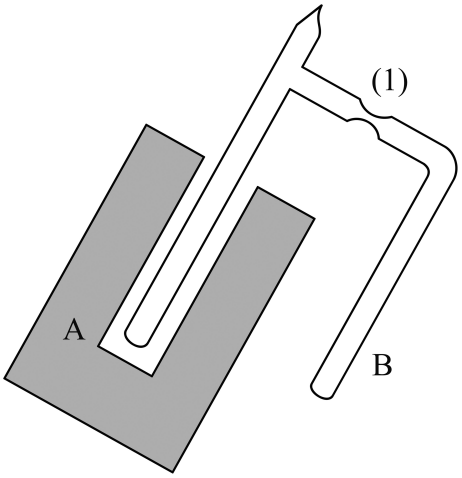

Figure 6.9: Crystallization by the "temperature difference" method.

crystals, on the walls or bottom of the thigh *A*. If the solution still remains colored, i.e. not all fullerides were precipitated, the solution could be decanted from *A* to *B* and put into the furnace with the thigh *B*. This would also often lead, nevertheless, to crystal formation, too.

6.4 Picking and mounting of single crystals for single crystal X-ray diffraction measurements

During the course of the experiments, crystals of different morphologies have been obtained, depending on the system studied and crystallization conditions. A common feature for all of them is reddish-black color, rather fragile, often intergrown and thin in one direction (plateletes).

For the single-crystal X-ray diffraction measurements "big" crystals often turned out to be intergrown single crystals (or twins), and when smaller "single" crystals were picked, they were too thin in this one direction.

The ampoules with crystals in solution were opened in air or in the glove-box, and the crystals were placed into immersion oil type NVH rapidly. The crystals were picked with a nylon cryo-loop and were placed directly to the single-crystal diffractometer.

7 New fullerides obtained

7.1 [K(DB24C8)(DME)]$_2$C$_{60}$·(DME)

7.1.1 Synthesis

48.2 mg (6.9×10^{-5} mol) of ground C_{60} have been reacted with 93.0 mg (20.8×10^{-5} mol) of dibenzo-24-crown-8 (DB24C8) and excess of metallic potassium in form of potassium mirror in 30 ml of dimethoxyethane (DME) in order to obtain C_{60}^{3-}-based fulleride as can be expected from the reaction scheme:

$$K_{ex.} + DB24C8 \stackrel{DME}{\longrightarrow} [K(DB24C8)]^+e^-$$

$$3K(DB24C8) + C_{60} \stackrel{DME}{\longrightarrow} [K(DB24C8)^+]_3C_{60}^{3-}.$$

Unexpectedly, already 2 days after performing the experiment, before applying the "temperature difference" crystal growth technique, big red-brown thin platelet-like crystals were observed at the bottom of the ampoule where it was stored, the solution still remainig with its original intense color. The solution was filtered in vacuum and crystals were picked from the precipitate on air under oil. Octane was added to the filtrate, the mixture obtained was subjected to the temperature difference method crystallization. No crystals were obtained after such treatment.

7.1.2 Crystal structure determination

The crystals picked from the precipitate were mounted on the single crystal diffractometer, quenched to 100 K and measured at 100 K with graphite-monochromated $Mo_{K\alpha}$ radiation (λ = 0.71073 Å). Measurement with Cu-radiation has been performed, too, but its quality was not better than of the one with Mo radiation. The crystallographic parameters are presented in Tab. 7.1 and in the Appendix A.

The systematic extinctions observed (*hkl*: $h + k = 2n$; and *h0l*: h, $l = 2n$) made the two space groups Cc (no. 9) or $C2/c$ (no. 15) possible, from which $C2/c$ has turned out to be the correct one during structure refinement.

Table 7.1: Crystallographic parameters for $[K(DB24C8)(DME)]_2C_{60}\cdot(DME)$.

Empirical formula	$C_{120}H_{94}K_2O_{22}$
T / K	100(2)
Formula weight	1966.15
Crystal system	monoclinic
Space group (no.), Z	$C2/c$ (15), 4
a / Å	31.133(4)
b / Å	15.1271(18)
c / Å	21.433(3)
β / °	117.506(2)
V / Å^3	8953.1(19)
Diffractometer	Smart Apex II
X-ray radiation, λ / Å	Mo-K_α, 0.7103
Density (calculated) / mg/m^3	1.459
Absorption coefficient / mm^{-1}	0.190
θ range for data collection / °	1.47 to 25.66
Reflections collected	33955
Independent reflections	8459 ($R_{int} = 0.0655$)
Parameters	748
Restraints	0
R_1 ($I > 2\sigma(I)$)	0.0576
wR_2 ($I > 2\sigma(I)$)	0.1503
R_1 (all data)	0.0967
wR_2 (all data)	0.1802
Wavelength, Å	0.71073
CCDC-no.	735151

The structure was solved in the Shelxtl program by direct methods and refined with standard difference Fourier and "least squares" techniques. All the atomic positions (potassium and crown-ether), except for fullerene, could be taken from the structure solution. The benzene rings of the crown-ethers were not fixed and were refined freely. The missing carbon atoms were found from subsequently calculated difference Fourier maps. For C_{60}, the individual atomic positions could not be identified. However, from the space filling and the difference Fourier map followed, that the C_{60} unit must be located around a special position (Wyckoff position $4e$ (0, y, $\frac{1}{4}$)) in a disordered manner, y being calculated to be ca. 0.5. As a result, it is not possible to find an ordered structure model for the fullerene in the space group $C2/c$.

In an alternative description, the structure was refined in Cc assuming twinning with the twofold axis as the twinning element. A manual transformation of the data to the Cc space group was performed by doubling the atomic coordinates of crown-ether, metal

and solvents and "inverting" the atomic coordinates for half of them. As to C_{60}, the coordinates have been left unchanged as appearing in the atomic list in $C2/c$. The occupancy for the carbon atoms of C_{60} was set to 1.0.

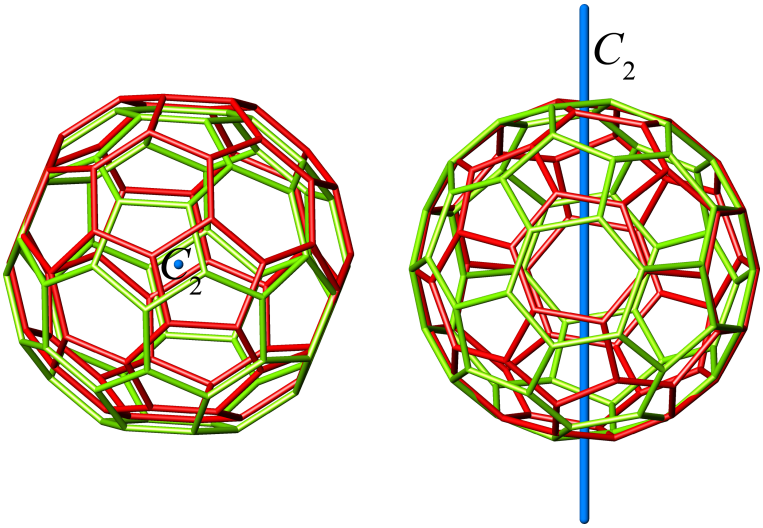

Figure 7.1: Two orientations of the C_{60} molecule in the crystal connected by the rotation about a C_2-axis in space group $C2/c$.

Same procedure was done for the second possible orientation of C_{60} (found in $C2/c$ (Fig. 7.1)). Atomic coordinates of the second possible orientation of C_{60} were calculated according to the following transformation:

$$\begin{pmatrix} x \\ y \\ z \end{pmatrix} \Rightarrow \begin{pmatrix} -x \\ y \\ \frac{1}{2} - z \end{pmatrix}.$$

However, no improvement of the fit between observed and calculated structure factors was obtained, confirming that the disorder is local and static. No indications on the preference of any of the two space groups considered was observed during refinement, hence, the solution in $C2/c$ was chosen to be the true one as the highest in symmetry.

For the final structure refinement strategy, the centrosymmetric space group $C2/c$ was chosen. All non-hydrogen atoms, including the carbon atoms of the fullerene, were refined independently and treated with anysotropic displacement parameters, without any restraints or constraints. The occupancies of carbon atoms of the fullerene were set to 0.5 because the symmetry operations for $C2/c$ generate two orientations on one site, which are connected by the rotation about a C_2-axis (Fig. 7.1). Afterwards, the positions of the hydrogen atoms were calculated geometrically, their isotropic displacement parameters

were restrained to 1.2 times the value of the respective attached carbon atom, and all non-hydrogen atoms were treated with anisotropic displacement parameters, including the carbon atoms of fullerenes. Correlations between the atomic coordinates and the displacement parameters of the carbon atoms within the fullerene could be avoided by separate refinement in blocks.

7.1.3 Results and discussion

$[K(DB24C8)(DME)]_2C_{60}\cdot(DME)$ crystallizes in the monoclinic space group *C2/c* (no. 15) with four formula units. Potassium atoms are coordinated by the crown-ether as well as by one solvent molecule, building $[K(DB24C8)(DME)]^+$ cations (Fig. 7.2).

The crown-ether, being too large for potassium, is twisted around the K-atom, whereby all eight oxygen atoms of the crown-ether coordinate the potassium atom at distances 2.800(3), 2.808(3), 2.810(4), 2.817(4), 2.818(3), 2.833(4), 2.904(3) and 3.233(3) Å. Additionally, the metal atom is coordinated by two oxygen atoms of the solvent at 2.935(3) and 2.954(2) Å, the solvent molecule being in *cis*-conformation (Fig. 7.2 and Fig. 7.3, left). The structure contains two $[K(DB24C8)(DME)]^+$ units per fullerene, thus, the resulting charge of C_{60} being –2, and one additional solvent molecule (DME) which is not coordinated to potassium. This second DME molecule is "isolated" and is present in *trans*-conformation (Fig. 7.3, right). Fig. 7.4 shows the arrangement of the three building units within the unit cell.

The C_{60}^{2-} units are arranged in hexagonal layers parallel to the *ab* plane, forming distorted trigonal prisms (Fig. 7.5). The fulleride anions, and the potassium cations develop a pseudobinary topology which is reminiscent of the CdI_2 type of structure, where C_{60}^{2-} occupy the positions of cadmium, and potassium - those of iodine (Fig. 7.6). In this layered structure, fully occupied and vacant layers of octehedral sites alternate. Each C_{60}^{2-} anion is thus enclosed in an octahedron built of potassium centered complexes. The non-coordinated DME solvent molecules are located in the remaining octahedral voids (Fig. 7.4).

The C_{60}^{2-} anions were found to be statically disordered, due to their location on a special crystallographic position (4*e*: 0, *y*, $\frac{1}{4}$), with the orientation of the crystallographic and molecular C_2 axes not matching. This disorder can be best and fully described by two orientations related to each other by the crystallographic C_2-axis (Fig. 7.1). As stated in the experimental section, in a first step to localize the atoms of the fulleride anion a predefined C_{60} unit was imported as a rigid body.

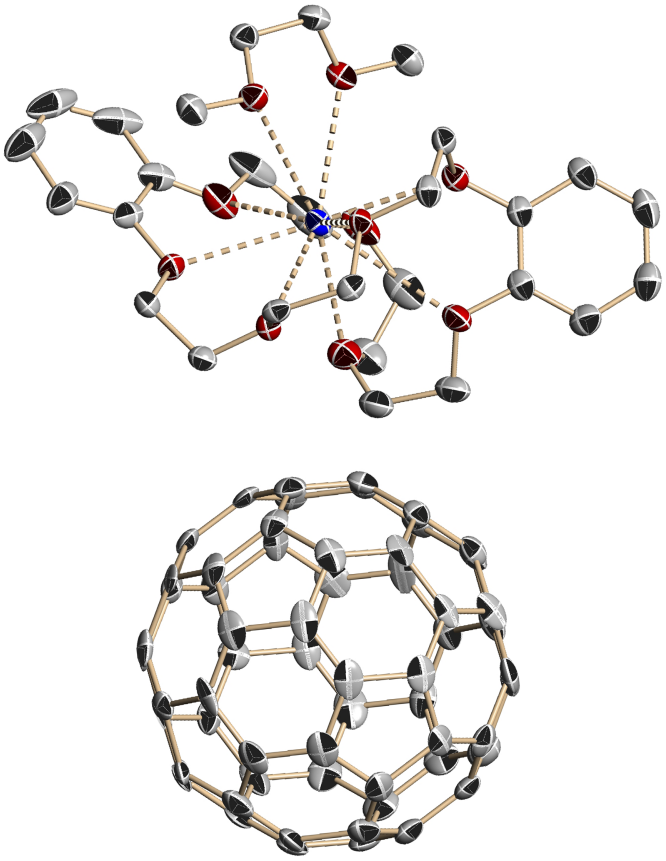

Figure 7.2: Fragment of the crystal structure showing the coordination of the potassium atom by one solvent molecule and crown-ether (dotted lines, above) together with one of two possible orientations of the next neighbouring fullerene (below). Displacement ellipsoids are drawn at the 50 % probability level, hydrogen atoms are omitted. Colour code: carbon (grey), oxygen (red), potassium (blue).

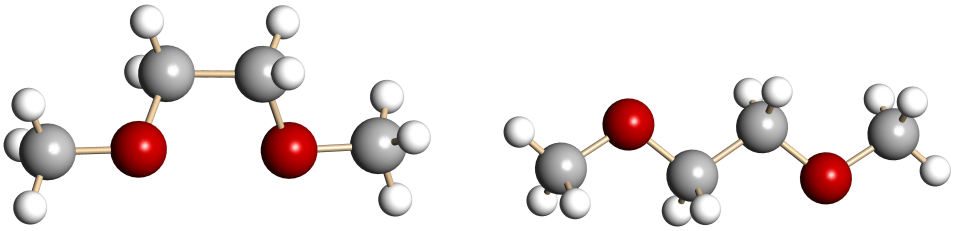

Figure 7.3: Two different conformations of the solvent in the crystal structure: DME which coordinates the potassium atom (left) and "isolated" DME (right).

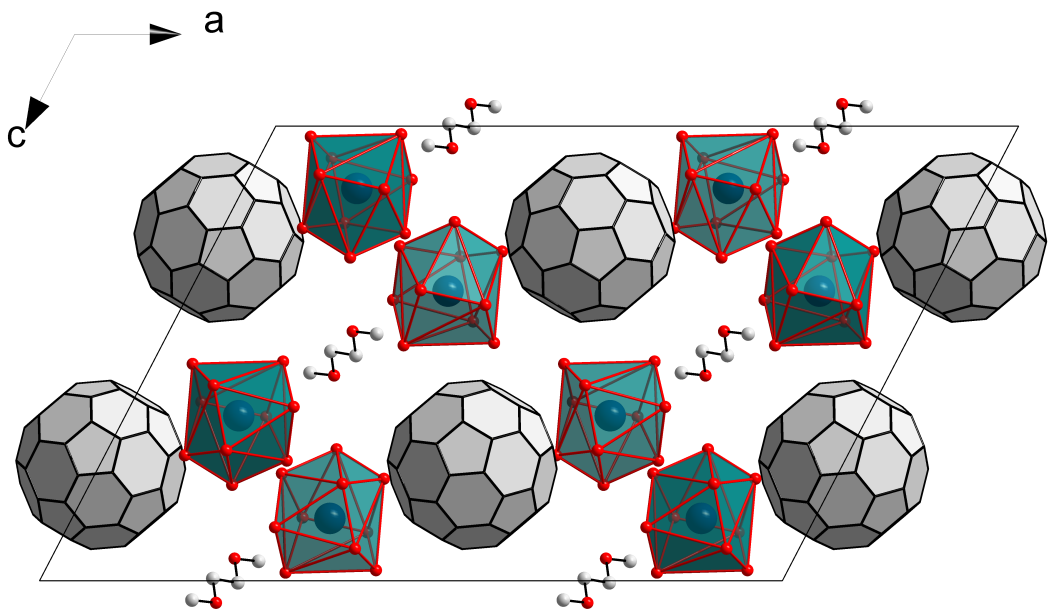

Figure 7.4: Projection of the crystal structure of $[K(DB24C8)(DME)]_2C_{60}$·DME along [010], with margins of the unit cell given. For clarity, only one orientation of the fullerene is displayed, the carbon atoms of the crown-ether and the DME coordinated to potassium are omitted. The coordination of potassium by 10 oxygen atoms (8 from DB24C8, and 2 from DME) is shown as a polyhedron.

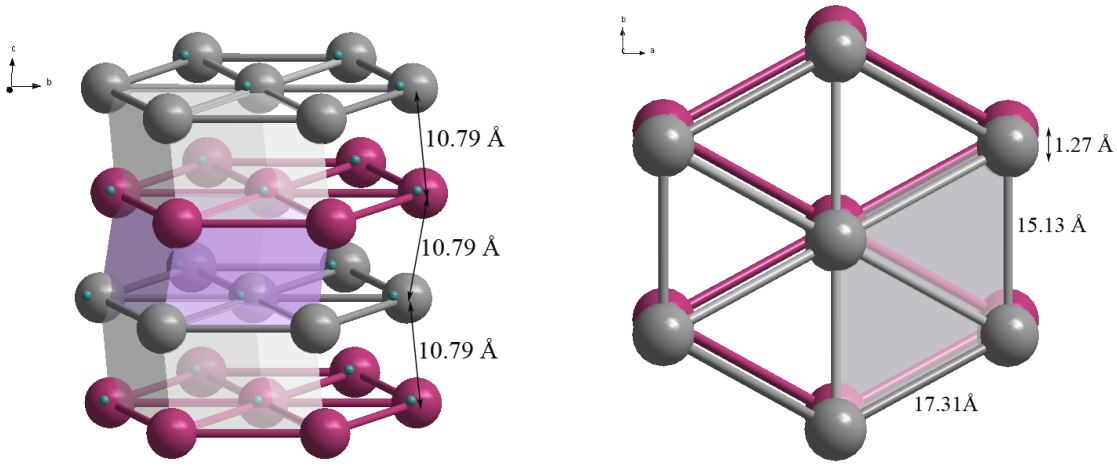

(a) (b)

Figure 7.5: Packing of the fullerene molecules, emphasizing the trigonal hexagonal primitive arrangement of C_{60}.

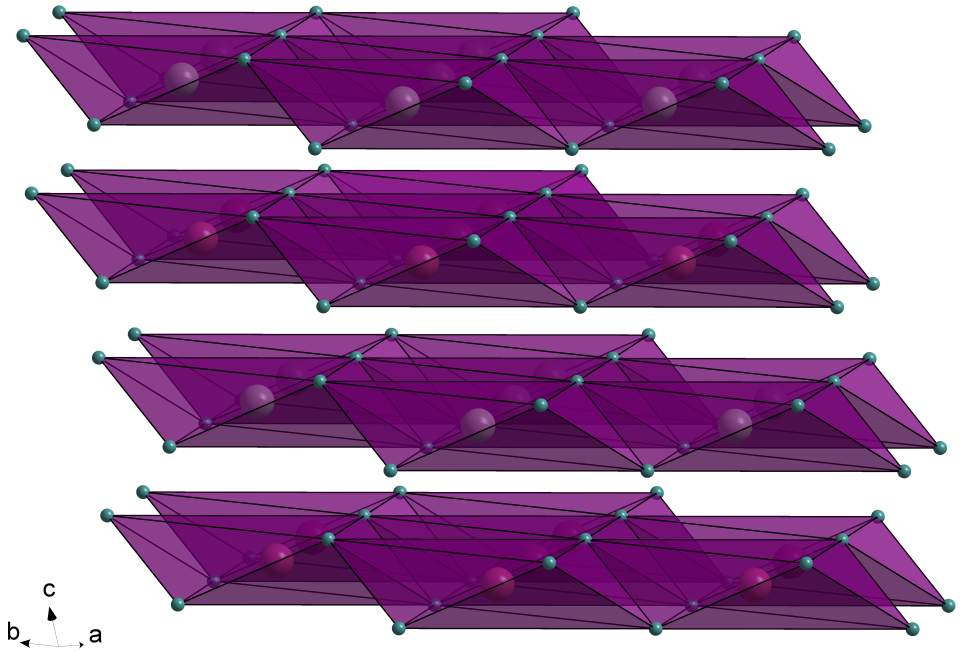

Figure 7.6: Polyhedral representation of K_2C_{60}, emphasizing the analogy to CdI_2.

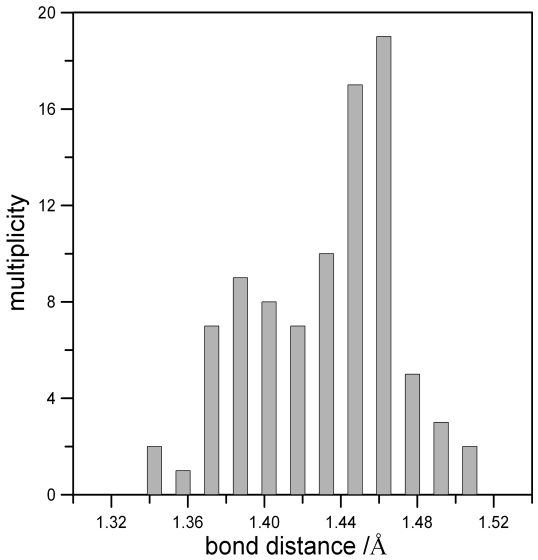

Figure 7.7: C-C bond length distribution within the fulleride anion C_{60}^{2-} in $[K(DB24C8)(DME)]_2C_{60}\cdot(DME)_2$.

Nevertheless, the refinement of the structure could be done without using any constraints and restraints. This has allowed to analyse the intramolecular fulleride bond distances, applying some sense of proportion, however.

In Fig. 7.7 a histogram is shown, representing the spread of the C-C distances in C_{60}^{2-}. One can clearly identify a dip in the distribution separating the shorter bonds between edge sharing hexagons [(6:6)-bonds] from those shared by hexagons and pentagons [(6:5)-bonds]. The frequency distribution of 1:2 fits well to the numbers of (6:6)-bonds (30) and the (6:5)-bonds (60) present.

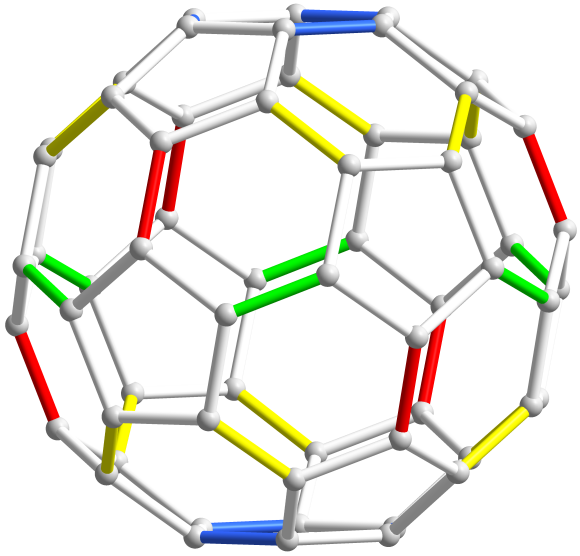

Figure 7.8: Positions of the symmetry inequivalent (6:6)-bonds in C_{60}^{2-} for the D_{3d} representation. The four different types are represented by different colours.

When examining the C-C bond lengths as determined for C_{60}^{2-} in $[Ba(NH_3)_7]C_{60}{\cdot}NH_3$ [14] with high accuracy, it has turned out that the C_{60}^{2-} displays a specific symmetry reduction from I_h to D_{3d} [205], just a minimal step needed for lifting the degeneracy of the t_{1u} orbital of the undistorted molecule. Thus, this has been the first observation of a static Jahn-Teller distortion in a C_{60}^{n-}- anion. The C-C bonds split up into four inequivalent types, which are represented in Fig. 7.8 by different colours (blue, yellow, red, green). In the case of $[Ba(NH_3)_7]C_{60}{\cdot}NH_3$, the red ones are elongated most, the yellow and green bonds in a moderate manner, and the blue ones are not significantly changed. This distortion pattern has been confirmed by HF and DFT type quantum chemical calculations, at the same time confirming an electronic singlet ground state

[205].

Table 7.2: Atomic C-C distances between two fused six-membered rings (6:6). For finding the correct orientation for the Jahn-Teller distorted $C_{60}{}^{2-}$ anion, the 30 6,6-bonds are colour coded according to the four different sets of bonding (red, yellow, green, blue) within the 10 possible orientations, given by the 10 three-fold axes passing through one C_{60} molecule.

Atomic contact		distance	1	2	3	4	5	6	7	8	9	10
C1M	C4M	1.3877										
C2M	C6M	1.3487										
C3M	C8M	1.4050										
C5M	C11M	1.3896										
C7M	C14M	1.4180										
C9M	C15M	1.4006										
C10M	C12M	1.3806										
C13M	C19M	1.4059										
C16M	C24M	1.4039										
C17M	C27M	1.3740										
C18M	C28M	1.3636										
C20M	C23M	1.3706										
C21M	C31M	1.3830										
C22M	C32M	1.4040										
C25M	C35M	1.3760										
C26M	C36M	1.4192										
C29M	C39M	1.3906										
C30M	C40M	1.4015										
C33M	C43M	1.3942										
C34M	C44M	1.3958										
C37M	C38M	1.3769										
C41M	C42M	1.4038										
C45M	C46M	1.3761										
C47M	C55M	1.3477										
C48M	C56M	1.4147										
C49M	C50M	1.3935										
C51M	C58M	1.3774										
C52M	C53M	1.3871										
C54M	C59M	1.3731										
C57M	C60M	1.3920										

Unfortunately the crystal structure analysis presented here is not of sufficient precision to directly allow identifying the distortion pattern. Therefore, the bond lengths of the four symmetry equivalent subsets in D_{3d} (Fig. 7.8) have been averaged for all ten possible orientations of the unique (three-fold) axis (Tab. 7.2). The result is summa-

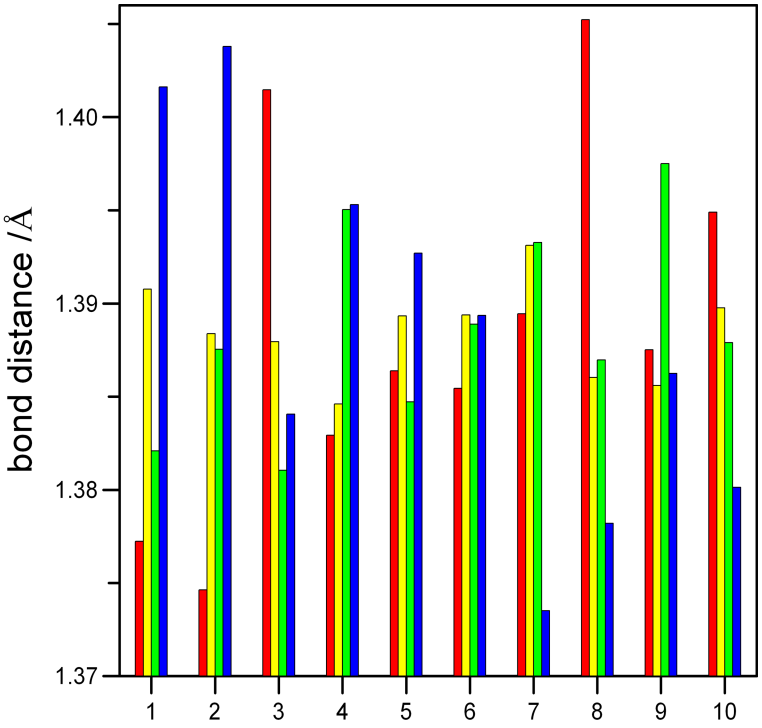

Figure 7.9: Average C-C bond distances between two condensed six-memebered rings (6:6), according to the colour code referring to the Jahn-Teller distortion, as a function of the 10 possible orientations, given by the 10 three-fold axes passing through one C_{60} molecule.

rized on Fig. 7.9. Indeed, there are two orientations (no. 3 and no. 8) that match the previous experimental and theoretical findings. The same situation was encountered in $[Mn(NH_3)_6]C_{60}{\cdot}6NH_3$ [17, 205]; it can be rationalized either by assuming an incoherent superposition of two orientations of the C_3 axis in the crystal structure or by assuming a lower point group symmetry D_{2h} which would be in full accordance with the overall distortion pattern since the orientations 3 and 8 are related by a twofold rotation axis. Such a symmetry reduction to D_{2h} is lifting the orbital degeneracy as well.

7.2 $KC_{60}\cdot(THF)_5\cdot(THF)_2$

7.2.1 Synthesis

150 mg (0.2×10^{-3} mol) of ground C_{60} have been reacted with 93.0 mg (0.2×10^{-3} mol) of dibenzo-24-crown-8 (DB24C8) and excess of metallic potassium in form of potassium mirror in 30 ml of tetrahydrofurane:

$$K_{ex.} + C_{60} + DB24C8 \xrightarrow{THF} KC_{60} + DB24C8.$$

The solution obtained was of a very intense "red wine" color. Almost all the amount of C_{60} reacted.

Octane was added to the solution (typically, 1.5 mL of octane to 6 mL of solution), and the mixture obtained was used for "temperature difference method" crystallization. In the course of 7 to 12 days, black needle-like crystals were obtained (Fig. 7.10).

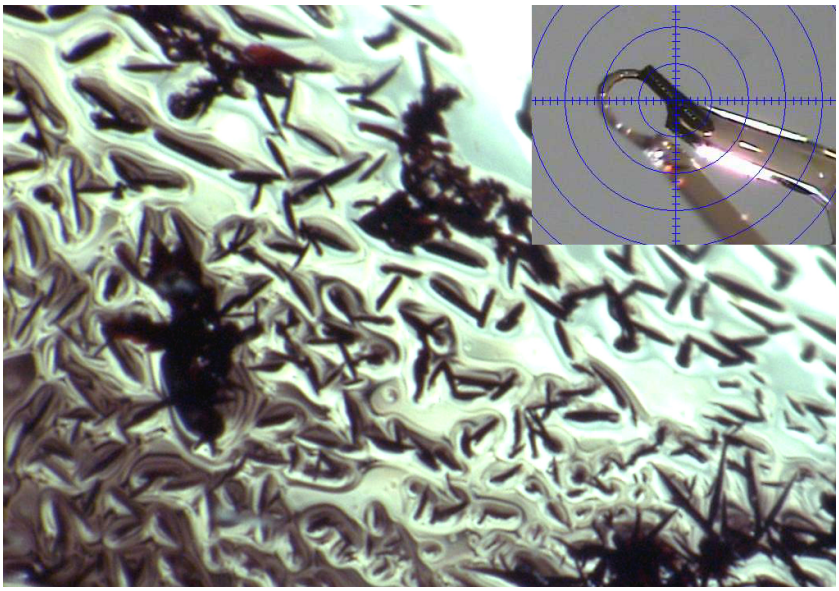

Figure 7.10: Crystals of $KC_{60}\cdot(THF)_5\cdot(THF)_2$ under the microscope (main), and needle mounted on a cryo-loop covered by oil for measurement at the single crystal diffractometer (inlay).

7.2.2 Crystal structure determination

The crystals were picked on air under oil with a nylon cryo-loop and mounted directly on the single crystal diffractometer (Fig. 7.10). Measurements were performed on a Smart

APEX II diffractometer with Mo-K_α radiation source after "slow" cooling and quenching to 100 K. The best dataset was obtained on quenching.

From systematic extinctions the polar space group $P2_12_12_1$ was deduced, with cell parameters $a = 17.80$ Å, $b = 30.10$ Å and $c = 9.85$ Å. The structure was solved by direct methods and refined by full-matrix least-squares fitting with the SHELXTL software package.

It was not possible to determine the absolute structure during the structure refinements; racemic twinning was assumed, which slightly improved the R-values. Experimental details on the crystallographic data and data collection are given in Tab. 7.3.

Table 7.3: Crystallographic parameters for $KC_{60}\cdot(THF)_5\cdot(THF)_2$.

Empirical formula	$C_{84}H_{48}KO_6$
T / K	100(2)
Formula weight	1192.32
Crystal system	orthorhombic
Space group (no.), Z	$P2_12_12$ (18), 4
Lattice constants / Å	$a = 17.802(5)$
	$b = 30.085(9)$
	$c = 9.863(3)$
Volume / Å^3	$V = 5283(3)$
Diffractometer	Smart APEX II
X-ray radiation, λ / Å	Mo-K$_\alpha$, 0.7103
Density (calculated) / g/cm^3	1.499
Absorption coefficient / mm^{-1}	0.170
θ range for data collection / °	1.77 to 20.88
Reflections collected	26190
Independent reflections, R_{int}	5563, 0.087
Parameters	821
Restraints	6
R_1 ($I > 2\sigma(I)$)	0.0692
wR_2 ($I > 2\sigma(I)$)	0.1698
R_1 (all data)	0.0996
wR_2 (all data)	0.1923
CCDC-no.	733614

The positions of the potassium atom and all 60 carbon atoms from the fullerene could be taken from the structure solution, and the missing O- and C-atoms belonging to the THF molecules were found from the difference Fourier map. The positions of the hydrogen atoms were calculated geometrically, and their isotropic displacement parameters were restrained to 1.2 times the value of the respective attached carbon atom. All

non hydrogen atoms were treated with anisotropic displacement parameters. The C_{60} molecule was completely ordered, while high values for the parameters of anisotropic thermal motion were observed for all THF molecules coordinated to potassium, and they can alternatively be described with a split-model comprising two orientations for each THF. There were problems in locating the exact positions of the uncoordinated solvent THF molecules. Their centres coincide with special positions ($2a$, 0 0 z and $2b$, 0 $\frac{1}{2}$ z) and large anisotropic displacement parameters were observed (see Appendix A with crystallographic data).

Carefully examining the diffraction data revealed very weak super structure reflections (Fig. 7.11), indicating a 5×1×2 super cell. This enlargement of the unit cell might be caused by a special kind of modulation of the THF molecules. However, due to the weak super cell intensity data, which could neither be overcome using Cu-K_α radiation, it was not possible to find and refine a fully ordered structure model in (3+1)D space.

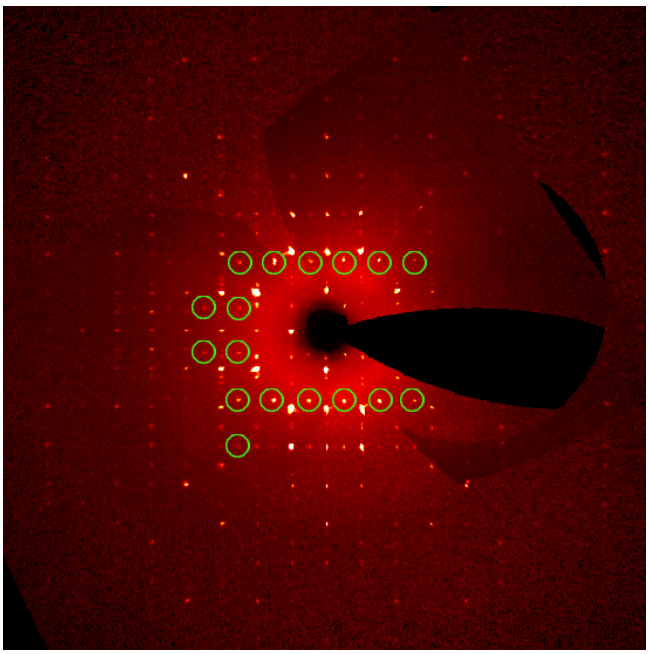

Figure 7.11: Precession images of $KC_{60}{\cdot}(THF)_5{\cdot}(THF)_2$ at *hk0* showing by green circles the reflections of the superstructure.

7.2.3 Results and discussion

$KC_{60}{\cdot}(THF)_5{\cdot}(THF)_2$ crystallizes in the orthorhombic space group $P2_12_12$ (no. 18) with four formula units per unit cell (Fig. 7.12). The structure contains one potassium atom per one C_{60} unit, therefore, the fulleride is an anion-radical $C_{60}^{\cdot -}$. Each potassium atom

is coordinated by five THF molecules acting as monodentate ligands forming a square pyramid with $d_{K-O} \approx 2.7$ Å (Fig. 7.13). The coordination sphere is completed by a hexagon of the fullerene, with an octahedral coordination resulting for the potassium atom. A similar coordination of potassium and THF molecules was observed before in $^{1}_{\infty}[\{K(THF)_5\}_2(C_{60})\{\mu\text{-}K(THF)_4\}]$ [206], with potassium to THF oxygen distances ranging from 2.61 Å to 2.74 Å. Two more solvent molecules are not coordinating and are located with their barycentres at special positions.

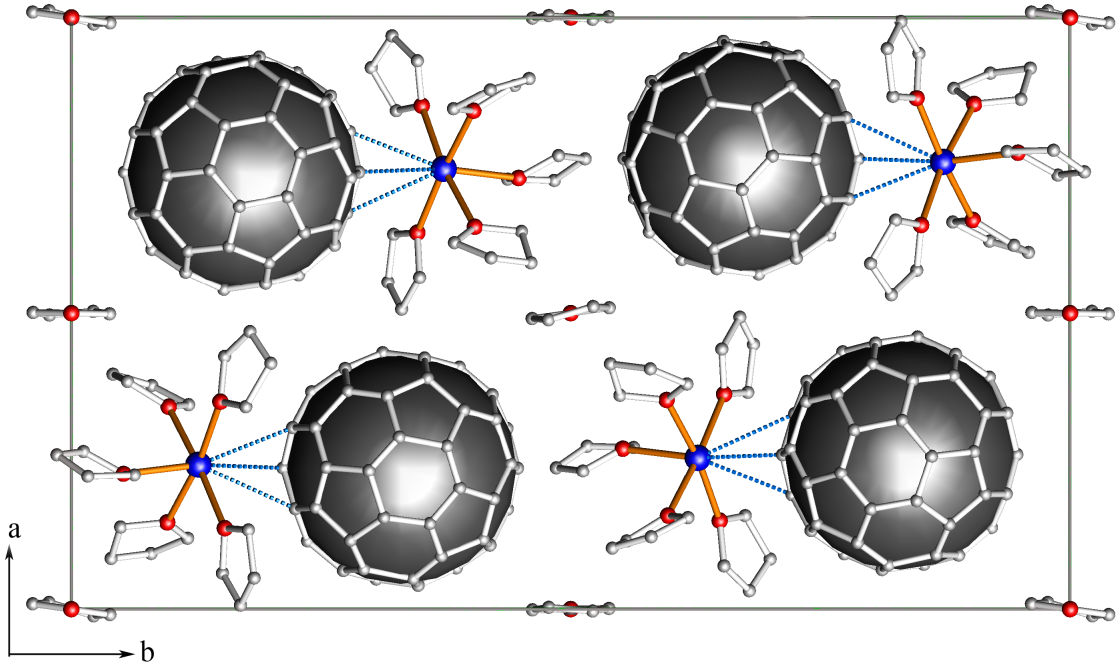

Figure 7.12: Projection of the crystal structure of $KC_{60}\cdot(THF)_5\cdot(THF)_2$ along [0 0 1], with margins of the unit cell given. Hydrogen atoms are omitted.

$C_{60}^{\cdot -}$ and K^+ form an ion pair, with potassium having shortest contact to three contiguous carbon atoms from a hexagon of C_{60} at 3.36, 3.21 and 3.43 Å (Fig. 7.13). The K-C distances to the three more remote carbon atoms are 3.70 Å, 3.76 Å and 3.90 Å. Thus, C_{60} clearly has a hapticity of three, corresponding to $[K(\eta^3\text{-}C_{60})(\eta^1\text{-}THF)_5]\cdot(THF)_2$. In this respect, the title compound differs evidently from $^{1}_{\infty}[\{K(THF)_5\}_2(C_{60})\{\mu\text{-}K(THF)_4\}]$, mentioned above, where all six C-atoms from one hexagon of the C_{60} molecule are coordinated to potassium (d_{K-C60} = 3.29-3.44 Å) [206]. A similar η^3-coordination between fullerides and alkali metal cations has been recently reported for $[Rb(benzo[18]crown\text{-}6)]_3[\eta^3\text{-}C_{60}](C_7H_8)\text{-}(C_3H_7NO)_{4.5}$ [206].

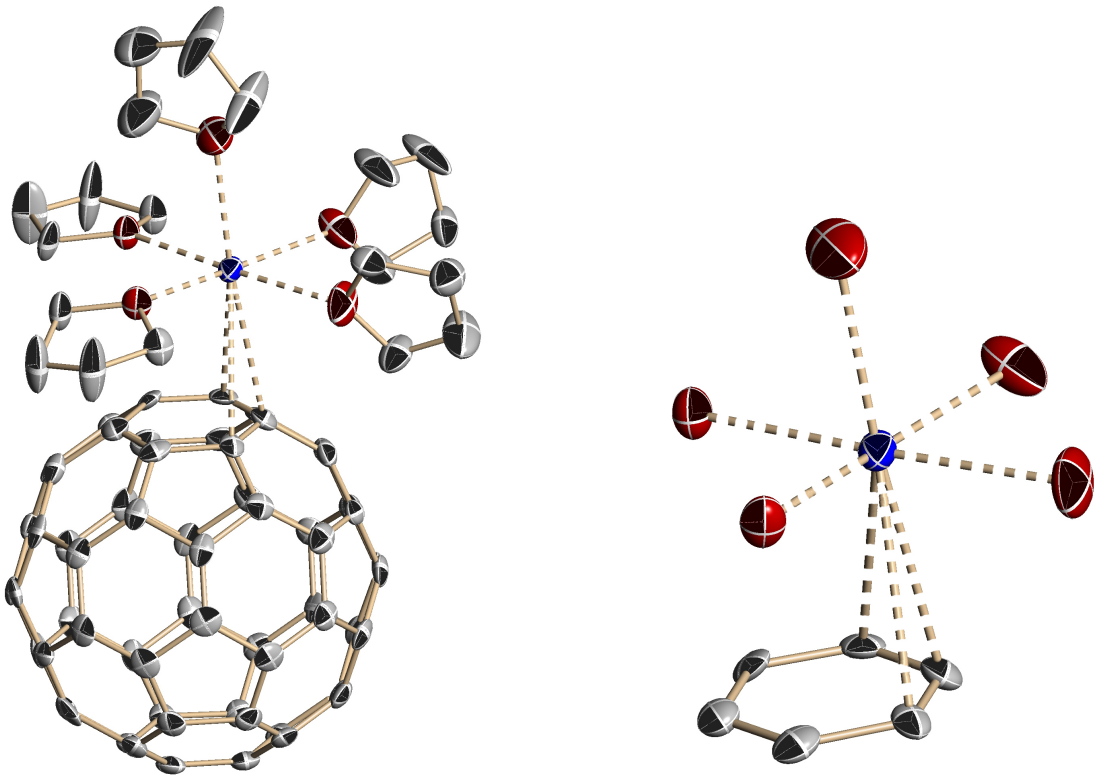

Figure 7.13: Fragments of the crystal structure showing the coordination of the potassium atom by the solvent molecules and fullerene cage (dotted lines). Displacement ellipsoids are drawn at the 50 % probability level, hydrogen atoms are omitted. Colour code: carbon (grey), oxygen (red), potassium (blue).

The ion pairs as described above are arranged in a way that the hydrogen bearing parts and the aromatic (fullerene) parts, respectively, flock together. This is a characteristic feature frequently encountered in crystal chemistry; the driving force is the optimization of the weak intermolecular interactions in the sense of "similar attracts similar".

$K^+C_{60}^{\cdot -}$ ion pairs thus form corrugated layers in the *ac* crystallographic plane. The interlayer separation is 15.06 Å (n in Fig. 7.14), the intralayer center-to-center fullerene distances being 10.12 Å (m in Fig. 7.14) and 9.86 Å along the c-axis. The layers are slightly shifted by 0.66 Å one from the other in the *ac* plane.

This way one of the objectives of our current project has been accomplished, namely, to create low-dimensional fulleride partial structures. As illustrated in Fig. 7.14 and mentioned above, the shortest interfulleride separations occur in layers parallel to (0 1 0).

In Fig. 7.15 a histogram is shown, representing the spread of the C-C distances in

$C_{60}^{\cdot -}$ as found by refinement of all positions involved individually and without using constraints. One can clearly identify a dip in the distribution separating the shorter bonds between edge sharing hexagons (6:6 bonds) from those shared by hexagons and pentagons (6:5 bonds).

Because of the rather high e.s.d.'s it has not been possible to identify some more detailed systematics in the bond lengths' distribution, potentially indicating some localization of the negative charge on the surface of the fullerene.

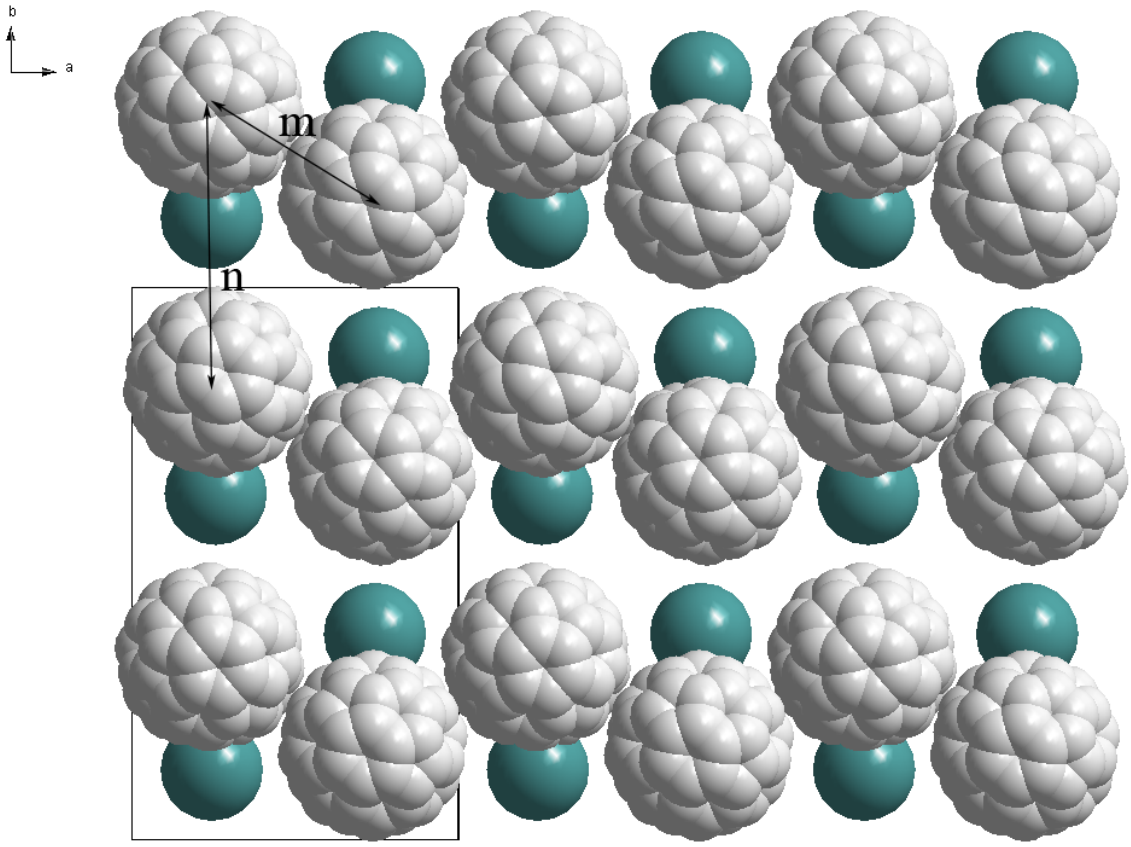

Figure 7.14: Space-filling model of the structure displaying van der Waals radii of fulleride anions and potassium cations, solvent molecules are omitted. K^{+}-$C_{60}^{\cdot -}$ ion pairs form layers in the *ac* crystallographic plane. The interlayer separation is 15.06 Å (n), the intralayer center-to-center fullerene distances are 10.12 Å (m) and 9.86 Å along the *c*-axis (not shown on the picture).

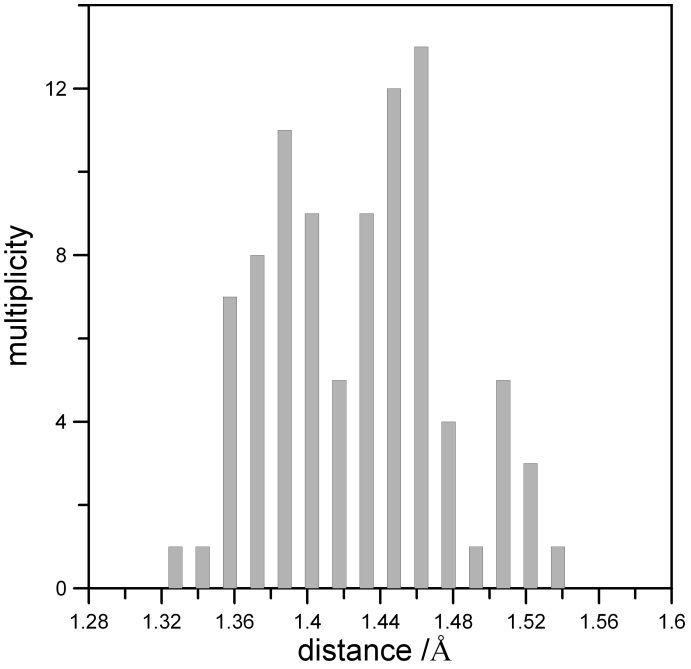

Figure 7.15: C-C bond length distribution within the fulleride anion in $KC_{60}\cdot(THF)_5\cdot(THF)_2$.

7.3 $[K(DB24C8)(THF)]_2C_{60}$·THF

7.3.1 Synthesis

50.0 mg (7.0×10^{-5} mol) of ground C_{60} have been reacted with 93.0 mg (20.8×10^{-5} mol) of dibenzo-24-crown-8 (DB24C8) and excess of metallic potassium in form of potassium mirror in 30 ml of tetrahydrofurane (THF) in order to obtain C_{60}^{3-}-based fulleride as can be expected from the reaction scheme:

$$K_{ex.} + DB24C8 \overset{DME}{\longrightarrow} [K(DB24C8)]^+e^-$$

$$3K(DB24C8) + C_{60} \overset{DME}{\longrightarrow} [K(DB24C8)^+]_3C_{60}^{3-}.$$

Octane was added to the solution, and single crystals were grown from it by the "temperature difference method".

7.3.2 Crystal structure determination

Black-reddish platelet-like crystals were picked as described in previous chapters. Single crystal X-ray diffraction data was collected using Mo-Kα radiation ($\lambda = 0.71073$ Å) after quenching to 100 K.

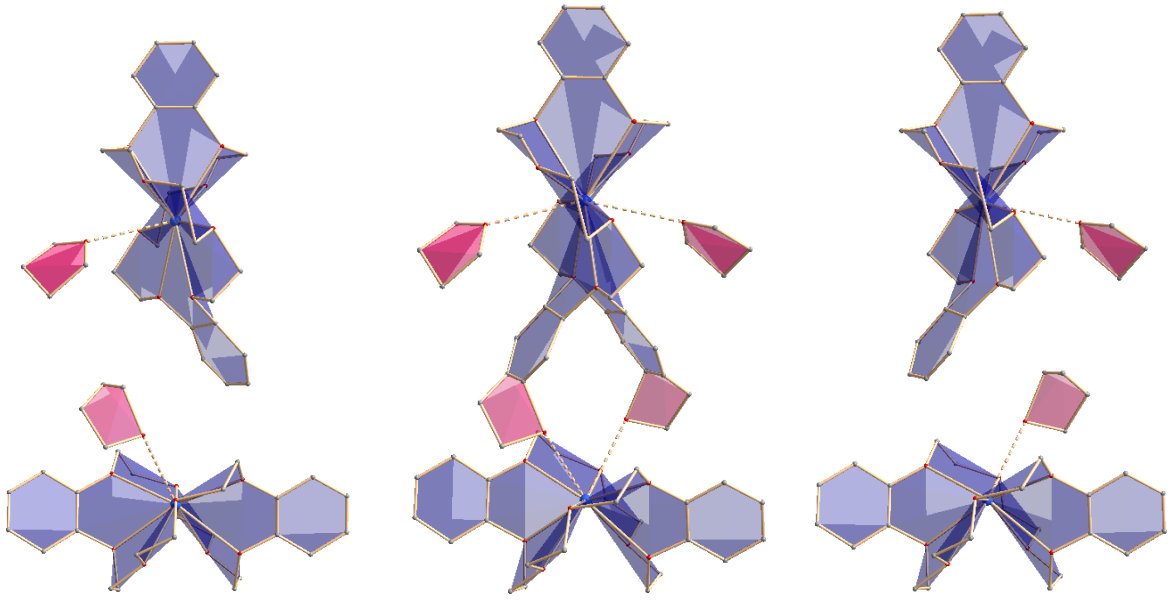

Figure 7.16: Disorder of the solvent and crown-ether in $[K(DB24C8)(THF)]_2C_{60}$·THF.

Two space groups - *C2/c* (no. 15) and *Cc* (no. 9) - were considered to be the possible solution. The disorder of crown-ether and solvent molecules having two different orientations has not been yet resolved (Fig. 7.16). The structure was checked for twinning but this has not brought to any improvement. The crystallographic parameters for the best solution are presented in Table 7.4. Atomic positions for potassium atoms and crown-ether molecules were taken from the structre solution. Fullerene molecules were found using the tangential expantion function (TEXP command) and imported with the FRAG comand. Only isotropic displacement parameters were refined.

Table 7.4: Crystallographic parameters for $[K(DB24C8)(THF)]_2C_{60}\cdot THF$.

Empirical formula	$C_{240}H_{96}K_4O_{38}$
T / K	100(2)
Formula weight	3743.57
Crystal system	monoclinic
Space group (no.), Z	Cc (9), 4
a / Å	27.132(3)
b / Å	26.064(3)
c / Å	29.336(3)
β / °	117.523(2)
V / Å^3	18397(3)
Diffractometer	Smart Apex II
X-ray radiation, λ / Å	Mo-K$_\alpha$, 0.7103
Density (calculated) / mg/m^3	1.352
Absorption coefficient / mm^{-1}	0.179
θ range for data collection / °	1.15 to 23.23
Reflections collected	57324
Independent reflections	25847 (R_{int} = 0.0978)
Parameters	1585
Restraints	2
R_1 ($I > 2\sigma(I)$)	0.1778
wR_2 ($I > 2\sigma(I)$)	0.4088
R_1 (all data)	0.3723
wR_2 (all data)	0.5261

7.3.3 Results and discussion

$[K(DB24C8)(THF)]_2C_{60}\cdot THF$ crystallizes in the space group *Cc* (no. 9) with four formula units, the latter consisting of two C_{60}, four potassium atoms, each complexed by one crown-ether molecule and coordinated by a solvent molecule, and two isolated THF molecules. The potassium to fullerene ratio is 2:1, therefore, the C_{60} units having a

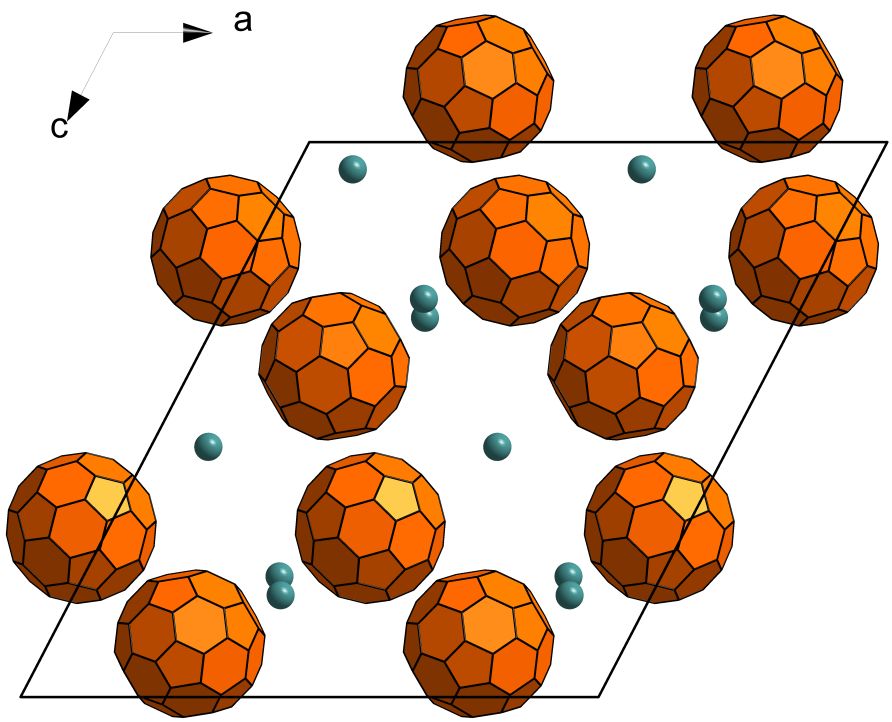

Figure 7.17: Unit cell of $[K(DB24C8)(THF)]_2C_{60}\cdot THF$. Only C_{60}^{2-} units and potassium atoms are shown.

charge -2. A view of the unit cell is presented in Figure 7.17. Crown-ethers and solvent molecules are disordered.

7.4 [K(DB24C8)(DME)]C_{60}

7.4.1 Synthesis

51.0 mg (7.0×10^{-5} mol) of ground C_{60} have been reacted with 31.0 mg (7.0×10^{-5} mol) of dibenzo-24-crown-8 (DB24C8) and excess of metallic potassium in form of potassium mirror in 30 ml of dimethoxyethane (DME). Octane was added to the solution, and single crystals were grown from it by the "temperature difference method".

7.4.2 Crystal structure determination

Table 7.5: Crystallographic parameters for [K(DB24C8)(DME)]C_{60}.

Empirical formula	$C_{176}H_{84}K_2O_{20}$
T / K	100(2)
Formula weight	2576.47
Crystal system	orthorhombic
Space group (no.), Z	$Pna2_1$ (33), 4
a / Å	27.485(5)
b / Å	16.662(3)
c / Å	25.503(5)
V / Å^3	11668(4)
Diffractometer	Smart Apex II
X-ray radiation, λ / Å	Mo-K_α, 0.7103
Density (calculated) / mg/m^3	1.467
Absorption coefficient / mm^{-1}	0.165
θ range for data collection / °	1.92 to 18.94
Reflections collected	35800
Independent reflections	9249 (R_{int} = 0.0694)
Parameters	1357
Restraints	1
R_1 ($I > 2\sigma(I)$)	0.1483
wR_2 ($I > 2\sigma(I)$)	0.3690
R_1 (all data)	0.2073
wR_2 (all data)	0.4267

Single crystals crystals were picked as described in previous chapters. Single crystal X-ray diffraction measurements were performed on both quenching to 100 K and slow cooling to 100 K (10 K/h) with Mo-K_α and Cu-K_α radiation. Because of the not good enough crystal quality and large lattice constants, the distance to the detector was increased from 6 cm to 9 cm (for the measurement with Mo radiation) in order to achieve

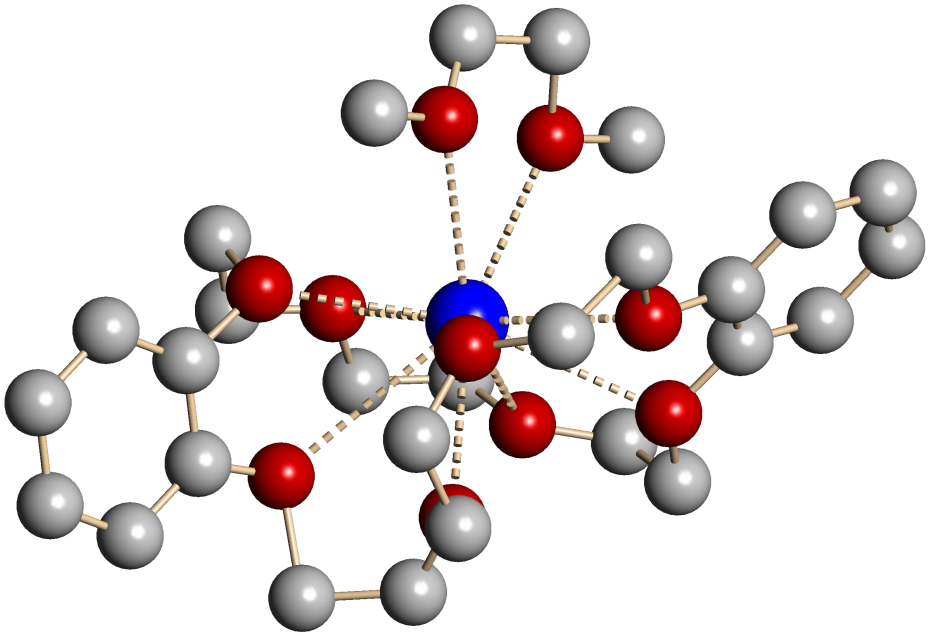

Figure 7.18: Coordination of the potassium atom by crown-ether and one DME solvent molecule.

a higher resolution and separating main and "false" reflections. The latter were caused by thin powder particles attached to the single crystal surface.

From systematic extinctions the $Pna2_1$ (no. 33) space group was deduced. All atomic coordinates were found during structure solution, except for one C_{60} unit which had to be imported using the FRAG command. Structure was refined isotropically and checked for twinning. The crystallographic parameters are presented in Table 7.5.

7.4.3 Results and discussion

[K(DB24C8)(DME)]C_{60} crystallizes in the space group $Pna2_1$ (no. 33) with four formula units consisting of two C_{60} cages and two potassium metals, complexed by a crown-ether and additionally coordinated by one DME solvent molecule (Fig. 7.18). Potassium-to-fullerene ratio is 1:1, therefore, fullerene is present in the form of anion-radicals. A view of the unit cell is shown in Figure 7.19.

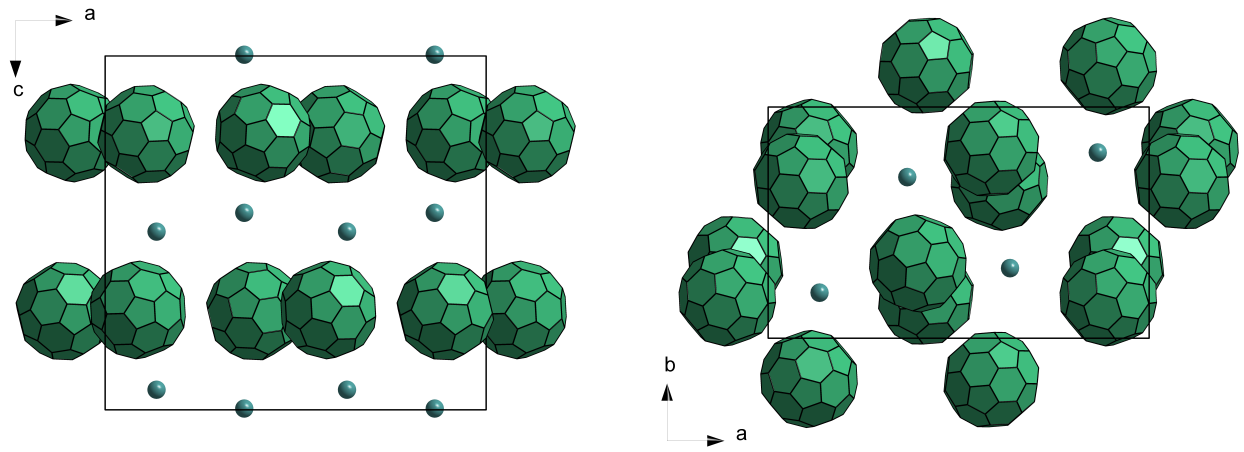

Figure 7.19: Unit cell of [K(DB24C8)(DME)]C_{60}. Crown-ether and solvent molecules are omitted.

7.5 $[K(DB24C8)(DME)]_2[C_{60}]_2$

7.5.1 Synthesis

53.0 mg (7.3×10^{-5} mol) of ground C_{60} have been reacted with 94.0 mg (21.9×10^{-5} mol) of dibenzo-24-crown-8 (DB24C8) and excess of metallic potassium in form of potassium mirror in 30 ml of dimethoxyethane (DME). Octane was added to the solution, and single crystals were grown from it by the "temperature difference method". The synthesis could not be reproduced.

7.5.2 Crystal structure determination

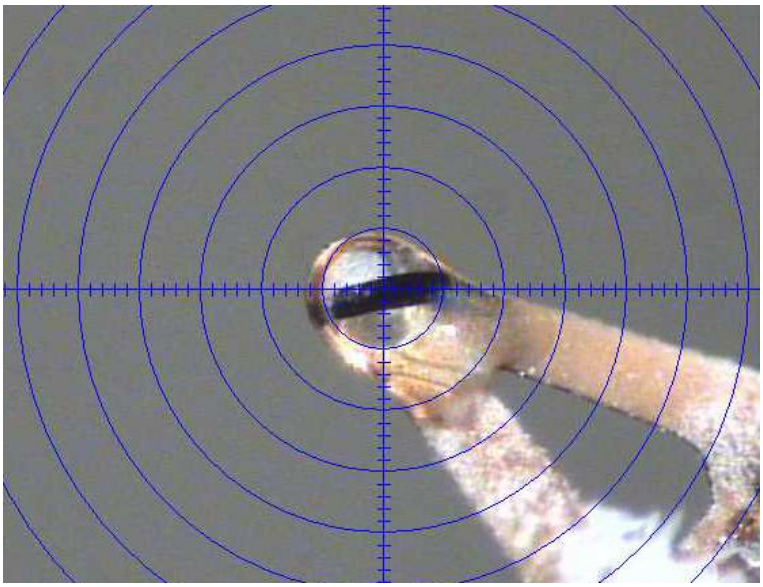

Figure 7.20: A single crystal of $[K(DB24C8)(DME)]_2[C_{60}]_2$ mounted on a cryo-loop covered by oil for measurement at the single crystal diffractometer.

A selected needle-like single crystal (Fig. 7.20) (size $0.15\times0.20\times0.30$ mm^3) was cooled from 270 K to 50 K with a rate of 10 K/h, performing measurements with Cu-K_α radiation with a 10-25 K step, annealing the crystal from 3 to 6 h before each long measurement. The $P2_1/c$ (no. 14) space group was determined from systematic extinctions. Potassium atoms, crown-ethers and solvent molecules could be found during the structure solution. C_{60} units were imported with the FRAG command. Hydrogen atoms were added as "riding" atoms. The crystallographic parameters are presented in Table 7.6.

Table 7.6: Crystallographic parameters for $[K(DB24C8)(DME)]_2[C_{60}]_2$.

Empirical formula	$C_{88}H_{42}KO_{10}$
T / K	50(2)
Formula weight	1298.32
Crystal system	monoclinic
Space group (no.), Z	$P2_1/c$, 4
a / Å	14.0145(2)
b / Å	25.0685(4)
c / Å	16.0233(3)
β /°	93.8040(10)
V / Å^3	5616.94(16)
Diffractometer	Smart Apex II
X-ray radiation, λ / Å	Cu-K$_\alpha$, 1.5418
Density (calculated) / mg/m^3	1.535
Absorption coefficient / mm^{-1}	1.451
θ range for data collection / °	3.16 to 64.45
Reflections collected	39953
Independent reflections	9296 (R_{int} = 0.0376)
Parameters	720
Restraints	0
R_1 ($I > 2\sigma(I)$)	0.1812
wR_2 ($I > 2\sigma(I)$)	0.5578
R_1 (all data)	0.1871
wR_2 (all data)	0.5720

7.5.3 Results and discussion

$[K(DB24C8)(DME)]_2[C_{60}]_2$ crystallizes in $P2_1/c$ (no. 14) with four formula units (consisting of a C_{60} and a potassium atom complexed by the crown ether and DME solvent - Fig. 7.21). The fullerene-to-metal ratio is 1:1, therefore, C_{60} has a charge -1.

At 50 K disordered dumbbells constitute the structure, the interfullerene single C-C bond being 1.57(3) Å. An interesting feature was observed: on cooling from 270 K, the c-axis of the unit cell increased, reached a maximum at ca. 250 K, and then decreased (Fig. 7.23).

The title compound and the one described in the previous chapter ($[K(DB24C8)(DME)]C_{60}$) have the same compositions, but different structures. Firstly, the conformations of the crown-ethers are different. Secondly, in $[K(DB24C8)(DME)]C_{60}$ the $C_{60}^{\cdot -}$ are present in monomeric form, while in the title compound - as dimer-dianions $(C_{60})_2^{2-}$. Besides, a temperature dependent transformation from $[K(DB24C8)(DME)]_2[C_{60}]_2$ to $[K(DB24C8)(DME)]C_{60}$ could not be detected.

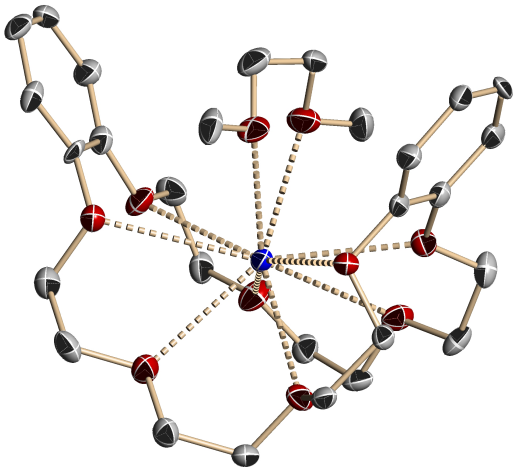

Figure 7.21: Complexation of the potassium atom in $[K(DB24C8)(DME)]_2[C_{60}]_2$. Thermal ellipsoids shown at the 50 % probability level. Hydrogen atoms are omitted.

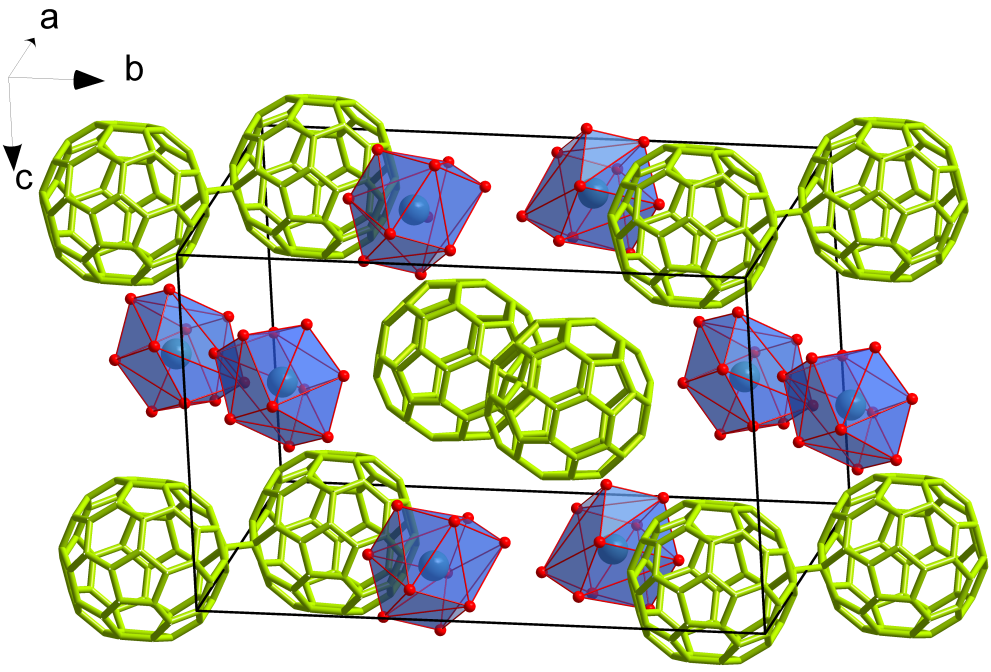

Figure 7.22: View of the unit cell of $[K(DB24C8)(DME)]_2[C_{60}]_2$ at 50 K. Coordination of potassium atoms by 10 oxygen atoms is shown as a polyhedron.

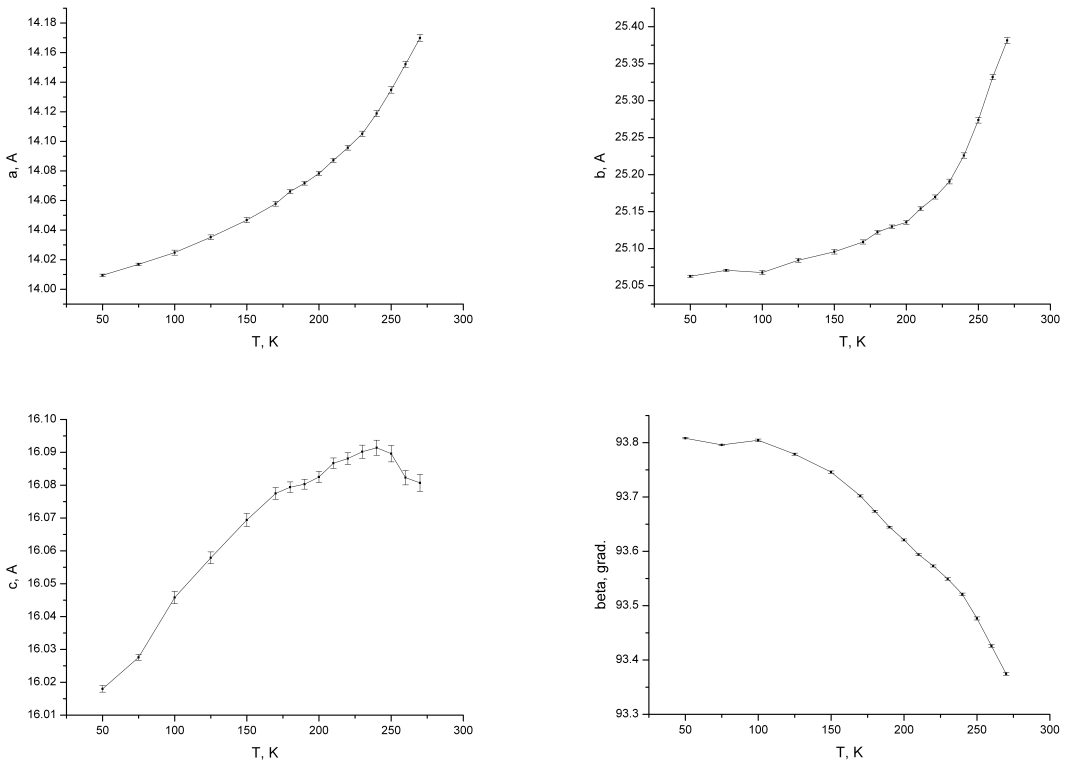

Figure 7.23: Change of the lattice constants with temperature for $[K(DB24C8)(DME)]_2[C_{60}]_2$. Note the unusual change of c.

7.5.4 SQUID from single crystals

Magnetic measurements were performed at 10000 Oe. The signal is negative because of small and few crystals measured, this bringing to a big error in centering of the sample. The mass of the sample could not be measured, therefore, the magnetic moment could neither be estimated. A hysteresis was noticed, indicating a monomer-dimer transition.

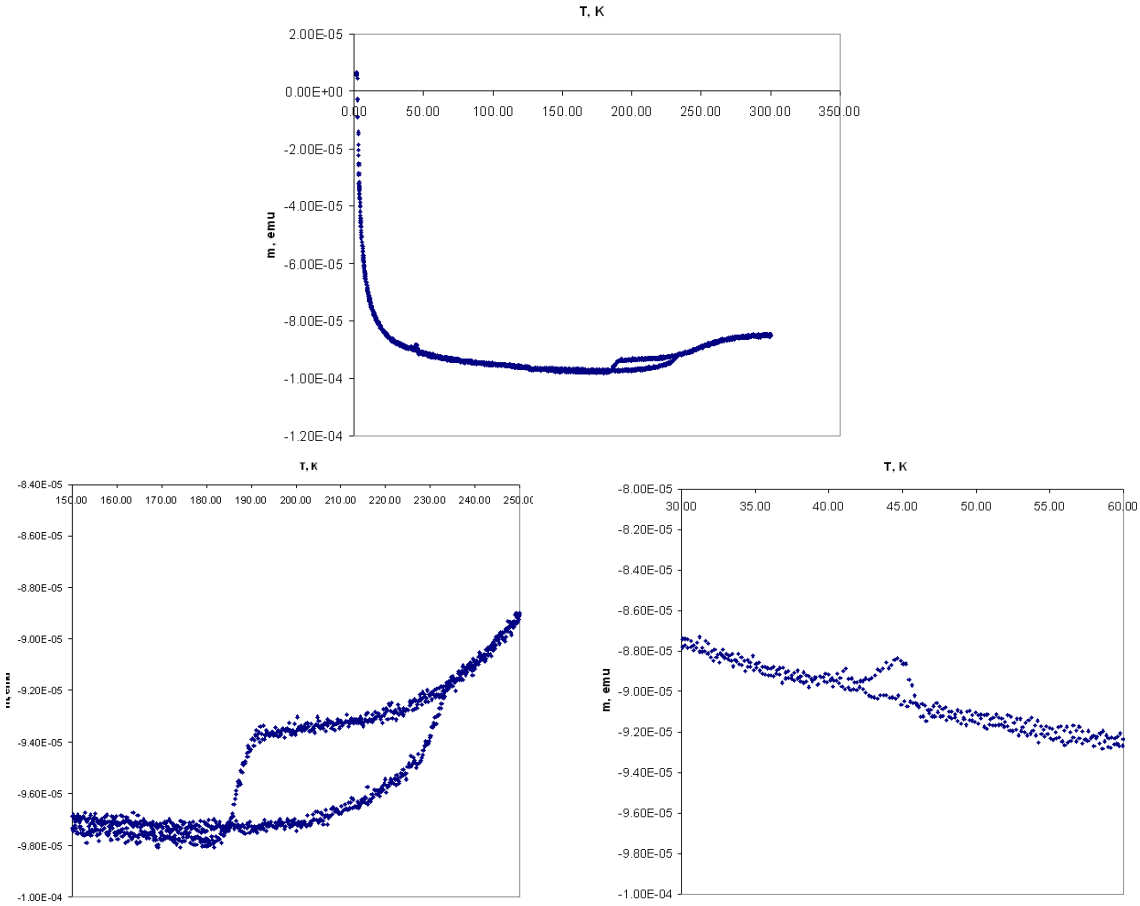

Figure 7.24: Magnetic moment of single crystals of $[K(DB24C8)(DME)]_2[C_{60}]_2$ vs temperature at 10000 Oe.

7.6 [4{K(DB18C6)($C_{60}^{\cdot-}$)}(THF)$_6$]·[C_{60}^{0}]·(THF)$_6$

7.6.1 Synthesis

100 mg (0.14×10^{-3} mol) of ground C_{60} have been reacted with 50.0 mg (0.14×10^{-3} mol) of dibenzo-18-crown-6 (DB18C6) and excess of metallic potassium in form of potassium mirror in 70 ml of tetrahydrofurane. After performing the synthesis and crystallizing by the "temperature difference method" with octane, reddish-black crystals were obtained, the morphology of the crystals being rather different in different "runs" (Fig. 7.25).

Single crystals were picked as described above and measured on the Smart APEX I diffractometer with Mo-K_α radiation source at 250, 220, 175, 140, 125 and 80 K on cooling from room temperature with a rate of 10 K/h, and annealing before each measurement from 3 to 6 h. The structure of crystals measured at different temperatures differed.

7.6.2 Structure at 80 K

7.6.2.1 Crystal structure determination

The systematic extinctions observed made two space groups, $C2/c$ (no. 15) and Cc (no. 9), possible, from which $C2/c$ has turned out to be the correct one during structure refinement. The structure was solved by direct methods and refined by full-matrix least-squares fitting. Reflections of superstructure were observed (Fig. 7.26) which results in a two times larger unit cell in comparison with the one at 220 K. All atomic positions except for one C_{60} unit could be taken from the structure solution. The remaining C_{60} unit was imported as a rigid body with the FRAG command using the parameters of [$Ba(NH_3)_7$]C_{60}·NH_3 [14], as described before. Isolated solvent molecules were heavily disordered and fixed with AFIX 59. Benzene rings in the crown-ether molecules were fixed. All anisotropic parameters were refined freely, except for one C_{60} molecule, for which the constraint DELU (SHELXTL) was applied, and the isolated THF molecules, for which EADP (SHELXTL) was applied. Hydrogen atoms were added as "riding" atoms. Experimental details on crystallographic data and data collection are given in Tab. 7.7.

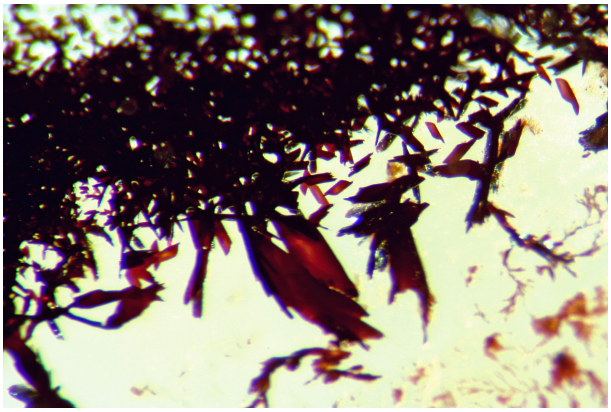

(a)

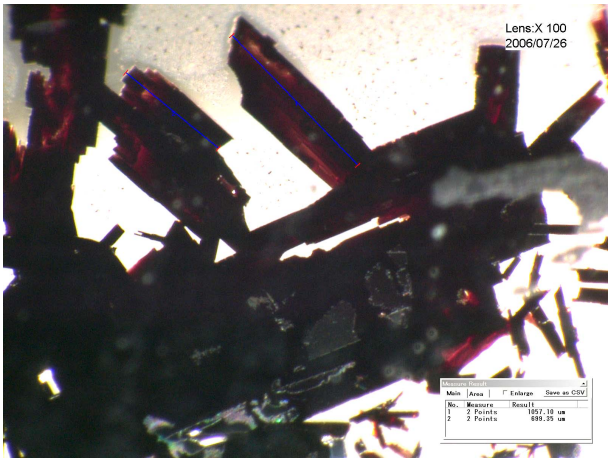

(b)

(c)

Figure 7.25: Different morphologies of $[4\{K(DB18C6)(C_{60}^{\cdot -})\}(THF)_6]\cdot[C_{60}^{0}]\cdot(THF)_6$ crystals: a - dendrite-like crystals, b - platele-like, c - block-like.

Table 7.7: Crystallographic parameters for $[4\{K(DB18C6)(C_{60}^{\cdot-})\}(THF)_6]\cdot[C_{60}^{0}]\cdot(THF)_6$ at 80 K.

Chemical formula	$C_{214}H_{96}K_2O_{18}$
T / K	80(2)
Formula weight	3031.09
Crystal system	monoclinic
Space group (no.), Z	$C2/c$ (15), 8
Lattice constants /Å	a = 56.131(5)
	b = 15.0951(14)
	c = 36.310(3)
	β= 121.904(2)
Volume /Å^3	V = 26118(4)
Diffractometer	Smart APEX I
X-ray radiation, λ /Å	MoK_α, 0.71073
Density (calculated) /g cm^{-3}	ρ = 1.542
Absorption coefficient μ /mm^{-1}	0.159
θ range / °	0.85 to 25.00
Reflections collected	93623
Independent reflections, R_{int}	22982, 0.0493
Parameters	1797
Restraints	270
R_1 ($I > 2\sigma(I)$)	0.1543
wR_2 ($I > 2\sigma(I)$)	0.4267
R_1 (all data)	0.2062
wR_2 (all data)	0.4689

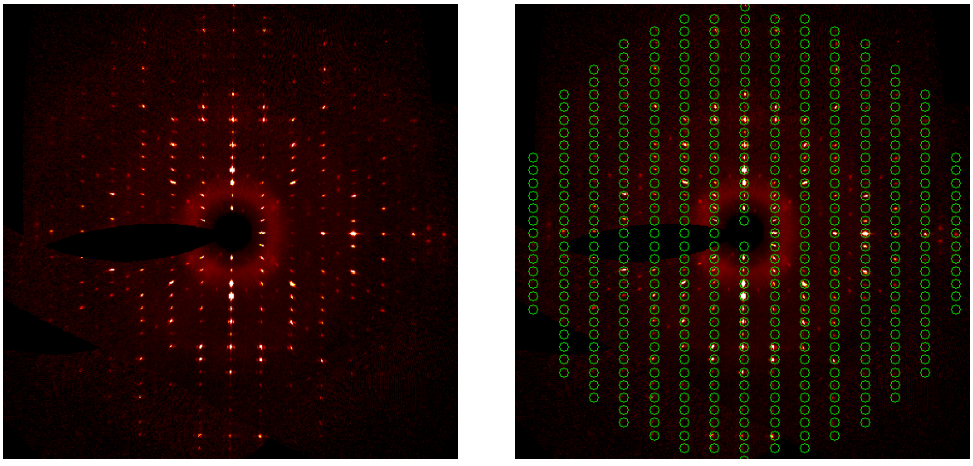

Figure 7.26: Superstructure reflections (not indexed) on the precession images at *0kl* of the crystal.

7.6.2.2 Structure description

$[4\{K(DB18C6)(C_{60}^{\cdot-})\}(THF)_6]\cdot[C_{60}^{0}]\cdot(THF)_6$ at 80 K has the monoclinic space group $C2/c$ (no. 15) with 8 formula units, the formula unit consisting of two K-crown complexes with three THF molecules coordinating K, 2.5 C_{60} units and 3 isolated THF molecules. The structure contains 1.25 C_{60} units per one potassium atom, therefore, 80 percent of C_{60} in the structure having a charge -1, and 20 % of C_{60} being uncharged.

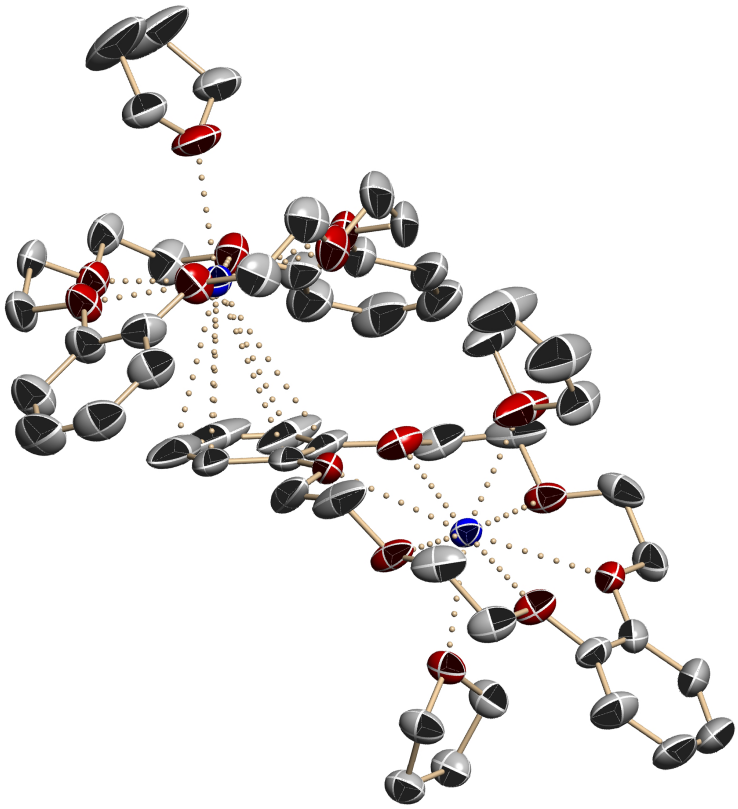

Figure 7.27: Coordination of the potassium atoms. Thermal ellipsoids are shown at the 50% probability level. Hydrogen atoms are omitted.

One can distinguish two different potassium-crown complexes (Fig. 7.27). In one, the potassium atom is coordinated by six oxygen atoms of the crown-ether at distances 2.73-2.80 Å, and by two THF molecules in axial positions. The second potassium atom is coordinated by six oxygen molecules from the crown-ether, as well, at 2.70-2.82 Å, one THF molecule in an axial position, and by the benzene ring of the crown-ether described previously, on the other axial positions, the three closest K-C distances being 3.19, 3.24

and 3.40 Å, and the three more remote – 3.62, 3.70 and 3.47 Å. Three remaining THF molecules are isolated, heavily disordered, and occupy the voids.

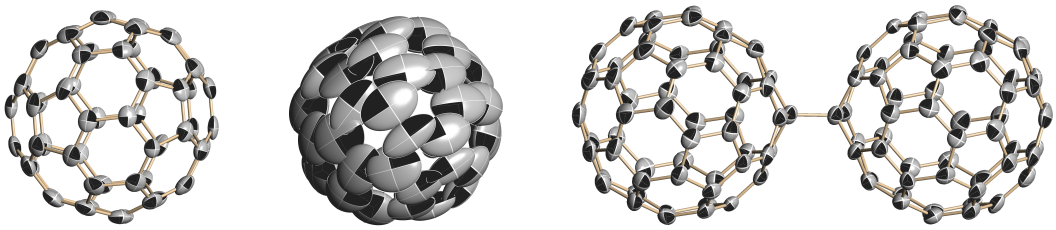

Figure 7.28: Three bonding states of fullerene in the structure: ordered monomer, disordered monomer, ordered dimer. Ellipsoids shown at the 50% probability level.

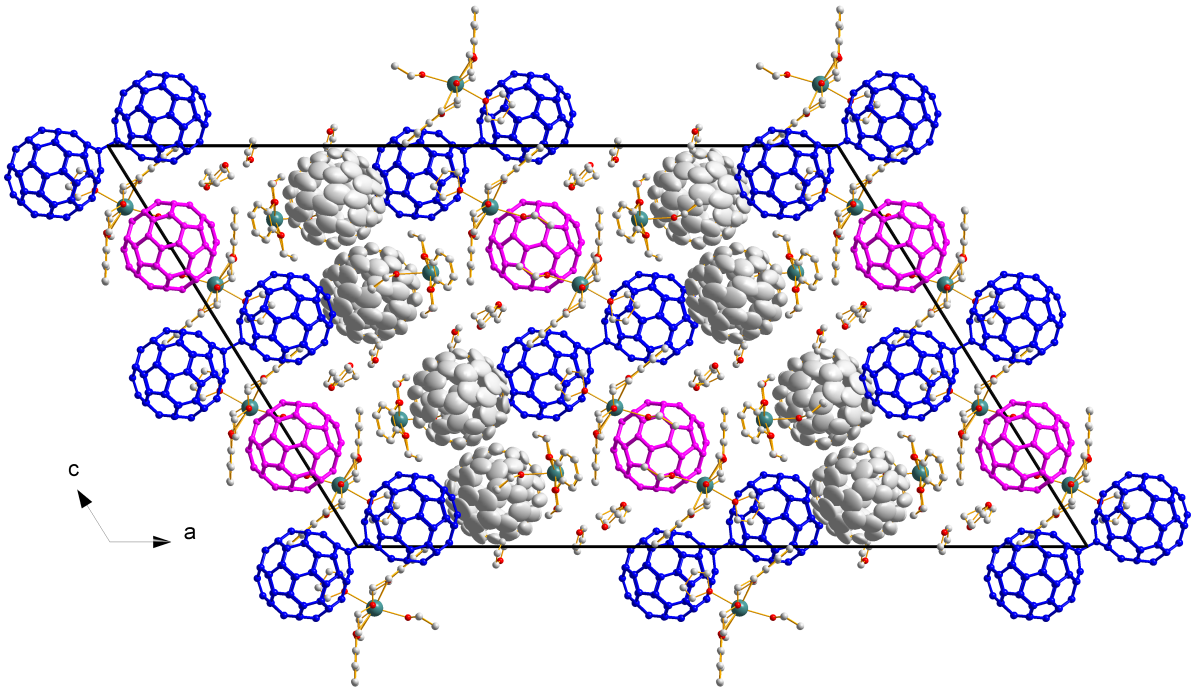

Figure 7.29: The unit cell of $[4\{K(DB18C6)(C_{60}^{\cdot-})\}(THF)_6]\cdot[C_{60}^{0}]\cdot(THF)_6$ at 80 K showing the fullerene in three different bonding states: blue - dimer-dianions, pink - ordered charged monomers, grey - disordered neutral fullerene. (Ellipsoid model for disordered C_{60}, 50 % probability level; ball-and-stick model for the rest of the unit cell content). Hydrogen atoms are omitted.

Fullerene is present in the structure in three different bonding states (Fig. 7.28, Fig. 7.29): as disordered isolated neutral C_{60}, ordered isolated anion-radicals $C_{60}^{\cdot-}$, and ordered dimer-dianions $(C_{60}^{-})^{2-}{}_2$. In the single-bonded dimer, the C-C bond between

two C_{60} units is 1.63(0) Å, the center-to-center interfullerene distance being 9.30(1) Å - less than the sum of the van der Waals radii. The single interfullerene bond lengths for dimers reported in literature are 1.597(7) Å [27], 1.55(5) Å [25] and 1.597(3) Å [207] found experimentally, and 1.618 Å - calculated [208]. The present structure is the first one reported for fullerenes in 3 bonding states.

7.6.3 Structure at 220 K

7.6.3.1 Crystal structure determination

Experimental details on crystallographic data and data collection are given in Table 7.8.

Table 7.8: Crystallographic parameters for $[4\{K(DB18C6)(C_{60}^{\cdot -})\}(THF)_6]\cdot[C_{60}^{0}]\cdot(THF)_6$ at 220 K.

Chemical formula	$C_{214}H_{96}K_2O_{18}$
T /K	220(2)
Formula weight	3033.1
Crystal system	monoclinic
Space group (no.), Z	$C2$ (5), 4
Lattice constants /Å	a = 49.055(11)
	b = 15.075(3)
	c = 18.312(4)
	β= 97.892(2)
Volume /Å^3	V = 13414(5)
Diffractometer	Smart APEX I
X-ray radiation, λ /Å	MoK_α, 0.71073
Density (calculated) /g cm^{-3}	ρ = 1.502
Absorption coefficient μ /mm^{-1}	0.155
θ range / °	1.12 to 18.20
Reflections collected	24610
Independent reflections, R_{int}	9497, 0.0458
Parameters	1142
Restraints	1581
R_1 ($I > 2\sigma(I)$)	0.2251
wR_2 ($I > 2\sigma(I)$)	0.5370
R_1 (all data)	0.2983
wR_2 (all data)	0.6009

The systematic extinctions observed made two space groups, $C2/m$ (no. 12) and $C2$ (no. 5), possible, from which $C2$ has turned out to be the correct one during structure refinement. The structure was solved by direct methods and refined by full-matrix

least-squares fitting. Only atomic positions of the crown-ether could be taken from the structure solution. All C_{60} units were imported as a rigid bodies with the FRAG command. Hydrogen atoms were added as "riding" atoms. Thermal parameters were refined with constraints.

7.6.3.2 Structure description

The unit cell of the structure at 220 K is two times smaller than at 80 K, the unit cell content being exactly two times less. $[4\{K(DB18C6)(C_{60}{}^{\cdot-})\}(THF)_6]\cdot[C_{60}{}^{0}]\cdot(THF)_6$ at 220 K has the space group $C2$, having four formula units. All C_{60} units are in monomeric form, as can be seen from Figure 7.30.

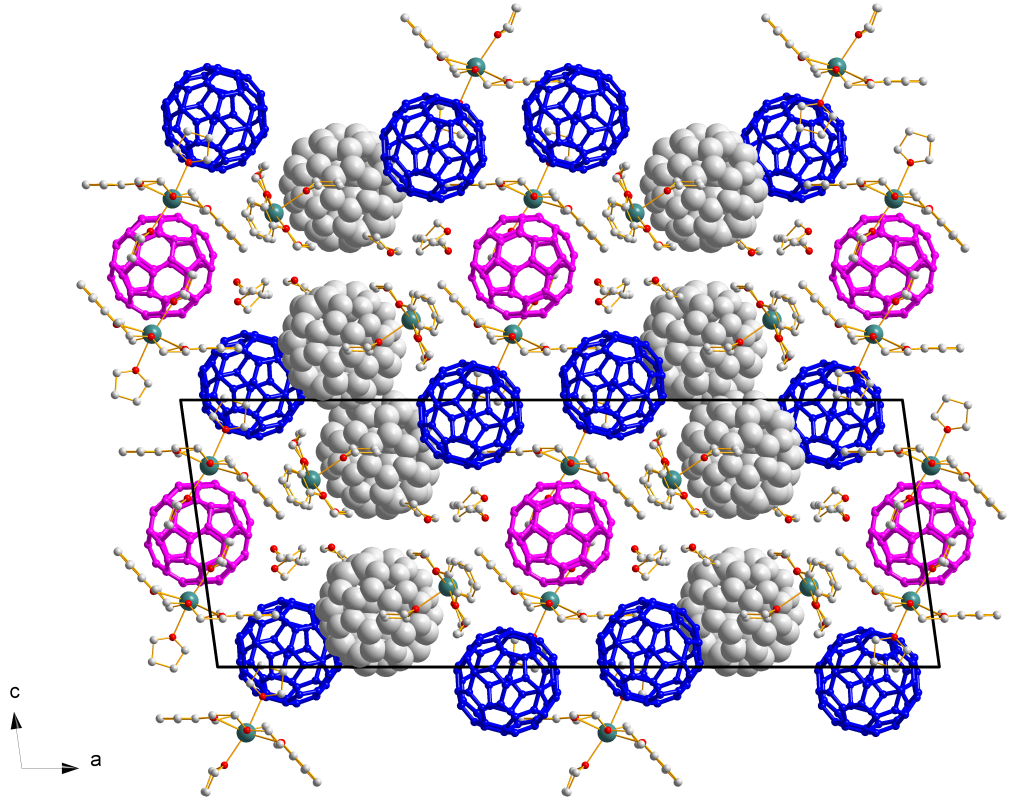

Figure 7.30: View of the unit cell of $[4\{K(DB18C6)(C_{60}{}^{\cdot-})\}(THF)_6]\cdot[C_{60}{}^{0}]\cdot(THF)_6$ at 220 K. The colour code is the same as for the structure at 80 K for ease of comparison. Hydrogen atoms are omitted. Center-to-center distance for blue colored fullerenes is 9.90 Å.

7.6.4 Discussion

In the dimer, the pentagons adjacent to the sp^3-hybridized carbon atoms are in *trans*-orientation with respect to the interfullerene C-C bond, while at 220 K these fullerene units are oriented in *gauche*-position (Fig. 7.31).

Figure 7.31: *Trans*-conformation of the fullerenes in dimer in the low-temperature phase (left) and *gauche*-orientation of the corresponding fullerenes in the high-temperature phase (right). View along the single C-C interfullerene bond.

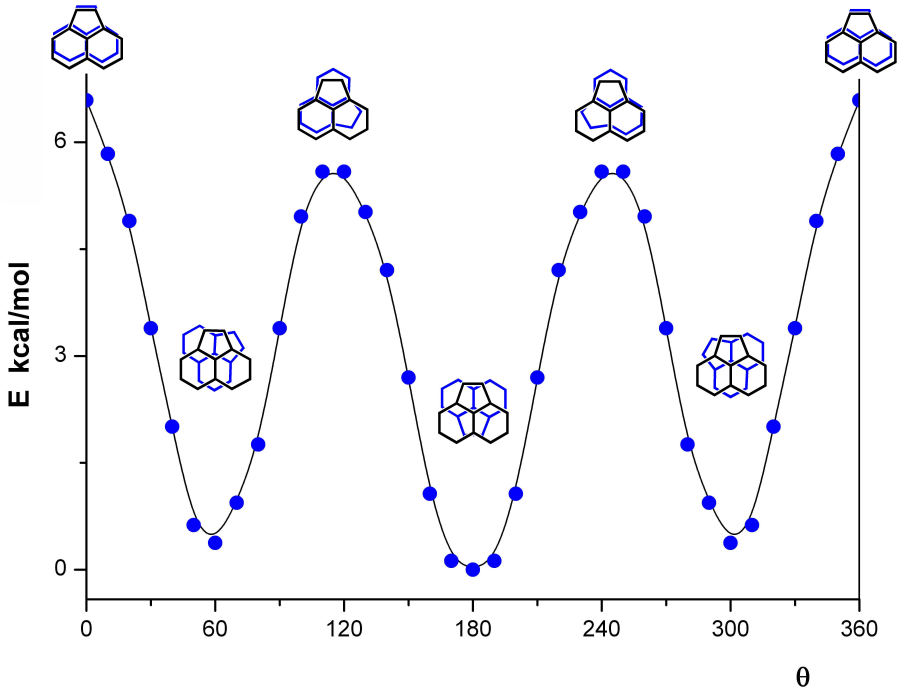

Figure 7.32: Energy landscape with respect to the rotation of fullerenes in the dimer. DFT, B3LYP, 6-31G basis set. The structural parameters were optimized for every given dihedral angle.

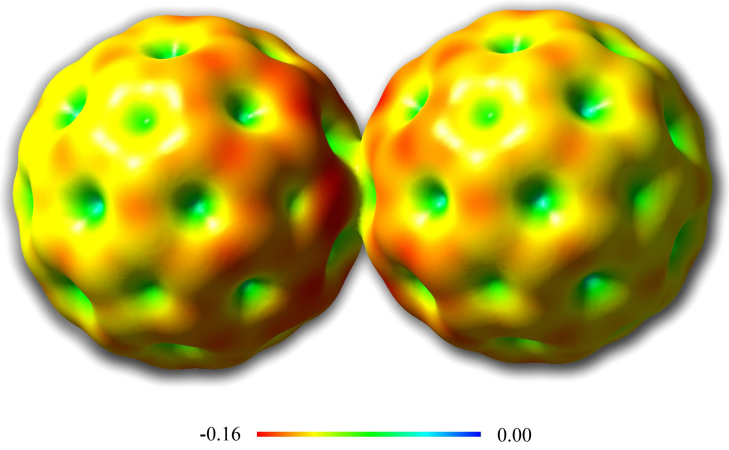

Figure 7.33: Electrostatic potential of an isosurface of the electron density of the dimer in the singlet state in *trans*-conformation. DFT, B3LYP, 6-31G basis set.

According to quantum chemical calculations [197], the dimer can exist in two different conformations (lowest in energy on Fig. 7.32). The difference between these minima is only 0.5 kcal/mol. Therefore, it is justified to expect that in the crystal structure they can exist in any of these two orientations. However, it is not the case, and the dimer exists in the crystal only in one conformation, the latter corresponding to *trans*-orientation of the pentagons. Therefore, it is worthy to notice that DFT shows qualitatively which conformation of the dimer is the most stable, however, this might be not correct quantitatively. The relative positions of the minima may be influenced by the basis set and the functional used.

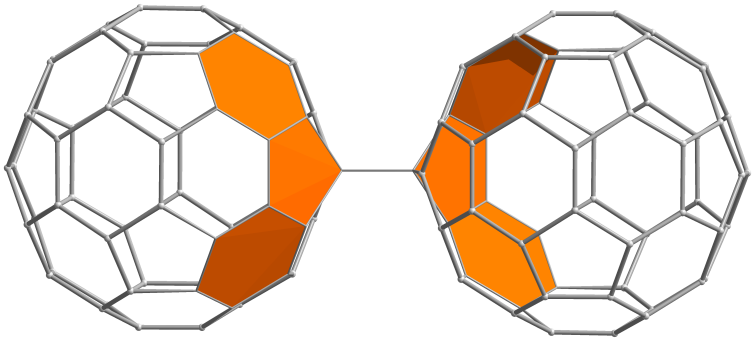

Figure 7.34: Fluorene fragments (colored) in *trans*-conformation in the dimer.

The electrostatic potential (Fig. 7.33) shows that the negative charge is equally distributed over the fluorene fragments (two hexagons fused with a pentagon, Fig. 7.34). This is an evidence for the aromatization of the pentagon in the fluorene fragment. Therefore, considering the Coulomb repulsion of the areas with localized charge on the C_{60} cage, the system has lowest energy only in the case of *trans*-orientation of the pentagons on two C_{60} units. This is an experimental proof of the fact that the charge is not delocalized over the whole C_{60} cage, but is localized on a rather small fragment of the molecule.

The analysis of the C-C bond lengths for the dimer, and comparison of experimental data with the results of the DFT calculations, prove the aromatization of the fluorene fragment, what follows from the lowering of bonds alternation in this fragment (Fig. 7.35).

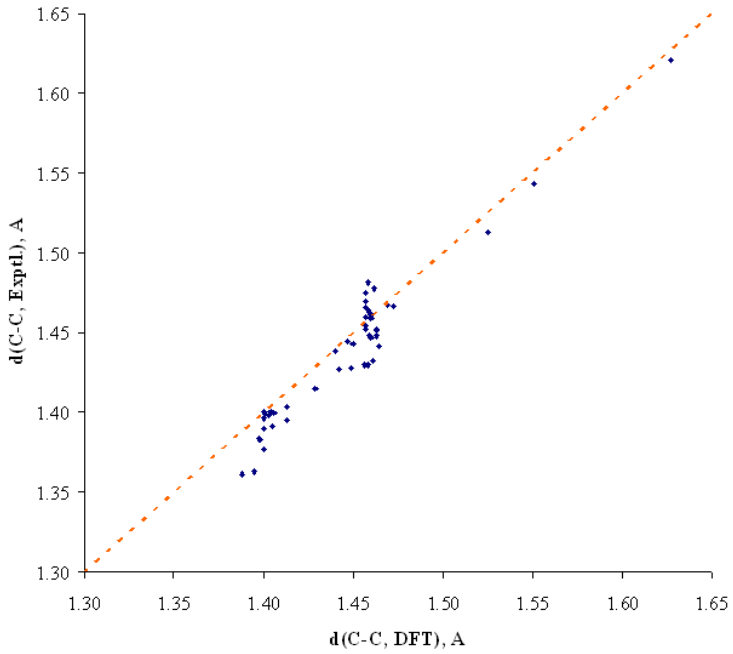

Figure 7.35: Correlation between the experimentally obtained and the DFT calculated C-C bond distances in the dimer.

Thus, it is evident that a radical recombination reaction takes place on cooling the compound under discussion. Therefore, the two different structures may be regarded as the "high-temperature phase" and the "low-temperature phase", although the term "phase" is not correct, since this transformation is not a "phase transition" in its common meaning, but a chemical reaction of radical recombination. It can be added that

dimerization temperatures for fullerenes reported in literature are in the range of 220 K [27] to 250 K [24, 25].

7.6.5 SQUID measurements

SQUID measurements were performed, bringing controversal results.

In the first run of experiments, a sample was prepared by evaporating the solution in THF as obtained after the synthesis under vacuum. The remaining solid was ground to powder in a mortar in the glove-box, and Suprasil ampoules with 50 mg sample were sealed under He and measured in the temperature range from 2 to 300 K in magnetic fields of 0.1 T, 1 T and 7 T. When evaluating the data, diamagnetic corrections were performed. According to the measurements, the transition temperature takes place at ca. 130 K (Appendix A, Fig. 8.4, 8.5, 8.6), the estimated magnetic moment for the low-temperature phase being 0.8 μ_B per one formula unit, whereas it is expected to be 1.73 per one electron.

However, the starting compound could have been not the pure phase, as it was the solid residue of everything what could have existed in the solution. Therefore, next sample was prepared from single crystals harvested from the solution exclusively. Prior to preparing the sample, several single-crystals were shortly measured at the diffractometer for proving to be the same compound by having the same cell parameters. The crystals were let to dry in the glove-box and ground. The as-obtained powder was used for measurements.

The data differed from the previous measurement (Appendix A, Fig. 8.7). Moreover, the powder X-ray diffraction pattern did not match with the calculated one of any of the two modifications, and did not show any crystallinity features. Most probably, the structure was destroyed either during evaporation of the solvent, or during mechanical grinding.

Finally, measurements of unground single crystals were performed. The crystals were placed into a Suprasil (or Parasil – quartz) ampoules, sealed under helium. The ampoule was placed into a brass sample holder and fixed. However, new problems emerged at this step. Since the measurement is performed in such a way that the ampoule placed vertically is vibrating, it can happen that the crystals are "jumping" during the measurement because the sample prepared in such a way is too loose. Next step would be to prepare a sample consisting of single crystals e.g. immersed in highly viscous oil (the problem would be to introduce the oil into a very narrow ampoule, few millimeters in diameter, without leaving oil residues on its wall, because it has to be sealed with a burner afterwards - i.e., avoid contamination during sealing off), or to measure a single crystal on a flat quartz sample holder. In the latter case, the crystal would have to be

immobilized, and besides, the transfer of the sample into the magnetometer would have to be performed on air.

Part V

Abstract

The present dissertation deals with the synthesis and characterization of fullerides. For the first time the so-called "break-and-seal" technique, used since 1970s in "living anionic polymerization" and for the synthesis of such highly air sensitive species in solution like alkalides and electrides, was applied. The method was modified exclusively for fulleride synthesis under highest purity conditions excluding any contaminations. The reaction, instead of using the conventional Schlenk-line, was performed in an all-glass apparatus under vacuum, avoiding the use of glass connections and use of grease. Besides the advantages mentioned above, the glassware could be heated completely under dynamic vacuum for getting rid of the possible organic impurities and moisture prior to each step of experiment, and the solutions prepared in such a way could have been stored for an incomparably longer time (years) than when prepared by conventional methods described in literature up to now. Reproducibility was very good. The "break-and-seal" method has one disadvantage: the preparation of the glassware and special purification of the educts is rather time consuming.

The modified "temperature difference method" was successfully used for growing single crystals from solution within a few days.

The problem of disorder is very often encountered for fullerides. In the present work, bulky cations – potassium complexed by crown-ethers – were used for overcoming this problem. It was shown that employment of "crowns" with aromatic groups favors "fixing" of the highly symmetrical C_{60} unit in the crystal structure.

Solutions of all fullerides were of dark intense "red wine" color, the crystals were obtained mostly as reddish-black thin platelets, although there were some needle-like, as well.

Six new potassium-containing fullerides have been synthesized.

In **[K(DB24C8)(DME)]$_2$C$_{60}$·(DME)** ($C2/c$, a = 31.133(4), b = 15.1271(18), c = 21.433(3) Å, β =117.506(2)°) the fullerene unit has a charge -2. C_{60} is disordered due to its location on a special position which does not coincide with the symmetry of the molecule, the two orientations being connected with each other by a rotation about a C_2-axis. The C_{60}^{2-} units are arranged in hexagonal layers parallel to the *ab* plane, forming distorted trigonal prisms. The fullerene anions and potassium cations develop a pseudobinary topology which is reminiscent of the CdI_2 structure type, where C_{60}^{2-} occupy the positions of cadmium, and potassium – those of iodine. The DB24C8 crown-ether is too big for potassium, therefore, the metal atom is additionally coordinated by one solvent molecule. The solvent – dimethoxyethane – is present in two different conformations in the structure: *trans* and *cis* - depending on whether it is isolated or coordinating the metal atom. Bond lengths' distribution in C_{60}^{2-} was examined. One

orientation of the dianion was found to match perfectly the one predicted by calculations.

$KC_{60}\cdot(THF)_5\cdot(THF)_2$ ($P2_12_12$, $a = 17.802(5)$, $b = 30.085(9)$, $c = 9.863(3)$ Å) crystallizes in a structure with fully ordered C_{60} units. $C_{60}^{\cdot-}$ anion-radicals and K^+ form ion pairs, potassium having shortest contacts to three contiguous carbon atoms from a C_{60} hexagon, the latter, therefore, having a hapticity of three. The ion pairs form corrugated layers in the *ac* crystallographic plane, the given compound being an example of a low-dimentional fulleride partial structure. Because of the rather high e.s.d.'s, it has not been possible to identify pronounced systematics in the bond lengths' distribution, although a dip in the distribution between (6:6) and (5:6) C-C bonds was clearly visible.

For the compound **$[K(DB24C8)(THF)]_2C_{60}\cdot THF$** ($Cc$, $a = 27.132(3)$, $b = 26.064(3)$, $c = 29.336(3)$ Å, $\beta = 117.523(2)°$) the structure solution was complicated by the disorder of crown-ether and solvent molecules which could not be overcome, although the C_{60}^{2-} unit was ordered.

$[K(DB24C8)(DME)]C_{60}$ fulleride ($Pna2_1$, $a = 27.485(5)$, $b = 16.662(3)$, $c = 25.503(5)$ Å) and **$[K(DB24C8)(DME)]_2[C_{60}]_2$** ($P2_1/c$, $a = 14.0145(2)$, $b = 25.0685(4)$, $c = 16.0233(3)$ Å, $\beta = 93.8040(10)°$), although have exactly the same composition, are not the same compounds. Thus, in these two structures crown-ethers crystallize in different conformations, and in the one the fullerene unit exists as a monomeric anion-radical, while in the other – as a dimer-dianion. The latter compound is an example of rather not many fulleride structures, where C_{60} exists in the form of dimers. The interfullerene C-C bond length is 1.57(3) Å. A temperature-dependent transformation from one structure to the other was not detected. An interesting feature was observed, i.e., the unusual behavior of one of the unit cell axes. On cooling from 270 K down, the *c*-axis increases, reaches a maximum at ca. 250 K and then decreases. The possibility for a phase transition was checked performing SQUID measurements from single crystals.

One more synthesized fulleride is **$[4\{K(DB18C6)(C_{60}^{\cdot-})\}(THF)_6]\cdot[C_{60}^{0}]\cdot(THF)_6$**. At temperatures above 220 K each of the four $C_{60}^{\cdot-}$ units exists in form of anion-radicals ($C2/c$, $a = 56.131(5)$, $b = 15.0591(14)$, $c = 36.310(3)$ Å, $\beta = 121.904(2)°$), and at lower temperatures – as a dimer-dianion ($C2$, $a = 49.055(11)$, b =15.0575(3), $c = 18.312(4)$ Å, $\beta = 97.892(2)°$), the interfullerene bond being 1.63(0) Å. The dimers are fully ordered. In addition, uncharged disordered C_{60} molecules are found, what follows from the charge balance. The low-temperature phase is a first example of a fulleride structure where fullerene exists in three different bonding states: anion-radical monomer, dianion-dimer, and neutral C_{60}. In the dimer, the pentagons adjacent to sp^3-hybridized carbon atoms, are in *trans*-conformation. This is a known fact from literature, as well, but no explanations for it have been given up to now. Only DFT calculations

were performed, for evaluating the energetical rotational barrier for such a dimer. The results obtained in the present work are in good agreement with literature data. But it is now for the first time that a localization of the negative charge on a small fragment of the C_{60} cage was found out, serving as additional evidence for the aromatization of this fragment. Knowing this, it becomes conclusive, considering the Coulombic repulsion, that the preferred orientation of two binded $C_{60}^{\cdot -}$ units is *trans*-orientation. Magnetic measurements were performed.

The method for fulleride synthesis used in the present work has a big potential for broadening by using different metals (e.g. alkali, alkali-earth), varying the complexing agents (crown-ethers, cryptands), as well as the organic solvent (or solvent mixtures).

Part VI

Zusammenfassung

Die vorliegende Dissertation handelt von der Synthese und Charakterisierung von Fulleriden. Zum ersten Mal wurde in diesem Zusammenhang die sogenannte "break-and-seal" Technik angewendet, die seit 1970 in anionischen Lebendpolymerisationen und in der Synthese von extrem luftempfindlichen Verbindungen in Lösung, wie Alkalide und Elektride, ihre Anwendung findet. Die Methode wurde speziell für die Synthese von Fulleriden unter höchsten Reinheitsbedingungen modifiziert. Die Reaktion wurde, anstatt mit der konventionellen Schlenk-Technik, in einer Voll-Glasapparatur unter Vakuum durchgeführt, um die Verwendung von Glasschliffen und Schlifffett zu vermeiden. Neben den oben erwähnten Vorteilen, kann die Glasapparatur vor jedem einzelnen Schritt eines Experiments, vollständig im dynamischen Vakuum ausgeheizt werden, um mögliche organische Verunreinigungen und Feuchtigkeit zu entfernen. Eine auf diese Weise hergestellte Lösung könnte für eine vergleichsweise längere Zeit (Jahre) aufbewahrt werden, als wenn sie nach konventionellen Methoden wie in der Literatur beschrieben hergestellt wäre. Die Reproduzierbarkeit ist sehr gut. Die "break-and-seal" Methode hat aber auch einen Nachteil: Die Herstellung der Glasapparaturen und besondere Reinigung der Edukte ist sehr zeitaufwendig.

Die modifizierte "Temperaturdifferenzmethode" wurde erfolgreich für die Zucht von Einkristallen aus Lösung innerhalb einiger Tage angewendet.

Häufig trifft man bei Fulleriden das Problem der Fehlordnung. Um dieses Problem zu umgehen, wurden in der vorliegenden Arbeit große Kationen — durch Kronenether komplexierte Kaliumionen — verwendet. Es konnte gezeigt werden, dass die Verwendung von Kronenethern mit aromatischen Gruppen die Fixierung der hochsymmetrischen C_{60} Einheit in der Kristallstruktur begünstigt.

Die Lösungen aller Fulleride waren intensiv dunkel-rot gefärbt. Obwohl auch einige nadelförmige Kristalle vorlagen, waren die meisten erhaltenen Kristalle rot-schwarze dünne Plättchen.

Es sind sechs neue Kalium-enthaltende Fulleride synthetisiert worden.

In **$[K(DB24C8)(DME)]_2C_{60}\cdot(DME)$** ($C2/c$, a = 31.133(4), b = 15.1271(18), c = 21.433(3) Å, β =117.506(2)°) hat die Fullereneinheit die Ladung 2-. Das C_{60} liegt auf einer speziellen kristallographischen Lage, welche nicht mit der Symmetrie des Molekühls übereinstimmt, und ist deshalb fehlgeordnet. Die zwei Orientierungen sind über eine Rotation um eine C_2-Achse ineinander überführbar. Die $C_{60}{}^{2-}$-Einheiten sind in hexagonalen Schichten parallel zur *ab*-Ebene angeordnet und bilden dabei verzerrte trigonale Prismen. Die Fullerenanionen und die Kaliumkationen bilden zusammen eine pseudobinäre Topologie, welche an die CdI_2-Struktur erinnert, wobei $C_{60}{}^{2-}$ die Positionen von Cadmium und Kalium die des Iodids besetzen. Der DB24C8-Kronenether ist zu

groß für Kalium, deshalb ist das Metallatom zusätzlich durch ein Lösungsmittelmolekühl koordiniert. Das Lösungsmittel - Dimethoxyethan - liegt in der Struktur in zwei verschieden Konformationen vor: *trans* und *cis*,- je nachdem ob es isoliert oder an das Metallatom koordiniert ist. Die Bindungslängenverteilung in C_{60}^{2-} wurde untersucht, wobei eine Orientierung des Dianions perfekt mit der durch quantenmechanische Rechnungen vorhergesagten Orientierung übereinstimmt.

KC_{60}·(THF)$_5$·(THF)$_2$ ($P2_12_12$, a = 17.802(5), b = 30.085(9), c = 9.863(3) Å) kristallisiert in einer Struktur mit vollständig geordneten C_{60}-Einheiten. Die $C_{60}^{\cdot-}$-Anion-Radikale und die K^+-Ionen bilden Paare, wobei die Kaliumionen kurze Kontakte zu drei angrenzenden Kohlenstoffatomen eines C_{60}-Sechsecks eingehen und somit eine Haptizität von drei aufweisen. Die Ionenpaare bilden gewellte Schichten parallel zur *ac*-Ebene, was die vorliegende Struktur zu einem Beispiel für eine Verbindung mit niedrigdimensionaler Fullerid-Teilstruktur macht. Aufgrund der relativ hohen Standardabweichungen war es hier nicht möglich, ein ausgeprägtes Muster in der Bindungslängenverteilung zu identifizieren, obwohl ein klarer Unterschied in der Häufigkeit der (6:6) im Vergleich zu (5:6) Bindungen gefunden wurde.

Die Strukturlösung für die Verbindung der Zusammensetzung **[K(DB24C8)(THF)]$_2$-C_{60}·THF** (Cc, a = 27.132(3), b = 26.064(3), c = 29.336(3) Å, β = 117.523(2)°) war durch die Fehlordnung der Kronenether- und Lösungsmittelmolekülen erschwert. Eine vollständige Strukturlösung war trotz geordneter C_{60}^{2-}-Einheiten hier nicht möglich.

Die Fulleride **[K(DB24C8)(DME)]C_{60}** ($Pna2_1$, a = 27.485(5), b = 16.662(3), c = 25.503(5) Å) und **[K(DB24C8)(DME)]$_2$[C_{60}]$_2$** ($P2_1/c$, a = 14.0145(2), b = 25.0685(4), c = 16.0233(3) Å, β = 93.8040(10)°) sind, trotz gleicher Zusammensetzung, unterschiedliche Verbindungen. So unterscheiden sich die Kronenether in diesen beiden Strukturen in ihren Konformationen und die Fullereneinheit liegt einmal als monomeres Anion-Radikal und das andere Mal als dimeres Dianion vor. Letztere Verbindung stellt eines der seltenen Beispiele einer Fulleridstruktur dar, in der C_{60} als Dimer vorliegt. Die interfulleren C-C-Bindungslänge beträgt 1.57(3) Å. Eine temperaturabhängige Umwandlung von der einen Struktur in die andere wird nicht beobachtet. Allerdings wurde eine interessante Eigenschaft beobachtet, nämlich das ungewöhnliche Verhalten einer Zellachse. Beim Abkühlen beginnend bei 270 K nimmt die Länge der c-Achse zunächst zu, erreicht bei ca. 250 K ein Maximum und nimmt dann wieder ab. Das Vorhandensein von Phasenübergängen wurde mittels SQUID-Messungen an Einkristallen überprüft.

Ein weiteres im Rahmen dieser Arbeit hergestelltes Fullerid ist **[4{K(DB18C6)-($C_{60}^{\cdot-}$)}(THF)$_6$]·[C_{60}^0]·(THF)$_6$**. Bei Temperaturen oberhalb von 220 K liegt jede der vier C_{60}^{2-} Einheiten als Radikal-Anion vor ($C2/c$, a = 56.131(5), b = 15.0591(14), c

= 36.310(3) Å, $\beta = 121.904(2)°$), bei niedrigeren Temperaturen hingegen zwei als dimeres Dianion ($C2$, $a = 49.055(11)$, b =15.0575(3), $c = 18.312(4)$ Å, $\beta = 97.892(2)°$). Die Interfullerenbindungslänge beträgt hier 1.63(0) Å. Die Dimere sind vollständig geordnet. Zusätzlich werden in der Struktur ungeladene C_{60}-Moleküle gefunden, was sich auch aus der Ladungsbilanz ergibt. Die Tieftemperaturphase ist das erste Beispiel einer Fulleridstruktur, in der Fullerene in drei unterschiedlichen Bindungszusänden vorliegen: als Radikal-anion Monomer, als Dianion-Dimer und als neutrales C_{60}. Im Dimer liegen die, den sp^3-hybridisierten Kohlenstoffatomen benachbarten, Fünfecke in *trans*-Konformation vor. Diese Beobachtung wird auch in der Literatur erwähnt, eine Erklärung dafür existiert bislang nicht. Es wurden nur DFT-Rechungen durchgeführt, um die Rotationsbarriere eines solchen Dimers zu bestimmen. Die in der vorliegenden Arbeit erhaltenen Ergebnisse stimmen gut mit diesen Literaturdaten überein. Allerdings wurde hier zum ersten Mal negative Ladung auf einem kleinen Teil des C_{60}-Käfigs lokalisiert, was einen zusätzlichen Hinweis für dessen Aromatizität liefert. Davon ausgehend leuchtet es ein, das, wenn man die Coulomb-Abstoßung betrachtet, die bevorzugte Orientierung zweier gebundener $C_{60}^{\cdot -}$-Einheiten die *trans*-Orientierung ist. Magnetische Messungen wurden ebenfalls durchgeführt.

Die in dieser Arbeit verwendete Methode zur Darstellung von Fulleriden hat ein großes Erweiterungspotenzial, beipielsweise durch Verwendung verschiedener Metalle (z.B. Alkali- und Erdalkalimetalle), Veränderung der Komplexierungsreagenzes (andere Kronenether und Kryptanden), sowie durch Veränderung des organischen Lösungsmittels bzw. durch Verwendung von Lösungsmittelgemischen.

Part VII

Bibliography

Bibliography

[1] K.S. Simeonov, K.Yu. Amsharov and M. Jansen. Connectivity of the Chiral D_2-Symmetric Isomer of C_{76} through a Crystal-Structure Determination of $C_{76}Cl_{18}{\cdot}TiCl_4$. *Angew. Chem. Int. Ed. Engl.*, 46:8419, 2007.

[2] K.S. Simeonov, K.Yu. Amsharov and M. Jansen. Chlorinated Derivatives of C_{78}-Fullerene Isomers with Unusually Short Intermolecular Halogen-Halogen Contacts. *Chem. Eur. J.*, 14:9585, 2008.

[3] K.S. Simeonov, K.Yu. Amsharov, E. Krokos and M. Jansen. An Epilogue on the C_{78}-Fullerene Family: the Discovery and Characterization of an Elusive Isomer. *Angew. Chem. Int. Ed. Engl.*, 47:6283, 2008.

[4] K.S. Simeonov, K.Yu. Amsharov and M. Jansen. $C_{80}Cl_{12}$: a Chlorine Derivative of the Chiral D_2-C_{80} Isomer - Empirical Rationale of Halogen-atom Addition Pattern. *Chem. Eur. J.*, 15:1812, 2009.

[5] M.S. Dresselhaus, G. Dresselhaus and P.C. Eklund. Fullerene Chemistry and Electrochemistry. In M.S. Dresselhaus, G. Dresselhaus and P.C. Eklund, editor, *Science of Fullerenes and Carbon Nanotubes: Their Properties and Applications*, pages 292–328. Academic Press Inc., San Diego, 1996.

[6] S.R. Wilson, D.I. Schuster, B. Nuber, M.S. Meier, M. Maggini, M. Prato and R. Taylor. Organic Chemistry of Fullerenes. In K.M. Kadish and R.S. Ruoff, editor, *Fullerenes: Chemistry, Physics and Technology*, pages 91–176. John Wiley and Sons, Inc., New York, 2000.

[7] A. Hirsch and M. Brettreich, editor. *Fullerenes: Chemistry and Reactions*. Wiley-VCH, Weinheim, 2005.

[8] F. Langa and P. de la Cruz. Basic Principles of the Chemical Reactivity of Fullerenes. In F. Langa and J.-F. Nierengarten, editor, *Fullerenes: Principles and Applications*, RSC Nanoscience and Nanotechnology, pages 15–50. The Royal Society of Chemistry, Thomas Graham House, Cambridge, 2007.

[9] L. Echegoyen, F. Diederich and L.E. Echegoyen. Electrochemistry of Fullerenes. In K.M. Kadish and R.S. Ruoff, editor, *Fullerenes: Chemistry, Physics and Technology*, pages 1–52. John Wiley and Sons, Inc., New York, 2000.

[10] C.A. Reed and R.D. Bolskar. Discrete Fulleride Anions and Fullerenium Cations. *Chem. Rev.*, 100:1075, 2000.

[11] K. Prassides and S. Margadonna. Structures of Fullerene-based Solids. In K.M. Kadish and R.S. Ruoff, editor, *Fullerenes: Chemistry, Physics and Technology*, pages 555–610. John Wiley and Sons, Inc., New York, 2000.

[12] L. Forró and L. Mihály. Electronic properties of Doped Fullerenes. *Rep. Prog. Phys.*, 64:649, 2001.

[13] Y. Iwasa and T. Takenobu. Superconductivity, Mott-Hubbard States and Molecular Orbital Order in Intercalated Fullerides. *J. Phys.: Condens. Matter*, 15:R495, 2003.

[14] K. Himmel and M. Jansen. Synthesis and Single-Crystal Structure Analysis of $[Ba(NH_3)_7]C_{60}{\cdot}NH_3$. *Inorg. Chem.*, 37:3437, 1998.

[15] K. Himmel and M. Jansen. Synthesis of $[Ni(NH_3)_6]C_{60}{\cdot}6NH_3$ via Ion Exchange in Liquid Ammonia - a New, Versatile Access to Ionic Fullerides. *Chem. Commun.*, 11:1205, 1998.

[16] K. Himmel and M. Jansen. Synthese und Einkristallstrukturanalyse von Bis(benzyltrimethylammonium)-fullerid-Ammoniakat; $(BzlNMe_3)_2C_{60}{\cdot}3NH_3$. *Z. Anorg. Allg. Chem.*, 624:1, 1998.

[17] K. Himmel and M. Jansen. On the Geometry of the Fulleride Dianion $C_{60}{}^{2-}$ in Crystalline Fullerides - Syntheses and Crystal Structures of $[M(NH_3)_6]C_{60}{\cdot}6NH_3$ ($M = Mn^{2+}$, Cd^{2+}). *Eur. J. Inorg. Chem.*, page 1183, 1998.

[18] H. Brumm and M.Jansen. Synthese und Einkristallstrukturanalyse von $[M(NH_3)_6]C_{60}{\cdot}6NH_3$ ($M = Co^{2+}$, Zn^{2+}). *Z. Anorg. Allg. Chem.*, 627:1433, 2001.

[19] H. Brumm, E. Peters and M. Jansen. Linear Polymeric $C_{70}{}^{2-}$ Ions. *Angew. Chem. Int. Ed. Engl.*, 40:2069, 2001.

[20] M. Panthöfer, U. Wedig, H. Brumm and M. Jansen. Geometric and Electronic Structure of Polymeric C_{70}-Fullerides: the Case of $[_\infty{}^1C_{70}{}^{3-}]$. *Solid State Sci.*, 6:619, 2004.

[21] T.F. Fässler, A. Spiekermann, M.E. Spahr and R. Nesper. Unprecedented Layered Structure of a Fulleride: Synthesis, Structure, amd Magnetic Pproperties of a Potassium-containing Salt with a C_{60}^{2-} Counterion. *Angew. Chem. Int. Ed. Engl.*, 36:486, 1997.

[22] Th.F. Fässler, R. Hoffmann, S. Hoffmann and M. Wörle. Triple-Decker Type Coordination of a Fullerene Trianion in $[K([18]crown\text{-}6)]_3$-$[\eta^6,\eta^6\text{-}C_{60}](\eta^3\text{-}C_6H_5CH_3)_2$ - Single Crystal Structure and Magnetic Properties. *Angew. Chem. Int. Ed. Engl.*, 39:2091, 2000.

[23] S.D. Hoffmann and T.F. Fässler. Synthesis and Crystal Structure Analysis of C_{60} Fulleride Dianions in Solvates of $[A([2.2.2]crypt)]_2[C_{60}]$ (A = K, Rb, Cs). *Z. Naturforsch.*, 59b:1579, 2004.

[24] A. Hönnerscheid, L. van Wüllen, M. Jansen, J. Rahmer and M. Mehring. Dimerformation in the Bis(arene)chromium Fulleride $Cr(C_7H_8)_2C_{60}$. *J. Chem. Phys.*, 115:7161, 2001.

[25] A. Hönnerscheid, R. Dinnebier and M. Jansen. Reversible Dimerization of C_{60} Molecules in the Crystal structure of the bis(arene)chromium Fulleride $[Cr(C_7H_8)]_2C_{60}$. *Acta Cryst. B*, 58:482, 2002.

[26] A. Hönnerscheid, L. van Wüllen, R. Dinnebier, M. Jansen, J. Rahmer and M. Mehring. Evidence for C_{60} Dimerisation in the Fulleride $[Cr(C_9H_{12})_2]^+C_{60}^-$. *J. Phys. Chem. Chem. Phys.*, 6:2454, 2004.

[27] D.V. Konarev, S.S. Khasanov, A. Otsuka and G. Saito. The Reversible Formation of a Single-bonded $(C_{60}^-)_2$ Dimer in Ionic Charge Transfer Complex: $Cp^*_2Cr{\cdot}C_{60}(C_6H_4Cl_2)_2$. The Molecular Structure of $(C_{60}^-)_2$. *J. Am. Chem. Soc.*, 124:8520, 2002.

[28] D.V. Konarev, S.S. Khasanov, G. Saito, A. Otsuka, Y. Yoshida and R.N. Lyubovskaya. Formation of Single-Bonded $(C_{60}^-)_2$ and $(C_{70}^-)_2$ Dimers in Crystalline Ionic Complexes of Fullerenes. *J. Am. Chem. Soc.*, 125:10074, 2003.

[29] D.V. Konarev, S.S. Khasanov, A.Y. Kovalevsky, G. Saito, A. Otsuka and R.N. Lyubovskaya. Structural Aspects of Two-stage Dimerization in an Ionic C_{60} Complex with Bis(benzene)chromium: $Cr(C_6H_6)_2{\cdot}C_{60}{\cdot}C_6H_4Cl_2$. *Dalton Trans.*, page 3716, 2006.

[30] J.L. Dye, C.W. Andrews and S.E. Mathews. Strategies for the Preparation of Compounds of Alkali Metal Anions. *J. Phys. Chem.*, 79:3065, 1975.

[31] J.L. Dye. Compounds of Alkali Metal Ions. *Angew. Chem. Int. Ed. Engl.*, 18:587, 1979.

[32] J.L. Dye. Preparation and Analysis of Metal/Solvent Solutions and the Formation of Alkali Metal Anions. *J. Phys. Chem.*, 84:1084, 1980.

[33] J.L. Dye. Recent Developments in the Synthesis of Alkalides and Electrides. *J. Phys. Chem.*, 1984:3842, 1984.

[34] M. Szwarc, editor. *Carbanions, Living Polymers and Electron Transfer Process.* Wiley-Interscience, New York, 1968.

[35] D.F. Shriver, editor. *The Manipulation of Air-sensitive Compounds.* McGraw-Hill Book Company, New York, 1969.

[36] H.W. Kroto, J.R. Heath, S.C. O'Brien, R.F. Curl and R.E. Smalley. C_{60}: Buckminsterfullerene. *Nature*, 318:162, 1985.

[37] W. Krätschmer, L.D. Lamb, K. Fostiropoulos and D.R. Huffman. Solid C_{60}: a New Form of Carbon. *Nature*, 347:354, 1990.

[38] D.E. Jones. *New Scientist*, 35:245, 1966.

[39] W.E. Barth and R.G. Lawton. Dibenzo[ghi,mno]fluoranthene. *J. Am. Chem. Soc.*, 88:380, 1966.

[40] E. Osawa. *Kagaku (Kyoto)*, 25:854, 1970.

[41] D.A. Bochvar and E.G.Galpern. Hypothetical Systems: Carbododecahedron, S-Icosahedron and Carbo-S-Icosahedron. *Dokl. Akad. Nauk SSSR*, 209:610, 1973.

[42] I.V. Stankevich, M.V. Nikerov and D.A. Bochvar. Structural Chemistry of Crystal Carbon: Geometry, Stability, Electronic Spectrum. *Uspekhi Khimii*, 53:1101, 1984.

[43] I. Hargittai. Wolfgang Krätschmer. In *Candid Science: Conversations with Famous Chemists*, pages 388–403. Imperial College Press, London, 2000.

[44] E.A. Rohlfing, D.M. Cox and A. Kaldor. Producion and Characterization of Supersonic Carbon Cluster Beams. *J. Chem. Phys.*, 81:3322, 1984.

[45] A.C. Cheung, D.M. Rank, C.H. Towmes, D.D. Thornton and W.J. Welch. Detection of NH_3 Molecules in Interstellar Medium by Their Microwave Emission. *Phys. Rev. Lett.*, 21:1701, 1968.

[46] H. Kroto. Symmetry, Space, Stars, and C_{60} (Nobel lecture). *Angew. Chem. Int. Ed. Engl.*, 36:1579, 1997.

[47] B.E. Turner. Detection of Interstellar Cyanoacetylene. *Astrophys. J*, 163:L35, 1971.

[48] L.W. Avery, N.W.Broten, J.M. MacLeod, T. Oka and H.W. Kroto. Detection of Heavy Interstellar Molecule Cyanodiacetylene. *Astrophys. J*, 205:L173, 1976.

[49] N.W. Broten, T. Oka, L.W. Avery, J.M. MacLeod and H.W. Kroto. The Detection of HC_9N in Interstellar Space. *Astrophys. J*, 223:L105, 1978.

[50] R.E. Smalley. Discovering the Fullerenes (Nobel lecture). *Angew. Chem. Int. Ed. Engl.*, 36:1595, 1997.

[51] I. Hargittai. Richard E. Smalley. In *Candid Science: Conversations with Famous Chemists*, pages 362–373. Imperial College Press, London, 2000.

[52] I. Hargittai. Robert F. Curl. In *Candid Science: Conversations with Famous Chemists*, pages 374–387. Imperial College Press, London, 2000.

[53] I. Hargittai. Harold W. Kroto. In *Candid Science: Conversations with Famous Chemists*, pages 332–357. Imperial College Press, London, 2000.

[54] R.B. Fuller, editor. *Synergetics: Explorations in the Geometry of Thinking*. Macmillan, New York, 1975.

[55] D.L.D. Caspar and A. Klug. Physical Principles in the Construction of regular Viruses. *Cold Spring Harbor Simposia on Quantitative Biology*, 27:1, 1962.

[56] S.J. Cyvin, E. Brendsal, B.N. Cyvin and J. Brunvoll. Molecular Vibrations of Footballene. *Chem. Phys. Lett.*, 143:377, 1998.

[57] W. Krätschmer, K. Fostiropoulos and D.R. Huffman. The Infrared and Ultraviolet Absorption Spectra of Laboratory-produced Carbon Dust: Evidence for the Presence of the C_{60} Molecule. *Chem. Phys. Lett.*, 170:167, 1990.

[58] A. Hirsch and M. Brettreich. Fullerene Production. In *Fullerenes: Chemistry and reactions*, pages 6–19. Wiley-VCH, Weinheim, 2005.

[59] T. Grösser, Dissertation, University of Tübungen, 1992.

[60] R. E. Haufler, J. Conceicao, L. P. F. Chibante, Y. Chai, N. E. Byrne, S. Flanagan, M. M. Haley, S. C. O'Brien, C. Pan, Z. Xiao, W. E. Billups, M. A. Ciufolini, R. H. Hauge, J. L. Margrave, L. J. Wilson, R. F. Curl, and R. E. Smalley. Efficient Production of C_{60} (Buckminsterfullerene), $C_{60}H_{36}$, and the Solvated Buckide Ion. *J. Phys. Chem.*, 94:8634, 1990.

[61] L.P.F. Chibante, A. Thess, J.M. Alford, M.D. Diener and R.E. Smalley. Solar Generation of the Fullerenes. *J. Phys. Chem.*, 97:8696, 1993.

[62] A. Weston, M. Murthy and S. Lalvani. Synthesis of Fullerenes from Coal. *Fuel Process. Technol.*, 45:203, 1995.

[63] M. Jansen, G. Peters and N. Wagner. Zur Bildung von Fullerenen und endohedralen Metallofullerenen: Darstellung im Hochfrequenzofen. *Z. Anorg. Allg. Chem.*, 621:689, 1995.

[64] G. Peters and M. Jansen. A New Fullerene Synthesis. *Angew. Chem. Int. Ed. Engl.*, 31:223, 1992.

[65] P.Gerhardt, S. Löffler and K.H. Homann. Polyhedral Carbon-Ions in Hydrocarbon Flames. *Chem. Phys. Lett.*, 137:306, 1987.

[66] P.Gerhardt, K.H. Homann. Ions and Charged Soot Particles in Hydrocarbon Flames. *J. Phys. Chem.*, 94:5381, 1990.

[67] J.B. Howard, J.T. McKinnon, Y. Makarovsky, A.l. Lafleur and M.E. Johnson. Fullerenes C_{60} and C_{70} in Flames. *Nature*, 352:139, 1991.

[68] J.M. Alford and J.D. Wright. *Book of abstracts, 212th ACS national meeting, Orlando, FL*, 1996.

[69] H. Takehara, M. Fujiwara, M.Arikawa, M.D. Diener and J.M. Alford. Experimental Study of Industrial Scale Fullerene Production by Combustion Synthesis. *Carbon*, 43:311, 2005.

[70] R. Taylor, G.J. Langley, H.W. Kroto and D.R.M. Walton. Formation of C_{60} by Pyrolysis of Naphtalene. *Nature*, 366:728, 1993.

[71] K.Yu. Amsharov and M. Jansen. Formation of Fullerenes by Pyrolysis of Perchlorofulvalene and its Derivatives. *Carbon*, 45:117, 2007.

[72] L.T. Scot, M.M. Hashemi, D.T. Meyer and H.B. Warren. Thermal Rearrangements of Aromatic Compounds. 14. Corannulene - a Convenient New Synthesis. *J. Am. Chem. Soc.*, 113:7082, 1991.

[73] S. Hagen, M.S. Bratcher, M.S. Erickson and G. Zimmermann. Novel Syntheses of Three $C_{30}H_{12}$ Bowl-Shaped Polycyclic Aromatic Hydrocarbons. *Angew. Chem. Int. Ed. Engl.*, 36:406, 1997.

[74] R.B.M. Ansems and L.T. Scott. Circumtrindene: a Geodesic Dome of Molecular Dimensions. Rational Synthesis of 60 percent of C_{60}. *J. Am. Chem. Soc.*, 122:2719, 2000.

[75] K.Yu. Amsharov and M. Jansen. C_{48} Buckybowl and C_{60} Fullerene Precursors on the Basis of Truxenone. *Z. Naturforsch. B*, 62:1497, 2007.

[76] K.Yu. Amsharov, K. Simeonov and M. Jansen. Formation of Fullerenes by Pyrolysis of 1,2'-Binaphthyl and 1,3-Oligonaphthylene. *Carbon*, 45:337, 2007.

[77] K.Yu. Amsharov and M. Jansen. A C_{78} Fullerene Precursor: Toward the Direct Synthesis of Higher Fullerenes. *J. Org. Chem.*, 73:2931, 2008.

[78] D.H. Parker, K. Chaterjee, P.Wurz, K.R. Lykke, M.J. Pellin and L.M. Stock. Fullerenes and Giant Fullerenes - Synthesis, Separation, and Mass Spectrometric Characterization. 30:1167, 1992.

[79] S. Iijima. Helical Microtubules of Graphitic Carbon. *Nature*, 354:56, 1991.

[80] T.W. Ebbesen and P.M. Ajayan. Large-scale Synthesis of Carbon Nanotubes. *Nature*, 358:220, 1992.

[81] T. Jovanovic, D. Koruga, B. Jovancicevic, J. Simic-Krstic. Modifications of Fullerenes Extractions and Chromatographies with Different Solvents. *Fullerenes, Nanotubes and Carbon Nanostructures*, 11:383, 2003.

[82] L. Saffaro. Cosmoids, Fullerenes and Continuous Polygons. In C. Taliani, G. Ruani and R. Zamboni, editor, *Proc. of the First Italian Workshop on Fullerenes: Status and Perspectives*, volume 2, page 55. World Scientific, Singapore, 1992.

[83] F. Chung and S. Strernberg. Mathematics and the Buckyball. *American Scientist*, 81:56, 1993.

[84] L. Euler. Elementa Doctrinae Solidorum. *Novi Commentarii Academiae Scientiarum Petropolitanae (Read in November 1750)*, 4:109–140, 1758.

[85] L. Euler. Demonstratio Nonnullarum Insignium Proprietatum Quibus Solida Hedris Planis Inclusa sunt Praedita. *Novi Commentarii Academiae Scientiarum Petropolitanae (Read in September 1751)*, 4:140–160, 1758.

[86] L. Euler. Specimen de usu Observationum in Mathesi Pura. *Novi Commentarii Academiae Scientiarum Petropolitanae (Read in September 1751)*, 6:185–230, 1756-7.

[87] P.W. Fowler and D.E. Manolopoulos. Fullerene Cages. In *An Atlas of Fullerenes*, The International Series of Monographs in Chemistry, pages 15–42. Oxford University Press Inc., New York, 1995.

[88] A. Hirsch and M. Brettreich. Structres. In *Fullerenes: Chemistry and reactions*, page 29. Wiley-VCH, Weinheim, 2005.

[89] T.G. Schmalz, W.A. Seitz, D.J. Klein and G.E. Hite. C_{60} Carbon Cages. *Chem. Phys. Lett.*, 130:203, 1986.

[90] H.W. Kroto. The Stability of the Fullerenes C_n, with n = 24, 28, 32, 36, 50, 60 and 70. *Nature*, 329:529, 1987.

[91] H.D. Beckhaus, C. Ruchardt, M. Kao, F. Diederich and C.S. Foote. The Stability of Buckminsterfullerene (C_{60}): Experimental Determination of the Heat of Formation. *Angew. Chem. Int. Ed. Engl.*, 31:63, 1992.

[92] H. Ajie, M.M. Alvarez, S.J. Anz, R.D. Beck, F. Diederich, K. Fostiropoulos, D.R. Huffman, W. Krätschmer, Y. Rubin, K.E. Shriver, D. Sensharma and R.L. Whetten. Characterization of the Soluble All-carbon Molecules C_{60} and C_{70}. *J. Phys. Chem.*, 94:8630, 1990.

[93] R.F. Curl. On the Formation of Fullerenes. *Phil. Trans. Royal Soc. London. Series A: Math., Phys., Eng. Sci.*, 343:19, 1993.

[94] H.D. Beckhaus, S. Verevkin, C. Ruchardt F. Diederich, C. Thilgen, H.U. Termeer, H. Mohn and W. Muller. C_{70} is more Stable than C_{60}: Experimental Determination of the Heat of Formation of C_{70}. *Angew. Chem. Int. Ed. Engl.*, 33:996, 1994.

[95] C.S. Yannoni, P.P. Bernier, D.S. Bethune, G. Meier and J.R. Salem. NMR Determination of the Bond Lengths in C_{60}. *J.Am. Chem. Soc.*, 113:3190, 1991.

[96] M.S. Dresselhaus, P.C. Eklund, G. Dresselhaus, editor. *Science of Fullerenes and Carbon Nanotubes: Their Properties and Applications.* Academic Press Inc., San Diego, 1996.

[97] D. A. Neumann, J. R. D. Copley, R. L. Cappelletti, W. A. Kamitakahara, R. M. Lindstrom, K. M. Creegan, D. M. Cox, W. J. Romanow, N. Coustel, J. P. McCauley, Jr., N. C. Maliszewskyj, J. E. Fischer, and A. B. Smith, III. Coherent Quasielastic Neutron Scattering Study of the Rotational Dynamics of C_{60} in the Orientationally Disordered Phase. *Phys. Rev. Lett.*, 67:3808, 1991.

[98] R.F. Kiefl, J.W. Schneider, A. Macfarlane, K. Chow, T.L. Duty, T.L. Estlel, B. Hitti, R.L. Lichti, E.J. Ansaldo, C. Schwab, P.W. Percival, G. Wei, S. Wlodek, K. Kojima, W.J. Romanow, J.P. Mccauley, N. Coustel, J.E. Fischer and A.B. Smith. Molecular Dynamics of μ^+-C_{60} Radical in Solid C_{60}. *Phys. Rev. Lett.*, 68:1347, 1992.

[99] A. Dworkin, H. Szwarc, S. Leach, J.P. Hare, T.I. Dennis, H.W. Kroto, R. Taylor and D.R.M. Walton. Thermodynamic Evidence For a Phase Transition in Crystalline Fullerene C_{60}. *C.R. Acad. Sci II*, 312:979, 1991.

[100] W.I.F. David, R.M. Ibberson, J.C. Matthewman, K. Prassides, T.J.S. Dennis, J.P. Hare, H.W. Kroto, R. Taylor and D.R.M. Walton. Crystal Structure and Bonding of Ordered C_{60}. *Nature*, 353:147, 1991.

[101] P. Lu, X.P. Li, R.M. Martin. Ground State and Phase Transitions in Solid C_{60}. *Phys. Rev. Lett.*, 68:1551, 1992.

[102] R.S. Ruoff, D.S. Tse, R. Malhotra and D.C. Lorents. Solubility of Fullerene C_{60} in a Variety of Solvents. *J. Phys. Chem.*, 97:3379, 1993.

[103] M.V. Korobov and A.L. Smith. Solubility of the Fullerenes. In K.M. Kadish and R.S. Ruoff, editor, *Fullerenes: Chemistry, Physics and Technology*, pages 53–91. John Wiley and Sons, Inc., New York, 2000.

[104] R.J. Sension, A.Z. Szarka, G.R. Smith and R.M. Hochstrasser. Ultrafast Photoinduced Electron Transfer to C_{60}. *Chem. Phys. Lett.*, 185:179, 1991.

[105] Y. Wang. Photophysical Properties of Fullerenes and Fullerene/*N,N*-diethylaniline Charge-transfer Complexes. *J. Phys. Chem.*, 96:764, 1991.

[106] Y. Kubozono, H. Maeda, Y. Takabayashi, K. Hiraoka, T. Nakai, S. Kashino, S. Emura, S. Ukita and T. Sogabe. Extractions of Y@C60, Ba@C60, La@C60, Ce@C60, Pr@C60, Nd@C60, and Gd@C60 with Aniline. *J. Am. Chem. Soc.*, 118:6998, 1996.

[107] M.T. Beck and G. Mandi. Solubility of C_{60}. *Fullerene Sci. Technol.*, 5:291, 1997.

[108] A.I. Vogel, editor. *A Text-Book of Practical Organic Chemistry.* Longman, London, 1971.

[109] S.H. Maron and C.F. Prutton, editor. *Principles of Physical Chemistry.* Collier Macmillan, London, 1969.

[110] R.S. Ruoff, R. Malhotra, D.L. Huestis, D.S. Tse and D.C. Lorents. Anomalous Solubility of C_{60}. *Nature*, 362:140, 1993.

[111] M.V. Korobov, A.L. Mirakian, N.V. Avramenko, E.F. Valeev, I.S. Neretin, Y.L. Slovokhotov, A.L. Smith, G. Olofsson and R.S. Ruoff. C_{60}·Bromobenzene Solvate: Crystallographic and Thermochemical Studies and their Relationship to C_{60} Solubility in Bromobenzene. *J. Phys. Chem. B*, 102:3712, 1998.

[112] A.L. Smith, E. Walter, M.V. Korobov and O.L. Gurvich. Some Enthalpies of Solution of C_{60} and C_{70}. Thermodynamics of the Temperature Dependence of Fullerene Solubility. *J. Phys. Chem.*, 100:6775, 1996.

[113] R.C. Haddon, L.E. Brus, K. Raghavachari. Electronic Structure and Bonding in Icosahedral C_{60}. *Chem. Phys. Lett*, 125:459, 1986.

[114] Q. Xie, E. Perez-Cordero, L. Echegoyen. Electrochemical Detection of ${C_{60}}^{6-}$ and ${C_{70}}^{6-}$: Enhanced Stability of Fullerides in Solution. *J. Am. Chem. Soc.*, 114:3978, 1992.

[115] Y. Ohsawa, T. Saji. Electrochemical Detection of ${C_{60}}^{6-}$ at Low Temperature. *J. Chem. Soc. Chem. Commun.*, 10:781, 1992.

[116] F.Zhou, C.Jeboulet, A.J. Bard. Reduction and Electrochemistry of Fullerene C_{60} in Liquid Ammonia. *J. Am. Chem. Soc.*, 114:11004, 1992.

[117] J. Chlistunoff, D. Cliffel and A.J. Bard. Electrochemistry of Fullerenes. In H.S. Nalwa, editor, *Handbook of Organic Conductive Molecules and Polymers. Vol. 1. Charge-transfer Salts, Fullerenes and Photoconductors*, page 382. Wiley, New York, 1997.

[118] K. Tanigaki, T.W. Ebbesen, S. Saito, J. Mizuki, J. S. Tsai, Y. Kubo and S. Kuroshima. Superconductivity at 33 K in $Cs_xRb_yC_{60}$. *Nature*, 352:222, 1991.

[119] R. Sijbesma, G. Srdanov, F. Wudl, J.A. Castro, C. Wilkins, S.H. Friedman, D.L. DeCamp and G.L. Kenyon. Synthesis of Fullerene Derivative for the Inhibition of HIV Enzymes. *J. Am. Chem. Soc.*, 115:6510, 1993.

[120] I. Tuñón, E. Silla and J.L. Pasculal-Ahuir. Molecular Surface Area and Hydrophobic Effect. *Prot. Eng.*, 5:715, 1992.

[121] H. Sinohara. Endohedral Metallofullerenes. *Rep. Prog. Phys.*, 63:843, 2000.

[122] J. Simic-Krstic. Effects of $C_{60}(OH)_{24}$ on Microtubule Assembly. *Arch. Oncol.*, 5:143, 1997.

[123] L.Y. Chiang, *Eur. Pat. Appl.*, EP 770577. [CAS 127:34015], 1997.

[124] S.R. Wilson. Biological Aspects of Fullerenes. In K.M. Kadish and R.S. Ruoff, editor, *Fullerenes: Chemistry, Physics and Technology*, pages 437–465. John Wiley and Sons, Inc., New York, 2000.

[125] L.Y. Chiang, L.-Y. Wang, J.W. Swircewski, S. Soled and S. Cameron. Efficient Synthesis of Polyhydroxylated Fullerene Derivatives via Hydrolysis of Polycyclosulfated Precursors. *J. Org. Chem.*, 59:3960, 1994.

[126] I.V. Podol'skii, E.V. Kondrat'eva, I.V. Shcheglov, M.A. Dumpis and L.B. Piotrovskii. Fullerene C_{60} Complexed with Poly(N-vinyl-pyrrolidone) Prevents the Disturbance of Long-term Memory Consolidation. *Phys. Sol. State*, 44:552, 2002.

[127] F.N. Tebbe, J.Y. Becker, D.B. Chase, L.E. Firment, E.R. Holler, B.S. Malone, P.J. Krusic and E. Wasserman. Multiple, Reversible Chlorination of C_{60}. *J. Am. Chem. Soc.*, 113:9900, 1991.

[128] J. Nacsa, J. Segesdi, A. Gyuris, T. Braun, H. Rausch, A. Buvaári-Barcza, L. Barcza, J. Minarovits and J. Molnar. Antiretroviral effects of nonderivatized C_{60} in vitro. *Fullerene Sci. Technol.*, 5:696, 1997.

[129] J.W. Arbogast, A.P. Darmanyan, C.S. Foote, F.N. Diederich, R.L. Whetten, Y. Rubin, M.M. Alvarez, S.J. Anz. Photophysical Properties of C_{60}. *J. Phys. Chem.*, 95:11, 1991.

[130] J.G. Levy. Photodynamic Therapy. *Tibtech*, 13:14, 1995.

[131] K. Miyazawa, F. Matsuzaki, T. Hariki and M. Yamaguchi, *Jpn. Kokai Tokkyo Koho*, JP 09278625. [CAS 127:34015], 1997.

[132] G. Andrievsky; V. Klochkov and L. Derevyanchenko. Is the C_{60} Fullerene Molecule Toxic?! *Fullerenes, Nanotubes and Carbon Nanostructures*, 13:363, 2005.

[133] B. Halford. Fullerene for the Face. *Chem. Eng. News*, 84:47, 2006.

[134] D.W. Murphy, M.J. Rosseinsky, R.M. Fleming, R. Tycko, A.P. Ramirez, R.C. Haddon, T. Siegrist, G. Dabbagh, J.C. Tully and R.E. Walstedt. Synthesis and Characterization of Alkali Metal Fullerides: A_xC_{60}. *J. Phys. Chem. Solids*, 53:1321, 1992.

[135] T. Shiroka, M. Riccò, F. Barbieri, E. Zannoni and M. Tomaselli. Clustering and Polymerization of $Li_{15}C_{60}$. *Phys. Sol. State*, 44:498, 2002.

[136] M.J. Rosseinsky. Fullerene Intercalation Chemistry. *J. Mater. Chem.*, 5:1497, 1995.

[137] R.C. Haddon. Electronic Structure, Conductivity, and Superconductivity of Alkali-Metal Doped C_{60}. *Acc. Chem. Res.*, 25:127, 1992.

[138] O.Gunnarson. Superconductivity in Fullerides. *Rev. Mod. Phys.*, 69:575, 1997.

[139] V. Buntar, H.W. Weber. Magnetic Properties of Fullerene Superconductors. *Supercond. Sci. Technol.*, 9:599, 1996.

[140] K. Tanigaki, K. Prassides. Conducting and Superconducting Properties of Alkali-metal C_{60} Fullerides. *J. Mater. Chem.*, 5:1515, 1995.

[141] G. Oszlányi, G. Baumgartner, G. Faigel and L. Forró. Na_4C_{60}: an Alkali Intercalated Two-dimensional Polymer. *Phys. Rev. Lett.*, 78:4438, 1997.

[142] D.V. Konarev, S.S. Khasanov, A. Otsuka, G. Saito and R.N. Lyubovskaya. Negatively Charged π-$(C_{60}^-)_2$ Dimer with Biradical State at Room Temperature. *J. Am. Chem. Soc.*, 128:9292, 2006.

[143] D.V. Konarev, S.S. Khasanov, G. Saito, A. Otsuka and R.N. Lyubovskaya. Ionic and Neutral C_{60} Complexes with Coordination Assemblies of Metal Tetraphenylporphyrins, $M^{II}TPP_2$·DMP (M = Mn, Zn). Coexistence of $(C_{60}^-)_2$ Dimers Bonded by One and Two Single Bonds in the Same Compound. *Inorg. Chem.*, 46:7601, 2007.

[144] U. Wedig, H. Brumm and M. Jansen. Synthesis, Characterization, and Bonding Properties of Polymeric Fullerides $AC_{70}{\cdot}nNH_3$ (A = Ca, Sr, Ba, Eu, Yb). *Chem. Eur. J.*, 8:2769, 2002.

[145] S. Margadonna, K. Prassides, K.D. Knudsen, M. Hanfland, M. Kosaka and K. Tanigaki. High Pressure Polymerization of the Li-Intercalated Fulleride Li_3CsC_{60}. *Chem. Mater.*, 11:2960, 1999.

[146] K. Prassides, C.M. Brown, S. Margadonna, K. Kordatos, K. Tanigaki, E. Suard, A.J. Dianouxb and K.D. Knudsen. Powder Diffraction and Inelastic Neutron Scattering Studies of the Na_2RbC_{60} Fulleride. *J. Mater. Chem.*, 10:1443, 2000.

[147] P.W. Stephens, G. Bortel, G. Faigel, M. Tegze, A. Janossy, S. Pekker, G. Oszlany and L. Forro. Polymeric Fullerene Chains in RbC_{60} and KC_{60}. *Nature*, 370:636, 1994.

[148] A. F. Hebard, M. J. Rosseinsky, R. C. Haddon, D. W. Murphy, S. H. Glarum, T. T. M. Palstra, A. P. Ramirez and A. R. Kortan. Superconductivity at 18 K in Potassium-doped C_{60}. *Nature*, 350:600, 1991.

[149] F. Bensebaa, B. Xiang, L.Kevan. A New Preparation Method for Superconducting Alkali-metal Doped Fullerenes - Comparison of Ac Susceptibility and Low-field Microwave Absorption Characterization. *J. Phys. Chem.*, 96:6118, 1992.

[150] D. R. Buffinger, R. P. Ziebarth, V. A. Stenger, C. Recchia and C. H. Pennington. Rapid and Efficient Synthesis of Alkali Metal-C_{60} Compounds in Liquid Ammonia. *J. Am. Chem. Soc.*, 115:9267.

[151] H.H. Wang , A.M. Kini, B.M. Savall, K.D. Carlson, J.M. Williams, K.R. Lykke, P. Wurz, D.H. Parker, M.J. Pellin, D.M. Gruen, U. Welp, W.K. Kwok, S. Fleshler, G.W. Crabtree. 1st Easily Reproduced Solution-Phase Synthesis And Confirmation of Superconductivity in the Fullerene K_xC_{60} (T_c=18.0+/-0.1 K). *Inorg. Chem.*, 30:2838, 1991.

[152] S.P. Kelty, C.-C. Chen, C.M. Lieber. Superconductivity at 30 K in Caesium-doped C_{60}. *Nature*, 352:223, 1991.

[153] C.-C. Chen, S.P. Kelty and C.M. Lieber. $(Rb_xK_{1-x})_3C_{60}$ Superconductors: Formation of a Continuous Series of Solid Solutions. *Science*, 253:886, 1991.

[154] A.V. Nikolayev, K. Prassides, K.H. Michel. Charge Transfer and Polymer Phases in AC_{60} (A=K, Rb, Cs) Fullerides. *J. Chem. Phys.*, 108:4912, 1998.

[155] Q. Zhu, O. Zhou, J.E. Fischer, A.R. McGhie, W.J. Romanow, R.M. Strongin, M.A. Cichy and A.B. Smith III. Unusual Thermal Stability of a Site-ordered MC_{60} Rocksalt Structure (M=K, Rb, or Cs). *Phys. Rev. B*, 47:13948, 1993.

[156] S. Pekker, A. Janossy, L. Mihaly O. Chauvet, M. Carrard, and L. Forró. Single-Crystalline $(KC_{60})_n$: A Conducting Linear Alkali Fulleride Polymer. *Science*, 265:1077, 1994.

[157] D. Koller, M.C. Martin, P.W. Stephens, L. Mihaly, S. Pekker, A. Janossy, O. Chauvet and L. Forro. Polymeric Alkali Fullerides are Stable in Air. *Appl. Phys. Lett.*, 66:1015, 1995.

[158] M.C. Martin, D. Koller, X. Du, P.W. Stephens and L. Mihaly. Insulating and Conducting Phases of RbC_{60}. *Phys. Rev. B*, 49:10818, 1994.

[159] M.C. Martin and D. Koller. Infrared and Raman Evidence for Dimers and Polymers in RbC_{60}. *Phys. Rev. B*, 51:3210, 1995.

[160] Y. Iwasa, T. Arima, R.M. Fleming, T. Siegrist, O. Zhou, R.C. Haddon, L.J. Rothberg, K.B. Lyons, H.L. Carter Jr., A.F. Hebard, R. Tycko, G. Dabbagh, J.J. Krajewski, G.A. Thomas and T. Yagi. New Phases of C_{60} Synthesized at High Pressure. *Science*, 264:1570, 1994.

[161] G. Oszlanyi and L. Forro. Two-dimensional Polymer of C_{60}. *Solid State Commun.*, 93:265, 1995.

[162] M. Núñez-Regueiro, L. Marques, J.-L. Hodeau, O. Béthoux and M. Perroux. Polymerized Fullerite Structures. *Phys. Rev. Lett.*, 74:278, 1995.

[163] Q. Zhu, D.E. Cox and J.E. Fischer. Phase Transitions in KC_{60}: Dimer Formation via Rapid Quenching. *Phys. Rev. B*, 51:3966, 1995.

[164] G.Oszlany, G.Bortel, G. Faigel, M. Tegze, L. Granasy, S. Pekker, P.W. Stephens G. Bendele, R. Dinnebier, G. Mihaly, A. Janossy, O. Chauvet and L. Forro. Dimerization in KC_{60} and RbC_{60}. *Phys. Rev. B*, 51:12228, 1995.

[165] J.R. Morton, K.F. Preston, P.J. Krusic, S.A. Hill and E. Wasserman. The Dimerization of Fullerene RC_{60} Radicals [R = alkyl]. *J. Am. Chem. Soc.*, 114:5454, 1992.

[166] J.C. Hummelen, B. Knight, J. Pavlovich, R. González and F. Wudl. Isolation of the Heterofullerene $C_{59}N$ and Its Dimer $(C_{59}N)_2$. *Science*, 269:1554, 1995.

[167] F. Bommeli, L. Degiorgi, P. Wachter, O. Legeza, A. Janossy, G. Oszlanyi, O. Chauvet and L. Forro. Metallic Conductivity and Metal-insulator Transition in $(AC_{60})_n$ (A = K, Rb, and Cs) Linear Polymer Fullerides. *Phys. Rev. B*, 51:14794, 1995.

[168] J. Stinchcombe, A. Penicaud, P. Bhyrappa, P.D.W. Boyd and C.A. Reed. Buckminsterfulleride(1-) Salts: Synthesis, EPR, and the Jahn-Teller Distortion of C_{60}^{-}. *J. Am. Chem. Soc.*, 115:5212, 1993.

[169] A. Penicaud, A. Perez-Benites and R. Gleason. Electrocrystallizing C_{60}: Synthesis, Single Crystal X-ray Structure, and Magnetic (ESR, SQUID) Characterization of $[(C_6H_5)_4P]_2[C_{60}][I]_x$. *J. Am. Chem. Soc.*, 115:10392, 1993.

[170] U.Bilow and M. Jansen. Electrocrystallisation and Crystal Structure Determination of $Ph_4PC_{60}{\cdot}Ph_4PCl$. *J. Chem. Soc. Chem. Commun.*, page 403, 1994.

[171] U. Bilow und M. Jansen. Uber die Elektrokristallisation von Fulleriden. *Z. Anorg. Allg. Chem.*, 621:982, 1995.

[172] V.V. Gritenko, O.A. Dyachenko, G.V. Shilov, N.G. Spitsina and E.B. Yagubski. Crystal and Molecular Structures of New Fullerides, $(Ph_4P)_2C_{60}Hal$ (Hal = Br or I) and $(Ph_4As)_2C_{60}Cl$. *Russ. Chem. Bull.*, 46:1878, 1997.

[173] W.C. Wan, X. Liu, G.M. Sweeney and W.E. Broderick. Structural Evidence for the Expected Jahn-Teller Distortion in Monoanionic C_{60}: Synthesis and X-ray Crystal Structure of Decamethylnickelocenium Buckminsterfulleride. *J. Am. Chem. Soc.*, 117:9580, 1995.

[174] B. Nuber and A. Hirsch. A New Route to Nitrogen Heterofullerenes and the First Synthesis of $(C_{59}N)_2$. *Chem. Commun.*, page 1421, 1996.

[175] M. Keshavarz-K., R. González, R.G. Hicks, G. Srdanov, V.I. Srdanov, T.G. Collins, J.C. Hummelen, C. Bellavia-Lund, J. Pavlovich, F. Wudl and K. Holczer. Synthesis of Hydroazafullerene $C_{59}HN$, the Parent Hydroheterofullerene. *Nature*, 383:147, 1996.

[176] W. Andreoni, A. Curioni, K. Holczer, K. Prassides, M. Keshavarz-K., J.-C. Hummelen and F. Wudl. Unconventional Bonding of Azafullerenes: Theory and Experiment. *J. Am. Chem. Soc.*, 118:11335, 1996.

[177] C. M. Brown, L. Cristofolini, K. Kordatos, K. Prassides, C. Bellavia, R. González, M. Keshavarz-K., F. Wudl, A. K. Cheetham, J. P. Zhang, W. Andreoni, A. Curioni, A. N. Fitch and P. Pattison. On the crystal structure of azafullerene $(C_{59}N)_2$. *Chem. Mater.*, 8:2548, 1996.

[178] R. Tycko, G. Dabbagh, M.J. Rosseinsky et al. C-13 NMR Spectroscopy of K_xC_{60}: Phase Separation, Molecular Dynamics, and Metallic Properties. *Science*, 253:884, 1991.

[179] A.J. Fowkes, J.M. Fox, P.F. Henry, S.J. Heyes and M.J. Rosseinsky. Expanded Close-packed Fullerides: the Reactivity of Na_2C_{60} with Ammonia. *J. Am. Chem. Soc.*, 119:10413, 1997.

[180] P. Paul, Z. Xie, R. Bau, P.D.W. Boyd and C.A.Reed. Ordered Structure of a Distorted ${C_{60}}^{2-}$ Fulleride Ion. *J. Am. Chem. Soc.*, 116:4145, 1994.

[181] P.D.W. Boyd, P. Bhyrappa, P. Paul, J. Stinchcombe, R.D. Bolskar, Y.P. Sun and C.A. Reed. The ${C_{60}}^{2-}$ Fulleride Anion. *J. Am. Chem. Soc.*, 117:2907, 1995.

[182] M.J. Rosseinsky. Recent Developments in the Chemistry and Physics of Metal Fullerides. *Chem. Mater.*, 10:2665, 1998.

[183] J. G. Bednorz and K. A. Müller. Possible High T_c Superconductivity in the Ba-La-Cu-O System. *Z. Phys. B*, 64:189, 1986.

[184] A.F. Hebard, M.J. Rosseinsky, R.C. Haddon, D.W. Murphy, S.H. Glarum, T.T.M. Palstra, A.P. Ramirez and A.R. Kortan. Superconductivity at 18 K in potassium-doped C_{60}. *Nature*, 350:600, 1991.

[185] R.M. Fleming, A.P. Ramirez, M.J. Rosseinsky, D.W. Murphy, R.C. Haddon, S.M. Zahurak and A.V. Makhija. Relation of structure and superconducting transition temperatures in A_3C_{60}. *Nature*, 352:787, 1991.

[186] K. Tanigaki, I. Hirosawa, T.W. Ebbesen, J.I. Mizuki, J.-S. Tsai. Structure and Superconductivity of C_{60} Fullerides. *J. Phys. Chem. Sol.*, 54:1645, 1994.

[187] T.M. Palstra, O. Zhou, Y. Iwasa, P.E. Sulewski, R.M. Fleming and B.R. Zegarski. Superconductivity at 40 K in Caesium Doped C_{60}. *Solid State Commun.*, 93:327, 1995.

[188] T. Yildirim, L. Barbedette, J.E. Fischer, C.L. Lin, J. Robert, P. Petit, and T.T.M. Palstra. T_c vs Carrier Concentration in Cubic Fulleride Superconductors. *Phys. Rev. Lett.*, 77:167, 1996.

[189] S. Margadonna, K. Prassides. Recent Advances in Fullerene Superconductivity. *J. Sol. St. Chem.*, 168:639, 2002.

[190] V. Buntar. Superconductivity in Fullerenes. In K.M. Kadish and R.S. Ruoff, editor, *Fullerenes: Chemistry, Physics and Technology*, pages 691–767. John Wiley and Sons, Inc., New York, 2000.

[191] P.-M. Allemand, K.C. Khemani, A. Koch, F. Wudl, K. Holczer, S. Donovan, G. Grüner and J.D. Thompson. Organic Molecular Soft Ferromagnetism in Fullerene C_{60}. *Science*, 253:301, 1991.

[192] P.W. Stephens, D. Cox, J.W. Lauher, L. Mihaly, J.B. Wiley, P.-M. Allemand, A. Hirsch, K. Kolczer, Q. Li, J.D. Thompson and F. Wudl. Lattice Structure of the Fullerene Ferromagnet TDAE-C_{60}. *Nature*, 355:331, 1992.

[193] F. Wudl, J.D. Thompson. Buckminsterfullerene C_{60} and Organic Ferromagnetism. *J. Phys. Chem. Solids*, 53:1449, 1992.

[194] Bruker Suite, Version 2008/3, Bruker AXS Inc., Madison, USA, 2008.

[195] G.M. Sheldrick, SADABS - *Bruker AXS Area Ddetector Scaling and Absorption*, Version 2007/4, University of Göttingen, Germany, 2007.

[196] G.M. Sheldrick. A Short History of ***SHELX***. *Acta Cryst., Sect. A*, 64:112, 2008.

[197] M.J. Frisch, G.W. Trucks, H.B. Schlegel, G.E. Scuseria, M.A. Robb, J.R. Cheeseman, J.A. Montgomery, T. Vreven, G. Scalmani, K.N. Kudin, S.S. Iyengar, J. Tomasi, V. Barone, B. Mennucci, M. Cossi, N. Rega, G.A. Petersson, H. Nakatsuji, M. Hada, M. Ehara, K. Toyota, R. Fukuda, J. Hasegawa, M. Ishida, T. Nakajima, Y. Honda, O. Kitao, H. Nakai, X. Li, H.P. Hratchian, J.E. Peralta, A.F. Izmaylov, E. Brothers, V. Staroverov, R. Kobayashi, J. Normand, J.C. Burant, J.M. Millam, M. Klene, J.E. Knox, J.B. Cross, V. Bakken, C. Adamo, J. Jaramillo, R. Gomperts, R.E. Stratmann, O. Yazyev, A.J. Austin, R. Cammi, C. Pomelli, J.W. Ochterski, P.Y. Ayala, K. Morokuma, G.A. Voth, P. Salvador, J.J. Dannenberg, V.G. Zakrzewski, S. Dapprich, A.D. Daniels, M.C. Strain, O. Farkas, D.K. Malick, A.D. Rabuck, K. Raghavachari, J.B. Foresman, J.V. Ortiz, Q. Cui, A.G. Baboul, S. Clifford, J. Cioslowski, B.B. Stefanov, G. Liu, A. Liashenko, P. Piskorz, I. Komaromi,

R.L. Martin, D.J. Fox, T. Keith, M. A. Al-Laham, C.Y. Peng, A. Nanayakkara, M. Challacompe, W. Chen, M.W. Wong, and J. A. Pople, Gaussian 03, Revision C.02, Gaussian, Inc., Wallingford CT., 2004.

[198] D. Trinschek and M. Jansen. A New and Simple Route to Alkali Metal Oxometallates. *Angew. Chem. Int. Ed.*, 38:133, 1999.

[199] M. Wu, X. Wei, L. Qi and Z. Xu. A New Method for Facile and Selective Generation of C_{60}^{-} and C_{60}^{2-} in Aqueous Caustic/THF (or DMSO). *Tetrahedron Lett.*, 37:7409, 1996.

[200] Z.Jedlinski, A.Stolarchewicz, Z.Grobelny. Decomposition of 18-Crown-6 Solutions in Tetrahydrofurane Containing Dissolved Potassium. *Makromol. Chem.*, 187:795, 1986.

[201] H. Arend, R. Perret, H. Wüst and P. Kerkoc. On the Solution Growth of Single Crystals of Solid Solutions. *J. Cryst. Growth*, 74:321, 1986.

[202] W.S.Wang, J.Hulliger and H.Arend. Soluiton Growth of Molecular Crystals: Exploratory Techniques. *Ferroelectrics*, 92:113, 1989.

[203] J. Hulliger. Chemistry and Crystal Growth. *Angew. Chem. Int. Ed. Engl.*, 33:143, 1994.

[204] O.König, P.Rechsteiner, B.Trusch, C.Andreoli and J.Hulliger. Equipment for Controlling Nucleation and Tailoring the Size of Solution-growth Single Crystals. *J. Appl. Cryst.*, 30:507, 1997.

[205] G. Stollhoff, M. Jansen and R. Ahlrichs. Jahn-Teller Distortion and the Electronic Ground State of C_{60}^{2-}, *Science, submitted*.

[206] C. Janiak, S. Mühle, H. Hemling and K. Köhler. The Solid-State Structure of $K_3C_{60}(THF)_{14}$. *Polyhedron*, 15:1559, 1996.

[207] G.A. Domrachev, Y.A. Shevelev, V.K. Cherkasov, G.K. Fukin, S.Y. Khorshev, G.V. Markin, B.S. Kaverin, V.L. Karnatsevich, G.A. Kirkin. Synthesis, Structure, and Thermodestruction of Bis(arene)chromium(l) Fullerides. *Doklady Chemistry*, 395:74, 2004.

[208] K.H. Lee, S.S. Park, Y. Suh, T. Yamabe, E. Osawa, H.P. Lüthi, P. Gutta and C. Lee. Similarities and Differences between $(C_{60})_2^{2-}$ and $(C_{59}N)_2$ Conformers. *J. Am. Chem. Soc.*, 123:11085, 2002.

Part VIII

Appendix A

8 Additional data on different compounds

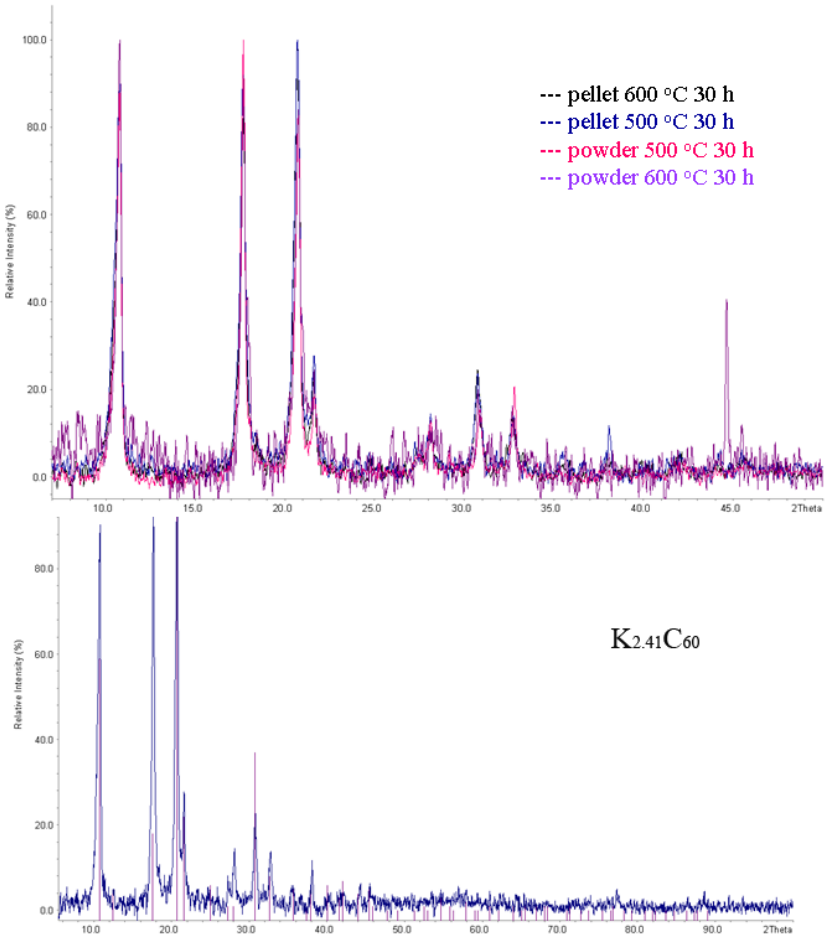

Figure 8.1: Powder XRD pattern obtained for the intercalated fullerides prepared along the azide-nitrate route.

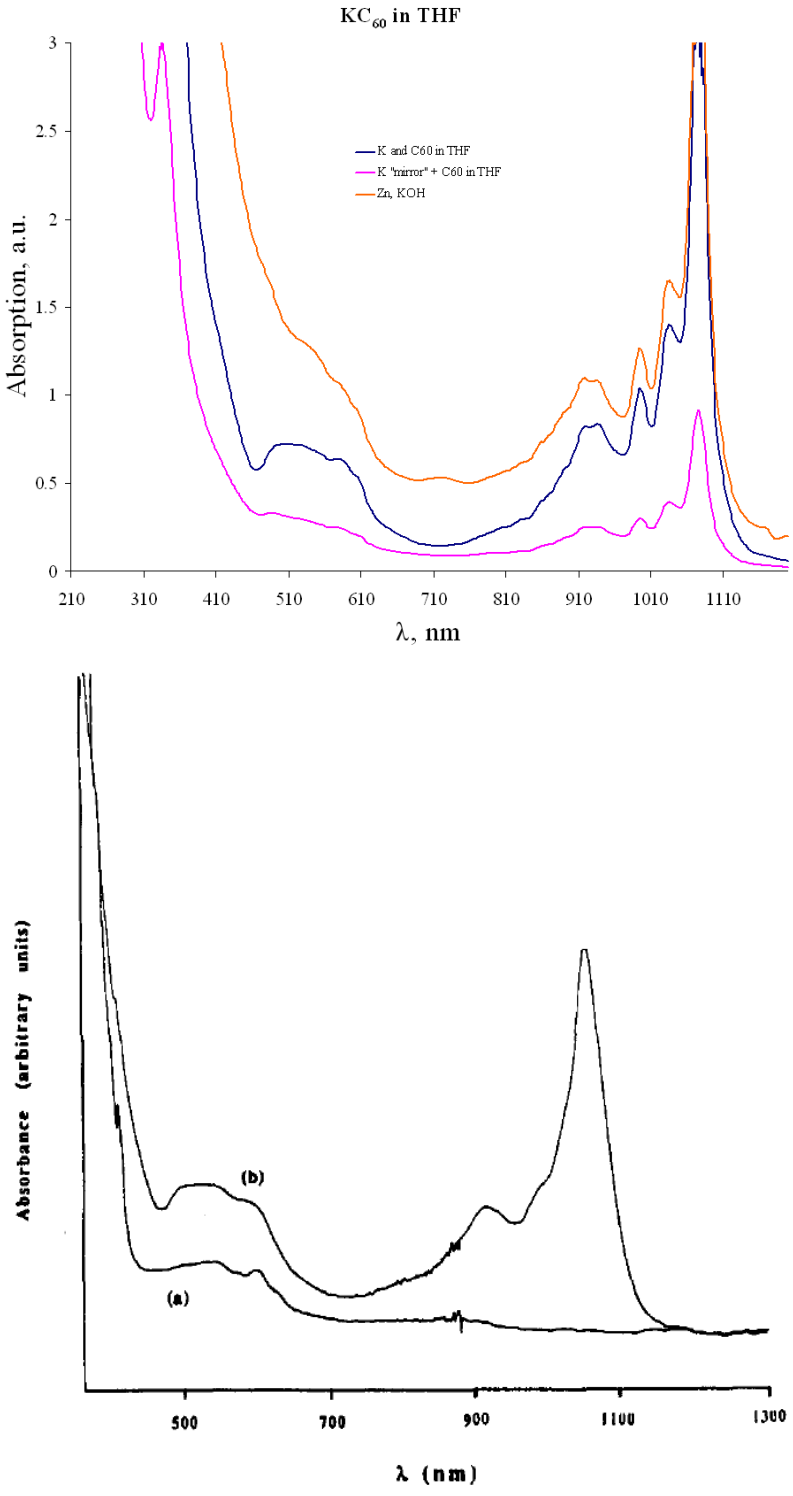

Figure 8.2: UV/Vis/NIR spectra of the fulleride solutions obtained (left) and comparison with the literature data (right).

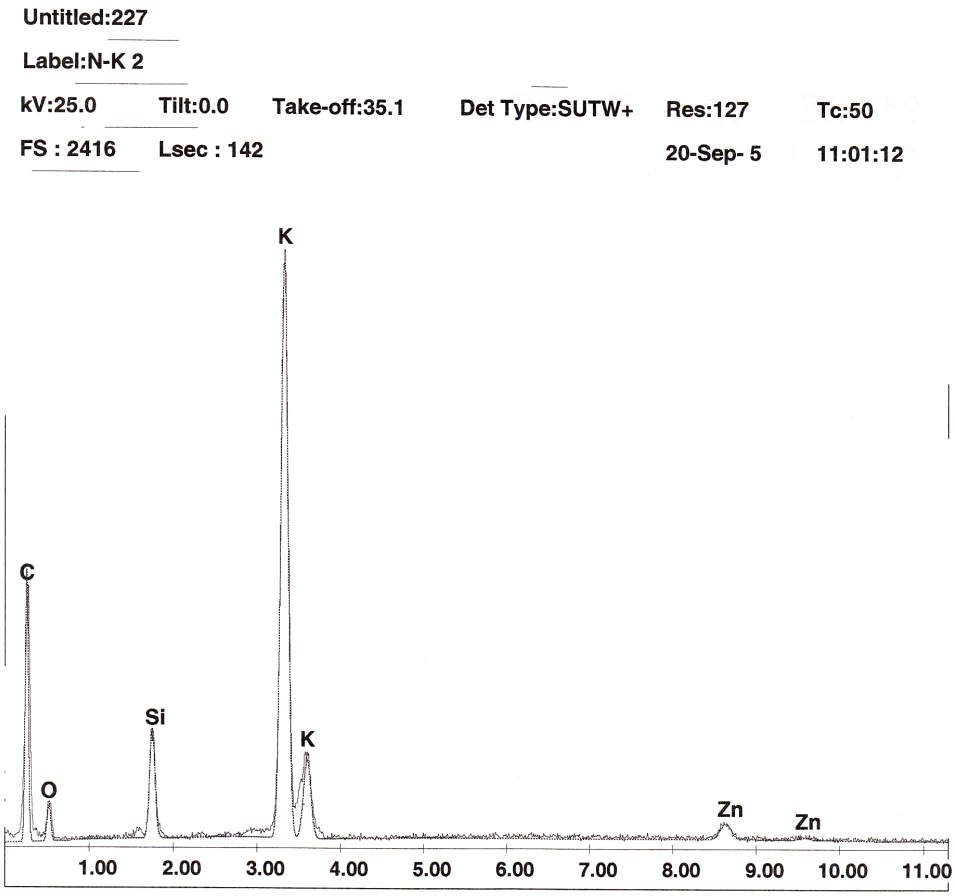

EDAX ZAF Quantification (Standardless)
Element Normalized

Element	Wt %	At %	K-Ratio	Z	A	F
C K	53.15	73.62	0.2152	1.0362	0.3907	1.0001
O K	10.69	11.12	0.0123	1.0204	0.1130	1.0002
SiK	4.22	2.50	0.0304	0.9819	0.7282	1.0073
K K	27.10	11.53	0.2521	0.9297	1.0009	1.0000
ZnK	4.83	1.23	0.0411	0.8474	1.0048	1.0000
Total	100.00	100.00				

Figure 8.3: Contaminations of Si and Zn in the crystals grown from the solution (synthesis in THF/H_2O mixture with Zn and KOH) clearly seen in the results of EDX analysis.

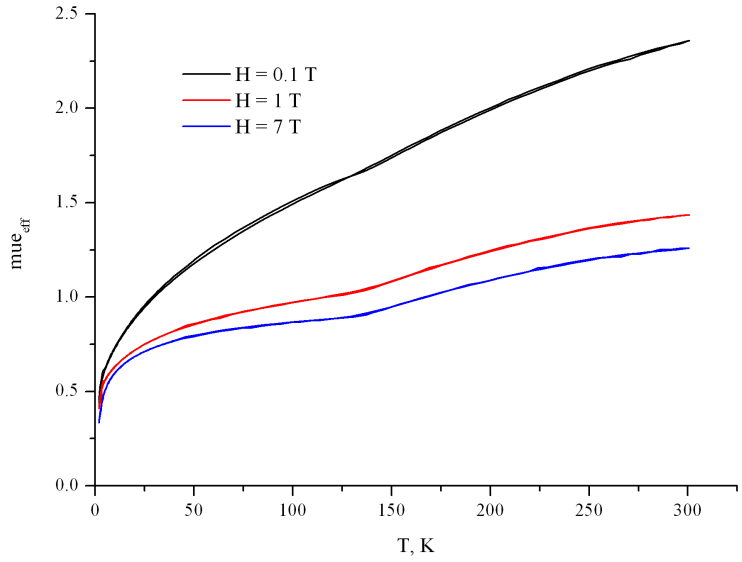

Figure 8.4: Effective magnetic moment vs temperature for [{4K(DB18C6)($C_{60}^{\cdot -}$)}$(THF)_6$]·[C_{60}^{0}]·$(THF)_6$ from precipitate.

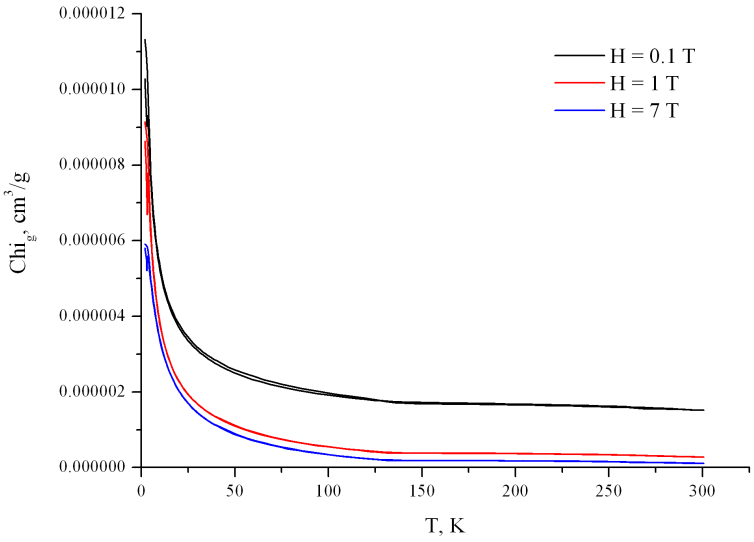

Figure 8.5: Specific magnetic susceptibility vs temperature for [{4K(DB18C6)($C_{60}^{\cdot -}$)}$(THF)_6$]·[C_{60}^{0}]·$(THF)_6$ from precipitate.

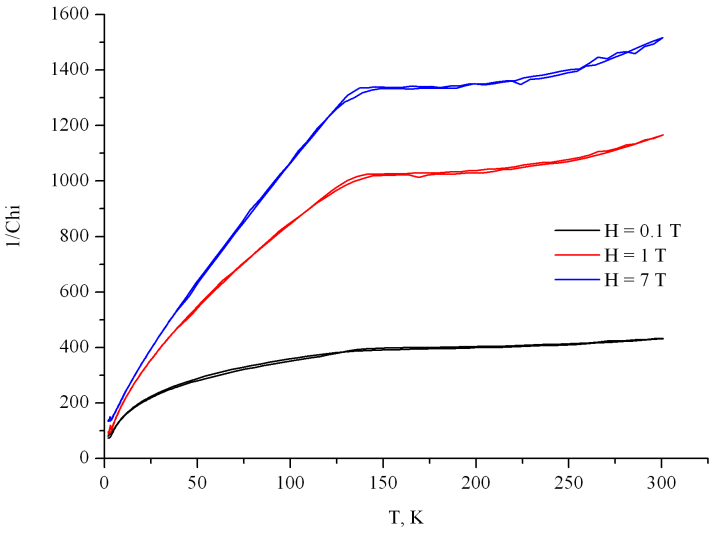

Figure 8.6: Reciprocal magnetic susceptibility vs temperature for $[\{4K(DB18C6)(C_{60}^{\cdot -})\}(THF)_6]\cdot[C_{60}^{0}]\cdot(THF)_6$.

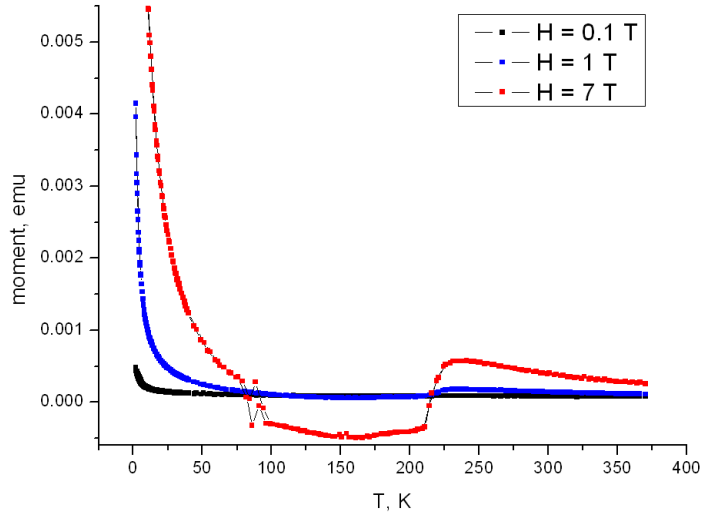

Figure 8.7: SQUID measurement for $[\{4K(DB18C6)(C_{60}^{\cdot -})\}(THF)_6]\cdot[C_{60}^{0}]\cdot(THF)_6$ from single crystals.

9 Crysrallographic data

9.1 [K(DB24C8)(DME)]$_2$C$_{60}$·(DME)

Table 9.1: Atomic coordinates ($\times 10^4$) and equivalent isotropic displacement parameters (Å$^2\times 10^3$) for [K(DB24C8)(DME)]$_2$C$_{60}$·(DME). U_{eq} is defined as one third of the trace of the orthogonalized U_{ij} tensor.

	x	y	z	U_{eq}
K(1B)	1528(1)	665(1)	1371(1)	25(1)
O(1B)	2488(1)	1001(1)	2358(1)	29(1)
O(2B)	1901(1)	2376(1)	1390(1)	26(1)
O(3B)	928(1)	2167(1)	1065(1)	26(1)
O(4B)	545(1)	624(1)	231(1)	30(1)
O(5B)	977(1)	-843(1)	703(1)	46(1)
O(6B)	1602(1)	-890(2)	2132(1)	44(1)
O(7B)	1078(1)	596(2)	2242(1)	40(1)
O(8B)	1921(1)	1601(2)	2892(1)	36(1)
C(1B)	2639(1)	1573(2)	1955(2)	30(1)
C(2B)	2409(1)	2473(2)	1848(2)	30(1)
C(3B)	1617(1)	3083(2)	1442(2)	27(1)
C(4B)	1105(1)	2950(2)	892(2)	26(1)
C(5B)	421(1)	2003(2)	636(2)	30(1)
C(6B)	322(1)	1470(2)	-5(2)	28(1)
C(7B)	496(1)	23(2)	-276(2)	33(1)
C(8B)	232(1)	162(3)	-991(2)	44(1)
C(9B)	226(2)	-497(3)	-1452(2)	67(1)
C(10B)	476(2)	-1264(3)	-1209(3)	73(2)
C(11B)	738(2)	-1408(3)	-491(3)	61(1)
C(12B)	752(1)	-774(2)	-13(2)	41(1)
C(13B)	1222(1)	-1649(2)	1035(3)	56(1)

Continued on next page

Table continued

	x	y	z	U_{eq}
C(14B)	1318(1)	-1624(3)	1780(3)	60(1)
C(15B)	1580(1)	-674(3)	2771(2)	59(1)
C(16B)	1123(1)	-184(3)	2634(2)	53(1)
C(17B)	1094(1)	1408(2)	2587(2)	41(1)
C(18B)	1584(1)	1612(3)	3180(2)	42(1)
C(19B)	2401(1)	1484(2)	3357(2)	30(1)
C(20B)	2602(1)	1648(2)	4079(2)	37(1)
C(21B)	3092(1)	1507(2)	4505(2)	40(1)
C(22B)	3381(1)	1194(2)	4221(2)	41(1)
C(23B)	3186(1)	1043(2)	3507(2)	34(1)
C(24B)	2697(1)	1190(2)	3071(2)	28(1)
O(1C)	1745(1)	742(1)	178(1)	32(1)
O(2C)	2205(1)	-537(1)	1176(1)	32(1)
C(1C)	1403(1)	1201(2)	-436(2)	39(1)
C(2C)	1899(1)	-60(2)	-6(2)	32(1)
C(3C)	2330(1)	-403(2)	626(2)	33(1)
C(4C)	2599(1)	-875(2)	1790(2)	37(1)
O(1A)	2470(1)	8490(2)	4513(1)	38(1)
C(1A)	2813(1)	9146(2)	4574(2)	38(1)
C(2A)	2683(1)	7842(2)	5047(2)	44(1)
C(1M)	1006(1)	6880(1)	2980(1)	26(2)
C(2M)	1192(1)	6233(1)	3542(1)	36(5)
C(3M)	997(1)	6478(1)	2362(1)	28(2)
C(4M)	639(1)	7451(1)	2913(1)	34(2)
C(5M)	1295(1)	5429(1)	3271(1)	29(3)
C(6M)	1001(1)	6191(1)	4013(1)	35(4)
C(7M)	1175(1)	5580(1)	2540(1)	30(2)
C(8M)	618(1)	6665(1)	1699(1)	35(2)
C(9M)	246(1)	7650(1)	2224(1)	36(2)
C(10M)	442(1)	7408(1)	3405(1)	34(2)
C(11M)	1201(1)	4615(1)	3477(1)	33(2)
C(12M)	619(1)	6789(1)	3943(1)	33(2)
C(13M)	907(1)	5338(1)	4233(1)	28(2)

Continued on next page

Table continued

	x	y	z	U_{eq}
C(14M)	965(1)	4907(1)	2049(1)	31(1)
C(15M)	235(1)	7264(1)	1630(1)	35(2)
C(16M)	402(1)	5963(1)	1188(1)	30(2)
C(17M)	-197(1)	7725(1)	2288(1)	38(2)
C(18M)	-74(1)	7576(1)	3020(1)	39(2)
C(19M)	1003(1)	4570(1)	3970(1)	34(2)
C(20M)	987(1)	3911(1)	2970(1)	32(3)
C(21M)	287(1)	6307(1)	4119(1)	37(2)
C(22M)	464(1)	5409(1)	4298(1)	47(3)
C(23M)	871(1)	4054(1)	2269(1)	27(2)
C(24M)	571(1)	5103(1)	1360(1)	36(2)
C(25M)	-217(1)	6932(1)	1076(1)	36(2)
C(26M)	-114(1)	6130(1)	805(1)	31(2)
C(27M)	-629(1)	7408(1)	1758(1)	38(2)
C(28M)	-392(1)	7111(1)	3187(1)	43(2)
C(29M)	666(1)	3835(1)	3763(1)	35(2)
C(30M)	657(1)	3429(1)	3147(1)	40(3)
C(31M)	-207(1)	6463(1)	3747(1)	46(2)
C(32M)	141(1)	4706(1)	4100(1)	46(3)
C(33M)	420(1)	3726(1)	1718(1)	34(2)
C(34M)	235(1)	4374(1)	1158(1)	31(2)
C(35M)	-638(1)	7002(1)	1142(1)	32(2)
C(36M)	-436(1)	5427(1)	607(1)	25(2)
C(37M)	-959(1)	6925(1)	1935(1)	40(3)
C(38M)	-843(1)	6783(1)	2636(1)	42(2)
C(39M)	245(1)	3905(1)	3829(1)	37(2)
C(40M)	225(1)	3111(1)	2617(1)	37(2)
C(41M)	-543(1)	5733(1)	3545(1)	48(3)
C(42M)	-374(1)	4874(1)	3716(1)	42(2)
C(43M)	102(1)	3261(1)	1885(1)	38(3)
C(44M)	-259(1)	4529(1)	786(1)	30(2)
C(45M)	-975(1)	6267(1)	935(1)	27(3)
C(46M)	-879(1)	5499(1)	672(1)	33(2)

Continued on next page

Table continued

	x	y	z	U_{eq}
C(47M)	-1173(1)	6222(1)	1428(1)	26(5)
C(48M)	-938(1)	5929(1)	2856(1)	42(2)
C(49M)	-207(1)	3573(1)	3276(1)	46(3)
C(50M)	-218(1)	3187(1)	2681(1)	36(2)
C(51M)	-590(1)	4171(1)	3206(1)	45(2)
C(52M)	-414(1)	3429(1)	1500(1)	33(2)
C(53M)	-591(1)	4047(1)	962(1)	30(2)
C(54M)	-973(1)	4645(1)	892(1)	30(2)
C(55M)	-1267(1)	5408(1)	1634(1)	30(3)
C(56M)	-1147(1)	5256(1)	2365(1)	39(2)
C(57M)	-611(1)	3385(1)	1992(1)	32(2)
C(58M)	-969(1)	4358(1)	2543(1)	40(2)
C(59M)	-1164(1)	4604(1)	1363(1)	25(2)
C(60M)	-978(1)	3956(1)	1924(1)	33(3)

Table 9.2: Anisotropic displacement parameters ($Å^2 \times 10^3$) for $[K(DB24C8)(DME)]_2C_{60}\cdot(DME)$. The anisotropic displacement factor exponent takes the form: $-2\pi^2[h^2a^{*2}U_{11} + \ldots + 2hka^*b^*U_{12}]$.

	U_{11}	U_{22}	U_{33}	U_{23}	U_{13}	U_{12}
K(1B)	22(1)	22(1)	30(1)	1(1)	11(1)	-1(1)
O(1B)	26(1)	29(1)	32(1)	0(1)	12(1)	-2(1)
O(2B)	22(1)	26(1)	27(1)	-5(1)	8(1)	-3(1)
O(3B)	25(1)	25(1)	27(1)	0(1)	10(1)	0(1)
O(4B)	32(1)	28(1)	28(1)	-6(1)	13(1)	1(1)
O(5B)	33(1)	23(1)	72(2)	-8(1)	16(1)	-1(1)
O(6B)	32(1)	36(1)	68(2)	21(1)	26(1)	3(1)
O(7B)	40(1)	45(2)	40(1)	8(1)	24(1)	2(1)
O(8B)	28(1)	46(1)	34(1)	7(1)	14(1)	10(1)
C(1B)	22(2)	39(2)	26(2)	-3(1)	10(1)	-4(1)

Continued on next page

Table continued

	U_{11}	U_{22}	U_{33}	U_{23}	U_{13}	U_{12}
C(2B)	28(2)	30(2)	29(2)	0(1)	9(1)	-6(1)
C(3B)	35(2)	20(2)	28(2)	-2(1)	16(1)	-1(1)
C(4B)	33(2)	22(2)	26(2)	0(1)	17(1)	4(1)
C(5B)	26(2)	32(2)	33(2)	0(1)	16(1)	3(1)
C(6B)	22(2)	32(2)	29(2)	0(1)	11(1)	1(1)
C(7B)	30(2)	36(2)	39(2)	-16(2)	21(2)	-14(1)
C(8B)	43(2)	54(2)	40(2)	-19(2)	23(2)	-23(2)
C(9B)	77(3)	84(4)	59(3)	-40(3)	48(3)	-50(3)
C(10B)	84(3)	73(3)	99(4)	-64(3)	74(3)	-54(3)
C(11B)	52(2)	41(2)	118(4)	-41(2)	62(3)	-27(2)
C(12B)	32(2)	32(2)	67(3)	-20(2)	29(2)	-15(2)
C(13B)	38(2)	20(2)	113(4)	0(2)	38(2)	2(2)
C(14B)	43(2)	36(2)	101(4)	25(2)	32(2)	3(2)
C(15B)	46(2)	70(3)	65(3)	41(2)	29(2)	11(2)
C(16B)	47(2)	62(3)	56(2)	26(2)	29(2)	8(2)
C(17B)	38(2)	51(2)	41(2)	8(2)	23(2)	12(2)
C(18B)	40(2)	52(2)	41(2)	10(2)	25(2)	16(2)
C(19B)	31(2)	27(2)	30(2)	8(1)	11(1)	4(1)
C(20B)	45(2)	35(2)	32(2)	7(2)	19(2)	6(2)
C(21B)	43(2)	42(2)	28(2)	8(2)	8(2)	-3(2)
C(22B)	28(2)	50(2)	36(2)	16(2)	7(2)	-3(2)
C(23B)	27(2)	37(2)	37(2)	11(2)	13(2)	1(1)
C(24B)	28(2)	26(2)	27(2)	5(1)	10(1)	-1(1)
O(1C)	36(1)	30(1)	31(1)	2(1)	16(1)	6(1)
O(2C)	28(1)	30(1)	39(1)	4(1)	17(1)	2(1)
C(1C)	30(2)	43(2)	40(2)	8(2)	15(2)	4(2)
C(2C)	30(2)	34(2)	34(2)	-6(1)	16(2)	-3(1)
C(3C)	30(2)	31(2)	43(2)	-2(1)	21(2)	2(1)
C(4C)	32(2)	32(2)	43(2)	7(2)	15(2)	6(1)
O(1A)	27(1)	38(1)	44(1)	6(1)	12(1)	3(1)
C(1A)	29(2)	46(2)	38(2)	-3(2)	16(2)	-1(2)
C(2A)	34(2)	41(2)	46(2)	5(2)	9(2)	3(2)
C(1M)	15(5)	12(5)	41(6)	0(4)	4(5)	-8(4)

Continued on next page

Table continued

	U_{11}	U_{22}	U_{33}	U_{23}	U_{13}	U_{12}
C(2M)	20(9)	18(10)	59(11)	-6(8)	8(9)	-13(7)
C(3M)	14(4)	35(4)	36(4)	9(3)	12(3)	-13(4)
C(4M)	36(4)	15(3)	41(5)	-7(3)	10(4)	-14(3)
C(5M)	19(6)	25(7)	38(6)	-2(5)	10(5)	-4(5)
C(6M)	18(7)	33(7)	32(8)	-4(6)	-8(6)	2(6)
C(7M)	20(4)	36(5)	34(4)	-3(3)	14(3)	-3(3)
C(8M)	29(4)	37(4)	41(4)	12(3)	18(4)	-9(3)
C(9M)	45(5)	6(3)	40(5)	3(3)	5(4)	-1(3)
C(10M)	28(4)	25(4)	36(4)	-22(3)	4(3)	-5(3)
C(11M)	17(4)	38(6)	38(4)	6(4)	9(4)	10(4)
C(12M)	41(6)	27(4)	25(4)	-14(3)	9(4)	-6(4)
C(13M)	17(5)	35(5)	20(4)	4(4)	0(4)	-1(4)
C(14M)	24(3)	36(4)	39(4)	1(3)	20(3)	4(3)
C(15M)	38(5)	22(4)	31(4)	18(3)	6(4)	-10(3)
C(16M)	37(5)	38(4)	22(4)	1(4)	19(4)	-11(4)
C(17M)	39(4)	13(3)	49(5)	-2(3)	10(3)	9(3)
C(18M)	38(5)	31(4)	38(5)	-20(4)	10(5)	4(3)
C(19M)	22(5)	27(5)	40(5)	14(4)	3(4)	2(4)
C(20M)	22(7)	21(7)	50(6)	-2(5)	13(5)	12(5)
C(21M)	34(4)	53(5)	26(4)	-20(4)	15(3)	-5(4)
C(22M)	54(9)	55(9)	34(5)	0(5)	21(6)	7(7)
C(23M)	21(4)	24(4)	33(4)	-7(4)	11(3)	11(3)
C(24M)	34(5)	49(5)	37(4)	-10(4)	26(4)	-5(4)
C(25M)	37(4)	27(4)	32(4)	21(3)	7(3)	2(3)
C(26M)	35(5)	42(4)	13(3)	10(3)	8(3)	-4(4)
C(27M)	26(5)	23(4)	50(6)	-1(4)	6(4)	11(3)
C(28M)	34(5)	47(5)	48(5)	-19(4)	19(4)	7(4)
C(29M)	36(4)	29(4)	31(4)	18(4)	8(4)	7(3)
C(30M)	37(6)	14(6)	41(5)	17(4)	-4(4)	11(5)
C(31M)	39(5)	68(6)	32(4)	-26(4)	17(4)	-1(4)
C(32M)	49(5)	67(6)	33(5)	11(5)	28(4)	-3(5)
C(33M)	41(6)	22(4)	39(5)	-8(3)	19(4)	13(4)
C(34M)	36(4)	38(4)	20(3)	-12(3)	14(3)	7(3)

Continued on next page

Table continued

	U_{11}	U_{22}	U_{33}	U_{23}	U_{13}	U_{12}
C(35M)	16(5)	28(4)	33(5)	16(3)	-5(4)	4(3)
C(36M)	22(5)	38(7)	5(3)	2(4)	-2(4)	4(5)
C(37M)	23(6)	41(8)	50(7)	-1(6)	13(6)	13(5)
C(38M)	13(4)	62(6)	44(5)	-22(4)	7(4)	5(4)
C(39M)	46(4)	34(4)	24(4)	10(3)	9(3)	-7(3)
C(40M)	46(4)	9(3)	53(6)	14(3)	20(5)	7(3)
C(41M)	36(5)	85(7)	38(5)	-25(5)	29(5)	-11(5)
C(42M)	54(7)	50(6)	36(5)	4(4)	32(5)	-8(5)
C(43M)	39(5)	13(4)	38(5)	-13(4)	-2(5)	5(3)
C(44M)	35(4)	35(4)	16(4)	-10(3)	8(3)	6(3)
C(45M)	22(7)	27(6)	22(6)	5(5)	2(6)	10(5)
C(46M)	28(5)	42(5)	13(4)	5(4)	-4(4)	-6(4)
C(47M)	10(8)	47(13)	15(7)	-2(7)	1(7)	-2(7)
C(48M)	19(4)	68(6)	47(5)	-15(4)	21(4)	2(4)
C(49M)	47(7)	45(7)	44(5)	18(5)	19(5)	-17(5)
C(50M)	37(5)	16(4)	41(6)	12(4)	6(4)	-7(3)
C(51M)	47(5)	56(6)	40(5)	3(5)	28(5)	-22(4)
C(52M)	31(4)	14(3)	43(4)	-11(3)	8(3)	-6(3)
C(53M)	29(4)	27(4)	25(4)	-12(3)	5(3)	-7(3)
C(54M)	24(5)	36(6)	12(3)	-7(3)	-6(3)	-7(4)
C(55M)	5(5)	46(9)	32(5)	-8(5)	2(5)	-4(5)
C(56M)	11(4)	62(6)	44(5)	-7(4)	14(4)	-4(3)
C(57M)	32(6)	22(6)	44(5)	-3(4)	20(4)	-11(5)
C(58M)	19(4)	54(6)	46(5)	12(5)	15(4)	-7(4)
C(59M)	4(4)	32(5)	28(4)	-6(3)	-1(3)	-8(3)
C(60M)	25(7)	37(8)	31(5)	-6(5)	6(5)	-15(6)

Table 9.3: Hydrogen coordinates ($\times 10^4$) and isotropic displacement parameters (Å$^2 \times 10^3$) for $[K(DB24C8)(DME)]_2C_{60}\cdot(DME)$.

	x	y	z	U_{eq}
H(1B1)	2549	1299	1491	36
H(1B2)	2996	1636	2203	36
H(2B1)	2462	2721	2306	37
H(2B2)	2555	2879	1637	37
H(3B1)	1741	3656	1368	33
H(3B2)	1635	3088	1915	33
H(4B1)	904	3464	879	31
H(4B2)	1091	2887	423	31
H(5B1)	249	2574	490	36
H(5B2)	293	1683	918	36
H(6B1)	-31	1402	-304	34
H(6B2)	460	1768	-284	34
H(8B)	57	696	-1167	53
H(9B)	44	-407	-1945	80
H(10B)	471	-1702	-1530	87
H(11B)	912	-1946	-324	74
H(13A)	1531	-1699	1010	67
H(13B)	1018	-2166	793	67
H(14A)	1006	-1598	1799	72
H(14B)	1487	-2173	2020	72
H(15A)	1864	-305	3071	71
H(15B)	1598	-1226	3030	71
H(16A)	839	-570	2371	63
H(16B)	1130	-28	3088	63
H(17A)	856	1385	2774	49
H(17B)	996	1894	2239	49
H(18A)	1583	2201	3381	50
H(18B)	1676	1164	3556	50
H(20B)	2403	1854	4277	44
H(21B)	3230	1626	4995	49
H(22B)	3715	1083	4518	50

Continued on next page

Table continued

	x	y	z	U_{eq}
H(23B)	3387	838	3313	41
H(1C1)	1556	1359	-730	58
H(1C2)	1296	1739	-294	58
H(1C3)	1123	818	-703	58
H(2C1)	1984	50	-391	39
H(2C2)	1634	-500	-170	39
H(3C1)	2438	-967	511	39
H(3C2)	2599	27	777	39
H(4C1)	2679	-1470	1695	56
H(4C2)	2510	-903	2172	56
H(4C3)	2881	-488	1928	56
H(1A1)	2917	9469	5016	57
H(1A2)	2665	9559	4178	57
H(1A3)	3095	8863	4568	57
H(2A1)	2802	8121	5516	53
H(2A2)	2962	7566	5020	53

9.2 $KC_{60}\cdot(THF)_5\cdot(THF)_2$

Table 9.4: Atomic coordinates ($\times 10^4$) and equivalent isotropic displacement parameters (Å$^2\times 10^3$) for $KC_{60}\cdot(THF)_5\cdot(THF)_2$. U_{eq} is defined as one third of the trace of the orthogonalized U_{ij} tensor.

	x	y	z	U_{eq}
K(1)	7439(1)	3730(1)	2413(2)	36(1)
O(1)	6359(3)	3471(2)	4164(6)	43(2)
C(11)	5610(5)	3492(4)	3604(9)	50(3)
C(12)	5097(6)	3302(5)	4608(11)	101(5)
C(13)	5522(5)	3161(5)	5663(13)	91(5)
C(14)	6319(5)	3225(3)	5400(9)	47(3)
O(2)	6477(4)	4048(2)	552(8)	71(2)
C(21)	6188(5)	3842(3)	-632(11)	51(3)
C(22)	5926(6)	4214(4)	-1522(11)	61(3)
C(23)	5888(8)	4595(4)	-646(18)	107(6)
C(24)	6349(11)	4498(4)	486(15)	126(7)
O(3)	8435(4)	4018(3)	531(8)	71(2)
C(31)	8458(7)	3848(4)	-778(13)	80(4)
C(32)	8780(9)	4190(4)	-1641(12)	95(5)
C(33)	8962(7)	4570(3)	-828(12)	66(3)
C(34)	8817(8)	4427(4)	571(13)	78(4)
O(4)	8514(3)	3509(2)	4153(6)	41(2)
C(41)	8431(5)	3252(3)	5390(9)	49(3)
C(42)	9147(5)	3031(5)	5642(12)	90(5)
C(43)	9666(6)	3226(5)	4757(12)	104(5)
C(44)	9264(5)	3457(3)	3676(9)	43(3)
O(5)	7333(7)	4480(3)	3779(7)	108(3)
C(51)	7269(14)	4403(5)	5249(13)	185(10)
C(52)	7250(10)	4826(4)	5800(14)	118(6)
C(53)	7586(16)	5112(5)	4925(11)	219(13)
C(54)	7713(14)	4843(4)	3729(13)	211(14)
O(6)	5000	5000	5850(30)	300(20)
C(61)	4884(17)	4621(7)	5040(30)	205(14)
C(62)	4913(15)	4781(6)	3720(20)	170(9)

Continued on next page

Table continued

	x	y	z	U_{eq}
O(7)	0	5000	5910(30)	281(17)
C(71)	25(14)	4623(6)	4940(20)	169(9)
C(72)	19(16)	4773(7)	3721(19)	203(14)
C(1X)	7289(5)	2803(3)	-974(8)	36(2)
C(2X)	7388(6)	2878(2)	461(7)	38(2)
C(3X)	6687(5)	2766(3)	1149(10)	34(2)
C(4X)	6159(5)	2629(3)	142(9)	30(2)
C(5X)	6501(5)	2643(3)	-1208(10)	40(3)
C(6X)	6375(5)	2327(3)	-2187(10)	46(3)
C(7X)	6975(6)	2162(3)	-2961(8)	41(3)
C(8X)	7703(5)	2296(3)	-2771(8)	37(2)
C(9X)	7858(5)	2634(3)	-1738(9)	40(2)
C(10X)	8550(5)	2541(3)	-1111(9)	34(2)
C(11X)	8685(5)	2595(3)	263(10)	36(2)
C(12X)	8067(5)	2774(2)	1068(9)	27(2)
C(13X)	8081(5)	2556(3)	2377(9)	31(2)
C(14X)	7412(5)	2448(2)	3022(7)	32(2)
C(15X)	6711(5)	2554(3)	2400(10)	36(2)
C(16X)	6179(5)	2201(3)	2665(10)	39(2)
C(17X)	5673(5)	2074(3)	1658(10)	44(3)
C(18X)	5652(5)	2281(3)	417(10)	47(3)
C(19X)	5510(5)	1948(3)	-636(10)	41(2)
C(20X)	5852(5)	1990(3)	-1852(10)	43(3)
C(21X)	6128(5)	1575(3)	-2492(9)	44(2)
C(22X)	6827(5)	1674(3)	-3161(8)	39(3)
C(23X)	7418(5)	1387(2)	-3195(7)	28(2)
C(24X)	8159(6)	1545(4)	-3015(9)	47(3)
C(25X)	8307(5)	1992(3)	-2790(9)	44(3)
C(26X)	8874(5)	2120(3)	-1784(10)	46(3)
C(27X)	9251(4)	1816(3)	-934(9)	42(3)
C(28X)	9334(4)	1888(4)	449(10)	46(3)
C(29X)	9068(5)	2263(3)	1085(10)	43(3)
C(30X)	8694(4)	2233(3)	2404(9)	32(2)

Continued on next page

Table continued

	x	y	z	U_{eq}
C(31X)	8602(5)	1834(3)	3066(9)	41(3)
C(32X)	7905(5)	1713(3)	3692(8)	43(3)
C(33X)	7332(5)	2020(3)	3715(7)	35(2)
C(34X)	6567(6)	1864(3)	3479(9)	46(3)
C(35X)	6440(6)	1408(3)	3271(9)	46(3)
C(36X)	5891(4)	1292(3)	2244(10)	41(2)
C(37X)	5514(5)	1585(3)	1441(10)	48(3)
C(38X)	5412(5)	1527(3)	51(8)	40(2)
C(39X)	5696(5)	1149(3)	-547(11)	45(3)
C(40X)	6078(5)	1171(3)	-1909(9)	39(2)
C(41X)	6696(5)	849(3)	-1867(10)	39(3)
C(42X)	7343(6)	965(3)	-2497(8)	42(2)
C(43X)	8058(6)	857(3)	-1911(9)	40(3)
C(44X)	8581(5)	1216(3)	-2201(9)	45(3)
C(45X)	9092(5)	1332(3)	-1189(10)	38(2)
C(46X)	9093(5)	1118(3)	67(10)	40(2)
C(47X)	9249(4)	1461(3)	1168(11)	45(3)
C(48X)	8900(4)	1424(3)	2395(9)	34(2)
C(49X)	8378(5)	1070(3)	2682(9)	39(2)
C(50X)	7768(5)	1244(3)	3454(9)	40(2)
C(51X)	7044(5)	1118(3)	3292(9)	33(2)
C(52X)	6854(5)	773(3)	2216(10)	42(3)
C(53X)	6174(5)	881(3)	1590(10)	38(2)
C(54X)	6091(5)	809(3)	210(10)	39(2)
C(55X)	6694(5)	637(2)	-575(9)	28(2)
C(56X)	7382(5)	530(2)	27(8)	31(2)
C(57X)	8061(5)	639(3)	-623(10)	38(2)
C(58X)	8624(5)	788(3)	364(10)	37(2)
C(59X)	8223(5)	760(3)	1722(10)	41(3)
C(60X)	7467(5)	602(2)	1445(8)	35(2)

Table 9.5: Anisotropic displacement parameters ($Å^2 \times 10^3$) for $KC_{60}\cdot(THF)_5\cdot(THF)_2$. The anisotropic displacement factor exponent takes the form: $-2\pi^2[h^2a^{*2}U_{11} + \ldots + 2hka^*b^*U_{12}]$.

	U_{11}	U_{22}	U_{33}	U_{23}	U_{13}	U_{12}
K(1)	47(1)	35(1)	26(1)	-2(1)	2(1)	-2(1)
O(1)	36(4)	63(4)	31(4)	9(3)	8(3)	-3(3)
C(11)	31(6)	89(8)	30(6)	11(6)	-4(5)	11(5)
C(12)	52(8)	208(16)	42(7)	67(9)	-8(6)	-18(8)
C(13)	23(6)	182(14)	70(9)	63(9)	15(6)	0(7)
C(14)	44(6)	72(7)	27(6)	11(5)	-9(5)	11(5)
O(2)	97(6)	44(5)	71(6)	24(4)	-36(5)	-18(4)
C(21)	50(6)	35(6)	68(7)	6(6)	-34(6)	-6(5)
C(22)	63(8)	63(7)	57(8)	9(7)	-9(6)	-20(6)
C(23)	113(11)	43(8)	165(17)	7(10)	-81(11)	-2(7)
C(24)	260(20)	46(9)	69(10)	-15(7)	-57(12)	14(10)
O(3)	89(6)	72(6)	51(5)	-2(4)	25(4)	-23(4)
C(31)	95(10)	69(8)	74(9)	-4(7)	20(7)	-14(7)
C(32)	184(15)	57(8)	44(8)	8(7)	2(8)	-48(9)
C(33)	100(9)	40(6)	59(8)	7(6)	23(7)	-13(6)
C(34)	125(11)	48(7)	62(9)	-1(6)	23(8)	11(8)
O(4)	32(4)	48(4)	42(4)	7(3)	6(3)	16(3)
C(41)	51(7)	70(7)	24(6)	13(5)	4(5)	7(5)
C(42)	38(7)	163(13)	68(8)	71(9)	14(6)	20(7)
C(43)	33(7)	223(16)	55(8)	79(10)	3(6)	18(8)
C(44)	35(6)	57(6)	36(6)	5(5)	-11(5)	-4(5)
O(5)	221(11)	58(5)	46(5)	-22(4)	-32(6)	5(7)
C(51)	400(30)	103(12)	54(9)	-19(8)	20(16)	-50(17)
C(52)	208(18)	56(8)	89(10)	-31(8)	31(11)	-33(10)
C(53)	530(40)	89(11)	37(7)	-23(8)	54(18)	-140(20)
C(54)	470(40)	94(11)	65(9)	-52(9)	129(16)	-178(19)
O(6)	460(50)	310(40)	120(20)	0	0	160(40)
C(61)	290(30)	114(19)	210(30)	13(19)	140(30)	42(18)
C(62)	250(30)	103(14)	160(20)	-21(13)	50(20)	-33(18)
O(7)	570(50)	143(19)	126(19)	0	0	-80(30)

Continued on next page

Table continued

	U_{11}	U_{22}	U_{33}	U_{23}	U_{13}	U_{12}
C(71)	260(30)	91(13)	160(20)	-15(15)	50(20)	-54(15)
C(72)	280(30)	240(30)	87(13)	-105(15)	-97(17)	180(20)
C(1X)	52(7)	25(5)	30(5)	12(4)	2(5)	6(4)
C(2X)	78(8)	14(4)	22(5)	3(3)	-7(6)	13(5)
C(3X)	48(6)	20(5)	35(6)	-15(5)	11(5)	-1(4)
C(4X)	39(6)	23(5)	28(6)	-1(4)	3(5)	6(4)
C(5X)	56(7)	27(5)	38(7)	4(5)	-27(5)	15(5)
C(6X)	38(6)	61(7)	38(6)	18(6)	-16(5)	3(6)
C(7X)	53(7)	56(7)	14(5)	9(4)	-11(5)	39(6)
C(8X)	52(7)	46(6)	13(5)	3(4)	2(5)	-13(5)
C(9X)	44(6)	34(6)	40(6)	15(5)	-8(5)	-1(5)
C(10X)	44(6)	40(6)	19(6)	3(4)	22(5)	-19(5)
C(11X)	38(6)	27(5)	43(7)	7(5)	-6(5)	-11(4)
C(12X)	40(6)	15(5)	24(5)	4(4)	5(5)	0(4)
C(13X)	39(6)	29(5)	27(6)	-4(5)	-7(5)	-10(4)
C(14X)	46(6)	30(5)	20(4)	-7(4)	0(5)	0(5)
C(15X)	55(6)	33(6)	21(6)	-15(5)	2(5)	1(5)
C(16X)	38(5)	49(6)	29(6)	-7(5)	13(5)	13(5)
C(17X)	23(5)	67(7)	41(6)	-23(6)	-3(5)	20(5)
C(18X)	43(6)	62(7)	37(7)	1(6)	10(5)	20(5)
C(19X)	24(5)	55(6)	45(7)	7(6)	-14(5)	3(5)
C(20X)	35(6)	55(7)	40(6)	4(5)	1(5)	11(5)
C(21X)	47(6)	73(8)	13(5)	3(5)	-6(5)	1(5)
C(22X)	41(6)	71(8)	6(5)	-3(5)	-11(4)	-27(6)
C(23X)	43(6)	29(5)	11(4)	-8(3)	-7(4)	0(5)
C(24X)	57(7)	64(7)	19(6)	-3(5)	7(5)	5(6)
C(25X)	60(7)	42(6)	29(6)	7(5)	19(5)	1(6)
C(26X)	40(6)	62(7)	36(6)	9(6)	16(5)	-36(6)
C(27X)	18(5)	78(8)	30(6)	13(6)	15(4)	4(5)
C(28X)	8(5)	81(8)	47(7)	-6(6)	-4(4)	-10(5)
C(29X)	29(5)	46(6)	53(7)	-28(6)	-5(5)	-23(5)
C(30X)	31(5)	48(6)	18(5)	-5(5)	-7(4)	-15(4)
C(31X)	32(6)	65(7)	27(6)	9(5)	-29(5)	-16(5)

Continued on next page

Table continued

	U_{11}	U_{22}	U_{33}	U_{23}	U_{13}	U_{12}
C(32X)	48(7)	67(7)	13(5)	3(5)	-6(4)	2(6)
C(33X)	33(6)	59(6)	12(4)	-1(4)	2(4)	2(5)
C(34X)	66(7)	47(7)	25(6)	-9(5)	32(5)	-14(6)
C(35X)	57(7)	60(7)	22(6)	12(5)	18(5)	-5(6)
C(36X)	25(5)	59(7)	38(6)	8(5)	13(5)	-3(5)
C(37X)	23(5)	67(7)	53(7)	9(6)	-10(5)	-7(5)
C(38X)	31(5)	68(7)	21(6)	3(5)	-7(4)	-5(5)
C(39X)	29(5)	41(6)	65(7)	-4(6)	4(5)	-1(5)
C(40X)	52(6)	39(6)	26(6)	-7(5)	-15(5)	-14(5)
C(41X)	35(6)	47(6)	36(7)	-29(5)	1(5)	-13(5)
C(42X)	60(7)	42(6)	24(5)	-13(4)	-24(6)	11(5)
C(43X)	63(7)	28(6)	29(6)	-13(5)	15(5)	10(5)
C(44X)	51(6)	52(6)	34(6)	-6(5)	36(6)	8(5)
C(45X)	27(5)	44(6)	45(7)	2(5)	24(5)	-2(4)
C(46X)	26(5)	45(6)	48(7)	5(5)	-8(5)	12(5)
C(47X)	17(5)	59(7)	59(7)	10(6)	-14(5)	18(4)
C(48X)	25(5)	52(6)	26(6)	13(5)	-19(5)	2(5)
C(49X)	47(6)	45(6)	24(5)	6(5)	-12(5)	11(5)
C(50X)	54(7)	37(6)	30(5)	17(4)	-11(5)	-10(5)
C(51X)	43(6)	33(5)	23(5)	10(4)	13(4)	-1(5)
C(52X)	51(7)	33(5)	40(7)	20(5)	7(5)	-9(5)
C(53X)	39(6)	31(6)	43(7)	16(5)	7(5)	-7(5)
C(54X)	53(7)	36(6)	28(6)	9(5)	1(5)	-23(5)
C(55X)	42(6)	19(5)	23(6)	-4(4)	-4(5)	-5(4)
C(56X)	46(6)	18(4)	28(5)	-6(3)	15(5)	-5(4)
C(57X)	51(6)	19(5)	42(6)	-13(5)	11(5)	23(4)
C(58X)	45(6)	32(6)	34(6)	3(5)	-2(5)	22(5)
C(59X)	56(7)	21(5)	45(7)	16(5)	-23(5)	13(5)
C(60X)	39(6)	21(4)	43(6)	6(4)	7(5)	15(5)

Table 9.6: Hydrogen coordinates ($\times 10^4$) and isotropic displacement parameters (Å$^2 \times 10^3$) for $KC_{60}\cdot(THF)_5\cdot(THF)_2$.

	x	y	z	U_{eq}
H(11A)	5584	3322	2747	60
H(11B)	5471	3805	3413	60
H(12A)	4732	3528	4915	121
H(12B)	4817	3049	4210	121
H(13A)	5423	2842	5830	110
H(13B)	5379	3328	6489	110
H(14A)	6558	3392	6149	57
H(14B)	6577	2935	5305	57
H(21A)	5766	3641	-401	61
H(21B)	6584	3666	-1091	61
H(22A)	6284	4266	-2273	73
H(22B)	5425	4147	-1910	73
H(23A)	6074	4863	-1122	129
H(23B)	5364	4649	-353	129
H(24A)	6833	4658	402	151
H(24B)	6099	4599	1328	151
H(31A)	7945	3771	-1089	95
H(31B)	8771	3576	-805	95
H(32A)	9239	4075	-2087	114
H(32B)	8416	4275	-2354	114
H(33A)	8641	4826	-1072	80
H(33B)	9495	4654	-947	80
H(34A)	9298	4393	1066	94
H(34B)	8509	4652	1046	94
H(41A)	8025	3030	5286	58
H(41B)	8303	3451	6157	58
H(42A)	9305	3073	6595	108
H(42B)	9104	2708	5461	108
H(43A)	9995	2995	4363	124
H(43B)	9985	3440	5259	124
H(44A)	9496	3751	3496	52

Continued on next page

Table continued

	x	y	z	U_{eq}
H(44B)	9273	3280	2830	52
H(51A)	6804	4238	5468	222
H(51B)	7707	4234	5593	222
H(52A)	6723	4918	5957	141
H(52B)	7517	4829	6681	141
H(53A)	8066	5224	5299	263
H(53B)	7255	5368	4719	263
H(54A)	7566	5013	2912	253
H(54B)	8254	4772	3655	253
H(61A)	5281	4397	5193	246
H(61B)	4389	4485	5227	246
H(62A)	5296	4614	3197	204
H(62B)	4420	4736	3271	204
H(71A)	485	4446	5087	203
H(71B)	-415	4428	5079	203
H(72A)	-419	4650	3228	244
H(72B)	481	4676	3245	244

9.3 [K(DB24C8)(THF)]$_2$C$_{60}$·THF

Table 9.7: Atomic coordinates ($\times 10^4$) and equivalent isotropic displacement parameters (Å$^2\times 10^3$) for [K(DB24C8)(THF)]$_2$C$_{60}$·THF. U_{eq} is defined as one third of the trace of the orthogonalized U_{ij} tensor.

	x	y	z	U_{eq}
K(1A)	3393(2)	8969(2)	2825(2)	86(2)
O(1A)	3648(8)	8699(7)	2020(8)	103(7)
O(2A)	4031(12)	8056(10)	2942(11)	182(12)
O(3A)	4449(8)	8842(9)	3687(8)	114(7)
O(4A)	3499(6)	8767(6)	3836(6)	78(5)
O(5A)	2549(6)	8742(7)	3045(6)	80(5)
O(6A)	2695(8)	9759(8)	2862(6)	104(6)
O(7A)	3882(12)	9977(8)	3252(8)	154(10)
O(8A)	4008(8)	9579(6)	2426(5)	87(6)
C(1A)	3975(12)	8149(12)	2093(11)	108(9)
C(2A)	3799(16)	7878(15)	2344(16)	126(13)
C(3A)	4661(15)	8217(13)	3169(13)	112(11)
C(4A)	4801(16)	8418(14)	3720(14)	136(12)
C(5A)	4458(9)	9023(8)	4104(9)	58(6)
C(6A)	4106(11)	8736(10)	4240(10)	84(8)
C(7A)	3130(12)	8506(11)	3911(11)	86(8)
C(8A)	3162(11)	8236(10)	4326(10)	77(7)
C(9A)	2765(11)	8054(10)	4389(10)	82(8)
C(10A)	2172(14)	7967(13)	3943(13)	112(11)
C(11A)	2114(12)	8280(11)	3508(11)	86(9)
C(12A)	2579(8)	8522(8)	3446(8)	48(5)
C(13A)	2069(13)	9063(12)	2754(12)	104(10)
C(14A)	2309(15)	9619(13)	3032(14)	115(12)
C(15A)	2945(16)	10224(16)	3138(15)	139(13)
C(16A)	3444(16)	10374(15)	3043(15)	135(12)
C(17A)	4438(16)	10056(14)	3232(14)	139(12)
C(18A)	4169(12)	10102(11)	2627(11)	92(8)
C(19A)	3911(12)	9565(11)	1911(11)	92(9)
C(20A)	3978(11)	9908(11)	1646(11)	92(9)

Continued on next page

Table continued

	x	y	z	U_{eq}
C(21A)	3871(13)	9839(12)	1085(12)	108(10)
C(22A)	3670(15)	9369(15)	937(13)	137(12)
C(23A)	3590(10)	8863(9)	1221(10)	80(7)
C(24A)	3766(16)	9048(16)	1737(16)	134(13)
K(1B)	5998(3)	4575(2)	5490(2)	76(1)
O(1B)	6302(6)	4233(7)	6482(5)	72(5)
O(2B)	7093(12)	4377(15)	6114(16)	270(20)
O(3B)	6839(7)	5297(6)	5641(5)	76(5)
O(4B)	5919(8)	5206(8)	4649(6)	93(6)
O(5B)	5665(6)	4176(7)	4503(5)	75(5)
O(6B)	4845(12)	4381(15)	4766(14)	200(16)
O(7B)	5138(8)	5290(7)	5362(7)	94(6)
O(8B)	6116(7)	5189(6)	6321(5)	76(5)
C(1B)	6828(15)	3914(13)	6768(13)	120(11)
C(2B)	7270(30)	4200(20)	6720(20)	240(20)
C(3B)	7472(19)	4865(18)	6344(18)	154(16)
C(4B)	7435(14)	5073(13)	5884(13)	114(11)
C(5B)	6662(11)	5666(10)	5167(10)	86(8)
C(6B)	6138(13)	5681(12)	4848(11)	92(9)
C(7B)	5956(8)	4936(8)	4270(8)	51(5)
C(8B)	6137(9)	5207(9)	3975(9)	65(7)
C(9B)	6300(10)	4992(9)	3646(10)	77(7)
C(10B)	6173(8)	4451(8)	3567(8)	52(6)
C(11B)	5964(10)	4147(9)	3839(9)	71(7)
C(12B)	5839(9)	4440(9)	4176(9)	56(6)
C(13B)	5124(12)	3983(10)	4276(10)	81(8)
C(14B)	4720(12)	4252(11)	4119(10)	90(8)
C(15B)	4510(20)	4860(20)	4545(19)	155(18)
C(16B)	4575(12)	5160(10)	5088(10)	82(8)
C(17B)	5152(10)	5582(9)	5772(9)	71(7)
C(18B)	5795(12)	5704(12)	6074(11)	88(9)
C(19B)	5953(10)	4975(9)	6679(9)	60(7)
C(20B)	5720(10)	5243(9)	6949(9)	68(7)

Continued on next page

Table continued

	x	y	z	U_{eq}
C(21B)	5688(10)	4900(10)	7355(9)	70(7)
C(22B)	5853(11)	4430(11)	7452(11)	90(8)
C(23B)	6077(10)	4208(9)	7186(9)	61(6)
C(24B)	6110(9)	4489(9)	6780(9)	68(7)
K(1C)	5995(3)	822(2)	5493(3)	114(2)
O(1C)	5980(18)	-157(8)	5979(8)	250(20)
O(2C)	5015(13)	295(7)	5264(11)	191(15)
O(3C)	5171(8)	948(8)	4523(6)	100(7)
O(4C)	5597(9)	1849(8)	5029(11)	155(10)
O(5C)	6378(5)	1805(7)	5931(7)	103(7)
O(6C)	6853(14)	943(13)	6465(9)	210(13)
O(7C)	7254(10)	363(9)	5879(8)	129(8)
O(8C)	6155(14)	-168(8)	4951(12)	183(12)
C(1C)	5198(12)	-94(10)	5871(11)	82(8)
C(2C)	4570(30)	-110(30)	5260(30)	310(40)
C(3C)	4637(14)	361(13)	4547(13)	122(11)
C(4C)	4670(20)	1098(19)	4392(18)	185(18)
C(5C)	5339(15)	1457(15)	4314(14)	147(12)
C(6C)	5074(15)	1779(13)	4470(13)	118(10)
C(7C)	5973(10)	2171(9)	5001(9)	78(6)
C(8C)	5912(12)	2557(10)	4622(11)	101(9)
C(9C)	6341(13)	2972(12)	4726(12)	115(10)
C(10C)	6707(13)	2967(11)	5278(12)	109(9)
C(11C)	6773(9)	2631(9)	5664(9)	78(6)
C(12C)	6377(10)	2244(10)	5504(9)	84(7)
C(13C)	6809(11)	1870(9)	6420(10)	73(7)
C(14C)	7410(80)	1860(70)	6740(70)	720(110)
C(15C)	7210(20)	1036(19)	6380(20)	170(20)
C(16C)	7470(12)	454(12)	6425(12)	105(9)
C(17C)	7195(16)	-131(16)	5655(15)	148(12)
C(18C)	6804(11)	-116(9)	5134(10)	74(7)
C(19C)	6130(12)	-645(12)	5311(13)	106(9)
C(20C)	6090(14)	-1134(14)	5040(13)	131(11)

Continued on next page

Table continued

	x	y	z	U_{eq}
C(21C)	6033(14)	-1581(14)	5256(15)	124(11)
C(22C)	6021(19)	-1486(19)	5700(20)	191(17)
C(23C)	5935(13)	-1033(13)	5942(12)	95(9)
C(24C)	6046(11)	-690(12)	5724(11)	88(9)
K(1D)	8583(3)	1021(3)	3166(2)	97(2)
O(1D)	8364(7)	1339(7)	3984(7)	117(7)
O(2D)	7963(8)	1871(8)	3082(7)	109(7)
O(3D)	7576(7)	1096(8)	2411(8)	111(7)
O(4D)	8467(7)	1279(8)	2130(7)	116(8)
O(5D)	9469(6)	1309(7)	2969(6)	79(5)
O(6D)	9299(7)	220(6)	3063(5)	80(5)
O(7D)	8157(7)	55(7)	2746(6)	77(5)
O(8D)	7913(8)	520(9)	3490(8)	129(8)
C(1D)	8169(12)	1829(12)	4031(11)	95(9)
C(2D)	8172(12)	2190(11)	3521(11)	102(9)
C(3D)	7450(17)	1767(14)	2887(15)	129(11)
C(4D)	7261(12)	1631(11)	2312(11)	101(8)
C(5D)	7557(19)	968(17)	1820(18)	170(17)
C(6D)	7945(14)	1299(12)	1624(13)	128(11)
C(7D)	8871(12)	1517(11)	2063(11)	80(8)
C(8D)	8777(11)	1736(10)	1626(10)	82(8)
C(9D)	9249(10)	2057(9)	1610(9)	76(7)
C(10D)	9764(10)	2006(10)	2038(10)	77(7)
C(11D)	9852(10)	1790(9)	2480(9)	66(6)
C(12D)	9499(11)	1552(10)	2498(10)	81(7)
C(13D)	9901(11)	928(10)	3205(10)	75(8)
C(14D)	9770(9)	442(9)	3017(8)	65(6)
C(15D)	8977(14)	-194(13)	2814(13)	108(10)
C(16D)	8553(13)	-370(12)	2934(11)	94(9)
C(17D)	7728(16)	-45(14)	2806(14)	129(12)
C(18D)	7689(14)	-16(14)	3337(13)	121(11)
C(19D)	8012(9)	545(9)	4036(9)	67(7)
C(20D)	7904(13)	186(12)	4323(13)	116(10)

Continued on next page

Table continued

	x	y	z	U_{eq}
C(21D)	8047(13)	311(12)	4831(12)	107(10)
C(22D)	8268(10)	762(10)	5048(10)	78(7)
C(23D)	8354(10)	1069(10)	4810(9)	70(7)
C(24D)	8267(10)	962(11)	4286(10)	74(7)
O(1AX)	2424(7)	8484(7)	1940(5)	83(5)
C(1AX)	2205(11)	8010(12)	2001(10)	86(8)
C(2AX)	1903(11)	7814(10)	1454(10)	88(8)
C(3AX)	1729(13)	8205(12)	1068(12)	107(10)
C(4AX)	2193(13)	8677(12)	1409(13)	107(10)
O(1BX)	5391(7)	3684(7)	5507(7)	111(6)
C(1BX)	5035(13)	3810(12)	5725(12)	119(10)
C(2BX)	5127(16)	3300(15)	6080(14)	144(13)
C(3BX)	5663(11)	2975(10)	6116(11)	91(8)
C(4BX)	5472(17)	3142(16)	5573(15)	159(13)
O(1CX)	5398(5)	1110(5)	6187(4)	55(3)
C(1CX)	5566(11)	1164(10)	6685(10)	93(8)
C(2CX)	5172(7)	1398(6)	6806(6)	42(4)
C(3CX)	4870(8)	1776(8)	6296(8)	64(6)
C(4CX)	4918(8)	1406(8)	5906(7)	62(5)
O(1DX)	9596(8)	1490(9)	4043(6)	110(7)
C(1DX)	9829(11)	1984(11)	3978(10)	81(7)
C(2DX)	9879(15)	2332(14)	4446(14)	140(13)
C(3DX)	10138(15)	1785(14)	4847(13)	124(12)
C(4DX)	9719(11)	1450(10)	4610(10)	88(8)
O(11I)	9291(10)	9885(13)	6400(15)	227(18)
C(11I)	8768(18)	9727(15)	6436(15)	149(13)
C(12I)	8530(10)	9415(9)	5988(9)	67(7)
C(13I)	8910(20)	9322(16)	5871(17)	166(15)
C(14I)	9412(14)	9400(14)	6355(13)	111(10)
O(21I)	2680(16)	37(18)	9549(17)	290(20)
C(21I)	2400(30)	610(20)	9680(20)	210(20)
C(22I)	3090(16)	768(14)	10127(14)	137(13)
C(23I)	3535(11)	505(10)	10021(10)	81(8)

Continued on next page

Table continued

	x	y	z	U_{eq}
C(24I)	3323(13)	65(12)	9618(12)	109(9)
C(1M)	8291(2)	3232(2)	6681(2)	210(30)
C(2M)	8668(2)	3433(2)	7184(2)	160(30)
C(3M)	8442(2)	3454(2)	6310(2)	190(20)
C(4M)	8114(2)	2727(1)	6628(1)	230(30)
C(5M)	9054(2)	3776(2)	7125(2)	139(18)
C(6M)	8848(2)	3116(2)	7612(2)	110(11)
C(7M)	8914(2)	3790(2)	6585(2)	270(40)
C(8M)	8410(2)	3158(2)	5902(2)	150(20)
C(9M)	8078(2)	2419(1)	6203(1)	150(20)
C(10M)	8302(2)	2398(2)	7076(1)	150(20)
C(11M)	9605(2)	3788(2)	7495(2)	300(40)
C(12M)	8662(2)	2589(2)	7556(1)	290(30)
C(13M)	9425(2)	3133(3)	8001(2)	101(12)
C(14M)	9335(2)	3814(2)	6440(2)	210(30)
C(15M)	8223(2)	2630(2)	5847(1)	190(20)
C(16M)	8848(2)	3186(2)	5751(2)	200(30)
C(17M)	8246(2)	1900(1)	6386(2)	95(12)
C(18M)	8383(2)	1888(2)	6926(2)	160(20)
C(19M)	9794(2)	3459(2)	7943(2)	117(15)
C(20M)	10044(2)	3818(2)	7346(2)	136(14)
C(21M)	9123(2)	2278(3)	7911(1)	93(9)
C(22M)	9595(2)	2613(3)	8186(1)	130(13)
C(23M)	9912(2)	3830(2)	6829(2)	137(17)
C(24M)	9300(2)	3506(2)	6015(2)	138(14)
C(25M)	8546(2)	2332(2)	5663(2)	660(140)
C(26M)	8930(2)	2676(3)	5603(2)	230(30)
C(27M)	8554(2)	1615(2)	6209(2)	135(13)
C(28M)	8826(2)	1591(2)	7265(2)	250(50)
C(29M)	10351(2)	3286(2)	8069(2)	170(20)
C(30M)	10504(2)	3508(2)	7701(2)	104(9)
C(31M)	9204(2)	1791(2)	7767(2)	141(16)
C(32M)	10128(2)	2448(3)	8307(2)	350(60)

Continued on next page

Table continued

	x	y	z	U_{eq}
C(33M)	10232(2)	3532(2)	6645(2)	163(19)
C(34M)	9854(2)	3332(3)	6143(2)	125(16)
C(35M)	8707(2)	1837(2)	5841(2)	330(40)
C(36M)	9463(2)	2510(3)	5724(2)	210(30)
C(37M)	9014(2)	1306(2)	6564(2)	250(30)
C(38M)	9146(2)	1293(2)	7081(2)	280(50)
C(39M)	10512(2)	2791(3)	8247(2)	129(16)
C(40M)	10813(2)	3224(2)	7524(2)	56(6)
C(41M)	9758(2)	1617(2)	7895(2)	62(7)
C(42M)	10210(2)	1938(3)	8159(2)	119(14)
C(43M)	10675(2)	3236(2)	6984(2)	68(6)
C(44M)	9936(2)	2845(3)	5999(2)	116(13)
C(45M)	9264(2)	1665(2)	5967(2)	190(30)
C(46M)	9634(2)	1991(3)	5909(2)	160(20)
C(47M)	9453(2)	1335(2)	6415(2)	240(30)
C(48M)	9724(2)	1309(2)	7470(2)	220(30)
C(49M)	10835(2)	2493(2)	8063(2)	89(10)
C(50M)	10980(2)	2704(2)	7707(2)	56(6)
C(51M)	10648(2)	1966(2)	8008(2)	93(11)
C(52M)	10757(2)	2725(3)	6835(2)	131(15)
C(53M)	10397(2)	2534(3)	6354(2)	103(9)
C(54M)	10210(2)	2007(3)	6298(2)	106(11)
C(55M)	10004(2)	1347(2)	6785(2)	118(12)
C(56M)	10144(2)	1334(2)	7325(2)	230(30)
C(57M)	10944(2)	2397(2)	7282(2)	94(10)
C(58M)	10616(2)	1670(2)	7600(2)	154(19)
C(59M)	10390(2)	1690(2)	6727(2)	126(15)
C(60M)	10767(2)	1892(2)	7229(2)	130(16)
C(1N)	3526(2)	1722(2)	4161(2)	290(40)
C(2N)	3047(2)	1386(2)	3934(2)	250(40)
C(3N)	3499(2)	2070(2)	3766(2)	200(30)
C(4N)	3721(2)	1893(2)	4661(2)	410(50)
C(5N)	2721(2)	1529(2)	3401(2)	230(30)

Continued on next page

Table continued

	x	y	z	U_{eq}
C(6N)	2786(2)	1237(2)	4223(2)	134(16)
C(7N)	3001(2)	1952(2)	3296(2)	490(70)
C(8N)	3667(2)	2579(2)	3890(1)	260(50)
C(9N)	3898(2)	2421(2)	4792(1)	150(18)
C(10N)	3448(2)	1736(2)	4962(2)	330(50)
C(11N)	2146(2)	1519(2)	3177(2)	180(30)
C(12N)	2990(2)	1415(2)	4746(2)	270(50)
C(13N)	2184(2)	1222(2)	3986(3)	720(150)
C(14N)	2690(2)	2347(3)	2970(2)	390(90)
C(15N)	3871(2)	2757(2)	4414(1)	156(18)
C(16N)	3344(2)	2989(2)	3550(2)	240(30)
C(17N)	3733(2)	2592(2)	5172(2)	150(20)
C(18N)	3455(2)	2167(2)	5277(2)	104(11)
C(19N)	1872(2)	1362(2)	3477(2)	95(11)
C(20N)	1822(2)	1926(3)	2835(2)	141(17)
C(21N)	2515(2)	1512(2)	4835(2)	108(15)
C(22N)	2016(2)	1394(2)	4365(2)	141(14)
C(23N)	2088(2)	2333(3)	2734(2)	150(20)
C(24N)	2866(2)	2875(3)	3100(2)	210(30)
C(25N)	3674(2)	3277(2)	4397(2)	210(30)
C(26N)	3350(2)	3419(2)	3864(2)	116(12)
C(27N)	3545(2)	3090(2)	5155(2)	180(20)
C(28N)	2999(2)	2261(3)	5359(2)	200(30)
C(29N)	1378(2)	1674(2)	3319(2)	89(9)
C(30N)	1347(2)	2022(3)	2922(2)	80(8)
C(31N)	2519(2)	1927(3)	5133(2)	100(11)
C(32N)	1542(2)	1693(2)	4214(2)	73(8)
C(33N)	1893(2)	2851(3)	2719(2)	690(120)
C(34N)	2373(2)	3185(3)	2945(2)	230(40)
C(35N)	3514(2)	3437(2)	4759(2)	190(30)
C(36N)	2876(2)	3718(2)	3713(2)	650(120)
C(37N)	3070(2)	3185(2)	5243(2)	93(10)
C(38N)	2804(2)	2779(3)	5344(2)	230(30)

Continued on next page

Table continued

	x	y	z	U_{eq}
C(39N)	1218(2)	1835(2)	3681(2)	121(11)
C(40N)	1159(2)	2519(3)	2906(2)	74(8)
C(41N)	2026(2)	2236(3)	4978(2)	380(60)
C(42N)	1548(2)	2123(3)	4528(2)	180(20)
C(43N)	1437(2)	2945(3)	2801(2)	100(11)
C(44N)	2377(2)	3600(2)	3243(2)	180(30)
C(45N)	3020(2)	3750(2)	4601(2)	145(14)
C(46N)	2708(2)	3889(2)	4092(2)	530(90)
C(47N)	2745(2)	3593(2)	4901(2)	138(17)
C(48N)	2202(2)	2765(3)	5108(2)	140(20)
C(49N)	1021(2)	2355(2)	3664(2)	84(8)
C(50N)	994(2)	2691(2)	3286(2)	87(9)
C(51N)	1225(2)	2533(3)	4188(2)	99(11)
C(52N)	1444(2)	3376(2)	3116(2)	150(20)
C(53N)	1902(2)	3697(2)	3332(2)	400(60)
C(54N)	2106(2)	3875(2)	3855(2)	170(20)
C(55N)	2171(2)	3583(2)	4677(2)	210(30)
C(56N)	1891(2)	3160(3)	4782(2)	280(40)
C(57N)	1171(2)	3218(2)	3417(2)	102(12)
C(58N)	1393(2)	3041(3)	4312(2)	180(20)
C(59N)	1844(2)	3726(2)	4144(2)	270(40)
C(60N)	1366(2)	3390(2)	3917(2)	170(20)

9.4 [K(DB24C8)(DME)]C_{60}

Table 9.8: Atomic coordinates ($\times 10^4$) and equivalent isotropic displacement parameters (Å$^2\times 10^3$) for [K(DB24C8)(DME)]C_{60}. U_{eq} is defined as one third of the trace of the orthogonalized U_{ij} tensor.

	x	y	z	U_{eq}
K(1A)	6349(1)	3039(2)	4964(1)	36(1)
O(1A)	6496(3)	1986(4)	4084(3)	38(3)
O(2A)	6644(4)	3574(5)	3928(4)	57(3)
O(3A)	7318(3)	3385(8)	4758(4)	92(4)
O(4A)	6997(3)	4410(7)	5448(4)	81(4)
O(5A)	6142(3)	4649(5)	5124(4)	62(3)
O(6A)	6113(3)	3616(4)	5992(3)	46(3)
O(7A)	6699(3)	2179(5)	5908(3)	48(3)
O(8A)	6820(3)	1455(5)	4933(3)	37(3)
C(1A)	6285(8)	2317(14)	3565(6)	136(10)
C(2A)	6648(6)	3021(9)	3499(7)	74(6)
C(3A)	7077(5)	4022(9)	3937(7)	72(6)
C(4A)	7445(6)	3602(10)	4249(6)	72(6)
C(5A)	7609(7)	3552(12)	5168(9)	121(9)
C(6A)	7593(6)	4331(12)	5436(11)	141(10)
C(7A)	6950(3)	5169(4)	5313(3)	59(5)
C(8A)	7292(3)	5783(5)	5298(4)	83(5)
C(9A)	7169(4)	6525(5)	5087(4)	172(9)
C(10A)	6703(5)	6653(5)	4892(4)	95(8)
C(11A)	6360(4)	6039(6)	4907(4)	66(5)
C(12A)	6484(3)	5297(5)	5118(3)	44(5)
C(13A)	5832(5)	4711(9)	5620(8)	90(7)
C(14A)	6079(4)	4433(8)	6076(5)	39(4)
C(15A)	6369(9)	3230(12)	6444(7)	122(9)
C(16A)	6387(6)	2432(9)	6385(5)	65(5)
C(17A)	6808(5)	1379(7)	5873(6)	52(5)
C(18A)	7081(5)	1224(11)	5377(5)	68(6)
C(19A)	6526(2)	946(4)	4678(3)	23(4)
C(20A)	6402(3)	183(4)	4853(3)	52(5)

Continued on next page

Table continued

	x	y	z	U_{eq}
C(21A)	6097(3)	-299(4)	4552(4)	102(7)
C(22A)	5917(3)	-19(6)	4077(4)	82(7)
C(23A)	6042(3)	744(6)	3902(3)	71(6)
C(24A)	6347(3)	1226(5)	4202(3)	46(5)
K(1B)	3652(1)	6977(2)	4432(1)	34(1)
O(1B)	3199(3)	8528(5)	4471(4)	52(3)
O(2B)	3317(4)	7769(6)	3478(4)	60(3)
O(3B)	3855(4)	6405(7)	3422(5)	77(4)
O(4B)	3863(3)	5277(5)	4303(3)	40(2)
O(5B)	2907(5)	5513(8)	3878(5)	101(4)
O(6B)	2668(3)	6639(5)	4712(4)	51(3)
O(7B)	3383(3)	6390(5)	5498(4)	49(3)
O(8B)	3559(4)	8032(5)	5341(4)	55(3)
C(1B)	2915(5)	8757(9)	4030(5)	53(5)
C(2B)	3216(6)	8620(10)	3558(6)	71(6)
C(3B)	3575(5)	7546(10)	3045(6)	61(5)
C(4B)	3573(5)	6696(8)	3003(5)	40(4)
C(5B)	3991(7)	5477(9)	3425(7)	84(6)
C(6B)	4215(5)	5273(9)	3873(5)	42(4)
C(7B)	3535(4)	4685(5)	4312(3)	56(5)
C(8B)	3732(5)	3993(6)	4530(4)	104(8)
C(9B)	3443(6)	3317(5)	4599(5)	280(20)
C(10B)	2956(6)	3333(7)	4450(5)	202(16)
C(11B)	2759(4)	4025(8)	4232(5)	167(11)
C(12B)	3048(4)	4701(6)	4163(4)	70(6)
C(13B)	2512(6)	6023(13)	3945(8)	144(8)
C(14B)	2375(6)	6341(12)	4325(7)	113(7)
C(15B)	2533(6)	6453(12)	5236(6)	87(7)
C(16B)	2953(5)	5926(8)	5412(6)	44(5)
C(17B)	3425(8)	6936(9)	5931(6)	91(7)
C(18B)	3704(5)	7655(7)	5787(5)	34(4)
C(19B)	3701(3)	8780(4)	5197(3)	37(4)
C(20B)	3999(3)	9267(5)	5501(3)	51(5)

Continued on next page

Table continued

	x	y	z	U_{eq}
C(21B)	4106(3)	10043(5)	5337(4)	98(8)
C(22B)	3913(4)	10332(4)	4869(5)	60(6)
C(23B)	3615(4)	9844(5)	4566(4)	65(6)
C(24B)	3508(3)	9068(5)	4730(3)	47(5)
O(1AX)	5438(3)	2157(5)	5166(3)	50(3)
O(2AX)	5465(3)	3380(5)	4412(4)	46(3)
C(1AX)	5414(5)	1350(7)	5429(5)	40(4)
C(2AX)	5049(6)	2236(8)	4756(6)	63(5)
C(3AX)	5040(5)	3072(8)	4623(5)	38(4)
C(4AX)	5471(4)	4088(7)	4142(6)	43(5)
O(1BX)	4481(3)	6662(6)	5014(4)	55(3)
O(2BX)	4573(3)	7861(5)	4250(4)	52(3)
C(1BX)	4594(7)	5776(10)	5252(6)	83(6)
C(2BX)	4983(5)	6819(9)	4791(6)	49(5)
C(3BX)	4900(4)	7790(8)	4660(5)	43(5)
C(4BX)	4569(6)	8667(8)	4069(6)	53(5)
C(1M)	4732(1)	9160(1)	6934(1)	353(10)
C(2M)	5059(1)	9629(1)	6610(1)	212(9)
C(3M)	4660(1)	8390(1)	6682(1)	79(6)
C(4M)	4760(1)	9208(1)	7476(1)	86(6)
C(5M)	5194(1)	9148(1)	6161(1)	450(20)
C(6M)	5401(1)	10126(1)	6847(1)	209(14)
C(7M)	4946(1)	8382(1)	6205(1)	139(8)
C(8M)	4622(1)	7697(1)	6986(1)	104(9)
C(9M)	4718(1)	8488(1)	7792(1)	226(13)
C(10M)	5116(1)	9728(1)	7721(1)	186(15)
C(11M)	5664(1)	9180(1)	5966(1)	400(30)
C(12M)	5429(1)	10177(1)	7412(1)	426(18)
C(13M)	5892(1)	10164(1)	6640(1)	230(9)
C(14M)	5183(1)	7681(1)	6051(1)	363(11)
C(15M)	4651(1)	7749(1)	7552(1)	510(40)
C(16M)	4868(1)	6969(1)	6824(1)	220(20)
C(17M)	5049(1)	8560(1)	8233(1)	176(14)

Continued on next page

Table continued

	x	y	z	U_{eq}
C(18M)	5294(1)	9329(1)	8188(1)	137(7)
C(19M)	6021(1)	9700(1)	6212(1)	171(11)
C(20M)	5910(1)	8454(2)	5803(1)	286(14)
C(21M)	5939(1)	10245(1)	7557(2)	298(12)
C(22M)	6226(1)	10237(1)	7080(2)	450(20)
C(23M)	5674(1)	7719(1)	5844(1)	262(18)
C(24M)	5142(1)	6962(1)	6367(1)	339(17)
C(25M)	4914(1)	7052(1)	7740(1)	72(6)
C(26M)	5047(1)	6572(1)	7290(1)	370(20)
C(27M)	5300(1)	7893(2)	8412(1)	330(20)
C(28M)	5782(1)	9392(2)	8324(1)	233(10)
C(29M)	6487(1)	9292(2)	6198(2)	108(7)
C(30M)	6418(1)	8524(2)	5945(2)	480(30)
C(31M)	6111(1)	9858(1)	8001(2)	400(20)
C(32M)	6672(1)	9846(1)	7066(2)	530(30)
C(33M)	5936(1)	7026(1)	6033(1)	288(12)
C(34M)	5607(1)	6559(1)	6356(1)	400(20)
C(35M)	5231(1)	7126(1)	8159(1)	185(12)
C(36M)	5493(1)	6181(1)	7278(1)	660(30)
C(37M)	5808(1)	7963(2)	8554(1)	125(10)
C(38M)	6044(1)	8698(2)	8513(1)	371(17)
C(39M)	6804(1)	9366(2)	6617(2)	336(10)
C(40M)	6669(1)	7857(2)	6124(2)	198(15)
C(41M)	6576(1)	9456(2)	7990(2)	312(17)
C(42M)	6851(1)	9448(2)	7533(2)	203(13)
C(43M)	6424(1)	7088(2)	6169(2)	130(11)
C(44M)	5780(1)	6173(1)	6800(1)	258(14)
C(45M)	5698(1)	6717(1)	8145(1)	224(14)
C(46M)	5826(1)	6254(1)	7717(1)	198(16)
C(47M)	6054(1)	7238(2)	8391(2)	310(20)
C(48M)	6536(1)	8736(2)	8306(2)	239(12)
C(49M)	7068(1)	8669(2)	6805(2)	175(12)
C(50M)	7000(1)	7929(2)	6565(2)	216(15)

Continued on next page

Table continued

	x	y	z	U_{eq}
C(51M)	7097(1)	8720(2)	7371(2)	170(13)
C(52M)	6603(1)	6690(1)	6636(2)	135(9)
C(53M)	6289(1)	6241(1)	6945(2)	176(12)
C(54M)	6317(1)	6291(1)	7510(2)	920(30)
C(55M)	6525(1)	7270(2)	8196(2)	227(15)
C(56M)	6772(1)	8036(2)	8152(2)	197(15)
C(57M)	6958(1)	7210(2)	6881(2)	360(20)
C(58M)	7058(1)	8027(2)	7675(2)	126(9)
C(59M)	6659(1)	6789(2)	7747(2)	700(30)
C(60M)	6986(1)	7258(2)	7423(2)	178(9)
C(1N)	4719(1)	4159(1)	8123(2)	290(20)
C(2N)	4631(1)	4809(1)	7757(1)	540(30)
C(3N)	4284(1)	4051(2)	8435(2)	530(30)
C(4N)	4991(1)	3499(1)	7970(2)	132(7)
C(5N)	4140(1)	5098(1)	7839(1)	193(14)
C(6N)	4822(1)	4764(1)	7253(1)	490(20)
C(7N)	3925(1)	4630(1)	8259(2)	1360(80)
C(8N)	4138(1)	3281(2)	8580(2)	203(13)
C(9N)	4841(1)	2698(1)	8122(2)	117(7)
C(10N)	5190(1)	3455(1)	7445(2)	720(50)
C(11N)	3858(1)	5329(1)	7416(1)	322(14)
C(12N)	5106(1)	4075(1)	7095(2)	314(16)
C(13N)	4527(1)	5013(1)	6810(1)	251(15)
C(14N)	3436(1)	4415(2)	8235(2)	240(15)
C(15N)	4423(1)	2592(1)	8421(2)	160(10)
C(16N)	3629(1)	3060(2)	8555(2)	144(9)
C(17N)	4945(1)	2157(1)	7691(2)	115(8)
C(18N)	5162(1)	2628(1)	7273(2)	252(10)
C(19N)	4056(1)	5285(1)	6889(1)	440(30)
C(20N)	3349(1)	5112(1)	7390(2)	265(12)
C(21N)	4988(1)	3894(1)	6553(2)	390(20)
C(22N)	4629(1)	4473(1)	6376(1)	1090(110)
C(23N)	3142(1)	4663(1)	7791(2)	610(60)

Continued on next page

Table continued

	x	y	z	U_{eq}
C(24N)	3286(1)	3614(2)	8386(2)	194(12)
C(25N)	4090(1)	1944(1)	8298(2)	163(8)
C(26N)	3600(1)	2234(2)	8382(2)	529(12)
C(27N)	4626(1)	1538(1)	7575(2)	129(7)
C(28N)	5046(1)	2456(1)	6755(2)	850(30)
C(29N)	3667(1)	5040(1)	6540(2)	91(7)
C(30N)	3231(1)	4934(1)	6849(2)	87(6)
C(31N)	4956(1)	3103(1)	6388(2)	1590(100)
C(32N)	4256(1)	4238(1)	6042(2)	320(18)
C(33N)	2811(1)	4017(2)	7669(2)	280(20)
C(34N)	2900(1)	3370(2)	8036(2)	248(19)
C(35N)	4190(1)	1432(1)	7884(2)	360(20)
C(36N)	3228(1)	1999(2)	8048(2)	214(11)
C(37N)	4508(1)	1361(1)	7034(2)	273(11)
C(38N)	4715(1)	1809(1)	6633(2)	158(9)
C(39N)	3767(1)	4528(1)	6126(2)	188(6)
C(40N)	2912(1)	4315(1)	6733(2)	80(6)
C(41N)	4571(1)	2858(1)	6038(2)	480(40)
C(42N)	4228(1)	3412(1)	5869(2)	233(13)
C(43N)	2695(1)	3845(2)	7151(2)	216(8)
C(44N)	2869(1)	2578(2)	7871(2)	459(11)
C(45N)	3800(1)	1188(1)	7535(2)	329(16)
C(46N)	3330(1)	1460(1)	7614(2)	570(40)
C(47N)	3999(1)	1144(1)	7009(2)	990(80)
C(48N)	4420(1)	2057(1)	6189(2)	740(30)
C(49N)	3433(1)	3880(1)	6003(2)	226(14)
C(50N)	3015(1)	3774(2)	6302(2)	89(7)
C(51N)	3719(1)	3191(1)	5844(2)	640(17)
C(52N)	2667(1)	3017(2)	6979(2)	209(9)
C(53N)	2751(1)	2397(2)	7329(2)	400(30)
C(54N)	3035(1)	1709(1)	7171(2)	350(30)
C(55N)	3716(1)	1374(1)	6585(2)	480(30)
C(56N)	3931(1)	1842(1)	6165(2)	450(30)

Continued on next page

Table continued

	x	y	z	U_{eq}
C(57N)	2866(1)	2973(2)	6454(2)	101(7)
C(58N)	3573(1)	2421(1)	5989(2)	360(19)
C(59N)	3226(1)	1664(1)	6667(2)	420(30)
C(60N)	3137(1)	2313(1)	6301(2)	470(30)

9.5 [K(DB24C8)(DME)]$_2$[C$_{60}$]$_2$

Table 9.9: Atomic coordinates ($\times 10^4$) and equivalent isotropic displacement parameters (Å$^2\times 10^3$) for [K(DB24C8)(DME)]$_2$[C$_{60}$]$_2$. U_{eq} is defined as one third of the trace of the orthogonalized U_{ij} tensor.

	x	y	z	U_{eq}
K(1A)	7056	8746	5434	20
O(1A)	7641	7904	4156	29
O(2A)	7238	7630	5744	31
O(3A)	7355	8210	7197	29
O(4A)	7785	9269	6979	25
O(5A)	6729	9968	6043	22
O(6A)	5354	9121	6179	27
O(7A)	5175	8669	4547	30
O(8A)	6709	8743	3499	24
C(1A)	8172	7481	4567	30
C(2A)	7535	7240	5187	28
C(3A)	6979	7401	6508	28
C(4A)	6610	7831	7059	25
C(5A)	7150	8602	7808	27
C(6A)	7917	9024	7786	30
C(7A)	8171	9763	6878	22
C(8A)	9073	9916	7225	28
C(9A)	9412	10423	7053	26
C(10A)	8869	10775	6546	28
C(11A)	7977	10620	6219	24
C(12A)	7626	10124	6387	22
C(13A)	6044	9930	6678	22
C(14A)	5151	9670	6301	21
C(15A)	4540	8826	5850	26
C(16A)	4379	8886	4913	28
C(17A)	5045	8688	3646	30
C(18A)	5876	8420	3295	31
C(19A)	7525	8576	3136	20
C(20A)	7823	8850	2442	26

Continued on next page

Table continued

	x	y	z	U_{eq}
C(21A)	8700	8689	2118	31
C(22A)	9210	8275	2485	31
C(23A)	8894	7999	3171	28
C(24A)	8051	8151	3489	23
O(1S)	8159	9519	4744	32
O(2S)	9050	8620	5475	34
C(1S)	7761	9897	4184	36
C(2S)	9073	9373	4574	38
C(3S)	9566	9074	5291	34
C(4S)	9458	8337	6175	42
C(1)	4553(2)	5184(1)	4897(2)	60(3)
C(2)	3570(2)	5026(1)	5176(2)	135(9)
C(3)	3402(2)	5262(1)	5960(2)	112(7)
C(4)	4134(2)	5642(1)	6157(2)	155(12)
C(5)	4770(2)	5651(1)	5503(2)	320(30)
C(6)	5138(1)	6130(1)	5249(2)	125(7)
C(7)	5211(1)	6258(1)	4367(2)	100(5)
C(8)	4829(2)	5887(1)	3775(2)	111(7)
C(9)	4466(2)	5388(1)	4001(2)	84(4)
C(10)	3660(2)	5276(1)	3454(2)	138(8)
C(11)	2832(3)	5028(1)	3725(2)	159(13)
C(12)	2799(3)	4917(1)	4609(2)	137(10)
C(13)	2265(2)	5842(1)	6636(1)	84(4)
C(14)	1278(2)	5200(1)	4111(2)	99(5)
C(15)	2962(2)	6200(2)	6833(1)	200(17)
C(16)	3541(2)	5699(1)	2832(2)	350(40)
C(17)	4916(2)	6612(2)	5682(2)	105(5)
C(18)	3159(2)	6799(1)	2600(1)	69(3)
C(19)	2646(3)	5872(1)	2527(1)	250(20)
C(20)	3613(2)	7638(1)	4408(2)	114(7)
C(21)	1669(2)	5233(1)	5626(2)	158(12)
C(22)	4331(2)	6606(2)	6353(2)	180(14)
C(23)	963(2)	7245(1)	5242(2)	92(5)

Continued on next page

Table continued

	x	y	z	U_{eq}
C(24)	4288(2)	6083(1)	3037(2)	90(5)
C(25)	1834(2)	5022(1)	4838(2)	144(10)
C(26)	1869(2)	6946(1)	6426(2)	206(18)
C(27)	423(2)	5817(1)	4987(2)	99(5)
C(28)	3528(2)	7425(1)	5836(2)	104(6)
C(29)	1115(2)	6553(1)	6221(2)	82(4)
C(30)	3942(2)	6107(2)	6595(1)	174(13)
C(31)	4838(2)	7041(1)	5076(2)	65(3)
C(32)	4096(2)	6625(1)	2922(2)	57(2)
C(33)	2011(2)	7387(1)	3265(2)	99(6)
C(34)	1275(2)	7003(1)	3067(2)	146(10)
C(35)	214(1)	6377(1)	4880(2)	89(4)
C(36)	4477(2)	7006(1)	3548(2)	138(9)
C(37)	2577(3)	7605(1)	5527(2)	156(11)
C(38)	633(2)	6987(1)	3762(2)	144(10)
C(39)	1851(2)	7617(1)	4085(2)	194(16)
C(40)	1765(2)	7370(1)	5813(2)	290(30)
C(41)	564(2)	6743(1)	5474(2)	88(5)
C(42)	1084(2)	6025(2)	2903(2)	250(20)
C(43)	1795(2)	5613(1)	2827(2)	202(17)
C(44)	1903(3)	5213(1)	3424(2)	129(9)
C(45)	476(2)	6012(1)	3558(2)	123(8)
C(46)	2468(2)	5351(1)	6203(2)	78(4)
C(47)	4158(2)	7441(1)	5138(2)	97(6)
C(48)	3761(2)	7414(1)	3627(2)	102(5)
C(49)	1307(2)	6020(1)	6321(2)	64(3)
C(50)	2625(2)	7734(1)	4633(2)	141(10)
C(51)	587(2)	5590(1)	4167(2)	67(3)
C(52)	953(2)	5639(1)	5697(2)	140(10)
C(53)	2774(2)	6772(1)	6722(1)	203(18)
C(54)	3615(2)	7019(1)	6431(2)	161(10)
C(55)	998(2)	7358(1)	4373(2)	70(4)
C(56)	5004(2)	6813(1)	4256(2)	105(5)

Continued on next page

Table continued

	x	y	z	U_{eq}
C(57)	2452(2)	6436(2)	2412(1)	220(19)
C(58)	259(1)	6506(1)	4000(2)	129(8)
C(59)	1478(2)	6529(2)	2646(1)	230(20)
C(60)	2940(2)	7290(1)	3043(2)	107(6)

Table 9.10: Anisotropic displacement parameters ($Å^2 \times 10^3$) for $[K(DB24C8)(DME)]_2[C_{60}]_2$. The anisotropic displacement factor exponent takes the form: $-2\pi^2[h^2a^{*2}U_{11} + \ldots + 2hka^*b^*U_{12}]$.

	U_{11}	U_{22}	U_{33}	U_{23}	U_{13}	U_{12}
K(1A)	17	27	15	0	1	1
O(1A)	30	39	19	5	7	7
O(2A)	44	24	26	6	12	-1
O(3A)	28	26	33	-6	12	0
O(4A)	26	25	24	0	0	-2
O(5A)	18	26	21	0	3	-2
O(6A)	23	27	31	-8	2	-5
O(7A)	26	40	25	-5	3	3
O(8A)	24	28	21	-2	1	0
C(1A)	21	34	34	1	-3	5
C(2A)	35	27	22	-2	-2	-5
C(3A)	33	29	20	6	0	-5
C(4A)	20	31	27	7	8	-1
C(5A)	35	30	18	6	10	8
C(6A)	43	28	19	-2	-4	0
C(7A)	24	28	14	-1	2	1
C(8A)	24	42	19	-9	6	1
C(9A)	13	44	21	-14	-2	-7
C(10A)	30	37	17	-4	5	-10
C(11A)	24	30	19	4	2	-1

Continued on next page

Table continued

	U_{11}	U_{22}	U_{33}	U_{23}	U_{13}	U_{12}
C(12A)	19	33	16	-9	3	-1
C(13A)	26	23	19	-4	2	-7
C(14A)	17	28	19	4	3	2
C(15A)	19	34	24	-1	5	-4
C(16A)	25	34	24	0	-3	3
C(17A)	22	32	33	-6	-9	3
C(18A)	33	36	25	-5	-1	-1
C(19A)	28	22	12	-6	11	-2
C(20A)	42	21	15	-2	5	-4
C(21A)	39	37	20	-1	13	-14
C(22A)	16	49	27	-9	3	-5
C(23A)	27	35	23	3	4	0
C(24A)	28	22	18	2	-1	-2
O(1S)	38	31	30	2	12	-14
O(2S)	21	46	36	6	3	0
C(1S)	57	33	17	2	0	-15
C(2S)	45	43	29	0	17	-11
C(3S)	18	58	26	-14	5	-10
C(4S)	28	75	23	-7	-5	5
C(1)	49(6)	60(5)	75(8)	31(5)	31(6)	25(4)
C(2)	106(11)	54(7)	260(20)	84(10)	130(14)	63(7)
C(3)	88(9)	138(12)	117(12)	101(11)	56(9)	72(9)
C(4)	62(9)	320(30)	85(12)	93(17)	-10(9)	49(15)
C(5)	30(7)	700(90)	240(30)	320(50)	-23(13)	6(19)
C(6)	40(6)	240(20)	90(11)	-2(13)	0(7)	66(10)
C(7)	27(5)	132(13)	144(16)	-28(10)	21(7)	-5(5)
C(8)	94(9)	117(10)	135(12)	90(10)	99(9)	90(9)
C(9)	77(7)	81(7)	90(9)	-24(7)	-17(7)	66(6)
C(10)	174(19)	126(14)	112(14)	-92(13)	-6(13)	76(13)
C(11)	340(40)	51(8)	91(11)	1(7)	87(18)	60(14)
C(12)	51(6)	17(4)	340(30)	-1(8)	-1(10)	3(4)
C(13)	126(11)	80(7)	50(6)	35(6)	47(7)	46(7)
C(14)	100(10)	40(5)	149(14)	0(7)	-50(10)	-48(6)

Continued on next page

Table continued

	U_{11}	U_{22}	U_{33}	U_{23}	U_{13}	U_{12}
C(15)	160(19)	410(50)	30(7)	47(13)	-22(10)	-170(30)
C(16)	520(60)	460(60)	54(11)	-130(20)	-70(20)	400(60)
C(17)	34(5)	138(13)	138(15)	6(11)	-40(7)	-23(6)
C(18)	73(6)	98(8)	40(5)	31(5)	21(5)	25(6)
C(19)	580(60)	145(15)	22(6)	-47(8)	104(17)	-240(30)
C(20)	116(12)	49(6)	167(16)	48(8)	-59(12)	-38(7)
C(21)	250(30)	59(8)	190(20)	-13(10)	170(20)	-61(12)
C(22)	128(14)	360(40)	45(7)	60(14)	-45(9)	-180(20)
C(23)	74(7)	85(8)	114(11)	-75(8)	-8(7)	42(6)
C(24)	100(10)	139(12)	37(6)	26(7)	39(7)	50(9)
C(25)	84(9)	47(7)	290(30)	78(11)	-80(13)	-39(6)
C(26)	111(14)	380(50)	131(19)	-190(30)	38(13)	-40(20)
C(27)	75(8)	134(13)	94(10)	-43(9)	42(8)	-61(9)
C(28)	58(6)	72(8)	178(17)	-97(10)	-19(9)	3(6)
C(29)	79(7)	129(11)	43(6)	28(6)	30(6)	40(8)
C(30)	180(20)	280(30)	63(11)	84(16)	-56(14)	-100(20)
C(31)	36(4)	113(9)	47(5)	2(5)	0(4)	-45(5)
C(32)	46(5)	92(7)	36(5)	17(5)	22(4)	7(4)
C(33)	115(11)	99(9)	89(10)	71(8)	42(9)	61(9)
C(34)	77(10)	220(20)	142(18)	109(18)	-25(12)	49(14)
C(35)	9(3)	142(12)	116(12)	-25(9)	6(5)	1(5)
C(36)	92(10)	290(30)	35(6)	-5(10)	20(7)	-125(14)
C(37)	350(40)	39(6)	82(10)	-7(6)	47(15)	59(12)
C(38)	97(12)	151(16)	170(20)	-72(16)	-63(14)	86(12)
C(39)	180(20)	82(10)	340(40)	107(17)	200(20)	95(13)
C(40)	550(70)	74(11)	280(40)	-120(17)	340(50)	-80(20)
C(41)	64(6)	86(8)	121(11)	47(8)	69(7)	48(6)
C(42)	146(16)	490(50)	94(13)	160(20)	-111(14)	-230(30)
C(43)	132(18)	290(40)	170(30)	-170(30)	-32(17)	-80(20)
C(44)	87(9)	71(9)	230(30)	-113(13)	1(13)	-9(7)
C(45)	51(6)	63(7)	240(20)	-15(10)	-76(10)	-1(5)
C(46)	57(6)	65(6)	118(10)	52(7)	49(7)	15(5)
C(47)	101(9)	35(5)	145(14)	19(6)	-65(10)	-34(6)

Continued on next page

Table continued

	U_{11}	U_{22}	U_{33}	U_{23}	U_{13}	U_{12}
C(48)	99(10)	68(8)	144(14)	17(8)	52(10)	-43(7)
C(49)	63(6)	82(7)	50(6)	7(5)	39(5)	-6(5)
C(50)	108(11)	12(4)	290(30)	9(8)	-57(14)	13(5)
C(51)	46(5)	106(9)	49(5)	-13(6)	8(4)	-49(6)
C(52)	148(15)	210(20)	65(8)	-43(11)	62(10)	-150(16)
C(53)	510(50)	82(9)	30(6)	-27(6)	88(16)	-133(19)
C(54)	145(18)	200(20)	122(18)	-65(17)	-76(16)	-29(18)
C(55)	51(5)	67(6)	96(8)	50(6)	43(6)	49(5)
C(56)	62(7)	116(11)	144(15)	-11(10)	59(9)	-38(7)
C(57)	170(20)	470(50)	10(5)	20(12)	-11(8)	-210(30)
C(58)	58(8)	220(20)	102(13)	-37(15)	-47(9)	72(12)
C(59)	260(30)	280(30)	130(20)	130(20)	-180(30)	-150(30)
C(60)	86(8)	89(8)	156(14)	99(10)	80(9)	31(7)

Table 9.11: Hydrogen coordinates ($\times 10^4$) and isotropic displacement parameters ($Å^2 \times 10^3$) for $[K(DB24C8)(DME)]_2[C_{60}]_2$.

	x	y	z	U_{eq}
H(1A1)	8765	7621	4858	36
H(1A2)	8348	7210	4156	36
H(2A1)	6968	7078	4885	34
H(2A2)	7886	6955	5505	34
H(3A1)	7542	7226	6796	33
H(3A2)	6478	7127	6393	33
H(4A1)	6036	8002	6782	31
H(4A2)	6435	7677	7597	31
H(5A1)	7157	8438	8371	33
H(5A2)	6511	8761	7674	33
H(6A1)	7847	9291	8233	36
H(6A2)	8560	8861	7863	36
H(8A)	9448	9677	7571	34
H(9A)	10023	10530	7286	31

Continued on next page

Table continued

	x	y	z	U_{eq}
H(10A)	9110	11119	6426	33
H(11A)	7603	10859	5873	29
H(13A)	5894	10291	6884	27
H(13B)	6315	9716	7156	27
H(14A)	4626	9709	6681	26
H(14B)	4952	9840	5760	26
H(15A)	3964	8952	6119	31
H(15B)	4632	8444	5990	31
H(16A)	3791	8695	4710	33
H(16B)	4306	9267	4762	33
H(17A)	5003	9063	3453	35
H(17B)	4445	8503	3455	35
H(18A)	5966	8059	3539	37
H(18B)	5767	8384	2681	37
H(20A)	7455	9134	2195	31
H(21A)	8930	8868	1649	38
H(22A)	9796	8173	2266	37
H(23A)	9256	7711	3413	34
H(1S1)	7861	9784	3611	54
H(1S2)	8068	10243	4293	54
H(1S3)	7074	9927	4255	54
H(2S1)	9447	9696	4456	46
H(2S2)	9045	9145	4067	46
H(3S1)	10216	8970	5145	41
H(3S2)	9631	9308	5789	41
H(4S1)	10036	8152	6019	63
H(4S2)	8996	8075	6358	63
H(4S3)	9623	8587	6631	63

9.6 [4{K(DB18C6)($C_{60}^{\cdot -}$)}(THF)$_6$]·[C_{60}^{0}]·(THF)$_6$ at 80 K

Table 9.12: Atomic coordinates ($\times 10^4$) and equivalent isotropic displacement parameters (Å$^2\times 10^3$) for [4{K(DB18C6)($C_{60}^{\cdot -}$)}(THF)$_6$]·[C_{60}^{0}]·(THF)$_6$ at 80 K. U_{eq} is defined as one third of the trace of the orthogonalized U_{ij} tensor.

	x	y	z	U_{eq}
K(1A)	287(1)	4997(1)	6531(1)	34(1)
O(1A)	763(1)	4075(2)	7176(1)	51(1)
O(2A)	289(1)	3218(2)	6460(1)	52(1)
O(3A)	-152(1)	4214(2)	5801(1)	48(1)
O(4A)	-139(1)	5931(2)	5838(1)	43(1)
O(5A)	308(1)	6779(2)	6553(1)	48(1)
O(6A)	767(1)	5778(2)	7232(1)	50(1)
C(1A)	716(1)	3155(4)	7146(2)	84(2)
C(2A)	570(1)	2877(3)	6686(2)	89(2)
C(3A)	138(1)	2924(3)	6022(2)	67(2)
C(4A)	-157(1)	3283(3)	5800(2)	58(2)
C(5A)	-408(1)	4643(2)	5554(1)	48(1)
C(6A)	-662(1)	4212(2)	5290(1)	71(2)
C(7A)	-907(1)	4701(3)	5047(1)	84(2)
C(8A)	-898(1)	5620(3)	5069(1)	84(2)
C(9A)	-644(1)	6051(2)	5334(1)	71(2)
C(10A)	-399(1)	5563(2)	5576(1)	45(1)
C(11A)	-132(1)	6880(3)	5867(2)	54(1)
C(12A)	175(1)	7147(3)	6126(2)	60(1)
C(13A)	599(1)	7063(3)	6830(2)	70(2)
C(14A)	728(1)	6685(4)	7262(2)	62(2)
C(15A)	910(1)	5330(2)	7617(1)	61(2)
C(16A)	1051(1)	5742(2)	8021(1)	107(3)
C(17A)	1190(1)	5235(4)	8397(1)	165(6)
C(18A)	1188(1)	4316(3)	8369(1)	178(6)
C(19A)	1046(1)	3904(2)	7966(2)	99(3)
C(20A)	908(1)	4412(2)	7590(1)	70(2)
K(1B)	1657(1)	4925(1)	8161(1)	41(1)

Continued on next page

Table continued

	x	y	z	U_{eq}
O(1B)	1614(1)	3333(2)	7764(1)	56(1)
O(2B)	1488(1)	4948(2)	7297(1)	65(1)
O(3B)	1602(1)	6542(2)	7770(1)	57(1)
O(5B)	1948(1)	4917(2)	9062(1)	48(1)
O(4B)	1794(1)	6505(2)	8590(1)	56(1)
O(6B)	1812(1)	3339(2)	8588(1)	53(1)
C(1B)	1491(1)	3363(4)	7299(2)	68(2)
C(2B)	1596(1)	4195(4)	7201(2)	74(2)
C(3B)	1595(1)	5721(4)	7210(2)	72(2)
C(4B)	1483(1)	6517(4)	7308(2)	72(2)
C(5B)	1527(1)	7244(2)	7916(1)	62(2)
C(6B)	1354(1)	7930(2)	7657(1)	75(2)
C(7B)	1277(1)	8597(2)	7837(2)	85(2)
C(8B)	1372(1)	8578(2)	8276(2)	91(2)
C(9B)	1544(1)	7892(3)	8536(1)	80(2)
C(10B)	1622(1)	7225(2)	8355(1)	60(2)
C(11B)	1916(1)	6496(4)	9049(2)	63(2)
C(12B)	2108(1)	5719(4)	9220(2)	55(2)
C(13B)	2116(1)	4141(3)	9219(2)	51(1)
C(14B)	1932(1)	3340(4)	9050(1)	60(2)
C(15B)	1638(1)	2621(2)	8352(1)	56(2)
C(16B)	1559(1)	1945(2)	8526(1)	71(2)
C(17B)	1386(1)	1266(2)	8261(1)	80(2)
C(18B)	1291(1)	1264(2)	7822(1)	73(2)
C(19B)	1370(1)	1941(2)	7647(1)	63(2)
C(20B)	1543(1)	2619(2)	7913(1)	56(2)
O(1AX)	-89(1)	5009(2)	6769(1)	44(1)
C(1AX)	-245(1)	5761(3)	6748(2)	52(1)
C(2AX)	-386(1)	5530(3)	6989(2)	53(1)
C(3AX)	-393(1)	4520(3)	6983(2)	53(1)
C(4AX)	-257(1)	4284(3)	6735(2)	55(1)
O(1BX)	2145(1)	4906(3)	8206(2)	75(1)
C(1BX)	2315(1)	5684(5)	8292(2)	74(2)

Continued on next page

Table continued

	x	y	z	U_{eq}
C(2BX)	2605(1)	5360(6)	8595(3)	130(4)
C(3BX)	2610(1)	4437(6)	8562(4)	153(5)
C(4BX)	2318(1)	4141(4)	8296(2)	70(2)
O(1CX)	556(1)	5188(4)	6114(1)	109(2)
C(1CX)	850(1)	5159(5)	6287(2)	85(2)
C(2CX)	885(2)	4733(7)	6021(2)	148(5)
C(3CX)	598(2)	4664(8)	5622(2)	158(5)
C(4CX)	437(1)	5126(5)	5669(2)	80(2)
O(1SX)	1443(1)	3066(6)	9512(2)	209(2)
C(1SX)	1143(2)	3529(9)	9338(4)	209(2)
C(2SX)	971(2)	2861(9)	9058(4)	209(2)
C(3SX)	1170(2)	2225(9)	9067(4)	209(2)
C(4SX)	1430(2)	2483(9)	9245(4)	209(2)
C(1D)	170(1)	9983(3)	5125(2)	42(1)
C(2D)	272(1)	9207(3)	4984(1)	43(1)
C(3D)	359(1)	9495(3)	4697(1)	41(1)
C(4D)	366(1)	10437(3)	4701(1)	39(1)
C(5D)	283(1)	10751(3)	4986(1)	39(1)
C(6D)	418(1)	11474(3)	5248(1)	44(1)
C(7D)	502(1)	11496(3)	5708(1)	46(1)
C(8D)	454(1)	10733(3)	5874(1)	43(1)
C(9D)	311(1)	9978(3)	5620(1)	41(1)
C(10D)	439(1)	9213(3)	5868(1)	41(1)
C(11D)	481(1)	8441(3)	5694(1)	43(1)
C(12D)	398(1)	8460(3)	5241(1)	43(1)
C(13D)	607(1)	7968(3)	5208(1)	44(1)
C(14D)	683(1)	8231(3)	4912(1)	47(1)
C(15D)	559(1)	9008(3)	4651(1)	41(1)
C(16D)	770(1)	9480(3)	4616(1)	44(1)
C(17D)	775(1)	10375(4)	4616(1)	42(1)
C(18D)	567(1)	10892(3)	4659(1)	39(1)
C(19D)	704(1)	11640(3)	4919(1)	47(1)
C(20D)	632(1)	11926(3)	5215(2)	44(1)

Continued on next page

Table continued

	x	y	z	U_{eq}
C(21D)	848(1)	12228(3)	5646(2)	51(1)
C(22D)	766(1)	11943(3)	5945(1)	46(1)
C(23D)	978(1)	11652(3)	6364(1)	45(1)
C(24D)	926(1)	10872(3)	6549(1)	43(1)
C(25D)	667(1)	10430(3)	6313(1)	40(1)
C(26D)	661(1)	9487(3)	6310(1)	43(1)
C(27D)	914(1)	9017(3)	6548(1)	47(1)
C(28D)	952(1)	8219(3)	6347(2)	49(1)
C(29D)	739(1)	7957(3)	5931(1)	42(1)
C(30D)	816(1)	7655(3)	5629(2)	49(1)
C(31D)	1097(1)	7614(3)	5754(2)	50(1)
C(32D)	1178(1)	7903(4)	5452(2)	53(1)
C(33D)	975(1)	8207(3)	5040(1)	47(1)
C(34D)	1029(1)	8964(4)	4857(1)	48(1)
C(35D)	1286(1)	9422(4)	5090(1)	50(1)
C(36D)	1294(1)	10353(4)	5095(2)	50(1)
C(37D)	1040(1)	10852(4)	4861(1)	49(1)
C(38D)	999(1)	11624(3)	5047(2)	46(1)
C(39D)	1207(1)	11889(4)	5467(2)	55(1)
C(40D)	1130(1)	12217(3)	5772(2)	54(2)
C(41D)	1347(1)	11914(3)	6201(2)	51(1)
C(42D)	1264(1)	11636(4)	6485(2)	54(1)
C(43D)	1396(1)	10841(4)	6754(1)	49(1)
C(44D)	1180(1)	10377(4)	6788(1)	47(1)
C(45D)	1173(1)	9461(4)	6785(1)	50(1)
C(46D)	1381(1)	8970(4)	6745(1)	51(2)
C(47D)	1237(1)	8199(3)	6470(2)	51(1)
C(48D)	1318(1)	7903(4)	6186(2)	56(2)
C(49D)	1528(1)	8370(4)	6146(2)	54(2)
C(50D)	1443(1)	8359(4)	5696(2)	51(1)
C(51D)	1498(1)	9099(4)	5520(2)	57(2)
C(52D)	1640(1)	9878(4)	5791(2)	56(2)
C(53D)	1511(1)	10654(4)	5524(2)	56(2)

Continued on next page

Table continued

	x	y	z	U_{eq}
C(54D)	1466(1)	11408(4)	5708(2)	54(2)
C(55D)	1550(1)	11402(4)	6158(2)	57(2)
C(56D)	1675(1)	10651(4)	6412(2)	59(2)
C(57D)	1595(1)	10375(4)	6718(2)	58(2)
C(58D)	1587(1)	9409(4)	6713(2)	53(2)
C(59D)	1661(1)	9099(4)	6402(2)	59(2)
C(60D)	1713(1)	9867(4)	6224(2)	57(2)
C(1)	743(1)	9984(3)	3026(2)	37(1)
C(2)	691(1)	10756(3)	3212(1)	42(1)
C(3)	614(1)	10460(3)	3515(1)	46(1)
C(4)	613(1)	9500(3)	3514(1)	47(1)
C(5)	691(1)	9206(3)	3213(2)	43(1)
C(6)	564(1)	8461(3)	2949(2)	44(1)
C(7)	483(1)	8471(3)	2509(2)	45(1)
C(8)	527(1)	9198(3)	2322(2)	48(1)
C(9)	662(1)	9979(3)	2588(2)	46(1)
C(10)	528(1)	10759(3)	2324(2)	47(1)
C(11)	485(1)	11482(3)	2508(2)	47(1)
C(12)	564(1)	11503(3)	2955(2)	43(1)
C(13)	358(1)	11975(3)	2994(2)	45(1)
C(14)	279(1)	11703(3)	3279(1)	45(1)
C(15)	408(1)	10928(3)	3548(1)	48(1)
C(16)	203(1)	10439(4)	3585(1)	47(1)
C(17)	203(1)	9517(4)	3585(1)	50(1)
C(18)	408(1)	9029(3)	3548(1)	46(1)
C(19)	281(1)	8256(3)	3281(1)	45(1)
C(20)	356(1)	7978(3)	2994(2)	45(1)
C(21)	140(1)	7693(3)	2558(2)	47(1)
C(22)	212(1)	7977(3)	2253(2)	47(1)
C(23)	312(1)	9512(4)	1889(1)	50(1)
C(24)	311(1)	10439(4)	1889(2)	51(1)
C(25)	212(1)	11979(3)	2254(2)	50(1)
C(26)	140(1)	12266(3)	2559(2)	46(1)

Continued on next page

Table continued

	x	y	z	U_{eq}
C(27)	-13(1)	11694(3)	3149(2)	53(1)
C(28)	-64(1)	10917(4)	3339(1)	50(1)
C(29)	-64(1)	9038(4)	3339(1)	53(1)
C(30)	-15(1)	8253(3)	3147(2)	52(1)
C(1N)	2942(1)	3540(1)	6709(1)	240(4)
C(2N)	2896(1)	3514(2)	7066(1)	233(4)
C(3N)	2727(1)	3006(1)	6360(1)	291(4)
C(4N)	3034(1)	4313(2)	6616(1)	220(3)
C(5N)	2652(1)	2971(1)	6937(1)	265(4)
C(6N)	2945(1)	4270(2)	7315(1)	200(3)
C(7N)	2547(1)	2655(1)	6500(1)	324(5)
C(8N)	2612(1)	3274(2)	5930(1)	299(5)
C(9N)	2915(1)	4591(2)	6171(1)	207(3)
C(10N)	3085(1)	5098(2)	6877(1)	227(4)
C(11N)	2465(1)	3205(2)	7059(1)	278(4)
C(12N)	3041(1)	5075(2)	7218(1)	196(3)
C(13N)	2751(1)	4509(2)	7446(1)	189(3)
C(14N)	2260(1)	2590(1)	6205(1)	324(4)
C(15N)	2708(1)	4082(2)	5835(1)	231(4)
C(16N)	2312(1)	3202(2)	5625(1)	277(4)
C(17N)	2891(1)	5548(2)	6154(1)	228(4)
C(18N)	2997(1)	5861(2)	6592(1)	223(4)
C(19N)	2516(1)	3992(2)	7320(1)	249(4)
C(20N)	2166(1)	3132(2)	6756(1)	337(5)
C(21N)	2906(1)	5817(2)	7290(1)	188(3)
C(22N)	2726(1)	5468(2)	7430(1)	197(3)
C(23N)	2065(1)	2830(1)	6337(1)	313(5)
C(24N)	2140(1)	2868(2)	5760(1)	314(5)
C(25N)	2468(1)	4509(2)	5470(1)	224(4)
C(26N)	2224(1)	3965(2)	5341(1)	226(4)
C(27N)	2661(1)	5955(2)	5804(1)	220(4)
C(28N)	2866(1)	6568(1)	6659(1)	240(4)
C(29N)	2247(1)	4401(2)	7176(1)	266(3)

Continued on next page

Table continued

	x	y	z	U_{eq}
C(30N)	2031(1)	3870(2)	6828(1)	318(5)
C(31N)	2819(1)	6544(1)	7015(1)	239(4)
C(32N)	2468(1)	5860(2)	7292(1)	234(4)
C(33N)	1826(1)	3257(2)	5973(1)	333(4)
C(34N)	1873(1)	3280(2)	5617(1)	320(4)
C(35N)	2446(1)	5424(2)	5457(1)	222(4)
C(36N)	1967(1)	4357(2)	5202(1)	235(3)
C(37N)	2526(1)	6694(2)	5877(1)	294(4)
C(38N)	2627(1)	6995(1)	6295(1)	267(5)
C(39N)	2225(1)	5316(2)	7163(1)	272(4)
C(40N)	1802(1)	4277(2)	6479(1)	332(4)
C(41N)	2552(1)	6956(1)	6873(1)	255(4)
C(42N)	2380(1)	6623(2)	7007(1)	266(4)
C(43N)	1696(1)	3964(2)	6040(1)	324(4)
C(44N)	1787(1)	4008(2)	5343(1)	283(4)
C(45N)	2176(1)	5833(2)	5312(1)	247(4)
C(46N)	1942(1)	5316(2)	5186(1)	217(4)
C(47N)	2227(1)	6620(2)	5573(1)	292(5)
C(48N)	2433(1)	7235(1)	6427(1)	317(6)
C(49N)	1984(1)	5743(2)	6798(1)	328(5)
C(50N)	1778(1)	5234(2)	6462(2)	329(4)
C(51N)	2081(1)	6551(2)	6702(1)	343(5)
C(52N)	1608(1)	4727(2)	5755(1)	331(5)
C(53N)	1652(1)	4749(2)	5414(1)	271(4)
C(54N)	1747(1)	5555(2)	5318(1)	325(4)
C(55N)	2040(1)	6854(2)	5696(1)	351(6)
C(56N)	2145(1)	7169(1)	6133(1)	331(5)
C(57N)	1659(1)	5512(2)	6016(1)	304(4)
C(58N)	1965(1)	6819(2)	6273(1)	305(4)
C(59N)	1796(1)	6311(2)	5567(1)	327(5)
C(60N)	1750(1)	6285(2)	5924(1)	357(5)
O(1T)	9002(2)	7177(7)	6032(2)	372(5)
C(1T)	8845(2)	7826(7)	5806(4)	372(5)

Continued on next page

Table continued

	x	y	z	U_{eq}
C(2T)	8600(2)	7516(10)	5534(3)	372(5)
C(3T)	8606(2)	6676(9)	5593(4)	372(5)
C(4T)	8854(2)	6466(6)	5900(4)	372(5)
O(1U)	1821(5)	10534(8)	9639(6)	790(20)
C(1U)	1996(6)	10524(11)	10001(7)	790(20)
C(2U)	2027(7)	9802(13)	10120(9)	790(20)
C(3U)	1872(8)	9366(9)	9832(10)	790(20)
C(4U)	1744(6)	9818(12)	9535(8)	790(20)

Table 9.13: Anisotropic displacement parameters ($Å^2 \times 10^3$) for $[4\{K(DB18C6)(C_{60}^{\cdot -})\}(THF)_6]\cdot[C_{60}{}^0]\cdot(THF)_6$ at 80 K. The anisotropic displacement factor exponent takes the form: $-2\pi^2[h^2a^{*2}U_{11} + \ldots + 2hka^*b^*U_{12}]$.

	U_{11}	U_{22}	U_{33}	U_{23}	U_{13}	U_{12}
K(1A)	29(1)	30(1)	40(1)	-1(1)	17(1)	-1(1)
O(1A)	34(2)	57(2)	56(2)	23(2)	19(1)	4(2)
O(2A)	30(1)	29(2)	86(2)	-3(2)	24(2)	1(1)
O(3A)	37(2)	39(2)	58(2)	-16(2)	19(1)	-5(1)
O(4A)	34(1)	44(2)	47(2)	13(1)	20(1)	7(1)
O(5A)	38(1)	32(2)	76(2)	-6(2)	31(1)	-6(1)
O(6A)	34(1)	56(2)	58(2)	-24(2)	22(1)	-4(2)
C(1A)	30(2)	53(3)	131(5)	51(3)	17(3)	-2(2)
C(2A)	42(3)	26(3)	182(6)	21(3)	47(3)	10(2)
C(3A)	59(3)	42(3)	112(4)	-25(3)	53(3)	-9(2)
C(4A)	47(2)	57(3)	69(3)	-24(3)	29(2)	-10(2)
C(5A)	29(2)	75(3)	35(2)	-2(2)	14(2)	2(2)
C(6A)	39(3)	88(4)	70(4)	-12(3)	18(3)	-12(3)
C(7A)	26(3)	136(6)	66(4)	15(4)	7(3)	-8(3)
C(8A)	34(3)	124(6)	79(4)	37(4)	19(3)	14(3)
C(9A)	43(3)	90(4)	67(3)	37(3)	21(2)	16(3)

Continued on next page

Table continued

	U_{11}	U_{22}	U_{33}	U_{23}	U_{13}	U_{12}
C(10A)	41(2)	51(3)	42(2)	14(2)	22(2)	7(2)
C(11A)	66(3)	34(3)	70(3)	14(2)	41(2)	7(2)
C(12A)	80(3)	30(3)	101(3)	3(2)	71(2)	-2(2)
C(13A)	56(2)	31(3)	141(4)	-36(3)	65(3)	-19(2)
C(14A)	39(2)	59(3)	78(3)	-32(3)	25(2)	-6(2)
C(15A)	21(2)	114(5)	46(3)	-8(3)	15(2)	9(3)
C(16A)	31(3)	230(9)	53(3)	-49(4)	18(2)	4(4)
C(17A)	32(3)	402(18)	62(4)	-34(6)	25(3)	2(6)
C(18A)	36(3)	447(18)	59(4)	80(6)	31(3)	32(6)
C(19A)	33(2)	191(7)	79(3)	69(4)	33(2)	25(4)
C(20A)	30(2)	128(5)	62(3)	40(3)	31(2)	14(3)
K(1B)	33(1)	60(1)	30(1)	3(1)	15(1)	4(1)
O(1B)	60(2)	59(2)	38(2)	-9(2)	20(1)	-18(2)
O(2B)	60(2)	84(3)	31(2)	4(2)	10(2)	-2(2)
O(3B)	53(2)	59(2)	45(2)	16(2)	16(2)	12(2)
O(5B)	43(2)	58(2)	32(2)	-1(1)	13(1)	2(2)
O(4B)	59(2)	56(2)	48(2)	6(2)	26(2)	18(2)
O(6B)	57(2)	63(2)	33(2)	-4(2)	19(1)	-19(2)
C(1B)	67(3)	88(4)	39(3)	-19(3)	21(2)	-23(3)
C(2B)	75(3)	95(5)	47(3)	-9(3)	29(3)	-12(4)
C(3B)	75(3)	89(5)	41(3)	17(3)	24(3)	2(4)
C(4B)	63(3)	88(4)	47(3)	34(3)	17(3)	9(3)
C(5B)	49(3)	60(4)	65(3)	22(3)	22(2)	9(3)
C(6B)	45(3)	67(4)	97(4)	36(3)	27(3)	11(3)
C(7B)	48(3)	60(4)	127(5)	23(4)	33(3)	11(3)
C(8B)	69(3)	53(4)	149(6)	-1(4)	57(4)	15(3)
C(9B)	72(3)	72(4)	101(4)	11(3)	49(3)	15(3)
C(10B)	54(3)	45(3)	87(3)	4(3)	42(2)	15(2)
C(11B)	68(3)	74(4)	44(3)	-12(3)	26(2)	6(3)
C(12B)	48(3)	71(4)	31(2)	-7(2)	10(2)	4(3)
C(13B)	39(2)	65(3)	32(2)	9(2)	7(2)	4(2)
C(14B)	58(3)	74(4)	37(3)	14(3)	18(2)	-10(3)
C(15B)	57(3)	49(3)	58(3)	-2(2)	29(2)	-19(2)

Continued on next page

Table continued

	U_{11}	U_{22}	U_{33}	U_{23}	U_{13}	U_{12}
C(16B)	84(3)	63(4)	71(3)	-2(3)	44(3)	-20(3)
C(17B)	78(3)	46(3)	115(5)	0(3)	51(3)	-24(3)
C(18B)	58(3)	58(4)	93(4)	-20(3)	33(3)	-21(3)
C(19B)	54(3)	57(3)	66(3)	-20(3)	24(3)	-17(3)
C(20B)	45(2)	63(4)	57(3)	-16(3)	24(2)	-14(3)
O(1AX)	54(2)	25(2)	67(2)	0(1)	40(1)	-1(1)
C(1AX)	68(3)	34(3)	72(3)	5(2)	49(2)	10(2)
C(2AX)	61(3)	39(3)	72(3)	3(2)	43(2)	8(2)
C(3AX)	54(2)	47(3)	68(3)	3(2)	38(2)	-4(2)
C(4AX)	65(3)	36(3)	78(3)	-6(2)	49(2)	-11(2)
O(1BX)	32(2)	103(4)	85(3)	-1(2)	28(2)	-1(2)
C(1BX)	41(3)	101(5)	78(4)	0(3)	30(3)	-5(3)
C(2BX)	33(3)	121(6)	166(8)	-34(6)	4(4)	0(4)
C(3BX)	35(4)	115(7)	217(10)	35(7)	2(5)	-9(4)
C(4BX)	43(3)	94(5)	72(3)	3(3)	30(2)	5(3)
O(1CX)	39(2)	242(7)	44(2)	-5(3)	21(2)	2(3)
C(1CX)	35(3)	152(7)	62(4)	-16(4)	21(3)	3(3)
C(2CX)	58(4)	330(14)	58(4)	-34(6)	31(3)	-1(6)
C(3CX)	68(4)	343(14)	56(4)	-12(6)	29(4)	-1(7)
C(4CX)	56(3)	145(7)	36(3)	-1(3)	22(2)	14(4)
O(1SX)	125(3)	289(7)	202(4)	-80(4)	78(3)	-96(4)
C(1SX)	125(3)	289(7)	202(4)	-80(4)	78(3)	-96(4)
C(2SX)	125(3)	289(7)	202(4)	-80(4)	78(3)	-96(4)
C(3SX)	125(3)	289(7)	202(4)	-80(4)	78(3)	-96(4)
C(4SX)	125(3)	289(7)	202(4)	-80(4)	78(3)	-96(4)
C(1D)	34(2)	54(3)	33(2)	-5(2)	15(2)	1(2)
C(2D)	32(2)	63(3)	28(2)	-9(2)	11(2)	-8(2)
C(3D)	29(2)	46(3)	33(2)	-4(2)	5(2)	-1(2)
C(4D)	30(2)	50(3)	26(2)	0(2)	7(2)	1(2)
C(5D)	28(2)	46(3)	34(2)	7(2)	12(2)	4(2)
C(6D)	37(2)	49(3)	40(2)	6(2)	17(2)	5(2)
C(7D)	48(2)	49(3)	42(2)	-5(2)	25(2)	3(2)
C(8D)	36(2)	57(3)	38(2)	-3(2)	21(2)	2(2)

Continued on next page

Table continued

	U_{11}	U_{22}	U_{33}	U_{23}	U_{13}	U_{12}
C(9D)	31(2)	57(3)	28(2)	2(2)	11(2)	2(2)
C(10D)	34(2)	52(3)	38(2)	-2(2)	20(2)	-6(2)
C(11D)	44(2)	47(3)	38(2)	5(2)	22(2)	-7(2)
C(12D)	30(2)	44(3)	41(2)	-7(2)	10(2)	-7(2)
C(13D)	45(2)	42(3)	42(2)	-6(2)	20(2)	-2(2)
C(14D)	39(2)	52(3)	42(2)	-9(2)	15(2)	-3(2)
C(15D)	33(2)	55(3)	27(2)	-11(2)	11(2)	-4(2)
C(16D)	48(2)	56(3)	25(2)	-3(2)	17(2)	-2(2)
C(17D)	40(2)	60(3)	21(2)	1(2)	13(2)	-2(2)
C(18D)	32(2)	55(3)	22(2)	5(2)	8(2)	-2(2)
C(19D)	49(2)	52(3)	40(2)	10(2)	24(2)	0(2)
C(20D)	46(2)	31(2)	50(3)	10(2)	22(2)	1(2)
C(21D)	56(3)	42(3)	48(3)	-1(2)	23(2)	-2(2)
C(22D)	57(2)	42(3)	42(2)	-11(2)	28(2)	-5(2)
C(23D)	52(2)	44(3)	38(2)	-14(2)	22(2)	-9(2)
C(24D)	50(2)	54(3)	24(2)	-9(2)	19(2)	-2(2)
C(25D)	32(2)	56(3)	35(2)	-6(2)	19(2)	-2(2)
C(26D)	39(2)	50(3)	38(2)	6(2)	20(2)	1(2)
C(27D)	46(2)	55(3)	34(2)	12(2)	16(2)	6(2)
C(28D)	58(3)	42(3)	48(3)	13(2)	28(2)	11(2)
C(29D)	50(2)	39(3)	37(2)	3(2)	23(2)	-11(2)
C(30D)	52(3)	38(3)	54(3)	-1(2)	26(2)	0(2)
C(31D)	55(3)	39(3)	50(3)	2(2)	24(2)	10(2)
C(32D)	50(2)	60(3)	49(3)	-3(2)	25(2)	15(2)
C(33D)	49(2)	47(3)	40(2)	-11(2)	20(2)	4(2)
C(34D)	35(2)	73(4)	34(2)	-7(2)	18(2)	8(2)
C(35D)	42(2)	72(4)	42(2)	-3(2)	28(2)	5(2)
C(36D)	32(2)	83(4)	33(2)	-1(2)	16(2)	-3(2)
C(37D)	46(2)	73(4)	32(2)	-3(2)	23(2)	-15(2)
C(38D)	41(2)	47(3)	48(2)	7(2)	22(2)	-10(2)
C(39D)	53(2)	66(3)	50(3)	-2(2)	31(2)	-20(3)
C(40D)	57(3)	41(3)	55(3)	-10(2)	23(2)	-21(2)
C(41D)	44(2)	54(3)	45(3)	-14(2)	16(2)	-23(2)

Continued on next page

Table continued

	U_{11}	U_{22}	U_{33}	U_{23}	U_{13}	U_{12}
C(42D)	54(3)	60(3)	40(3)	-25(2)	19(2)	-24(3)
C(43D)	36(2)	71(4)	25(2)	-11(2)	7(2)	-13(2)
C(44D)	42(2)	71(3)	21(2)	-5(2)	11(2)	-6(3)
C(45D)	44(2)	70(4)	27(2)	3(2)	13(2)	1(3)
C(46D)	33(2)	73(4)	32(2)	9(2)	7(2)	13(2)
C(47D)	51(3)	54(3)	37(2)	17(2)	16(2)	16(2)
C(48D)	52(3)	62(3)	44(3)	19(2)	18(2)	24(3)
C(49D)	33(2)	76(4)	41(3)	-1(3)	11(2)	15(3)
C(50D)	38(2)	56(3)	56(3)	10(2)	23(2)	18(2)
C(51D)	30(2)	95(4)	37(2)	-9(3)	11(2)	13(3)
C(52D)	24(2)	92(5)	51(3)	3(3)	19(2)	3(2)
C(53D)	37(2)	87(4)	48(3)	-6(3)	25(2)	-12(3)
C(54D)	31(2)	70(4)	51(3)	-2(3)	15(2)	-21(2)
C(55D)	35(2)	79(4)	50(3)	-15(3)	19(2)	-20(3)
C(56D)	31(2)	82(4)	42(3)	-5(3)	3(2)	-13(3)
C(57D)	29(2)	91(4)	29(3)	-2(3)	-1(2)	-12(3)
C(58D)	37(2)	68(4)	35(3)	6(2)	7(2)	9(3)
C(59D)	37(2)	90(4)	42(3)	7(3)	16(2)	17(3)
C(60D)	21(2)	95(5)	45(3)	-5(3)	12(2)	-2(2)
C(1)	26(2)	37(3)	40(2)	-3(2)	13(2)	0(2)
C(2)	25(2)	45(3)	40(2)	0(2)	5(2)	-5(2)
C(3)	26(2)	54(3)	32(2)	-8(2)	-2(2)	-1(2)
C(4)	29(2)	53(3)	33(2)	6(2)	-1(2)	4(2)
C(5)	25(2)	43(3)	43(2)	3(2)	7(2)	9(2)
C(6)	30(2)	37(3)	52(3)	6(2)	13(2)	13(2)
C(7)	42(2)	32(2)	65(3)	-1(2)	30(2)	12(2)
C(8)	38(2)	60(3)	56(3)	-9(2)	32(2)	5(2)
C(9)	29(2)	56(3)	62(3)	0(2)	30(2)	2(2)
C(10)	40(2)	56(3)	51(2)	4(2)	29(2)	-8(2)
C(11)	43(2)	35(3)	64(3)	6(2)	30(2)	-9(2)
C(12)	36(2)	34(3)	49(3)	-6(2)	17(2)	-10(2)
C(13)	41(2)	22(2)	58(3)	-16(2)	17(2)	-8(2)
C(14)	50(2)	35(3)	40(2)	-17(2)	16(2)	-6(2)

Continued on next page

Table continued

	U_{11}	U_{22}	U_{33}	U_{23}	U_{13}	U_{12}
C(15)	52(3)	53(3)	29(2)	-17(2)	14(2)	-12(2)
C(16)	49(2)	69(3)	19(2)	-4(2)	15(2)	4(3)
C(17)	51(3)	70(4)	21(2)	13(2)	15(2)	0(3)
C(18)	48(2)	50(3)	33(2)	13(2)	17(2)	7(2)
C(19)	52(3)	34(3)	37(2)	16(2)	16(2)	8(2)
C(20)	38(2)	25(2)	59(3)	11(2)	17(2)	6(2)
C(21)	44(2)	18(2)	66(3)	-3(2)	22(2)	4(2)
C(22)	54(2)	28(2)	61(3)	-8(2)	33(2)	6(2)
C(23)	52(2)	72(4)	40(2)	-10(2)	34(2)	-1(3)
C(24)	51(2)	72(4)	43(2)	8(2)	33(2)	0(3)
C(25)	55(2)	36(3)	60(3)	7(2)	33(2)	-9(2)
C(26)	46(2)	21(2)	62(3)	-2(2)	22(2)	-7(2)
C(27)	64(3)	48(3)	54(3)	-21(2)	37(2)	-3(2)
C(28)	59(2)	61(3)	38(2)	-9(2)	31(2)	2(2)
C(29)	65(3)	65(4)	37(2)	13(2)	31(2)	-2(3)
C(30)	64(3)	43(3)	54(3)	23(2)	35(2)	8(2)
C(1N)	196(6)	343(9)	172(6)	73(5)	91(5)	160(6)
C(2N)	145(6)	306(9)	156(6)	64(5)	17(5)	99(6)
C(3N)	312(7)	238(10)	268(6)	-57(6)	117(6)	109(7)
C(4N)	79(5)	381(7)	160(6)	-1(6)	36(5)	93(6)
C(5N)	280(6)	189(9)	261(7)	105(6)	98(5)	49(7)
C(6N)	128(5)	298(7)	128(6)	38(6)	36(5)	53(6)
C(7N)	341(6)	140(11)	304(7)	19(7)	44(6)	65(7)
C(8N)	228(7)	302(10)	260(7)	-100(7)	56(7)	67(7)
C(9N)	108(6)	402(8)	130(5)	10(5)	76(5)	43(6)
C(10N)	110(7)	440(9)	134(5)	-13(6)	67(5)	10(6)
C(11N)	206(6)	293(9)	222(8)	143(6)	37(6)	-51(6)
C(12N)	50(4)	388(9)	127(6)	-14(5)	32(4)	-24(5)
C(13N)	95(5)	348(8)	95(6)	54(6)	31(4)	0(5)
C(14N)	428(7)	118(9)	326(7)	-13(7)	130(6)	-100(7)
C(15N)	151(5)	357(8)	187(6)	-110(6)	90(5)	50(6)
C(16N)	305(6)	275(9)	228(7)	-157(6)	125(6)	-44(6)
C(17N)	176(7)	382(8)	136(6)	-35(5)	89(5)	-96(7)

Continued on next page

Table continued

	U_{11}	U_{22}	U_{33}	U_{23}	U_{13}	U_{12}
C(18N)	90(5)	359(8)	166(6)	-7(6)	31(5)	-77(6)
C(19N)	194(6)	397(9)	132(7)	37(7)	71(5)	-56(6)
C(20N)	256(7)	413(11)	293(8)	22(7)	112(6)	-199(6)
C(21N)	134(5)	288(7)	125(6)	-77(6)	56(5)	-71(6)
C(22N)	146(5)	343(8)	105(6)	-46(6)	69(5)	-6(6)
C(23N)	344(7)	255(11)	262(6)	-35(7)	107(6)	-189(7)
C(24N)	323(7)	295(13)	225(7)	-51(8)	76(5)	-98(8)
C(25N)	117(5)	401(7)	151(7)	-91(6)	70(5)	-22(6)
C(26N)	177(5)	356(9)	117(7)	-71(7)	59(5)	-20(6)
C(27N)	210(6)	301(8)	157(6)	61(5)	102(5)	-76(6)
C(28N)	229(6)	277(10)	259(6)	-59(6)	158(5)	-132(6)
C(29N)	115(5)	597(8)	102(6)	12(7)	68(4)	-76(6)
C(30N)	179(6)	602(9)	184(7)	-1(8)	103(6)	-86(8)
C(31N)	229(6)	256(9)	169(6)	-76(6)	63(5)	-116(7)
C(32N)	205(5)	414(9)	126(5)	-44(6)	117(4)	49(6)
C(33N)	257(7)	411(10)	273(7)	-53(7)	99(6)	-237(7)
C(34N)	209(7)	415(10)	233(7)	-48(7)	47(6)	-197(6)
C(35N)	133(5)	413(8)	124(7)	54(6)	71(5)	-21(6)
C(36N)	105(5)	493(9)	76(6)	-50(6)	26(4)	-74(6)
C(37N)	347(7)	263(10)	282(7)	97(6)	173(6)	-66(7)
C(38N)	300(7)	250(13)	251(6)	53(7)	145(6)	-29(8)
C(39N)	176(6)	554(8)	151(7)	3(7)	130(5)	18(7)
C(40N)	112(6)	648(9)	199(7)	-37(6)	58(6)	-160(7)
C(41N)	356(6)	163(9)	291(7)	-97(6)	200(5)	5(7)
C(42N)	274(7)	299(10)	187(7)	-96(7)	97(6)	54(6)
C(43N)	102(6)	567(8)	204(7)	22(6)	13(6)	-153(7)
C(44N)	118(6)	465(8)	183(8)	-39(7)	23(6)	-105(7)
C(45N)	197(6)	395(9)	133(7)	128(6)	76(5)	46(6)
C(46N)	102(5)	423(9)	74(6)	54(6)	10(4)	35(5)
C(47N)	304(6)	286(11)	214(8)	117(8)	88(6)	50(7)
C(48N)	372(7)	188(15)	355(8)	34(8)	169(6)	37(8)
C(49N)	227(8)	595(10)	126(7)	-56(7)	69(7)	6(8)
C(50N)	122(6)	702(9)	229(7)	3(6)	138(5)	39(7)

Continued on next page

Table continued

	U_{11}	U_{22}	U_{33}	U_{23}	U_{13}	U_{12}
C(51N)	243(7)	417(11)	379(8)	17(7)	172(6)	194(6)
C(52N)	72(7)	630(9)	190(6)	-21(7)	1(6)	-37(8)
C(53N)	67(5)	595(9)	104(6)	-25(7)	12(5)	-26(7)
C(54N)	89(6)	498(9)	285(9)	95(8)	29(6)	81(7)
C(55N)	346(7)	349(15)	306(8)	92(9)	138(6)	120(9)
C(56N)	335(7)	220(12)	406(8)	49(8)	173(6)	161(7)
C(57N)	64(6)	606(8)	142(6)	-59(6)	-14(5)	71(7)
C(58N)	233(7)	323(11)	285(6)	34(8)	88(6)	208(6)
C(59N)	227(8)	442(11)	234(8)	85(7)	70(6)	212(7)
C(60N)	163(7)	475(11)	371(8)	127(8)	98(7)	215(7)
O(1T)	305(8)	305(9)	280(8)	6(7)	0(6)	-201(7)
C(1T)	305(8)	305(9)	280(8)	6(7)	0(6)	-201(7)
C(2T)	305(8)	305(9)	280(8)	6(7)	0(6)	-201(7)
C(3T)	305(8)	305(9)	280(8)	6(7)	0(6)	-201(7)
C(4T)	305(8)	305(9)	280(8)	6(7)	0(6)	-201(7)
O(1U)	980(30)	1150(60)	441(17)	290(13)	500(19)	218(17)
C(1U)	980(30)	1150(60)	441(17)	290(13)	500(19)	218(17)
C(2U)	980(30)	1150(60)	441(17)	290(13)	500(19)	218(17)
C(3U)	980(30)	1150(60)	441(17)	290(13)	500(19)	218(17)
C(4U)	980(30)	1150(60)	441(17)	290(13)	500(19)	218(17)

Table 9.14: Hydrogen coordinates ($\times 10^4$) and isotropic displacement parameters (Å$^2\times 10^3$) for [4{K(DB18C6)($C_{60}^{\cdot -}$)}$(THF)_6$]·[C_{60}^0]·$(THF)_6$ at 80 K.

	x	y	z	U_{eq}
H(1A1)	601	2999	7270	100
H(1A2)	898	2840	7314	100
H(2A1)	672	3104	6551	107
H(2A2)	565	2222	6668	107
H(3A1)	133	2268	6012	81
H(3A2)	231	3136	5871	81
H(4A1)	-266	3064	5498	70

Continued on next page

Table continued

	x	y	z	U_{eq}
H(4A2)	-249	3071	5953	70
H(6A)	-668	3583	5274	85
H(7A)	-1081	4406	4866	101
H(8A)	-1066	5954	4903	101
H(9A)	-638	6680	5349	85
H(12A)	270	6931	5979	71
H(12B)	190	7801	6145	71
H(13A)	706	6882	6697	84
H(13B)	605	7718	6852	84
H(14A)	911	6975	7459	74
H(14B)	606	6777	7379	74
H(16A)	1053	6370	8039	128
H(17A)	1286	5516	8672	199
H(18A)	1282	3969	8626	213
H(19A)	1045	3276	7947	119
H(1B1)	1284	3375	7147	82
H(1B2)	1547	2835	7201	82
H(2B1)	1804	4208	7378	89
H(2B2)	1537	4202	6891	89
H(3B1)	1538	5728	6901	86
H(3B2)	1802	5721	7391	86
H(4B1)	1535	7059	7213	86
H(4B2)	1276	6486	7154	86
H(6B)	1289	7942	7356	90
H(7B)	1159	9066	7660	102
H(8B)	1319	9034	8400	109
H(9B)	1609	7879	8836	96
H(11A)	1768	6440	9118	76
H(11B)	2021	7050	9180	76
H(12C)	2244	5752	9126	66
H(12D)	2214	5724	9541	66
H(13C)	2223	4137	9541	61
H(13D)	2252	4134	9124	61

Continued on next page

Table continued

	x	y	z	U_{eq}
H(14C)	2044	2795	9182	72
H(14D)	1783	3370	9117	72
H(16B)	1624	1946	8827	86
H(17B)	1332	804	8380	96
H(18B)	1173	801	7640	88
H(19B)	1305	1940	7347	75
H(1A1)	-386	5910	6442	63
H(1A2)	-119	6277	6884	63
H(2A1)	-578	5778	6841	64
H(2A2)	-278	5757	7290	64
H(3A1)	-286	4276	7280	64
H(3A2)	-588	4297	6833	64
H(4A1)	-139	3747	6860	65
H(4A2)	-401	4167	6427	65
H(1B1)	2264	6154	8428	89
H(1B2)	2294	5918	8021	89
H(2B1)	2735	5631	8521	156
H(2B2)	2667	5529	8896	156
H(3B1)	2701	4164	8854	184
H(3B2)	2716	4265	8425	184
H(4B1)	2283	3876	8022	84
H(4B2)	2277	3691	8453	84
H(1C1)	926	5766	6324	102
H(1C2)	948	4861	6573	102
H(2C1)	963	4138	6136	178
H(2C2)	1014	5053	5958	178
H(3C1)	602	4866	5366	189
H(3C2)	534	4040	5575	189
H(4C1)	249	4848	5529	96
H(4C2)	418	5719	5540	96
H(1S1)	1109	3637	9575	250
H(1S2)	1123	4089	9183	250
H(2S1)	844	3094	8761	250

Continued on next page

Table continued

	x	y	z	U_{eq}
H(2S2)	857	2588	9162	250
H(3S1)	1168	1689	9222	250
H(3S2)	1101	2047	8764	250
H(4S1)	1563	1990	9397	250
H(4S2)	1466	2746	9030	250
H(1T1)	8923	8119	5649	447
H(1T2)	8833	8268	5997	447
H(2T1)	8548	7645	5234	447
H(2T2)	8458	7794	5582	447
H(3T1)	8468	6508	5672	447
H(3T2)	8558	6359	5323	447
H(4T1)	8938	6038	5794	447
H(4T2)	8848	6187	6142	447
H(1U1)	2173	10759	10040	954
H(1U2)	1943	10898	10170	954
H(2U1)	1992	9749	10359	954
H(2U2)	2222	9610	10229	954
H(3U1)	1975	8916	9770	954
H(3U2)	1745	9055	9901	954
H(4U1)	1542	9775	9428	954
H(4U2)	1772	9636	9298	954

9.7 [4{K(DB18C6)($C_{60}^{\cdot-}$)}(THF)$_6$]·[C_{60}^{0}]·(THF)$_6$ at 220 K

Table 9.15: Atomic coordinates ($\times 10^4$) and equivalent isotropic displacement parameters (Å$^2\times 10^3$) for [4{K(DB18C6)($C_{60}^{\cdot-}$)}(THF)$_6$]·[C_{60}^{0}]·(THF)$_6$ at 220 K. U_{eq} is defined as one third of the trace of the orthogonalized U_{ij} tensor.

	x	y	z	U_{eq}
K(1R)	4729(1)	6154(3)	2467(2)	53(1)
O(1R)	5163(2)	5246(8)	1887(7)	65(1)
O(2R)	4713(2)	4331(8)	2371(7)	65(1)
O(3R)	4257(2)	5252(8)	2835(7)	65(1)
O(4R)	4272(2)	6984(8)	2844(7)	65(1)
O(5R)	4713(2)	7919(8)	2378(7)	65(1)
O(6R)	5142(3)	6969(8)	1885(7)	65(1)
C(1R)	5164(4)	4353(12)	1808(11)	63(3)
C(2R)	4851(4)	4005(12)	1808(12)	63(3)
C(3R)	4416(4)	4046(12)	2407(11)	63(3)
C(4R)	4284(4)	4341(11)	2902(11)	63(3)
C(5R)	4116(2)	5562(9)	3326(5)	63(3)
C(6R)	3972(3)	5101(10)	3806(7)	124(6)
C(7R)	3837(2)	5561(15)	4308(6)	124(6)
C(8R)	3846(3)	6482(15)	4330(7)	124(6)
C(9R)	3991(3)	6944(10)	3850(9)	124(6)
C(10R)	4126(3)	6484(9)	3348(7)	63(3)
C(11R)	4319(4)	7913(13)	2908(12)	78(3)
C(12R)	4449(4)	8307(14)	2225(11)	78(3)
C(13R)	4860(4)	8165(14)	1815(12)	78(3)
C(14R)	5133(4)	7924(13)	2000(12)	78(3)
C(15R)	5405(2)	6546(10)	1948(5)	78(3)
C(16R)	5650(2)	7017(10)	1958(7)	96(4)
C(17R)	5896(2)	6566(13)	1951(7)	96(4)
C(18R)	5899(2)	5645(13)	1932(8)	96(4)
C(19R)	5655(3)	5174(10)	1921(9)	96(4)
C(20R)	5408(2)	5624(10)	1929(7)	78(3)
K(1Q)	3347(1)	6124(4)	2999(2)	59(1)

Continued on next page

Table continued

	x	y	z	U_{eq}
O(1Q)	3208(3)	7681(9)	3577(7)	69(1)
O(2Q)	3070(2)	6139(11)	4200(5)	69(1)
O(3Q)	3214(3)	4538(8)	3588(7)	69(1)
O(4Q)	3413(3)	4526(8)	2298(7)	69(1)
O(5Q)	3506(2)	6128(11)	1612(5)	69(1)
O(6Q)	3399(3)	7725(9)	2364(7)	69(1)
C(1Q)	3097(4)	7765(13)	4225(11)	71(3)
C(2Q)	2923(4)	6954(12)	4177(11)	71(3)
C(3Q)	2890(4)	5354(12)	4261(11)	71(3)
C(4Q)	3089(4)	4615(13)	4251(11)	71(3)
C(5Q)	3389(2)	3786(7)	3471(7)	71(3)
C(6Q)	3489(3)	3103(9)	3943(7)	102(5)
C(7Q)	3667(3)	2475(8)	3714(10)	102(5)
C(8Q)	3745(3)	2530(9)	3014(10)	102(5)
C(9Q)	3645(3)	3213(11)	2542(8)	102(5)
C(10Q)	3467(3)	3841(9)	2770(7)	71(3)
C(11Q)	3537(4)	4508(14)	1695(10)	75(3)
C(12Q)	3378(4)	5361(13)	1226(10)	75(3)
C(13Q)	3421(5)	6891(14)	1274(11)	75(3)
C(14Q)	3461(5)	7630(14)	1569(10)	75(3)
C(15Q)	3473(2)	8448(6)	2785(5)	75(3)
C(16Q)	3634(2)	9167(7)	2640(6)	62(3)
C(17Q)	3691(3)	9837(7)	3161(7)	62(3)
C(18Q)	3586(3)	9787(8)	3827(6)	62(3)
C(19Q)	3424(3)	9068(8)	3972(6)	62(3)
C(20Q)	3368(2)	8399(7)	3451(6)	75(3)
O(1W)	5094(1)	6090(3)	3685(2)	98(5)
C(1W)	5239(1)	5328(3)	3970(2)	130(5)
C(2W)	5394(1)	5565(3)	4697(2)	130(5)
C(3W)	5416(1)	6591(3)	4676(2)	130(5)
C(4W)	5274(1)	6812(3)	3905(2)	130(5)
O(1E)	2855(1)	6052(3)	2163(2)	98(5)
C(1E)	2707(1)	6776(3)	1816(2)	141(5)

Continued on next page

Table continued

	x	y	z	U_{eq}
C(2E)	2411(1)	6622(3)	1850(2)	141(5)
C(3E)	2390(1)	5608(3)	1973(2)	141(5)
C(4E)	2685(1)	5300(3)	1968(2)	141(5)
O(1Y)	4434(1)	6348(3)	1110(2)	263(17)
C(1Y)	4583(1)	5891(3)	620(2)	151(7)
C(2Y)	4391(1)	5693(4)	-59(2)	151(7)
C(3Y)	4101(1)	5748(3)	189(2)	151(7)
C(4Y)	4168(1)	5949(3)	1009(2)	151(7)
C(1A)	541(1)	4836(4)	-627(2)	130(4)
C(2A)	615(1)	5510(5)	-1127(2)	137(4)
C(3A)	485(1)	6334(5)	-955(2)	157(4)
C(4A)	330(1)	6167(4)	-349(2)	146(4)
C(5A)	364(1)	5242(4)	-150(2)	146(4)
C(6A)	387(1)	4988(4)	586(2)	144(4)
C(7A)	585(1)	4323(4)	873(2)	140(4)
C(8A)	754(1)	3936(4)	415(2)	133(4)
C(9A)	731(1)	4201(4)	-351(2)	125(4)
C(10A)	1006(1)	4208(4)	-562(2)	140(4)
C(11A)	1077(1)	4854(4)	-1040(2)	152(5)
C(12A)	879(1)	5520(5)	-1328(2)	144(4)
C(13A)	1023(1)	6353(5)	-1366(2)	153(4)
C(14A)	899(1)	7141(5)	-1199(2)	142(4)
C(15A)	625(1)	7133(5)	-990(2)	160(4)
C(16A)	613(1)	7799(4)	-423(2)	146(4)
C(17A)	465(1)	7638(4)	155(2)	154(4)
C(18A)	321(1)	6804(4)	192(2)	144(4)
C(19A)	344(1)	6540(4)	960(2)	135(4)
C(20A)	375(1)	5655(4)	1151(2)	140(5)
C(21A)	569(1)	5401(4)	1791(2)	146(5)
C(22A)	698(1)	4577(4)	1617(2)	130(4)
C(23A)	975(1)	4437(3)	1868(2)	121(4)
C(24A)	1151(1)	4030(3)	1390(2)	128(4)
C(25A)	1043(1)	3782(4)	678(2)	135(4)

Continued on next page

Table continued

	x	y	z	U_{eq}
C(26A)	1199(1)	3951(4)	74(2)	147(5)
C(27A)	1455(1)	4354(4)	207(2)	156(4)
C(28A)	1528(1)	5031(4)	-289(2)	163(5)
C(29A)	1345(1)	5276(4)	-899(2)	165(5)
C(30A)	1311(1)	6199(4)	-1102(2)	157(4)
C(31A)	1462(1)	6846(4)	-685(2)	142(5)
C(32A)	1333(1)	7669(4)	-512(2)	135(4)
C(33A)	1056(1)	7810(4)	-762(2)	124(4)
C(34A)	880(1)	8217(4)	-284(2)	141(4)
C(35A)	988(1)	8464(4)	428(2)	149(4)
C(36A)	832(1)	8296(4)	1032(2)	159(5)
C(37A)	576(1)	7892(4)	899(2)	164(5)
C(38A)	503(1)	7215(4)	1395(2)	151(5)
C(39A)	686(1)	6970(4)	2005(2)	158(4)
C(40A)	720(1)	6047(4)	2207(2)	154(4)
C(41A)	1008(1)	5893(3)	2471(2)	152(4)
C(42A)	1132(1)	5105(3)	2305(2)	156(4)
C(43A)	1406(1)	5114(3)	2096(2)	153(4)
C(44A)	1417(1)	4447(3)	1529(2)	131(4)
C(45A)	1566(1)	4609(3)	950(2)	141(4)
C(46A)	1709(1)	5443(3)	914(2)	140(4)
C(47A)	1686(1)	5707(4)	146(2)	144(4)
C(48A)	1656(1)	6592(4)	-46(2)	150(5)
C(49A)	1644(1)	7259(4)	520(2)	145(4)
C(50A)	1445(1)	7923(4)	233(2)	158(5)
C(51A)	1276(1)	8311(4)	691(2)	153(4)
C(52A)	1300(1)	8045(3)	1457(2)	145(4)
C(53A)	1025(1)	8039(3)	1667(2)	154(4)
C(54A)	953(1)	7392(3)	2146(2)	156(5)
C(55A)	1152(1)	6727(3)	2434(2)	140(4)
C(56A)	1416(1)	6736(3)	2233(2)	138(4)
C(57A)	1546(1)	5913(3)	2061(2)	152(4)
C(58A)	1701(1)	6079(3)	1455(2)	150(4)

Continued on next page

Table continued

	x	y	z	U_{eq}
C(59A)	1667(1)	7005(3)	1255(2)	152(4)
C(60A)	1490(1)	7410(3)	1733(2)	141(5)
C(1B)	675(1)	6915(4)	4935(2)	116(4)
C(2B)	583(1)	6578(4)	4134(2)	104(4)
C(3B)	594(1)	5590(4)	4238(2)	102(4)
C(4B)	672(1)	5359(4)	4948(2)	92(4)
C(5B)	727(1)	6196(4)	5417(2)	95(4)
C(6B)	653(1)	6173(4)	6127(2)	114(4)
C(7B)	524(1)	7021(5)	6352(2)	124(5)
C(8B)	476(1)	7721(4)	5895(2)	132(4)
C(9B)	538(1)	7699(4)	5100(2)	130(4)
C(10B)	345(1)	8092(4)	4610(2)	115(4)
C(11B)	269(1)	7813(4)	3916(2)	125(4)
C(12B)	380(1)	6998(4)	3683(2)	126(5)
C(13B)	188(1)	6465(4)	3208(2)	120(4)
C(14B)	186(1)	5546(4)	3289(2)	110(4)
C(15B)	402(1)	5131(4)	3790(2)	107(4)
C(16B)	265(1)	4361(4)	4091(2)	84(4)
C(17B)	346(1)	4099(4)	4827(2)	87(4)
C(18B)	563(1)	4654(4)	5334(2)	87(4)
C(19B)	481(1)	4714(4)	6008(2)	109(4)
C(20B)	524(1)	5481(5)	6432(2)	123(5)
C(21B)	208(1)	8207(5)	5807(2)	134(5)
C(22B)	125(1)	8443(4)	5097(2)	130(5)
C(23B)	-27(1)	7759(4)	3634(2)	143(5)
C(24B)	-81(1)	6977(4)	3170(2)	116(4)
C(25B)	-314(1)	6511(4)	3140(2)	128(5)
C(26B)	-325(1)	5585(4)	3206(2)	144(5)
C(27B)	-76(1)	5102(4)	3259(2)	127(4)
C(28B)	-20(1)	4294(4)	3768(2)	96(5)
C(29B)	143(1)	3859(4)	5260(2)	89(4)
C(30B)	218(1)	4196(5)	6026(2)	114(5)
C(1S)	2752(1)	-643(3)	2802(4)	283(5)

Continued on next page

Table continued

	x	y	z	U_{eq}
C(2S)	2510(1)	-1103(3)	2450(4)	316(5)
C(3S)	2289(1)	-951(3)	2886(4)	307(5)
C(4S)	2395(1)	-399(3)	3510(4)	313(5)
C(5S)	2681(1)	-214(3)	3459(3)	262(4)
C(6S)	2791(1)	615(3)	3659(3)	296(5)
C(7S)	2975(1)	1044(3)	3217(3)	305(4)
C(8S)	3042(1)	631(3)	2589(3)	250(5)
C(9S)	2927(1)	-231(3)	2378(4)	270(5)
C(10S)	2870(1)	-257(3)	1581(4)	312(5)
C(11S)	2638(1)	-695(3)	1241(4)	317(5)
C(12S)	2454(1)	-1126(3)	1683(4)	324(5)
C(13S)	2175(1)	-998(3)	1322(4)	337(5)
C(14S)	1963(1)	-851(3)	1740(4)	307(5)
C(15S)	2021(1)	-826(3)	2538(4)	306(5)
C(16S)	1848(1)	-150(3)	2801(3)	337(5)
C(17S)	1951(1)	376(3)	3399(3)	430(5)
C(18S)	2230(1)	249(3)	3756(3)	411(5)
C(19S)	2344(1)	1113(3)	3968(3)	396(5)
C(20S)	2618(1)	1290(3)	3923(3)	393(5)
C(21S)	2696(1)	2141(3)	3640(2)	413(5)
C(22S)	2916(1)	1987(3)	3205(3)	331(4)
C(23S)	2926(1)	2473(3)	2565(2)	309(5)
C(24S)	2998(1)	2040(3)	1911(2)	329(5)
C(25S)	3055(1)	1139(3)	1923(3)	307(5)
C(26S)	2948(1)	590(3)	1296(3)	344(5)
C(27S)	2790(1)	965(3)	689(3)	392(5)
C(28S)	2548(1)	510(3)	340(3)	360(5)
C(29S)	2473(1)	-301(3)	606(4)	343(5)
C(30S)	2187(1)	-490(3)	657(4)	351(5)
C(31S)	1987(1)	141(3)	438(3)	357(5)
C(32S)	1766(1)	295(3)	874(3)	363(4)
C(33S)	1756(1)	-190(3)	1514(4)	301(5)
C(34S)	1685(1)	242(3)	2168(3)	300(5)

Continued on next page

Table continued

	x	y	z	U_{eq}
C(35S)	1627(1)	1144(3)	2156(3)	307(5)
C(36S)	1734(1)	1692(3)	2782(3)	339(5)
C(37S)	1892(1)	1317(3)	3389(3)	448(5)
C(38S)	2135(1)	1772(3)	3739(3)	384(5)
C(39S)	2210(1)	2584(3)	3473(2)	338(5)
C(40S)	2495(1)	2772(3)	3422(2)	421(5)
C(41S)	2508(1)	3280(3)	2756(2)	401(5)
C(42S)	2719(1)	3133(3)	2339(2)	344(5)
C(43S)	2661(1)	3109(3)	1541(2)	353(5)
C(44S)	2834(1)	2432(3)	1277(2)	357(5)
C(45S)	2731(1)	1906(3)	680(3)	364(5)
C(46S)	2453(1)	2034(3)	323(3)	348(5)
C(47S)	2338(1)	1170(4)	111(3)	348(5)
C(48S)	2064(1)	992(4)	156(3)	376(5)
C(49S)	1891(1)	1667(3)	420(3)	346(5)
C(50S)	1707(1)	1238(3)	862(3)	317(5)
C(51S)	1640(1)	1651(3)	1489(3)	263(5)
C(52S)	1755(1)	2513(3)	1701(2)	270(5)
C(53S)	1812(1)	2539(3)	2498(2)	290(5)
C(54S)	2044(1)	2977(3)	2838(2)	305(5)
C(55S)	2229(1)	3408(3)	2396(2)	365(5)
C(56S)	2173(1)	3385(3)	1628(2)	346(5)
C(57S)	2393(1)	3234(3)	1192(2)	348(5)
C(58S)	2287(1)	2682(3)	569(2)	334(5)
C(59S)	2001(1)	2496(3)	620(2)	335(4)
C(60S)	1930(1)	2926(3)	1276(2)	312(5)
O(1T)	1006(1)	3368(4)	4420(2)	337(5)
C(1T)	1073(1)	2571(4)	4081(2)	337(5)
C(2T)	1363(1)	2638(3)	3939(2)	337(5)
C(3T)	1421(1)	3650(3)	3946(2)	337(5)
C(4T)	1146(1)	4042(3)	4072(2)	337(5)
O(1H)	980(1)	8861(3)	3683(2)	337(5)
C(1H)	1204(1)	8409(3)	4088(2)	337(5)

Continued on next page

Table continued

	x	y	z	U_{eq}
C(2H)	1401(1)	9085(3)	4433(2)	337(5)
C(3H)	1329(1)	9932(3)	3964(3)	337(5)
C(4H)	1100(1)	9611(3)	3379(3)	337(5)
O(1O)	1809(6)	5810(20)	4484(15)	337(5)
C(2O)	1974(7)	5740(30)	3911(18)	337(5)
C(3O)	2110(8)	6620(30)	3850(20)	337(5)
C(4O)	1928(11)	7280(20)	4220(30)	337(5)
C(5O)	1700(7)	6680(30)	4430(20)	337(5)

Table 9.16: Anisotropic displacement parameters ($Å^2 \times 10^3$) for $[4\{K(DB18C6)(C_{60}^{\cdot -})\}(THF)_6]\cdot[C_{60}{}^0]\cdot(THF)_6$ at 220 K. The anisotropic displacement factor exponent takes the form: $-2\pi^2[h^2a^{*2}U_{11} + \ldots + 2hka^*b^*U_{12}]$.

	U_{11}	U_{22}	U_{33}	U_{23}	U_{13}	U_{12}
K(1R)	48(2)	43(2)	67(2)	-8(3)	6(2)	4(3)
O(1R)	61(3)	50(3)	80(3)	-12(4)	0(2)	-6(4)
O(2R)	61(3)	50(3)	80(3)	-12(4)	0(2)	-6(4)
O(3R)	61(3)	50(3)	80(3)	-12(4)	0(2)	-6(4)
O(4R)	61(3)	50(3)	80(3)	-12(4)	0(2)	-6(4)
O(5R)	61(3)	50(3)	80(3)	-12(4)	0(2)	-6(4)
O(6R)	61(3)	50(3)	80(3)	-12(4)	0(2)	-6(4)
C(1R)	64(5)	39(5)	87(6)	-18(5)	7(5)	14(5)
C(2R)	64(5)	39(5)	87(6)	-18(5)	7(5)	14(5)
C(3R)	64(5)	39(5)	87(6)	-18(5)	7(5)	14(5)
C(4R)	64(5)	39(5)	87(6)	-18(5)	7(5)	14(5)
C(5R)	64(5)	39(5)	87(6)	-18(5)	7(5)	14(5)
C(6R)	59(7)	233(16)	76(8)	-25(14)	-4(5)	-10(13)
C(7R)	59(7)	233(16)	76(8)	-25(14)	-4(5)	-10(13)
C(8R)	59(7)	233(16)	76(8)	-25(14)	-4(5)	-10(13)
C(9R)	59(7)	233(16)	76(8)	-25(14)	-4(5)	-10(13)

Continued on next page

Table continued

	U_{11}	U_{22}	U_{33}	U_{23}	U_{13}	U_{12}
C(10R)	64(5)	39(5)	87(6)	-18(5)	7(5)	14(5)
C(11R)	65(5)	76(6)	98(6)	-5(6)	21(5)	23(6)
C(12R)	65(5)	76(6)	98(6)	-5(6)	21(5)	23(6)
C(13R)	65(5)	76(6)	98(6)	-5(6)	21(5)	23(6)
C(14R)	65(5)	76(6)	98(6)	-5(6)	21(5)	23(6)
C(15R)	65(5)	76(6)	98(6)	-5(6)	21(5)	23(6)
C(16R)	66(6)	115(9)	111(7)	-28(12)	25(6)	-10(11)
C(17R)	66(6)	115(9)	111(7)	-28(12)	25(6)	-10(11)
C(18R)	66(6)	115(9)	111(7)	-28(12)	25(6)	-10(11)
C(19R)	66(6)	115(9)	111(7)	-28(12)	25(6)	-10(11)
C(20R)	65(5)	76(6)	98(6)	-5(6)	21(5)	23(6)
K(1Q)	63(2)	70(2)	47(2)	-12(3)	13(2)	-27(3)
O(1Q)	81(3)	67(3)	60(3)	10(4)	19(2)	0(4)
O(2Q)	81(3)	67(3)	60(3)	10(4)	19(2)	0(4)
O(3Q)	81(3)	67(3)	60(3)	10(4)	19(2)	0(4)
O(4Q)	81(3)	67(3)	60(3)	10(4)	19(2)	0(4)
O(5Q)	81(3)	67(3)	60(3)	10(4)	19(2)	0(4)
O(6Q)	81(3)	67(3)	60(3)	10(4)	19(2)	0(4)
C(1Q)	64(5)	76(6)	78(5)	-26(6)	30(4)	-6(6)
C(2Q)	64(5)	76(6)	78(5)	-26(6)	30(4)	-6(6)
C(3Q)	64(5)	76(6)	78(5)	-26(6)	30(4)	-6(6)
C(4Q)	64(5)	76(6)	78(5)	-26(6)	30(4)	-6(6)
C(5Q)	64(5)	76(6)	78(5)	-26(6)	30(4)	-6(6)
C(6Q)	73(8)	94(10)	133(12)	10(9)	-6(9)	-8(7)
C(7Q)	73(8)	94(10)	133(12)	10(9)	-6(9)	-8(7)
C(8Q)	73(8)	94(10)	133(12)	10(9)	-6(9)	-8(7)
C(9Q)	73(8)	94(10)	133(12)	10(9)	-6(9)	-8(7)
C(10Q)	64(5)	76(6)	78(5)	-26(6)	30(4)	-6(6)
C(11Q)	87(6)	94(6)	46(5)	1(6)	14(4)	18(7)
C(12Q)	87(6)	94(6)	46(5)	1(6)	14(4)	18(7)
C(13Q)	87(6)	94(6)	46(5)	1(6)	14(4)	18(7)
C(14Q)	87(6)	94(6)	46(5)	1(6)	14(4)	18(7)
C(15Q)	87(6)	94(6)	46(5)	1(6)	14(4)	18(7)

Continued on next page

Table continued

	U_{11}	U_{22}	U_{33}	U_{23}	U_{13}	U_{12}
C(16Q)	78(7)	48(7)	70(7)	0(5)	40(6)	-8(6)
C(17Q)	78(7)	48(7)	70(7)	0(5)	40(6)	-8(6)
C(18Q)	78(7)	48(7)	70(7)	0(5)	40(6)	-8(6)
C(19Q)	78(7)	48(7)	70(7)	0(5)	40(6)	-8(6)
C(20Q)	87(6)	94(6)	46(5)	1(6)	14(4)	18(7)
O(1W)	121(9)	46(7)	110(10)	-25(11)	-43(8)	-19(11)
C(1W)	162(11)	98(8)	115(9)	10(13)	-34(8)	40(12)
C(2W)	162(11)	98(8)	115(9)	10(13)	-34(8)	40(12)
C(3W)	162(11)	98(8)	115(9)	10(13)	-34(8)	40(12)
C(4W)	162(11)	98(8)	115(9)	10(13)	-34(8)	40(12)
O(1E)	67(8)	93(10)	120(10)	-4(12)	-40(8)	24(11)
C(1E)	87(7)	134(10)	202(12)	77(12)	20(10)	45(11)
C(2E)	87(7)	134(10)	202(12)	77(12)	20(10)	45(11)
C(3E)	87(7)	134(10)	202(12)	77(12)	20(10)	45(11)
C(4E)	87(7)	134(10)	202(12)	77(12)	20(10)	45(11)
O(1Y)	48(8)	700(50)	52(9)	70(20)	38(7)	50(20)
C(1Y)	114(10)	152(13)	187(16)	-16(13)	26(11)	7(11)
C(2Y)	114(10)	152(13)	187(16)	-16(13)	26(11)	7(11)
C(3Y)	114(10)	152(13)	187(16)	-16(13)	26(11)	7(11)
C(4Y)	114(10)	152(13)	187(16)	-16(13)	26(11)	7(11)
C(1A)	124(7)	135(7)	129(7)	-14(5)	9(5)	-13(5)
C(2A)	138(6)	141(6)	127(8)	-5(5)	-4(6)	-4(6)
C(3A)	156(7)	154(6)	156(7)	4(6)	4(5)	1(5)
C(4A)	134(8)	149(6)	149(7)	-4(5)	1(6)	9(7)
C(5A)	139(8)	150(6)	149(6)	-7(6)	20(6)	-4(6)
C(6A)	137(8)	144(7)	151(6)	2(5)	18(6)	-18(6)
C(7A)	142(7)	139(8)	141(6)	6(6)	23(5)	-16(6)
C(8A)	140(6)	121(8)	138(6)	4(6)	17(6)	-14(6)
C(9A)	135(6)	113(8)	124(6)	-12(6)	12(6)	-15(6)
C(10A)	150(6)	134(8)	138(7)	-22(5)	22(5)	5(6)
C(11A)	162(6)	152(7)	143(8)	-19(6)	23(6)	-4(5)
C(12A)	159(6)	142(6)	130(8)	-10(7)	21(6)	-13(5)
C(13A)	162(6)	155(6)	145(8)	5(6)	26(6)	-12(5)

Continued on next page

Table continued

	U_{11}	U_{22}	U_{33}	U_{23}	U_{13}	U_{12}
C(14A)	153(6)	139(7)	131(8)	16(6)	11(6)	-7(5)
C(15A)	160(6)	161(7)	158(8)	2(5)	14(6)	-5(6)
C(16A)	150(6)	144(8)	143(6)	11(6)	14(5)	7(6)
C(17A)	149(8)	150(7)	163(6)	4(6)	25(5)	9(6)
C(18A)	132(8)	147(7)	152(6)	-2(5)	12(7)	9(6)
C(19A)	118(8)	141(6)	148(6)	-10(5)	29(6)	4(6)
C(20A)	129(8)	149(6)	146(7)	7(5)	35(6)	-8(7)
C(21A)	141(8)	155(6)	145(7)	0(6)	30(5)	-6(5)
C(22A)	135(6)	126(7)	130(7)	15(6)	24(6)	-22(6)
C(23A)	135(6)	114(7)	116(7)	27(6)	27(5)	-7(6)
C(24A)	137(6)	122(8)	128(6)	15(6)	24(5)	3(6)
C(25A)	142(6)	117(8)	143(6)	2(6)	10(5)	-5(7)
C(26A)	152(6)	140(8)	148(7)	-13(6)	21(5)	8(6)
C(27A)	157(7)	152(8)	161(6)	-13(5)	28(6)	10(6)
C(28A)	161(8)	166(7)	163(7)	-9(5)	27(5)	0(6)
C(29A)	162(7)	168(6)	166(8)	-6(6)	30(6)	2(6)
C(30A)	166(6)	163(6)	146(8)	-10(6)	33(6)	-8(6)
C(31A)	140(8)	147(6)	144(7)	4(6)	38(5)	-17(5)
C(32A)	135(6)	134(7)	138(6)	20(6)	24(6)	-19(6)
C(33A)	139(6)	119(8)	115(7)	26(6)	23(5)	-8(6)
C(34A)	150(7)	131(8)	142(6)	11(6)	23(5)	5(6)
C(35A)	161(6)	132(9)	152(6)	2(6)	12(5)	-3(7)
C(36A)	162(6)	152(8)	162(7)	-8(7)	21(5)	13(6)
C(37A)	163(7)	162(8)	167(6)	-8(5)	26(6)	8(6)
C(38A)	150(8)	151(7)	155(7)	-18(5)	28(5)	11(6)
C(39A)	157(6)	159(6)	158(8)	-12(6)	27(6)	-2(6)
C(40A)	157(6)	161(6)	148(8)	-3(6)	37(6)	-14(6)
C(41A)	161(6)	152(6)	145(8)	6(6)	22(6)	-14(5)
C(42A)	164(6)	156(7)	149(8)	2(6)	21(6)	-9(6)
C(43A)	150(6)	152(6)	154(8)	-1(5)	4(6)	2(6)
C(44A)	130(6)	128(8)	132(6)	15(5)	6(5)	8(6)
C(45A)	137(8)	138(7)	148(6)	6(6)	19(5)	17(6)
C(46A)	119(8)	149(7)	151(6)	0(5)	20(7)	10(6)

Continued on next page

Table continued

	U_{11}	U_{22}	U_{33}	U_{23}	U_{13}	U_{12}
C(47A)	134(8)	152(6)	151(6)	-6(6)	36(6)	8(6)
C(48A)	143(8)	153(6)	158(7)	2(5)	33(6)	-6(7)
C(49A)	139(8)	147(7)	150(6)	3(5)	20(6)	-25(6)
C(50A)	161(7)	155(8)	158(6)	1(6)	23(5)	-16(6)
C(51A)	158(6)	145(8)	157(6)	5(6)	22(6)	-15(6)
C(52A)	153(6)	137(8)	142(6)	-9(6)	8(6)	-13(6)
C(53A)	160(6)	150(8)	151(7)	-16(6)	17(5)	4(6)
C(54A)	155(6)	158(7)	154(8)	-17(6)	20(6)	-4(5)
C(55A)	156(6)	140(7)	123(8)	-4(7)	17(6)	-16(5)
C(56A)	138(6)	138(6)	132(8)	-14(5)	-1(6)	-1(6)
C(57A)	148(8)	152(6)	153(7)	2(6)	3(5)	7(5)
C(58A)	139(8)	153(6)	152(7)	-5(5)	1(6)	0(7)
C(59A)	150(8)	154(6)	153(6)	-5(6)	20(6)	-3(6)
C(60A)	136(7)	145(7)	141(7)	-18(5)	12(6)	-11(5)
C(1B)	105(8)	117(6)	123(6)	7(5)	10(6)	-7(6)
C(2B)	95(7)	114(6)	109(6)	14(6)	36(6)	-3(6)
C(3B)	97(7)	111(6)	104(6)	-13(6)	28(6)	2(6)
C(4B)	79(8)	93(6)	107(6)	3(5)	20(6)	11(6)
C(5B)	74(7)	99(6)	108(6)	-5(5)	1(5)	-5(7)
C(6B)	104(7)	122(6)	113(6)	3(6)	1(6)	-3(5)
C(7B)	121(8)	126(6)	122(8)	-10(5)	10(6)	-12(6)
C(8B)	128(7)	127(7)	134(6)	-6(6)	0(6)	-11(6)
C(9B)	126(8)	121(7)	141(6)	-2(6)	12(5)	-10(6)
C(10B)	113(7)	106(8)	128(6)	10(6)	25(5)	-10(6)
C(11B)	134(6)	119(7)	126(7)	9(6)	30(6)	-8(6)
C(12B)	127(7)	128(7)	123(8)	10(5)	22(5)	-3(5)
C(13B)	124(6)	124(6)	116(8)	-1(6)	29(6)	-4(5)
C(14B)	115(6)	115(6)	103(8)	-5(6)	20(6)	8(5)
C(15B)	106(7)	109(7)	109(8)	-4(5)	24(5)	-1(5)
C(16B)	90(6)	77(7)	88(6)	-17(6)	29(6)	15(6)
C(17B)	81(6)	76(7)	104(6)	-6(6)	13(5)	9(6)
C(18B)	74(7)	77(7)	106(6)	0(5)	5(5)	13(5)
C(19B)	105(7)	109(7)	110(6)	14(5)	0(6)	6(6)

Continued on next page

Table continued

	U_{11}	U_{22}	U_{33}	U_{23}	U_{13}	U_{12}
C(20B)	118(8)	126(7)	125(8)	7(5)	15(6)	7(6)
C(21B)	144(7)	126(8)	132(6)	-14(6)	17(6)	1(6)
C(22B)	131(8)	125(8)	136(6)	0(6)	24(6)	9(6)
C(23B)	150(6)	136(7)	141(8)	7(6)	17(6)	-1(7)
C(24B)	129(6)	116(7)	101(8)	24(6)	15(7)	6(5)
C(25B)	130(7)	136(6)	117(8)	7(7)	11(7)	5(6)
C(26B)	149(7)	144(6)	138(9)	-6(7)	16(7)	-4(6)
C(27B)	137(6)	127(7)	117(8)	-4(6)	15(7)	-11(5)
C(28B)	102(6)	92(7)	95(8)	-27(5)	17(6)	-4(6)
C(29B)	92(7)	72(8)	101(6)	21(6)	9(5)	7(6)
C(30B)	122(7)	110(8)	112(7)	20(6)	18(6)	2(6)
C(1S)	286(7)	285(8)	281(7)	1(5)	51(5)	12(6)
C(2S)	314(7)	315(9)	319(6)	-5(7)	45(5)	-5(6)
C(3S)	306(6)	305(9)	309(7)	7(6)	40(5)	1(7)
C(4S)	304(6)	321(8)	311(8)	16(6)	35(6)	-33(6)
C(5S)	268(6)	259(7)	255(7)	7(6)	20(6)	14(6)
C(6S)	299(7)	292(6)	292(8)	9(6)	17(6)	-23(5)
C(7S)	307(8)	315(6)	297(7)	-13(6)	55(6)	3(6)
C(8S)	237(9)	251(7)	257(6)	4(5)	15(6)	11(6)
C(9S)	266(8)	261(7)	284(6)	-1(6)	35(6)	4(6)
C(10S)	314(8)	322(7)	301(6)	-12(6)	41(6)	10(6)
C(11S)	315(7)	315(8)	323(7)	-10(6)	49(5)	4(6)
C(12S)	329(6)	322(9)	322(6)	-4(7)	48(5)	0(7)
C(13S)	332(6)	340(9)	341(7)	-6(6)	50(5)	5(7)
C(14S)	308(7)	303(8)	306(6)	-1(7)	31(6)	-4(6)
C(15S)	305(7)	307(8)	305(6)	7(7)	37(6)	-14(6)
C(16S)	330(8)	338(8)	346(7)	27(5)	55(6)	15(6)
C(17S)	429(7)	440(6)	416(8)	-21(6)	48(6)	-17(7)
C(18S)	417(7)	406(6)	413(9)	-17(7)	70(6)	17(5)
C(19S)	396(6)	399(7)	392(9)	3(7)	51(7)	15(5)
C(20S)	395(6)	394(7)	395(9)	-15(6)	67(7)	24(6)
C(21S)	412(7)	423(7)	411(8)	-4(6)	79(5)	-3(5)
C(22S)	339(8)	317(6)	330(7)	10(6)	19(6)	-7(7)

Continued on next page

Table continued

	U_{11}	U_{22}	U_{33}	U_{23}	U_{13}	U_{12}
C(23S)	306(8)	311(8)	310(6)	-7(5)	36(6)	-16(6)
C(24S)	330(9)	324(6)	335(7)	-10(6)	55(6)	0(7)
C(25S)	307(9)	315(6)	303(7)	28(5)	49(7)	-4(7)
C(26S)	349(9)	340(7)	348(7)	-10(5)	62(6)	-6(6)
C(27S)	392(7)	391(6)	390(8)	2(6)	40(6)	6(6)
C(28S)	366(7)	358(6)	360(9)	10(6)	61(6)	14(5)
C(29S)	346(6)	345(7)	338(8)	-3(6)	40(6)	7(6)
C(30S)	353(6)	350(8)	349(8)	-2(6)	49(7)	-2(6)
C(31S)	357(7)	359(7)	354(8)	-9(6)	38(5)	2(5)
C(32S)	373(8)	354(6)	364(7)	20(6)	58(6)	4(7)
C(33S)	294(8)	301(8)	306(6)	-20(5)	32(6)	-6(6)
C(34S)	296(9)	301(6)	305(7)	-6(6)	49(6)	-8(7)
C(35S)	307(9)	306(6)	309(6)	20(5)	48(7)	2(7)
C(36S)	340(9)	330(7)	353(7)	-18(5)	75(6)	-21(6)
C(37S)	444(7)	451(6)	441(8)	13(6)	28(6)	1(6)
C(38S)	398(7)	380(6)	380(9)	12(6)	72(6)	13(5)
C(39S)	354(6)	335(7)	321(8)	-12(6)	25(6)	25(6)
C(40S)	406(6)	428(8)	433(7)	9(6)	72(7)	-10(6)
C(41S)	392(6)	407(9)	406(7)	-8(6)	66(5)	10(7)
C(42S)	345(7)	333(8)	349(6)	8(7)	30(6)	2(6)
C(43S)	355(6)	353(8)	352(6)	2(7)	46(6)	-3(6)
C(44S)	357(8)	358(8)	357(7)	5(5)	48(6)	1(6)
C(45S)	356(7)	375(6)	360(8)	1(6)	49(6)	-8(7)
C(46S)	354(7)	344(6)	346(9)	1(6)	52(6)	4(5)
C(47S)	355(6)	347(7)	339(9)	0(7)	42(7)	3(5)
C(48S)	373(6)	379(7)	378(9)	2(6)	63(7)	-1(5)
C(49S)	348(8)	347(6)	344(8)	11(6)	45(6)	-12(5)
C(50S)	313(8)	335(6)	303(7)	-18(6)	41(6)	2(6)
C(51S)	250(9)	262(7)	275(6)	2(5)	25(6)	3(6)
C(52S)	269(8)	265(7)	276(6)	-6(6)	30(6)	8(6)
C(53S)	286(8)	300(7)	282(6)	-9(6)	35(6)	15(6)
C(54S)	304(7)	299(8)	310(7)	-16(6)	31(5)	9(6)
C(55S)	377(7)	366(9)	359(6)	4(7)	68(6)	-10(7)

Continued on next page

Table continued

	U_{11}	U_{22}	U_{33}	U_{23}	U_{13}	U_{12}
C(56S)	340(6)	343(9)	353(6)	-4(7)	43(5)	-6(6)
C(57S)	350(6)	344(9)	348(7)	0(6)	48(5)	-5(7)
C(58S)	336(6)	335(8)	331(8)	11(6)	47(6)	1(6)
C(59S)	335(6)	337(7)	335(7)	-3(6)	47(6)	6(6)
C(60S)	312(7)	314(9)	313(7)	19(6)	50(6)	2(6)
O(1T)	335(8)	334(8)	343(8)	-2(6)	49(6)	2(6)
C(1T)	335(8)	334(8)	343(8)	-2(6)	49(6)	2(6)
C(2T)	335(8)	334(8)	343(8)	-2(6)	49(6)	2(6)
C(3T)	335(8)	334(8)	343(8)	-2(6)	49(6)	2(6)
C(4T)	335(8)	334(8)	343(8)	-2(6)	49(6)	2(6)
O(1H)	335(8)	334(8)	343(8)	-2(6)	49(6)	2(6)
C(1H)	335(8)	334(8)	343(8)	-2(6)	49(6)	2(6)
C(2H)	335(8)	334(8)	343(8)	-2(6)	49(6)	2(6)
C(3H)	335(8)	334(8)	343(8)	-2(6)	49(6)	2(6)
C(4H)	335(8)	334(8)	343(8)	-2(6)	49(6)	2(6)
O(1O)	335(8)	334(8)	343(8)	-2(6)	49(6)	2(6)
C(2O)	335(8)	334(8)	343(8)	-2(6)	49(6)	2(6)
C(3O)	335(8)	334(8)	343(8)	-2(6)	49(6)	2(6)
C(4O)	335(8)	334(8)	343(8)	-2(6)	49(6)	2(6)
C(5O)	335(8)	334(8)	343(8)	-2(6)	49(6)	2(6)

Table 9.17: Hydrogen coordinates ($\times 10^4$) and isotropic displacement parameters (Å$^2\times 10^3$) for [4{K(DB18C6)($C_{60}^{\cdot -}$)}(THF)$_6$]·[C_{60}^0]·(THF)$_6$ at 220 K.

	x	y	z	U_{eq}
H(1R1)	5286	4081	2216	76
H(1R2)	5230	4192	1344	76
H(2R1)	4744	4163	1334	76
H(2R2)	4855	3356	1840	76
H(3R1)	4310	4195	1931	76
H(3R2)	4416	3398	2446	76
H(4R1)	4381	4192	3390	76

Continued on next page

Table continued

	x	y	z	U_{eq}
H(4R2)	4101	4065	2853	76
H(6R)	3965	4478	3791	148
H(7R)	3739	5249	4633	148
H(8R)	3755	6793	4669	148
H(9R)	3998	7567	3865	148
H(11A)	4444	8033	3363	94
H(11B)	4145	8213	2944	94
H(12A)	4350	8107	1752	94
H(12B)	4457	8957	2235	94
H(13A)	4846	8808	1739	94
H(13B)	4783	7872	1355	94
H(14A)	5198	8072	2515	94
H(14B)	5249	8232	1685	94
H(16R)	5648	7640	1971	115
H(17R)	6061	6885	1958	115
H(18R)	6066	5340	1927	115
H(19R)	5657	4550	1909	115
H(1Q1)	2987	8307	4233	85
H(1Q2)	3239	7754	4657	85
H(2Q1)	2813	6961	4586	85
H(2Q2)	2795	6977	3717	85
H(3Q1)	2810	5364	4722	85
H(3Q2)	2742	5319	3844	85
H(4Q1)	3235	4689	4668	85
H(4Q2)	2994	4057	4326	85
H(6Q)	3436	3066	4417	122
H(7Q)	3734	2013	4034	122
H(8Q)	3865	2105	2860	122
H(9Q)	3697	3250	2068	122
H(11C)	3504	3948	1426	90
H(11D)	3735	4609	1810	90
H(12C)	3410	5355	709	90
H(12D)	3179	5350	1246	90

Continued on next page

Table continued

	x	y	z	U_{eq}
H(13C)	3503	6912	815	90
H(13D)	3222	6836	1131	90
H(14C)	3349	8065	1264	90
H(14D)	3655	7789	1561	90
H(16Q)	3705	9201	2189	75
H(17Q)	3800	10323	3062	75
H(18Q)	3624	10240	4179	75
H(19Q)	3353	9035	4423	75
H(1W1)	5367	5134	3633	156
H(1W2)	5111	4844	4024	156
H(2W1)	5577	5291	4763	156
H(2W2)	5295	5372	5099	156
H(3W1)	5321	6866	5055	156
H(3W2)	5609	6784	4744	156
H(4W1)	5170	7366	3911	156
H(4W2)	5410	6879	3564	156
H(2E1)	2740	6821	1301	169
H(2E2)	2767	7330	2068	169
H(3E1)	2299	6802	1389	169
H(3E2)	2350	6952	2260	169
H(4E1)	2326	5476	2445	169
H(4E2)	2265	5329	1574	169
H(5E1)	2730	4820	2325	169
H(5E2)	2711	5085	1477	169
H(1Y1)	4658	5339	846	181
H(1Y2)	4736	6258	500	181
H(2Y1)	4425	5100	-246	181
H(2Y2)	4410	6130	-445	181
H(3Y1)	3991	6224	-70	181
H(3Y2)	4002	5186	105	181
H(4Y1)	4031	6354	1166	181
H(4Y2)	4169	5401	1297	181
H(1T1)	951	2483	3616	405

Continued on next page

Table continued

	x	y	z	U_{eq}
H(1T2)	1052	2066	4405	405
H(2T1)	1385	2379	3460	405
H(2T2)	1487	2335	4324	405
H(3T1)	1567	3810	4346	405
H(3T2)	1474	3848	3476	405
H(4T1)	1173	4568	4387	405
H(4T2)	1039	4214	3601	405
H(1H1)	1294	8027	3760	405
H(1H2)	1139	8038	4469	405
H(2H1)	1591	8900	4414	405
H(2H2)	1375	9186	4949	405
H(3H1)	1265	10410	4261	405
H(3H2)	1488	10140	3741	405
H(4H1)	962	10078	3259	405
H(4H2)	1175	9445	2928	405
H(2O1)	1860	5599	3445	405
H(2O2)	2113	5278	4023	405
H(3O1)	2115	6774	3336	405
H(3O2)	2299	6607	4113	405
H(4O1)	2032	7551	4659	405
H(4O2)	1855	7742	3876	405
H(5O1)	1645	6870	4899	405
H(5O2)	1539	6710	4048	405

Part IX

Appendix B

10 Acknowledgements

I must say that I write this part of my thesis with my greatest pleasure.

I would like to thank Professor Thomas Schleid and Professor Frank Gießelmann for accepting being my examiners, reading thoroughly the thesis and giving valuable comments and remarks.

I give my special thanks to Professor Martin Jansen, for giving me the opportunity of working in his group, and getting much new valuable experience, scientific as well as personal. It was very important and helpful for me to feel his constant interest in the project, his ready availability at any time for solving any issue, and his support and motivation when not everything was going as one would like to. The "bottleneck" of my work was the solution of the crystal structures. Besides general supervision of my PhD project, Professor Jansen had the most active role in the "crystal solution group" (may be a "funny" name, but the most correct, I think, because a number of people were involved in this, building a perfect team at the end), examining each structure in detail and leading and participating in the very process of crystal structure solution in each and every step. I am very grateful to him for "struggling" with us, the other members of this "crystal group", and teaching us to be extremely careful and tedious during all the process, doing everything step by step, and going back to the very beginning, no matter of the progress achieved already, when necessary, and starting again. I am grateful because finally it was this his attitude which enabled us to solve successfully a number of such unconventional and "big" structures, with twinning, disorder and many other nice things because of which crystallographers like they job (the impression I got...).

I thank Dr. Konstantin Amsharov for suggesting to use the "break-and-seal" technique for the task I was proposed and introducig me into this method. The first crystal obtained and structure solved were together with him. DFT calculations performed is his contribution to the present work, as well.

My special thanks go to Mr. Gerhard Preininger, the glassblower who was making for several years the glassware I used for my experiments, and his colleagues. I am very happy that from the very beginning we had a very friendly relationship, in spite of my numerous orders, and that often I needed things being done very fast. And they did it.

Is a pity Mr. Preininger leaves the institute now. He was not only making a perfect glassware, but was also always interested for what it is and how it will be used in the experiment, was making his own suggestions for improving and was an often guest in the lab where I was working. I will remember our Check-Russian communication for long.

I thank Dr. Jürgen Nuß for taking over the task of picking and measuring all the single crystals, making the absorption corrections, and his constant help in all the structures solutions. I am beyond all bounds grateful to Jürgen for his invaluable help in proof-reading of the part of the manuscript dealing with single crystal measurements, structure solution and results interpretation. I would also like to say I enjoyed very much writing articles with him. Was all very smooth, fast and easy cooperation, often bringing some nice and funny moments.

Mrs. Eva-Maria Peters contributed much, as well, to the crystal structure solutions, till the very time she left the department. EDX measurements were performed by her, too.

I am very grateful to Dr. Martin Schulz-Dobrick for introducing me into the program for crystal structure solution SHELX.

The magnetic measurements were carried out by Mrs. Eva Brücher and Mr. Michael Schulz. Mr. Schulz helped me in learning to operate the machine, as well.

UV/Vis/NIR measurements were recorded by Mr. Wolfgang König.

I thank Prof. Dr. Robert Dinnebier for his help with powder X-ray diffraction measurements.

With the help of Dr. Ulrich Wedig and Dr, Klaus Doll it was possible to perform theoretical calculations for the dimer. Besides, I thank Uli very much for his help with all kind of technical problems which occured during typing of the manuscript.

Mrs. Regine Noack "rescued" with very fast and professional making of several drawings needed to be done in a very short tiome slot included in the present work.

I am also very thankful to my officemate Dr. Hanne Nuß for her helpful comments on various issues during writing of the thesis, and taking over the full "German part" of it, and the total quietness she provided me when I needed it during writing.

And am thankful to Jörg Tomada, Vago Krokos, as well as to the rest of the "fullerene group" and my other friends – for making "noise" when I also needed it...

I am grateful to all my colleagues for having spent four years with you in one group in this nice, easy and friendly atmosphere we were creating for ourselves.

Taking advantage of that I give "acknowledgements", I would like to say more than a thanks to my family: my parents and my sister Sonya. "Taking advantage" - because there are always few opportunities or occasions when one (at least myself) can openly

thank the closest and most important people. All what I am, and will ever be, I owe to my family. I thank my parents for all their support in everything, and my sister, although she is much younger than me, for encouraging me with her example not to give up and go on, what she did when finishing high school and entering the university, at the same time I was finishing the thesis.

11 Curriculum vitae

Personal data

Name:	Nina Valeryevna Kozhemyakina
Date of birth:	11.05.1983
Place of birth:	Moscow, Russia
Merital status:	single

School education

09.1990-06.1999	Middle school under the USSR/Russian Embassy in Mexico City, Mexico
09.1999-12.1999	Specialized school in English № 1279 under the Russian State Humanitarian University, Moscow, Russia
01.2000-06.2000	School № 199, Moscow, Russia

Academic study

09.2000-06.2005	M.V. Lomonosov Moscow State University, Department of Chemistry, Moscow, Russia
01.2005-06.2005	Diploma thesis in the laboratory of Chemical Thermodynamics under supervision of Prof. Dr. M.V. Korobov "Aggregation of Fullerene C_{60} in the Solvent *N*-Methylpyrrolidone"
since 07.2005	PhD work under supervision of Prof. Dr. Dr. h. c. Martin Jansen, MPI für Festkörperforschung, Stuttgart. "Synthesis of New Fullerides via the "Break-and-Seal" Approach and their Characterization"

Practice

11.2004	Joint Institute for Nuclear Research, Dubna, Moscow reg., Russia
07.2004	Industrial-technological practice at the Moscow Oil-Processing Factory. Focus on cracking and platforming.

12 Publications

1. Nina V. Kozhemyakina, Jürgen Nuss, and Martin Jansen. Demonstration of the "Break-and-Seal" Approach to Fullerides of Complex Cations at the Example of $KC_{60}\cdot(THF)_5\cdot 2(THF)$. Z. Anorg. Allg. Chem., 635:1355, 2009.

2. Nina V. Kozhemyakina, Jürgen Nuss, and Martin Jansen. Synthesis and Crystal Structure of a New C_{60}^{2-} Fulleride: $[K(DB24C8)(DME)]_2C_{60}\cdot DME$. Eur. J. Inorg. Chem., 2009:3900, 2009.

3. Nina V. Kozhemyakina, Konstantin Amsharov, and Martin Jansen. Synthesis and Structure Analysis of $[K(DB18C6)]_{16}(C_{60})_{16}(C_{60})_4\cdot(THF)_{32}$, Containing C_{60} in Three Different Bonding States. Chem. Eur. J. *In preparation.*

Hiermit versichere ich an Eides statt, dass ich diese Dissertation unter Verwendung der angegebenen Hilfsmittel selbständig angefertigt und bisher noch keinen Promotionsversuch unternommen habe.

Stuttgart, den

Nina Kozhemyakina